Investigation of Quantitative Magnetization Transfer Magnetic Resonance Imaging as a Non-Invasive Technique to Assess the Biochemical, Mechanical, and Histologic Properties of Healthy and Osteoarthritic Meniscus and Cartilage

A Thesis Submitted to the

College of Graduate and Postdoctoral Studies

In Partial Fulfillment of the Requirements

For the Degree of Master of Science

In the Division of Biomedical Engineering

University of Saskatchewan

Saskatoon

By

KIRSTIN DON OLSEN

Permission to use

In presenting this thesis in partial fulfillment of the requirements for a Postgraduate degree from the University of Saskatchewan, I agree that the Libraries of this University may make it freely available for inspection. I further agree that permission for copying of this thesis in any manner, in whole or in part, for scholarly purposes may be granted by the professor or professors who supervised my thesis work or, in their absence, by the Head of the Department or the Dean of the College in which my thesis work was done. It is understood that any copying or publication or use of this thesis or parts thereof for financial gain shall not be allowed without my written permission. It is also understood that due recognition shall be given to me and to the University of Saskatchewan in any scholarly use which may be made of any material in my thesis.

Disclaimer

References in this thesis to any specific commercial products, process, or service by trade name, trademark, manufacturer, or otherwise, does not constitute or imply its endorsement, recommendation, or favoring by the University of Saskatchewan. The views and opinions of the author expressed herein do not state or reflect those of the University of Saskatchewan and shall not be used for advertising or product endorsement purposes.

Requests for permission to copy or to make other uses of materials in this thesis in whole or part should be addressed to:

Head of the Division of Biomedical Engineering

57 Campus Drive

University of Saskatchewan

Saskatoon, Saskatchewan S7N 5A9

Canada

OR

Dean

College of Graduate and Postdoctoral Studies

University of Saskatchewan

116 Thorvaldson Building, 110 Science Place

Saskatoon, Saskatchewan S7N 5C9

Canada

Abstract

Osteoarthritis is a degenerative disease affecting entire joints and leading to pain, stiffness, and loss of mobility. It affects around 13% of the Canadian population and commonly presents in the knee. Traditionally, osteoarthritis has been visualized using radiography because it is the most accessible imaging method and can detect bone alterations, but this method is unable to show changes to the articular cartilage and meniscus, which have been shown to play an important role in the disease process. Quantitative magnetic resonance imaging (qMRI) is able to provide images of the soft tissue within the knee joint as well as numerical values representative of the state of the tissue health. One particular qMRI technique is quantitative magnetization transfer (qMT), and it allows for the determination of the properties of the bound pool within tissues (macromolecules such as proteoglycan and collagen) that has resonance too short to be captured with conventional MRI. Because qMT probes the properties of the hydrogen bound to macromolecules, it is expected to be more sensitive to the changes in composition of a tissue associated with osteoarthritis. The primary objective of this research is to establish a relationship between qMT parameters (f, k, T_{2b} relaxation time, T_{2f} relaxation time, and T_{1f} relaxation time) and the biochemical, histological, and mechanical properties of human articular cartilage and meniscus, and a secondary objective is to compare *in vivo* to *ex situ* qMT parameters. Two separate studies were conducted using differing populations in order to accomplish these objectives.

The first study assessed six human cadaver knees with no history of injury or illness in order to validate the methods and gain a baseline of values to be expected in a healthy population. Intact cadaver knees were imaged using qMT MRI techniques and qMT parameters extracted. Subsequent to imaging, core samples were taken from each meniscus and digested and assayed to determine the liquid, collagen, and proteoglycan contents. Menisci were dissected into pieces for histology and scored using an established histological scoring system customized to the meniscus. Pearson product moment and Spearman's rho correlation coefficients were calculated for the biochemistry and histology results respectively compared to the qMT parameters to

determine if any of the imaging metrics were predictive of the biochemical content or histological score. Results of this study showed several significant correlations between the qMT parameters and tissue properties. Some of these key findings included correlations in the collective samples where increasing liquid content was associated with decreasing bound pool fraction ($r=-0.248$, $p<0.5$); increasing collagen per dry mass showed increasing T_{1f} ($r=0.413$, $p<0.01$) and T_{2f} ($r=0.510$, $p<0.01$); and an increase in total histology score was related to a decrease in T_{1f} ($\rho=-0.232$, $p<0.05$), T_{2f} ($\rho=-0.277$, $p<0.01$), and T_{2b} ($\rho=-0.207$, $p<0.05$). In the medial side samples, key correlations were observed between increasing collagen per dry mass and increasing T_{1f} ($r=0.477$, $p<0.01$), T_{2f} ($r=0.585$, $p<0.01$), and T_{2b} ($r=0.415$, $p<0.05$); and increasing histology score and decreasing T_{1f} ($\rho=-0.232$, $p<0.05$), T_{2f} ($\rho=-0.277$, $p<0.01$), and T_{2b} ($\rho=-0.207$, $p<0.05$). In the lateral side samples, key correlations were between increasing liquid content and decreasing f ($r=-0.380$, $p<0.05$) and increasing sulfated glycosaminoglycan (sGAG) per wet mass was associated with increases in f ($r=0.391$, $p<0.05$) and k_f ($r=0.404$, $p<0.05$).

The second study focused on an end-stage osteoarthritis population by assessing total knee arthroplasty patients. The aim of this study was to explore the relationships between qMT parameters and tissue properties in damaged tissue. Two patients were scanned using the qMT MRI protocol prior to their surgery, and the excised tissues were scanned post-operatively using the same sequence. From these samples, seven separate articular cartilage and meniscus surfaces (both medial and lateral) were assessed. After imaging, the surfaces underwent mechanical indentation testing and the instantaneous modulus, elastic fit mean squared error, and tissue thicknesses were determined. Core samples were then removed from the surfaces for biochemical and histological analysis. Biochemistry protocols were the same as utilized in the cadaver study, and histology preparation was the same as well with different scoring methods used depending on the tissue type (articular cartilage versus meniscus). Pearson and Spearman correlation coefficients were once again determined in order to assess correlations between the qMT parameters and the tissue properties. A Wilcoxon signed rank test was performed to assess differences between *in vivo* and *ex situ* qMT results. The key results of this study showed significant correlations in the *in vivo* cartilage between increasing instantaneous modulus and

decreasing T_{1f} (r=-0.221, p<0.05) and T_{2f} (r=-0.233, p<0.05) in the lateral side samples; increasing liquid content and T_{1f} (r=0.836, p<0.05) in the lateral samples; and histology score and f in the combined samples (ρ=0.670, p<0.05) and medial samples (ρ=1.000, p<0.01). In the *ex situ* cartilage, significant correlations were found between increasing histology score and decreasing T_{2b} (ρ=-0.896, p<0.01) in the lateral samples. In the lateral menisci samples *in vivo,* key correlations were found between increasing liquid content and decreasing k_f (r=-0.890, p<0.05); increasing sGAG/dry mass and increasing T_{2b} (r=0.869, p<0.05); and increasing collagen/wet mass and increasing k_f (r=0.820, p<0.05). In the lateral *ex situ* menisci, a negative correlation was observed between instantaneous modulus and T_{2f} (r=-0.563, p<0.05). In the global surface analysis (combining all cartilage and meniscus surfaces), key correlations were between increasing liquid content and increasing T_{1f} (r=0.926, p<0.01) and T_{2f} (r=0.864, p<0.05); increasing sGAG/dry mass and increasing T_{1f} (r=826 p<0.05) and T_{2f} (r=0.964, p<0.01); increasing collagen/dry mass and decreasing T_{1f} (r=-0.780, p<0.05); and increasing histology score and increasing T_{2f} (ρ=0.893, p<0.01). Significant decreases in T_1obs, T_{1f}, T_{2f} and T_{2b} were also found from *in vivo* to *ex situ* scanning environments.

The findings in the correlation analysis of this project show the potential of qMT MRI imaging as a valuable modality for determining the structure, function, and composition of osteoarthritic articular cartilage and meniscus. It has been shown that *ex situ* qMT parameters are not the same as *in vivo* but steps have been made in a direction towards quantifying the relationships between the differing environments. Possible uses of this technique lie in early diagnosis of OA, monitoring of disease progression, and evaluation of potential treatments.

Acknowledgements

There are several people I would like to thank without whom this work would not have been possible. To my supervisor Dr. Emily McWalter, I owe the biggest thanks for guiding me through this process and offering support and encouragement throughout. I have gained invaluable experience and knowledge through your mentorship and have sincerely appreciated the many instances of reassurance and confidence in me when I had little in myself. To Dr. Adi Manek in the Histology Core Facility, thank you for teaching and supporting me through the entire histology portion of my project. You always went above and beyond to provide instruction, suggestions, and help troubleshooting and I am so lucky to have been able to learn from the best. I would also like to thank Dr. Steve Machtaler for all the assistance with biochemistry and access to lab space and equipment. Thank you as well for introducing me to your student Una Goncin who was also a huge help with my biochemistry and offered moral support and friendship throughout my struggles in the lab. Thank you to Rob Peace for all the help in the engineering lab and discussions about figure skating.

To my engineering lab group members, I owe my sanity throughout this degree. Kadin, Amy, Ibk, Dylan, Alvaro, Pablo, Nima, Lumeng, Brennan, and Dena thank you for all the support, advice, outings, and winter Wednesday's. Without you all I would not have been able to finish or even start this project. To Lumeng, thank you for all the help with the MRI components of the project and thank you for helping me understand and pass our MRI physics class. To Brennan, thank you for your patience and assistance with the registration component. Without your coding expertise and instruction, I would not have been able to compile my results or provide any valuable conclusions.

Lastly, thank you to my family and friends. Thank you to my parents Linda and Karl for all the love, support, and encouragement at every stage of this project. Thank you to the rest of my family as well (especially Chris for letting me live with you longer than anticipated) for everything you did for me during my time here in Saskatoon. Also thank you to my amazing friends (especially Jade, my biggest cheerleader) for always believing in me and supporting everything I do.

Table of Contents

Permission to use i

Disclaimer i

Abstract iii

Acknowledgements vi

List of Figures xi

List of Tables xvii

List of Abbreviations xx

1. Introduction 1

1.1. Motivation 1

1.2. Research Objectives 3

1.3. Changes to project due to COVID-19 3

1.4. Thesis Organization 4

2. Background 5

2.1. Cartilage and meniscus of the knee 5

2.1.1. Articular cartilage composition and function 5

2.1.2. Meniscus composition and function 7

2.2. Osteoarthritis 9

2.2.1. Role of cartilage in osteoarthritis progression 10

2.2.2. Role of meniscus in osteoarthritis progression 10

2.2.3. Diagnosing osteoarthritis 10

2.3. Quantitative Magnetization Transfer Magnetic Resonance Imaging 11

2.3.1. Magnetic resonance imaging physics background 12

2.3.2. Quantitative magnetic resonance imaging 13

2.3.3. Specifics of quantitative magnetization transfer 15

2.4. Mechanical Testing 17

2.4.1. Mechanical testing methods in cartilage and meniscus 17

2.4.2. Mechanical properties of cartilage and meniscus 19

2.4.3. Changes of mechanical properties with osteoarthritis 21

2.5. Biochemical analysis of knee cartilage and meniscus 21

2.5.1. Proteoglycan 21
2.5.2. Collagen 24
2.6. Histological analysis of cartilage and meniscus 25
2.6.1. Staining in histology 25
2.6.2. Histological scoring 27
2.7. Validation of qMRI metrics in the literature 33
2.7.1. Validation of qMT metrics in the literature 40
2.8. Gaps in the literature 40
3. General Methodology 43
3.1. qMT image acquisition 43
3.2. Image processing 44
3.2.1. Image segmentation for binary masks 44
3.2.2. Determining qMT parameters from MRI data 45
3.2.3. Model registration 47
3.3. Biochemical content analysis 49
3.3.1. Proteinase K digestion 49
3.3.2. Quantification of proteoglycan in the tissues 49
3.3.3. Quantification of collagen in the tissues 50
3.4. Histology 50
3.4.1. Sample fixation, processing, and paraffin embedding 51
3.4.2. Sectioning and staining 52
3.4.3. Scoring 53
4. Validation of qMT MRI in Cadaver Menisci 54
4.1. Introduction to the cadaver study 54
4.2. Methods specific to the cadaver study 54
4.2.1. Specimens 55
4.2.2. Sample retrieval for biochemistry and histology 55
4.2.3. Histology 57
4.2.4. Image processing 57
4.2.5. Statistical analysis specific to the cadaver study 58
4.3. Results of the cadaver study 59
4.3.1. qMT imaging parameter results 60

4.3.2. Biochemistry results 63
4.3.3. Histology results 63
4.3.4. Biochemistry correlation analysis 65
4.3.5. Histology correlation analysis 68
4.4. Cadaver study discussion 68
4.4.1. qMT parameter analysis – comparison to literature 69
4.4.2. Correlations between tissue properties and qMT parameters 71
4.4.3. Connections between biochemistry and histology results 73
4.5. Limitations of the cadaver study 77
4.6. Cadaver study conclusion 77
5. qMT MRI of Articular Cartilage and Meniscus in Total Knee Arthroplasty Patients 78
5.1. Introduction to the TKA study 78
5.2. Methods specific to the TKA study 79
5.2.1. Patient recruitment 80
5.2.2. *In vivo* participant qMT MRI scanning 80
5.2.3. Specimen retrieval 80
5.2.4. *Ex Situ* specimen qMT MRI scanning 81
5.2.5. Mechanical testing using the Mach-1 82
5.2.6. Sample retrieval for biochemistry and histology 87
5.2.7. Creation of surface and sample models 88
5.2.8. Statistical analysis specific to the TKA study 90
5.3. Results of the TKA study 91
5.3.1. qMT imaging parameters *in vivo* versus *ex situ* 91
5.3.2. Mechanical testing results 93
5.3.3. Biochemistry results 96
5.3.4. Histology results 99
5.3.4.1. Histology score correlations to qMT parameters 102
5.3.5. Combined tissue correlation 103
5.4. Discussion of the TKA study 105
5.4.1. Comparison of *in vivo* to *ex situ* results 105
5.4.2. Correlations between qMT parameters and the TKA tissue properties 108
5.4.3. Comparison of qMT parameters to literature 111

5.5. Limitations of the TKA study 116
5.6. Conclusion of the TKA study 116
6. Integrated discussion 118
6.1. qMT parameters of meniscus in healthy versus diseased knees 118
6.2. Medial versus lateral qMT parameters in healthy and diseased knees 121
6.3. Strengths and limitations 122
7. Conclusion 125
References 127
Appendix A: qMT scanning protocols 138
Appendix B: MRI screening form 139
Appendix C: Consent form 141
Appendix D: Participant demographic survey 147
Appendix E: KOOS pain survey 148
Appendix F: TKA Study Ethics Certificate 152
Appendix G: Mach-1 Indentation Testing SOP 153
Appendix H: Cadaver Study Ethics Certificate 158
Appendix I: Significant correlations for combined cadaver data 159
Appendix J: qMT parameter filtering prior to registration for the TKA study 161
Appendix K: qMT imaging results of the TKA study – *in vivo* and *ex situ* 162
Appendix L: Thickness testing results for the TKA study 166
Appendix M: Mechanical testing results color maps for TKA study 167
Appendix N: Correlation coefficient tables for the TKA study 174
Appendix O: Correlation scatterplots for TKA data with N=3 and N=2 sample sizes 179
Appendix P: Discussion of connections between the mechanical, biochemistry, and histology results of the TKA study 184
Appendix Q: Correlations between tissue properties for the TKA study 189

List of Figures

Figure 2.1: Anatomical diagram of a right human knee. Cartilage and meniscus labels are boxed. Image in public domain (Author unidentified, Wikimedia Commons). fewhbeiwbfwik 6

Figure 2.2: Layers of cartilage and percentage of collagen within each region (reproduced with permission from original publisher)[25] 6

Figure 2.3Figure 2.4: Description of vascularization and cell population by region in the meniscus (reproduced with permission from original publisher) [28] 8

Figure 2.5: The effect of a radiofrequency pulse on net magnetization (M) during magnetic resonance image acquisition 13

Figure 2.6: K-space (left) is the Fourier transform (FT) of an MR image (right). Courtesy of Allen D. Elster, MRIquestions.com 13

Figure 2.7: Visualization of longitudinal (T_1) and transverse (T_2) relaxation times. Courtesy of Allen D. Elster, MRIquestions.com 14

Figure 2.8: Magnetization transfer binary spin bath model. Modified from Simard and Henkelman[20,76] 16

Figure 2.9: Repeating disaccharide units of various glycosaminoglycans (reproduced with permission from original publisher) [99] 22

Figure 2.10: Structure of collagen fibers up to nanoscale (amino acids). HYP represents hydroxyproline and PRO proline (image copyright 2006 National Academy of Sciences) [112] 24

Figure 2.11: Staining of human knee articular cartilage with Hematoxylin and Eosin (A) and Safranin O (B). Modified from Pauli *et al*. Reprodcued with permission from original publisher [123] 26

Figure 2.12: Picrosirius red stained porcine femeropatellar articular cartilage. Images from public access article[126] 27

Figure 2.13: Goldner's trichrome stained canine menisci (A shows healthy meniscus and B compressed meniscus). Images from public access article[127] 27

Figure 2.14: Normal articular cartilage (grade 0). Safranin O stained 5X. Reproduced with permission from original publisher[128] 28
Figure 2.15: Examples of OARSI grades 1-6. Briefly, grade 1: surface intact with superficial fibrillation, grade 2: surface discontinuity, fibrillation extends further through the superficial zone, grade 3: fissures extending to mid zone, grade 4: erosion, grade 5: denudation, grade 6: deformation. Safranin O stained, 5X. Reproduced with permission from original publisher[128] 30
Figure 2.16: Pauli meniscus histology scoring system surface integrity component. (A,B) normal meniscus - score 0, (C,D) mild changes, slight fibrillation - score 1, (E,F) moderate fibrillation and some clefts - score 2, (G,H) severe damage – score 3. Safranin O/fast green stained 4X. Reproduced with permission from original publisher[140] 32
Figure 2.17: Pauli meniscus histology scoring system cellularity component. A) normal cells – score 0, B) diffuse hypercellularity – score 1, C) hypo- to a-cellular regions – score 2, D) hypocellularity – score 3. H&E 40X. Reproduced with permission from original publisher[140] 32
Figure 2.18: Pauli meniscus histology scoring system matrix and collagen fiber organization component. A) normal appearance – score 0, B) diffuse foci of degenerated extracellular matrix – score 1, C) bands or confluent foci of degenerated extracellular matrix, collagen fibers disorganized – score 2, D) fibrocartilaginous separation, unorganized collagen fibers – score 3. Safranin O/fast green 4X. Reproduced with permission from original publisher[140] 33
Figure 2.19: Pauli meniscus histology scoring system safranin o staining intensity component. A) no stain – score 0, B) slight intensity – score 1, C) moderate staining – score 2, D) strong staining intensity – score 3. Safranin O/fast green 4X. Reproduced with permission from original publisher[140] 33
Figure 3.1: A) Binary mask of cartilage created using Analyze 14.0 overlaid onto the corresponding MR image slice. B) Binary mask of just the top surface of the cartilage for the same slice. 45
Figure 3.2: A) Binary mask of meniscus created using Analyze 14.0 overlaid onto the corresponding MR image slice. B) Binary mask of just the top surface of the meniscus for the same slice. 45

Figure 3.3: Gaussian lineshape fit for *in vivo* cartilage. The upper data has MT flip angle = 126°, and lower data has MT flip angle = 426°. 47

Figure 3.4: Matlab registration figures. A) Mach-1 surface and sample cylinder registered to analyze surface B) Transformed cylinder registered to the MRI mask. 48

Figure 3.5: A) Single slice showing the cartilage mask overlapped with the cylinder B) region of overlap between the cartilage and cylinder 48

Figure 3.6: Description of steps involved in automatic tissue processing for histology (Image copyright 2020 Leica Biosystems division of Leica Microsystems, Inc.)[150] 51

Figure 3.7: Tissue sample embedded in paraffin for histological sectioning. 52

Figure 4.1: Methodology for the cadaver study. This study included qMT MRI scanning of the whole cadaver knee, dissection for tissue retrieval and sample procurement, biochemistry and histology, and then registration 55

Figure 4.2: Depiction of histology blocks taken from cadaver menisci and the regions represented in sections taken from each block 56

Figure 4.3: A) Modified photograph of meniscus dissected into blocks for histology (Science Care does not permit publication of pictures of cadaver specimens. B) Image of blocks created in Fusion 360 to represent the locations of the histology samples taken. The blocks were also split into 3 regions, the anterior, central, and posterior portions of each block. 58

Figure 4.4: Resulting figure from registration code run on cadaver histology blocks. Red represents the surface model, blue the analyze surface, and green the histology block. The average shape match error for all 6 cadaver knee registrations was 0.676 ± 0.056 mm. Not all data points will necessarily exist in both surface and analyze models 58

Figure 4.5: Color maps representing the ranges of qMT values across a single slice of human cadaver menisci 62

Figure 4.6: Distribution of histology scores in all, medial, and lateral samples for the cadaver study. G1 = normal tissue, G2 = mild degeneration, G3 = moderate degeneration, G4 = severe degeneration 64

Figure 4.7: Examples of each grade of histology sample observed in the cadaver study A. Grade 1, B. Grade 2, C. Grade 3 64

Figure 4.8: Correlation between the transverse relaxation time of the free pool and the percentage of collagen per dry mass in human cadaver menisci 67

Figure 5.1: Overall TKA study methodology. *(1) Prior to TKA, patients underwent MRI assessment. (2) After surgery, excised tibial plateaus with attached menisci were scanned again. (3) Mechanical testing. (4) Tissue retrieval. (5) Small samples were procured from the tissue specimens for testing. (6) Registration of mechanical, histological, and biochemical values to location of samples followed.* 79

Figure 5.2: Specimen set-up for MRI scanning of TKA samples 82

Figure 5.3: Mach-1 mechanical testing system set-up (Mach-1, Biomomentum, Laval, QC, Canada). Image copyright 2013 Biomomentum. 83

Figure 5.4: Specimen in Mach-1 testing chamber for cartilage mechanical testing 84

Figure 5.5: Samples selected for analysis using the Mach-1 mapping toolbox software 85

Figure 5.6: Cartilage surface (left) and lateral meniscus surface (right) after samples removed for biochemistry and histology. On the cartilage surface, tan colored tissue is the cartilage while the pink and red areas are subchondral bone. Pink areas of the meniscus are the surrounding ligaments 88

Figure 5.7: Plot of the force experienced in the Z direction by the Mach-1 indenter over time for finding the point of contact of the indenter with the tissue. The units of the force in this figure do not have meaning but represent the force experienced in newtons. 89

Figure 5.8: Bar graphs comparing *in vivo* to *ex situ* qMT parameters across surfaces for the TKA study 92

Figure 5.9: Color map showing variation of instantaneous modulus values across the surface of the lateral cartilage of knee 1 95

Figure 5.10: Very strong correlation between T_{1f} and liquid content for *in vivo* lateral cartilage 98

Figure 5.11: Examples of stained cartilage slides for the TKA study. A) grade 0 stage 0 B) grade 1 stage 1 C) grade 3.5 stage 4 D) grade 4.5 stage 3 E) grade 4.5 stage 4. All sides show the femoral side or top surface of the cartilage at the top of the image. The cut out portions in A and B should be ignored because they were by-products of sample extraction and do not influence the scoring. 100

Figure 5.12: Meniscus histology results for the TKA study. G1 = normal tissue, G2 = mild degeneration, G3 = moderate degeneration, G4 = severe degeneration 101

Figure 5.13: Examples of stained meniscus slides for the TKA study A) grade 1 B) Grade 2 C) grade 4 101

Figure 5.14: Significant correlations for TKA cartilage histology correlation analysis A: *in vivo* combined surfaces, B: *in vivo* medial surfaces, and C: *ex situ* lateral surfaces 102

Figure 5.15: Very strong significant correlations for TKA study *in vivo* surfaces. Red data points are from meniscus, green from articular cartilage. A-C) correlations between T_1obs, T_{1f}, and T_{2f} (respectively) and liquid content, D-F) correlations between T_1obs, T_{1f}, and T_{2f} (respectively) and sGAG/dry mass, F) correlation between T_{2f} and sGAG/wet mass, and H) correlation between T_{2f} and histology score 104

Figure 6.1: Bar graphs comparing the cadaver meniscus to *ex situ* TKA meniscus and cartilage qMT results. Cadaver results are taken from the qMT parameters of the corresponding biochemistry samples. 119

Figure K.1: qMT parameter maps for a single slice of *in vivo* cartilage (knee 2 lateral) 163

Figure K.2: qMT parameter maps for a single slice of *ex situ* cartilage (knee 2 lateral) 165

Figure O.1: Relationships between qMT parameters and biochemical properties in the *in vivo* medial cartilage samples 179

Figure O.2: Relationships between qMT parameters and biochemical properties in the *ex situ* medial cartilage samples 180

Figure O.3: Relationships between qMT parameters and biochemical properties in the *ex situ* lateral cartilage samples 181

Figure O.4: Relationships between qMT parameters and biochemical properties in the *ex situ* meniscus samples 182

Figure O.5: Relationships between qMT parameters and histology score in the *ex situ* meniscus samples ... 183

Figure P.1: Scatterplots for representative tissue property relationships in the cartilage..... 187

Figure P.2: Scatterplots for representative tissue property relationships in the meniscus 188

List of Tables

Table 2.1: Description of cartilage structural zones[21] 6

Table 2.2: Description of three commonly used mechanical property testing methods 18

Table 2.3: Direct and indirect methods for obtaining Young's modulus, aggregate modulus, and Poisson's ration from unconfined, confined, and indentation compression tests (reproduced with permission from original publisher) [79] 20

Table 2.4: Description of cartilage scoring systems 28

Table 2.5: qMRI validation against tissue mechanical properties in the literature 34

Table 2.6: qMRI validation against tissue biochemical properties in the literature 37

Table 2.7: qMRI validation against histological score in the literature 39

Table 3.1: Scanning parameters for the cadaver and TKA studies 43

Table 3.2: Safranin O/Fast Green Staining Protocol Modified from Schmitz et al 52

Table 4.1: Breakdown of number of samples taken from each knee for histology and biochemistry 59

Table 4.2: qMT parameter results for the cadaver study 61

Table 4.3: Average biochemistry results for the cadaver study 63

Table 4.4: Pearson correlation coefficients and significance values for biochemical properties and the qMT parameters using A) all biochemistry samples taken from the cadaver menisci, B) only samples taken from medial menisci, and C) only samples taken from lateral menisci 65

Table 4.5: Spearman's rho correlation coefficients and significance values for histological scores and the qMT parameters using A) all samples obtained, B) only samples from medial menisci, and C) only samples from lateral menisci 68

Table 4.6: qMT values in meniscus – comparison to literature 69

Table 4.7: Biochemistry values in meniscus - comparison to literature for cadaver study 74

Table 4.8: Comparison between histology and biochemistry results for a small sampling of data with differing tissue health 76
Table 5.1: Mach-1 parameters specified for tissue indentation testing 85
Table 5.2: Mach-1 parameters specified for tissue thickness testing 86
Table 5.3: Parameters chosen for Mach-1 indentation analysis 87
Table 5.4: List of statistical methods used to perform the various analyses in the TKA study 90
Table 5.5: Number of samples for each knee and side for the tissue property tests performed in the TKA study 91
Table 5.6: Wilcoxon signed ranks test results for comparison of the *in vivo* to *ex situ* qMT parameter results 92
Table 5.7: Average mechanical property results for the TKA study 94
Table 5.8: Average biochemistry results for the TKA study 97
Table 5.9: Cartilage histology results for the TKA study 99
Table 5.10: Comparison of TKA study meniscus qMT results to values from the literature 107
Table 5.11: Comparison of TKA study cartilage qMT results to values from the literature 113
Table J.1: qMT raw data filtering ranges for each parameter in the TKA study 161
Table K.1: *In Vivo* qMT parameter results for the TKA study 162
Table K.2: Ex Situ qMT parameters for the TKA study 164
Table L.1: Average tissue thickness for TKA study samples 166
Table N.1: Pearson correlation coefficients with significance values in brackets for A: *in vivo* and B: *ex situ* cartilage qMT to mechanical properties: all samples, medial samples, and lateral samples 174
Table N.2: Pearson correlation coefficients with significance values in brackets for A: *in vivo* and B: *ex situ* meniscus qMT to mechanical properties 174
Table N.3: Pearson correlation coefficients with significance values in brackets for A: *in vivo* and B: *ex situ* cartilage qMT to biochemistry: all samples, medial samples, and lateral samples 175

Table N.4: Pearson correlation coefficients with significance values in brackets for *in vivo* meniscus qMT to biochemistry 176

Table N.5: Spearman's rho correlation coefficients with significance values in brackets for A: *in vivo* and B: *ex situ* cartilage qMT to histological score: all samples, medial samples, and lateral samples 176

Table N.6: Spearman's rho correlation coefficients with significance values in brackets for *in vivo* meniscus qMT to histological score 177

Table N.7: Correlation coefficients for combined A. *in vivo* and B. *ex situ* surfaces – comparison of qMT parameters to all evaluated tissue properties. All coefficients reported in table are Pearson except for histology score which is Spearman. Significance values in brackets. 178

Table P.1: Comparison of my results to the literature for cartilage and meniscus in the TKA study 186

Table Q.1: Pearson correlation coefficients calculated between various representative tissue properties in the TKA study 189

List of Abbreviations

Abbreviation	Meaning
B_0	Main, static magnetic field
B_1	Magnetic field generated by radiofrequency pulse
DMMB	1:9-dimethylmethylene blue
ECM	Extracellular matrix
F	Bound pool fraction
FT	Fourier transform
FOV	Field of view
GAG	Glycosaminoglycan
H&E	Hematoxylin and eosin
HA	Hyaluronic acid
H_b	Restricted hydrogen pool
H_f	Free hydrogen pool
HHGS	Histologic Histochemical Grading System
IM	Instantaneous modulus
k_f	Exchange rate of magnetization between the free and the bound hydrogen pools
KL	Kellgren-Lawrence
KOOS	Knee Injury and Osteoarthritis Outcome Score
MRI	Magnetic resonance imaging
MT	Magnetization transfer
MTR	Magnetization transfer ratio
NBF	Neutral buffered formalin
OA	Osteoarthritis
OARSI	Osteoarthritis Research Society International
PBS	Phosphate buffered saline
pDAB	p-dimethylaminobenzaldehyde
PTFE	Polytetrafluoroethylene
qMRI	Quantitative magnetic resonance imaging
qMT	Quantitative magnetization transfer
RF	Radiofrequency
sGAG	Sulphated glycosaminoglycans
SPGR	Spoiled gradient recalled echo
T	Tesla
T_1	Longitudinal relaxation time
$T1_b$	Longitudinal relaxation time of the bound pool
$T1_f$	Longitudinal relaxation time of the free pool
$T_{1\rho}$	Relaxation time due to spin-lattice interactions in the rotating frame

T_2	Transverse relaxation time
T_2*	Observed transverse relaxation time due to inhomogeneity in the magnetic field
$T2_b$	Transverse relaxation time of the bound pool
TE	Time to echo
TKA	Total knee arthroplasty
TR	Repetition time

1. Introduction

Osteoarthritis is commonly referred to as a disease of ageing and it currently affects 240 million people worldwide[1]. Despite the vast population it impacts, the disease process is still not well understood, especially in its early stages. Current treatments are lacking[1] and are limited by the inability to non-invasively detect changes in the joints impacted by the disease[2]. Imaging techniques to further understand the disease process and observe changes in the joint over time are required to validate potential therapies[2]. The purpose of this project is to further understand osteoarthritis and explore a potential new way to non-invasively image the soft tissue in knee joints, which may provide quantitative parameters that are related to the properties and health of the tissue. This chapter provides further details on the motivation and research objectives of this project and explains the changes made due to COVID-19 as well as the organization of this thesis.

1.1. Motivation

Osteoarthritis (OA) is a degenerative disease that involves the entire synovial joint and is characterized by a loss in soft tissue and bone as well as structural modification[3–5]. It is the most common type of arthritis – affecting 13% of Canadians – but this number is projected to increase to 19% by the year 2031, alongside an increase in $4.7 billion in direct costs (hospitalization, outpatient services, drugs, etc.)[6–8]. There are two subgroups of OA: primary (or idiopathic), where there is no known cause of the disease; and secondary (or post-traumatic), in which a known injury or other disease is related to the development of OA[9]. Some of the signs of OA include joint pain, stiffness, focal areas of fibrillation, fissures, bone sclerosis, osteophyte formation, and loss of mobility in the affected joint [4,10]. Two of the tissues affected by OA in the human knee joint specifically are the articular cartilage and the meniscus. As OA advances, the proteoglycan and collagen within the cartilage and meniscus becomes depleted and disorganized[11]. The critical role these two tissues play in the progression of the disease make them the focal point of this research. OA is a debilitating disease with very few remedies available[1]. The lack of treatment options is largely due to an inability to measure changes in the

joint soft tissues early in the disease process and thus verify the efficacy of proposed therapies[2]. A method of tracking changes in cartilage or meniscus that may be the result of an applied treatment would be useful in determining levels of success for the intervention. This project begins to fill this gap in knowledge by investigating a non-invasive method of assessing tissue composition, structure and function in articular cartilage and meniscus.

Traditionally, OA has been assessed using radiography because it is the most accessible imaging method and it is able to detect alterations of the bones in the joint [12]. However, traditional radiography does not image articular cartilage and menisci directly. Magnetic resonance imaging (MRI) is a powerful tool that differs from other imaging modalities as it can be used to provide images of soft tissues, such as articular cartilage and meniscus[2]. This makes it beneficial for OA research, as it is a non-invasive method of analyzing the tissue within the joints of OA patients[2]. A more specific application of MRI is quantitative magnetic resonance imaging (qMRI), which allows for numerical values to be measured as well as morphological images rendered. Specifically, qMRI allows for various parameters to be obtained which have previously been correlated to the structure[13,14], function[15,16], and content[16] of the tissues.

Quantitative magnetization transfer (qMT) is a specific qMRI approach that allows for the indirect observation of hydrogen atoms with resonance too short (on the order of microseconds) to be captured with conventional MRI[17]. It is a powerful MRI contrast that allows for the determination of the properties of the restricted pool within tissues (specifically the macromolecules such as proteoglycan and collagen within articular cartilage and meniscus) that cannot be detected using conventional MRI[17]. Based on this and the fact that proteoglycan and collagen are key players in OA, it is hypothesized that qMT has the potential to give greater insight into tissue degeneration due to OA than other qMRI techniques. Previous studies have shown moderate correlations between qMT parameters and the biochemical properties of cartilage as well as changes in some properties with presence of OA[18,19]. These findings support the potential of qMT MRI as a useful tool for assessing soft tissue function, but further work must be done to include other tissue properties such as mechanical properties

and histological scoring. Furthermore, there is currently a relatively small body of knowledge on qMT analysis in cartilage, but it is even smaller in the meniscus with only one other qMT study analyzing the meniscus in existence[20]. Because the meniscus plays a critical role in OA progression, it is important to understand its structure and function as well as that of cartilage. There are also no studies comparing *in vivo* and *ex situ* qMT parameters in either cartilage or meniscus; this is essential for understanding the applicability of qMT to OA *in vivo* since much of the validation work is done *ex situ*. Research in this field is necessary to more fully understand the OA disease process *in vivo* and to have an objective tool that can be used to evaluate treatment strategies.

1.2. Research Objectives

The main objectives of this research were to establish a relationship between qMT parameters and the mechanical, biochemical, and histological properties of human knee articular cartilage and meniscus and compare the qMT parameters obtained *in vivo* to *ex situ*. This would allow for the investigation of qMT as a non-invasive imaging technique for the assessment of tissue properties. These main objectives were carried out through two studies with connected purposes.

Study 1 Objective: To evaluate qMT MRI as a non-invasive marker of healthy menisci tissue content (biochemical properties) and structure (histology score) in cadaver knees.

Study 2 Objective: To evaluate qMT MRI as a non-invasive marker of articular cartilage and meniscus tissue content (biochemical properties), structure (histology score), and function (mechanical properties) in an end stage OA population (total knee arthroplasty (TKA) patients) and to compare qMT results between *in vivo* and *ex situ* scanning environments.

1.3. Changes to project due to COVID-19

Due to the international COVID-19 pandemic, modifications to the original plan for this project had to be made. Initially, the goal was to include 15 participants in the TKA study but the lockdown and cancellation of elective

surgeries at the onset of the pandemic prevented this from happening. Prior to the major shutdown, all data had been collected for two participants with seven tissue surfaces in total; so, these results were analyzed and compiled into this report as an initial investigation. This limited sample size is recognized as a limitation of this work, but it is the intent for this project to be continued by another student in the future in order to validate my results and assess the same relationships and properties in a larger population.

1.4. Thesis Organization

This thesis contains six further chapters to present the work completed. Chapter 2 gives the background information and literature review of the main topics required to understand the work carried out and the results obtained. Chapter 3 provides a description of the general methodologies, in particular those of which are used in both the cadaver and TKA studies. Chapter 4 is dedicated to the cadaver study, outlining the cadaver specific methods, results, and discussion of the findings. Chapter 5 then covers the same content but for the TKA study. The sixth chapter is an integrated discussion which highlights the interconnectedness of the two studies and outlines the broad takeaways from the work as a whole. Finally, chapter 7 is a conclusion stating the key findings and providing suggestions for future research directions.

2. Background

This chapter gives a background on knee anatomy and OA, as well as biochemistry, histology, and mechanical testing methods that have been used in the past for OA research. It will also describe qMT MRI as it pertains to cartilage and meniscus.

2.1. Cartilage and meniscus of the knee

In order to diagnose and treat osteoarthritis (OA), it is first necessary to understand the structure and function of normal articular cartilage and meniscus as well as the effects and etiology of the disease on these tissues. This section will provide background on the composition and function of both cartilage and meniscus.

2.1.1. Articular cartilage composition and function

Articular cartilage is a specialized connective tissue covering the articulating surfaces of bones in the diarthrodial joints of vertebrate animals (Figure 2.1) which functions to provide a smooth and lubricated surface to facilitate joint motion and to distribute loads to the bone extremities[21,22]. Cartilage is a viscoelastic tissue, demonstrating a behavior dependent on exposure time when a constant load is applied[21,23]. Furthermore, cartilage lacks blood vessels, nerves, and lymphatics which ultimately limits its ability to repair and heal if damaged[21]. Composition wise cartilage contains mostly water (80% of wet weight) but it also contains an extracellular matrix (ECM) consisting of collagen fibers, proteoglycans, and small amounts of other matrix proteins[21,24]. Also distributed within the ECM are chondrocytes, which are highly specialized and metabolically active cells originating from mesenchymal cells that are responsible for the synthesis of various matrix components including glycosaminoglycan (GAG) side chains and proteins[21,24]. Structurally, cartilage has three zones varying in content and collagen organization (Figure 2.2, Table 2.1).

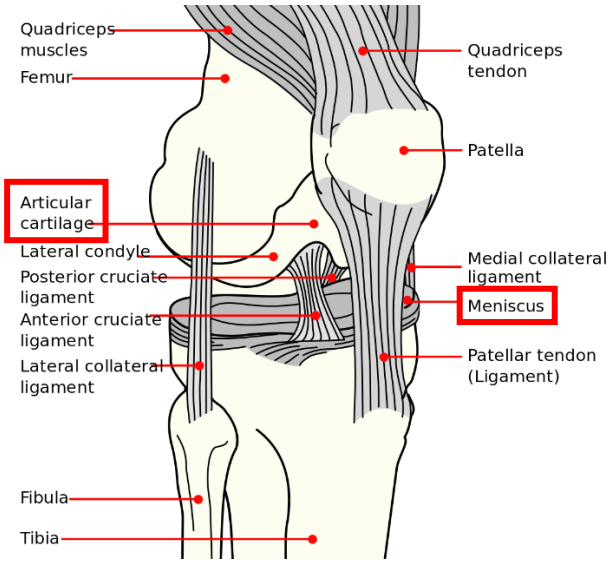

FIGURE 2.1: ANATOMICAL DIAGRAM OF A RIGHT HUMAN KNEE. CARTILAGE AND MENISCUS LABELS ARE BOXED. IMAGE IN PUBLIC DOMAIN (AUTHOR UNIDENTIFIED, WIKIMEDIA COMMONS). FEWHBEIWBFWIK

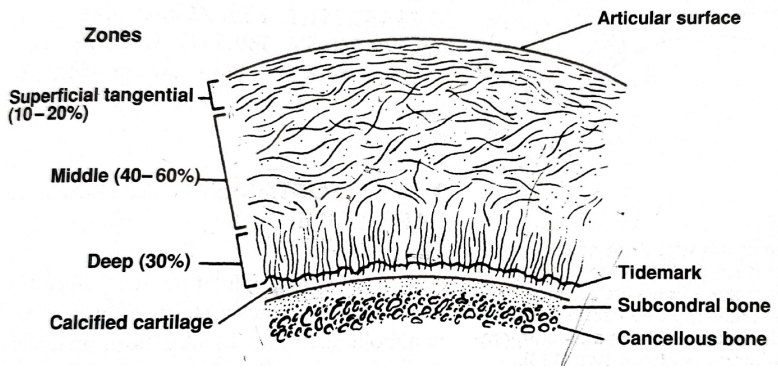

FIGURE 2.2: LAYERS OF CARTILAGE AND PERCENTAGE OF COLLAGEN WITHIN EACH REGION (REPRODUCED WITH PERMISSION FROM ORIGINAL PUBLISHER)[25]

TABLE 2.1: DESCRIPTION OF CARTILAGE STRUCTURAL ZONES[21]

Name	Collagen Fibers	Proteoglycans
Superficial zone	- Packed tightly, parallel to articular surface	Smallest concentration
Middle zone	- Organized randomly (appearing obliquely at times)	Medium concentration
Deep zone	- Perpendicular to articular surface	Highest concentration

As mentioned previously, the main components of the articular cartilage ECM are collagen and proteoglycan. Collagen makes up about 60% of the dry weight of the matrix and serves to provide shape and form to the tissue[21,24]. Of this collagen, 90-95% is Type II and forms fibers that intertwine with the proteoglycan aggregates[21]. Typically, this collagen contains hydroxylysine as well as large amounts of glycine and hydroxyproline[22]. Proteoglycan makes up 10-15% of the dry weight of the ECM, and consists of a protein core with chains of GAGs covalently attached[21,22]. The main type of GAG in cartilage is chondroitin-6-sulfate, but smaller amounts of keratan sulfate and chondroitin-4-sulfate are also present[22]. The biochemical composition of articular cartilage gives rise to its mechanical properties and allows the tissue to withstand and distribute the loads experienced by the knee joint. When compressed, the negatively charged proteoglycan molecules encased in and limited by the surrounding collagen framework are forced closer together, increasing the repulsion forces and therefore stiffness of the tissue[26]. This allows the tissue to support and distribute forces across the knee joint, thereby contributing to overall joint health and function[27]. By understanding the composition, organization, and function of cartilage, it is possible to more fully understand the effects and implications of diseases that affect it.

2.1.2. Meniscus composition and function

Another important soft tissue in the knee joint specifically is the meniscus. The meniscus consists of medial and lateral crescent shaped components with wedge-like cross sections that act to protect the underlying articular cartilage in the tibiofemoral joint (Figure 2.1)[28]. Each meniscus consists of two distinct regions, the outer or red-red zone (vascularized) and the inner or white-white zone (completely avascular)[28,29]. The cross-over section of the two zones is referred to as the white-red region (Figure 2.3)[28].

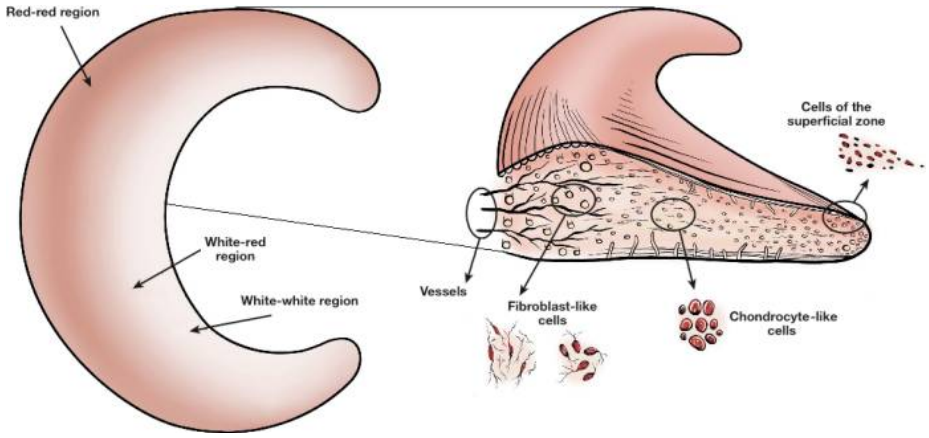

FIGURE 2.3FIGURE 2.4: DESCRIPTION OF VASCULARIZATION AND CELL POPULATION BY REGION IN THE MENISCUS (REPRODUCED WITH PERMISSION FROM ORIGINAL PUBLISHER) [28]

Peripheral connective tissue is responsible for attaching the meniscus to the joint capsule and also functions to give nutrients and oxygen to the red zone[30]. Because the capacity of the menisci to heal is directly related to circulation of blood, the white zone is vulnerable to tears caused by injury as well as degeneration[28]. The meniscus primarily consists of water (72%) with the remaining components being ECM and meniscus cells[28]. There are two types of cells in the meniscus, fibrochondrocytes and fibroblasts (Figure 2.3)[31,32]. The fibrochondrocytes are round or oval shaped cells located in the inner and middle areas of the meniscus, which appear chondrocytic but synthesize a fibrocartilage matrix rather than a hyaline cartilage matrix (as articular chondrocytes do)[30,31]. The fibroblasts are located in the outer one-third of the meniscus and are contained inside dense connective tissue[31,32]. The ECM consists mostly of collagen (75% of dry weight) but also contains GAGs (17% of dry weight) as well as small amounts of DNA, adhesion glycoproteins, and elastin[28,29]. The type of collagen present varies by location. In the red zone, it is predominantly type I collagen (80% of the dry weight) with trace amounts of type II, III, IV, and XVIII (<1%)[28]. In the white zone, collagen accounts for 70% of the dry weight with 60% of that being type II collagen and the remaining 40% being collagen type I[28]. In a normal adult human, the types of GAGs found in the meniscus are chondroitin-6-sulfate (40%), chondroitin-4-sulfate (10-20%), dermatan sulfate (20-30%), and keratin sulfate (15%)[28,29]. The meniscal horns (ends) and inner half of the menisci (the primary weight bearing areas) tend to have the highest concentrations of GAGs[29]. These

molecules enable the meniscus to absorb water, contributing to the viscoelastic compressive properties and supporting the tissue when it experiences compression[28,29].

The meniscus functions to increase the area over which forces are transmitted through the knee, stabilize the joint, and lubricate the underlying articular cartilage[28,29,33]. Structurally, the meniscus occupies 60% of the area of contact within the tibiofemoral joint and transmits over 50% of the compressive forces applied to the joint[34]. It's shape and attachments at the horns allow for vertical forces of compression to be converted into horizontal hoop stresses[28]. Collagen fibers arranged circumferentially within the menisci elongate as they are compressed to allow the structure to withstand the tension, effectively converting the load into tensile strain[35,36]. In order to avoid longitudinal splitting, the menisci are also equipped with radial fibers which act as ties[35]. The meniscus is compositionally similar to articular cartilage but organizationally distinct and plays an important role in the protection of articular cartilage and the health of the knee joint overall.

2.2. Osteoarthritis

OA is the most common type of arthritis and is a degenerative disease involving the whole synovial joint (including the cartilage, meniscus, tendons, ligaments, synovium, and bone). It can be either primary (idiopathic) or secondary (post-traumatic), and it is characterized by loss of cartilage, meniscal damage, bone alterations and overall joint modification[3–6,9]. Some effects of OA include joint pain, stiffness, focal areas of cartilage fibrillation or fissures, bone sclerosis (hardening), capsular fibrosis or inflammation (synovitis), effusion, and osteophyte formation (bony protrusions on the joint periphery)[4,10]. It has been shown that OA of the knee, hand, and hip all have similar prevalence's of around 20-30% of adults in various populations, with women being affected more frequently than men[37]. In Canada, 13% of the population (1 in 8 people) live with OA[7]. Some of the modifiable risk factors include obesity, abnormal joint loading, occupational factors, sports participation, muscle weakness, and nutritional factors[10,38]. Non-preventable risks to developing OA include genetics, ethnicity, age, and female sex[3,10].

2.2.1. Role of cartilage in osteoarthritis progression

Cartilage is one of the main soft tissues impacted by OA; displaying thinning and fibrillation as disease progresses, which may eventually lead to exposure of the underlying subchondral bone[5]. With disease, cartilage experiences an increase in water content and decrease in proteoglycan and collagen concentrations[39,40]. Lower cartilage volume has been associated with early OA[41] and early OA has been shown to negatively affect cartilage permeability and collagen network stiffness[42]. The study of cartilage is essential for further understanding OA because it is so heavily involved in the disease process.

2.2.2. Role of meniscus in osteoarthritis progression

The meniscus is another important soft tissue involved in OA disease progression. The meniscus can be involved in OA through two different pathways. Firstly, through primary OA, whereby the meniscus is damaged due to degeneration of the joint, likely resulting in meniscal tears (horizontal cleavages, flaps, complex tears, or maceration)[46]. And secondly, through secondary OA, where meniscal tears or extrusion (medial displacement of the meniscus from the central margin of the tibial plateau[47]) from trauma to the joint cause OA to develop and further trigger a loss in function of the meniscus[46,48]. One study found meniscal lesions in 70.7% of early OA knees[49], and another showed meniscus extrusion to be predictive of radiographic OA[50]. Similarly to cartilage, the meniscus also experiences degenerative matrix changes and loss in volume with OA[43–45]. Degeneration of the meniscus leads to increased water content and decreased proteoglycan and collagen concentrations within the tissue[51]. It is clear that the meniscus plays a key role in OA and is an important soft tissue to study.

2.2.3. Diagnosing osteoarthritis

Traditionally, OA has been assessed and diagnosed based on radiographs. This is the most accessible and common imaging modality for the evaluation of osteoarthritic joints [12,52]. These radiographs are used to analyze the formation of osteophytes and the degree of joint space narrowing, which is a decrease in the space between the bones and represents cartilage thinning as well as damage to and extrusion of the meniscus [12].

To apply these radiographs to OA diagnosis, several radiographic atlases have been developed [53]. The most commonly used system was developed by Kellgren and Lawrence (KL) [12,54]. This scale presents the following features to be evidence of OA: osteophyte formation, periarticular ossicles, joint space narrowing, pseudocystic areas within the subchondral bone, and a modification of the shape of bone ends [54]. The KL scale results in the assignment of a grade from 1-4 based on standard films for each of the grades for all eleven of the joints analyzed [54]. In all joints, a grade of 4 represents the most damage and cannot increase any further regardless of additional destruction to the structure [55]. According to the American College of Rheumatology, diagnosis of OA is a combination of radiographic as well as symptomatic OA [56,57]. The common symptoms contributing to a diagnosis of OA include joint pain and stiffness, decreased function, cracking or grinding noises accompanied by joint movement, and knob-like swelling at the affected joint [57]. In a study by Riddle *et al,* it was found that KL scores of 4 paired with severe symptoms and an age over 55 years most commonly led to the appropriate treatment of a patient by performing a total knee arthroplasty (TKA) [58]. TKA is the most common treatment of end-stage knee OA and is both cost-effective and successful in pain reduction for recipients [59]. In Canada, 98.8% of TKA patients from 2017-2018 had an underlying diagnosis of OA [60]. TKA patients are a useful group to study because they are a model of end-stage OA. Imaging techniques more specific to soft tissues (such as MRI) could potentially provide more information about the condition of the knee joint than traditional radiography is able to.

2.3. Quantitative Magnetization Transfer Magnetic Resonance Imaging

Magnetic resonance imaging (MRI) is a powerful tool because it provides superior soft tissue contrast and, therefore, is becoming increasingly popular as a non-invasive method for analyzing the joints of OA patients for research purposes. This section will provide a brief background on how MR imaging works as well as discussing more specific applications of MRI as related to this project.

2.3.1. Magnetic resonance imaging physics background

The use of MRI requires magnets, electronics, radiofrequency (RF) generators, coils, and gradients to allow for localization, excitation, and finally development of an image[61]. Patients lie in a bore surrounded by a magnet that generates a very strong, constant magnetic field (B_0) with strength being measured in units of Tesla (T) - one T is 20,000 times the strength of the earth's natural magnetic field[62,63]. Hydrogen atoms in the body are naturally dipolar and randomly oriented but when they are placed in a strong magnetic field, they will align with (parallel) or against (antiparallel) B_0 – a phenomena referred to as magnetization [63]. They will then move in a particular way called precession, which is similar to the way a spinning top wobbles in a cone shape[63]. The speed of this precession is named the Larmor frequency, and it is proportional to the magnetic field strength[63]. A series of magnetic oscillations can be created by the RF generators and transmitted to the body through gradient coils, disturbing the protons to fall out of their alignment with B_0. (Figure 2.5)[62,63]. This disturbance occurs when the RF pulse transfers energy to the protons, which can only occur if the RF pulse is the same as the Larmor frequency[63]. The hydrogen atoms will then align with the field generated by the RF pulses, which is known as B_1 (or excitation) [64]. When the RF pulse is turned off, the hydrogen atoms will return to their original alignment with B_0 (lowest energy state) by resonating and as the tipped magnetization passes the receiver coil during precession, a signal is induced in the coil which measures the energy required to return to equilibrium[62]. These signals then each make up a data point in k-space, which is an array of numbers that represents the spatial frequencies of MR images[65]. By using a Fourier transform, these frequencies can be converted into the final image (Figure 2.6)[65,66]. Understanding the basics of MR image generation is essential to the comprehension of other MR methods and protocols that can be used to recognize disease in tissues.

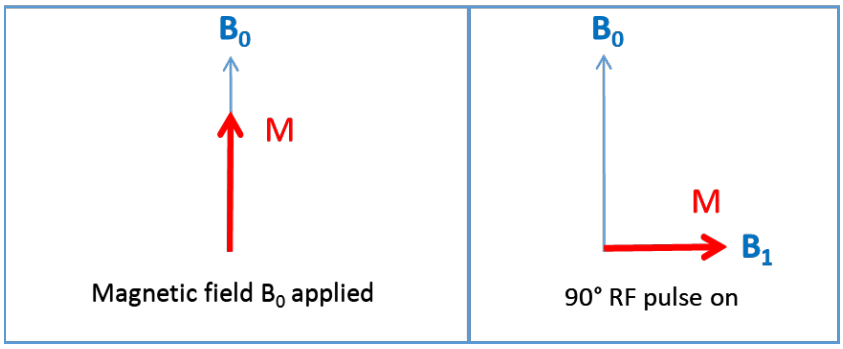

FIGURE 2.5: THE EFFECT OF A RADIOFREQUENCY PULSE ON NET MAGNETIZATION (M) DURING MAGNETIC RESONANCE IMAGE ACQUISITION

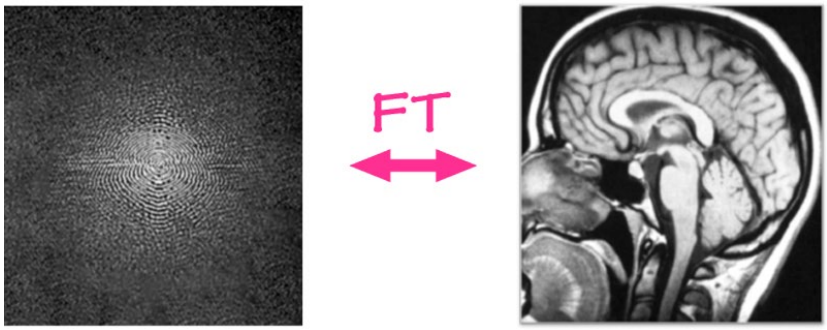

FIGURE 2.6: K-SPACE (LEFT) IS THE FOURIER TRANSFORM (FT) OF AN MR IMAGE (RIGHT). COURTESY OF ALLEN D. ELSTER, MRIQUESTIONS.COM

2.3.2. Quantitative magnetic resonance imaging

Quantitative magnetic resonance imaging (qMRI) involves the estimation of physical parameters of the tissue which have a particular unit and can be compared in differing subjects or regions [67]. Two of the most common qMRI parameters are T_1 and T_2 relaxation times; these parameters refer to the time required for the hydrogen atoms to return to equilibrium after the RF pulse is turned off (Figure 2.7). T_1 relaxation time is the longitudinal relaxation time and is the time required for the longitudinal signal to fully recover[61,64].

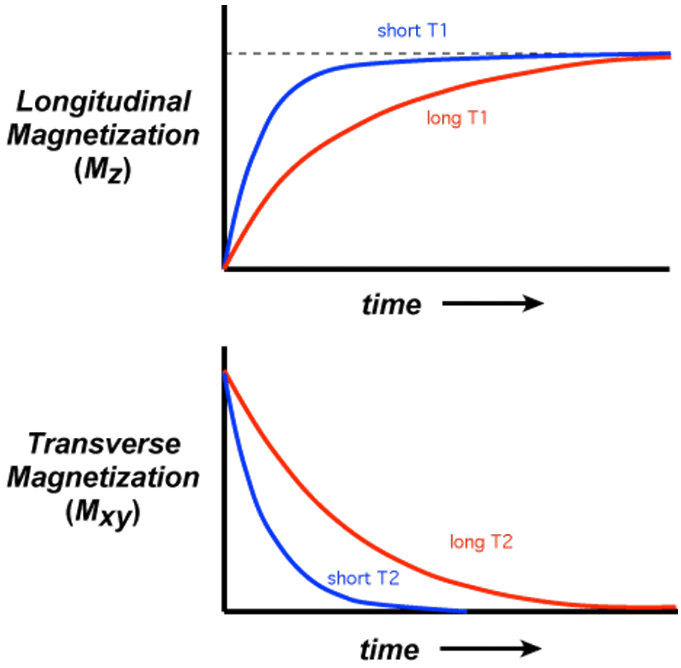

FIGURE 2.7: VISUALIZATION OF LONGITUDINAL (T_1) AND TRANSVERSE (T_2) RELAXATION TIMES. COURTESY OF ALLEN D. ELSTER, MRIQUESTIONS.COM

Another important qMRI measure is T_2 (Figure 2.7), which is the transverse relaxation time and occurs when protons lose phase coherence after the RF pulse is turned off; it occurs due to spin-spin interactions in the tissue, or in other words because of the interactions between the spinning nuclei and their local magnetic environment[63,68]. In humans, transverse relaxation occurs much faster than longitudinal relaxation; T_1 is about 5-10 times longer than T_2[63]. In articular cartilage, the T_2 relaxation value is associated with hydration of the tissue and collagen content and organization[69,70]. When there is degradation of the collagen matrix, water mobility increases which increases the T_2 relaxation time possibly due to the decrease in spin-spin interactions[16,69]. Several studies confirmed this, all showing an increase in the T_2 relaxation time in subjects with cartilage or meniscus damage or OA[13,15,16]. A similar parameter, called T_2* relaxation time, can also be measured. It is also the result of dephasing due to spin-spin interactions but also includes the dephasing of magnetization due to inhomogeneities in the local static magnetic field (B_0)[63]. This type of imaging has also been utilized to identify subclinical damage to the meniscus that shows as a change in the collagen structure[71]. Quantitative magnetic resonance imaging has proven to be a valuable imaging modality for differentiating

between healthy and OA tissue through examination of the transverse and longitudinal relaxation times of hydrogen atoms.

Another valuable qMRI metric is $T_{1\rho}$, which is the relaxation time caused by spin-lattice interactions (interactions with the surrounding external environment of the spins) in the rotating frame (reference frame rotating at the Larmor frequency)[16,66]. Mapping of $T_{1\rho}$ has shown to be sensitive to the content of proteoglycans in cartilage with one study finding an average of 71±4% GAG calculated from a $T_{1\rho}$ imaging method and 75±5% from a spectrophotometric assay in bovine patellar cartilage[72]. Other studies have demonstrated $T_{1\rho}$ to detect changes in proteoglycan, with one observing 33% greater $T_{1\rho}$ values in proteoglycan degraded bovine articular cartilage specimens as opposed to collagen-degraded or normal samples[73], and another finding $T_{1\rho}$ relaxation rate ($1/T_{1\rho}$) values to be 25% lower in porcine patellae cartilage injected with interleukin-1β (to induce cartilage matrix changes) than in the saline injected contralateral patellae[74]. Several studies found an increase in $T_{1\rho}$ times from healthy to OA patients in cartilage and meniscus, which is logical because this type of relaxation depends on interactions with and the transfer of energy to surrounding atoms (the "lattice") and so, if there are fewer atoms to transfer this energy to due to diminishing proteoglycans, it will take longer for the magnetization to fully recover[14–16].

2.3.3. Specifics of quantitative magnetization transfer

Another qMRI metric is quantitative magnetization transfer (qMT); it is the main focus of this thesis. Magnetization transfer (MT) is a form of contrast that allows for the indirect observation of hydrogen atoms with resonance too short to be captured with conventional MRI[17]. qMT uses a two-pool model where the hydrogen atoms are either in the mobile liquid state (free pool-H_f), or in the semisolid state attached to the macromolecules (restricted or bound pool-H_b)[75]. The macromolecular spins can be preferentially saturated by using an off-resonance RF pulse which is then transferred to the liquid spins (H_f) through proton exchange or magnetization exchange. This transfer results in a change in the magnetization in the free pool which can then be detected by conventional MRI sequences[76]. This phenomenon is illustrated in Figure 2.8 below. The

quantitative measures obtained from this technique are the bound pool fraction (f), the exchange rate of magnetization transfer between the free and the bound pools (k), the longitudinal and transverse relaxation times of the bound pool (T_{1b} and T_{2b}), and the longitudinal relaxation time of the free pool (T_{1f})[20,76]. A previous study by Stikov *et al* showed moderate correlations between f and proteoglycan content (r=0.58-0.85, p<0.05) as well as k and T_{1b} and collagen (r=0.39-0.41, p<0.05, and r=-0.54, p<0.05 respectively) in human knee cartilage[18]. Furthermore, Sritanyaratana *et al* found OA patients had significantly lower k and higher T_{2b} values than healthy individuals[19]. These findings support the potential of qMT MRI as a powerful tool for assessing cartilage and meniscus structure. Because qMT probes the bound hydrogen atoms, qMT can directly measure the properties of the macromolecules within a tissue. This is the key feature of the qMT technique that makes it particularly well suited to study OA. We know that OA progression is characterized by degeneration of the macromolecules (proteoglycan and collagen) and we know that qMT probes these macromolecules, thus we hypothesize that qMT may be more sensitive to OA changes than other qMRI techniques.

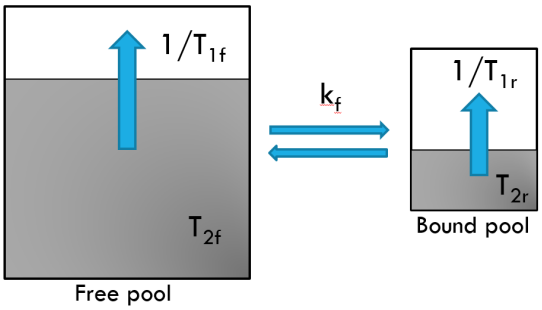

FIGURE 2.8: MAGNETIZATION TRANSFER BINARY SPIN BATH MODEL. MODIFIED FROM SIMARD AND HENKELMAN[20,76]

2.4. Mechanical Testing

Mechanical testing of cartilage and meniscus provides various properties representing the functional state of the tissue. Relevant material properties and testing methods will be discussed in this section.

2.4.1. Mechanical testing methods in cartilage and meniscus

Cartilage and meniscus is comprised of roughly 70-80% water (most of which can be exchanged with the outside medium, synovial fluid, through diffusion), while the remaining 20-30% is primarily the fixed proteoglycans and collagens[29,77]. In aqueous conditions, such as that of a tissue in the body, proteoglycans are polyanionic and will repel each other causing the aggregated proteoglycan molecules to take up more space in the tissue and press against the collagen framework[26]. When the tissue is compressed, the negatively charged sites are forced closer together, which increases their repulsion forces and creates compressive stiffness in the tissue[26]. Essentially, the macromolecules within the tissue are responsible for the mechanical integrity of the tissues. There are three methods used for the determination of the main material properties of cartilage and meniscus: the confined compression test, the unconfined compression test, and the indentation test. These tests are summarized in Table 2.2 below.

TABLE 2.2: DESCRIPTION OF THREE COMMONLY USED MECHANICAL PROPERTY TESTING METHODS

Method	Description	Properties Obtained
Confined Compression 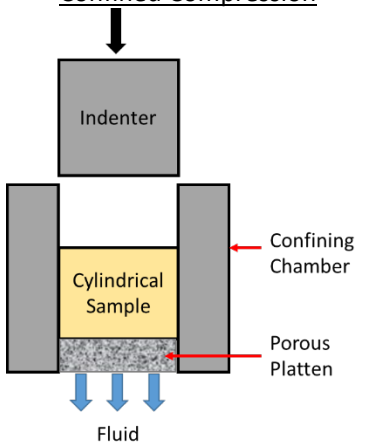	A small cylindrical sample of cartilage or meniscus tissue is taken from the joint and placed in a well with either a porous indenter or porous platen to allow for fluid flow, lateral expansion is prevented [25,26,78]	Young's modulus [79] Aggregate modulus [26] Permeability [26]
Unconfined Compression 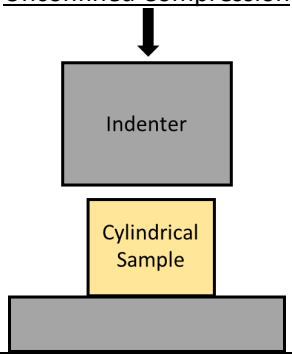	A cylindrical sample of cartilage or meniscus tissue is procured in the same manner as for confined compression and then the sample is squeezed between two impermeable smooth plates, lateral expansion is allowed [80–82]	Young's modulus [81] Poisson's ratio [81] Permeability [81]
Indentation Testing 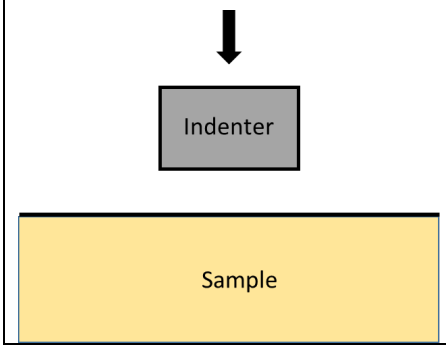	Cartilage on bone or dissected meniscus (no special preparation required) is compressed by a small, hemispherical, smooth and free-draining indenter [25,83]	Young's modulus [79] Aggregate modulus [26] Poisson's ratio [26] Permeability [26]

All three of these methods can test the creep or stress-relaxation behaviour of the tissue. In a creep test, a constant load is applied and the tissue displacement is measured over time, while in a stress-relaxation test, a constant displacement is applied while the resulting force is measured over time[26]. In the literature, indentation testing is the most commonly utilized method[77,81,84,85]. This method is much more appealing than

the others because it requires no special preparation of specimens and also the material properties are determined in a condition more closely associated with the physiological circumstance of the sample[81]. It is also interesting to note that one study found indentation tests to result in 30-79% higher values for Young's modulus as compared to unconfined compression testing[79]. Drawbacks of indentation testing are that it can be much more challenging and time consuming without the use of a specialized testing system. Although all three mechanical testing procedures are useful, indentation testing should be utilized when possible as it gives rise to all the important material properties and more closely resembles the physiological state of the tissue, and therefore is the most representative of the properties of the tissue inside the body.

2.4.2. Mechanical properties of cartilage and meniscus

Since cartilage and meniscus are predominantly loaded in compression, the compression test provides the most significant biomechanical properties. These include the aggregate modulus, Young's modulus, Poisson's ratio, and permeability. The aggregate modulus represents a measure of the stiffness of the tissue when all fluid flow has stopped and equilibrium is reached[26] . A higher value of this property means a tissue will deform less under a given load. The Young's modulus is similar to the aggregate modulus in that it is the proportionality constant between stress and strain in the linear elastic region, but it represents the stiffness of a linear elastic isotropic object[81]. Poisson's ratio is the ratio of the transverse to longitudinal strain[81]. This value is typically less than 0.4 in both cartilage and meniscus, showing both are somewhat compressible (incompressible = 0.5, highly compressible = 0)[26,81,86,87]. Lower Poisson's ratios mean that a material is less likely to laterally expand when a given load is vertically applied. Lastly, permeability is the resistance of fluid flow through the solid matrix in the tissue; the lower this value is, the more difficult it is to force fluid through the tissue (indicative of healthy tissue)[26,81]. These biomechanical properties can be used to understand the functional state of the tissue.

In order to extract these parameters from compression testing data, mathematical models are usually fit. Previous models presented in the literature have been based on the assumptions of articular cartilage behaving as elastic[88], viscoelastic[89], biphasic[90], and triphasic[91], with most considering the tissue to be homogeneous and

isotropic[79]. For indentation tests, the Hayes model is commonly utilized. This model considers the tissue to be an infinitely wide elastic layer which is bonded to a rigid half-space, requiring the thickness of the elastic layer (e.g. cartilage layer over the subchondral bone in the case of articular cartilage) for parameter extraction[88,92]. Permeability can be determined through curve fitting stress strain data obtained either in creep or relaxation tests using all three mechanical testing methods[81].

Alternatively to models, the aggregate modulus may also be calculated directly from the data of a confined compression test by dividing the load applied by the strain at equilibrium in the linear range of the stress-strain curve[81]. Similarly, Young's modulus can also be obtained from the linear stress-strain data of an unconfined compression test[79]. For measuring the Poisson's ratio, an optical method can alternatively be used, this involves the visual observation of lateral expansion at equilibrium in unconfined compression or indentation testing[79,81]. Korhonen *et al* compiled information of how to obtain each of these parameters from the various compression tests (Table 2.3)[79]. It is important to select an appropriate model or property extraction method based on the tissue type and the compression test carried out.

TABLE 2.3: DIRECT AND INDIRECT METHODS FOR OBTAINING YOUNG'S MODULUS, AGGREGATE MODULUS, AND POISSON'S RATION FROM UNCONFINED, CONFINED, AND INDENTATION COMPRESSION TESTS (REPRODUCED WITH PERMISSION FROM ORIGINAL PUBLISHER) [79]

	Direct	Indirect
Young's modulus	Unconfined	Confined: $E_S = \frac{(1+\nu_S)(1-2\nu_S)}{1-\nu_S} H_A$
		Indentation: $E_S = \frac{(1-\nu_S^2)\pi a}{2\kappa h} E$
Aggregate modulus	Confined	Unconfined: $H_A = \frac{1-\nu_S}{(1+\nu_S)(1-2\nu_S)} E_S$
		Indentation:[a] $H_A = \frac{1-\nu_S}{(1+\nu_S)(1-2\nu_S)} E_S$
Poisson's ratio	Optical	Unconfined vs. indentation: $\nu_S = \sqrt{1 - \frac{2\kappa h}{\pi a}\frac{E_S}{E}}$
		Unconfined vs. confined: $\nu_S = \frac{\frac{E_S}{H_A} - 1 + \sqrt{\left(\frac{E_S}{H_A} - 1\right)^2 - 8\left(\frac{E_S}{H_A} - 1\right)}}{4}$

[a] The Young's modulus (E_S) indicates the value from indentation test.
In the formulae above, a is the radius of the indenter, h the cartilage thickness, ν_S the Poisson's ratio (from optical measurement), E the slope of the equilibrium stress–strain curve in indentation geometry, κ the theoretical scaling factor (Hayes et al., 1972; Jurvelin et al., 1990), H_A the aggregate modulus (determined in confined compression) and E_S the Young's modulus (determined in unconfined compression), if not stated otherwise.

2.4.3. Changes of mechanical properties with osteoarthritis

In some cases, the mechanical properties can give insight into the condition of the cartilage. As OA disease progresses, proteoglycans are lost from the soft tissue decreasing its ability to resist loads[81]. Naturally, this causes a decrease in the stiffness of the tissue as indicated by decreasing aggregate and Young's moduli; in fact, there is a direct correlation between the aggregate modulus and proteoglycan content[25]. This was found to be experimentally true in both the meniscus and cartilage of osteoarthritis patients[84,93]. Damage to the tissue also results in degradation of the extracellular matrix, which leads to an increase in water in the tissue correlating with an increased permeability[25,26]. Evidence of this was shown in several studies by proof of increased tissue swelling accompanied by collagen degradation in osteoarthritic human cartilage and an increased fluid permeability in rabbit cartilage after experiencing blunt trauma (a single blow to the joint)[94–96]. The mechanical properties of a tissue sample are essential for understanding the condition of the cartilage and meniscus as well as the progression of OA disease.

2.5. Biochemical analysis of knee cartilage and meniscus

The strength of cartilage and meniscus tissues come from the macromolecules that comprise them, therefore, it is essential to the study of OA to be able to examine the characteristics of their composition, which can be accomplished through biochemical analysis. The two main macromolecules in cartilage and meniscus are proteoglycan and collagen. The composition and methods for quantifying these molecules will be discussed in this section.

2.5.1. Proteoglycan

The first essential biochemical assessment in cartilage and meniscus tissue analysis is the quantification of proteoglycans through the sulfated glycosaminoglycans (sGAG) within the tissues. Overall, GAGs are polymers with a negative charge that form chains of repeating disaccharides that can covalently attach to a core protein to form large complex proteoglycan molecules[25,97]. The most prevalent proteoglycan in cartilage as well as meniscus is aggrecan, which consists of chondroitin sulfate and keratin sulfate GAGs[25]. In cartilage, aggrecan

contains more chondroitin sulfate (~100 chains) than keratin sulfate (~60 chains) and, in meniscus, the GAG chains consist of 40% chondroitin-6-sulfate, 10-20% chondroitin-4-sulfate, 20-30% dermatan sulfate, and 15% keratin sulfate – all of which are sGAGs[29,98]. Another important (but non-sulfated) GAG is hyaluronan, or hyaluronic acid (HA), which functions to link the ECM to the chondrocytes in cartilage and interact with aggrecan to form immobilized macromolecular aggregates[25]. The disaccharide units and features of these GAGs are depicted in Figure 2.9 below. sGAGs are important because there are not any direct methods of measuring proteoglycans and so the sGAGs (which make up most of the GAGs and represent the majority of the proteoglycans) is quantified instead.

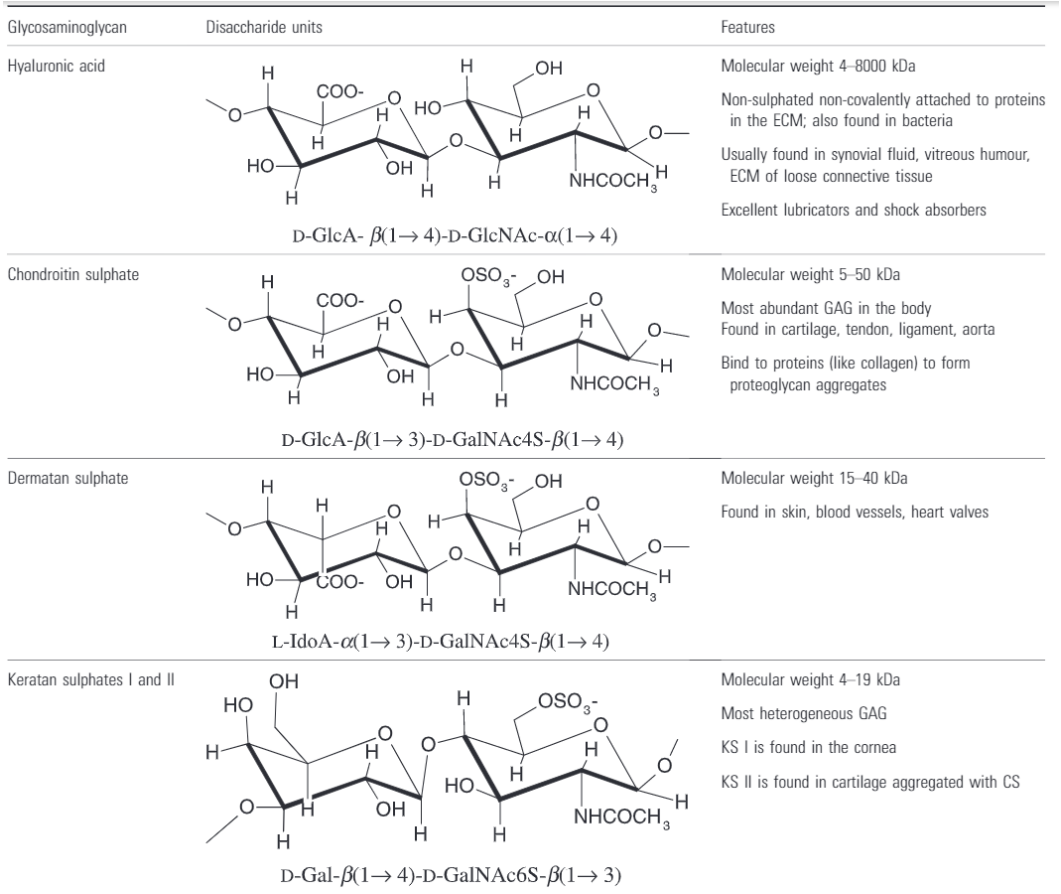

FIGURE 2.9: REPEATING DISACCHARIDE UNITS OF VARIOUS GLYCOSAMINOGLYCANS (REPRODUCED WITH PERMISSION FROM ORIGINAL PUBLISHER) [99]

In the literature, there are two main methods for quantifying these GAGs: the 1:9-dimethylmethylene blue (DMMB) assay, and the Alcian blue dot test. The DMMB dye was first described by Taylor and Jeffree in 1968 but the most commonly referenced DMMB procedure in the literature is the modification presented by Farndale, Buttle, and Barrett that allows for an improved specificity to sulfated GAGs[100,101]. This represents a faster and more convenient procedure that also eliminates any interference from other polyanions[101]. One potential drawback of this method is that the sample cannot be assayed directly, it first requires digestion with papain[98]. Over time there have been several modification to the overall procedure in order to accommodate slightly different circumstances, for instance Enobakhare *et al* adapted the Farndale method to be suitable for the measurement of GAGs in carboxylate alginate, and Carroll changed the assay slightly to be effective for synovial fluid[98,102]. Despite changes to the procedure, the commonality between all methods is that the DMMB color reagent is added to the GAG mixture and the absorbance is read using a spectrophotometer, the GAG content can then be determined from a standard curve[101].

The Alcian blue method was introduced in 1973 by Whiteman with the intention of precipitating urinary GAGs[103]. In this test, GAGs are complexed with Alcian blue to form a precipitate that elutes the dye which can then be measured colorimetrically to determine GAG quantity[104]. One major drawback of this method is that the resulting precipitate is very finely dispersed which makes it difficult to harvest without centrifugation[105]. Although the Alcian blue dot blot method was originally developed for urinary GAGs, it has also been applied to other biological fluids and therefore is still a useful procedure for quantifying GAGs in cartilage and meniscus samples[97].

One other method of importance in the quantification of GAGs using biochemical assessment is that of gel electrophoresis combined with toluidine blue staining. This technique is especially useful for identifying and quantifying any contaminants of other unimportant polysaccharides within GAG preparations[106]. It is highly sensitive and allows the detection of low levels of GAGs within tissue extracts but it is not typically used for the quantitative analysis of GAGs because the toluidine blue tends to react with other negatively charged

molecules that are unrelated[106,107]. For the quantification of GAGs in cartilage and meniscus, the DMMB method is the best choice because it has the fewest potential drawbacks and is also the most common in the literature and therefore should be used in order to compare results to previous work[16,74,108–110].

2.5.2. Collagen

In the biochemical assessment of cartilage and meniscus, it is also essential to quantify the collagen. This can be done by measuring the amount of hydroxyproline, which is the main amino acid that makes up collagen and is used as a measure of the prevalence of collagenous material within a tissue sample[111]. The structure of collagen fibers is shown in Figure 2.10.

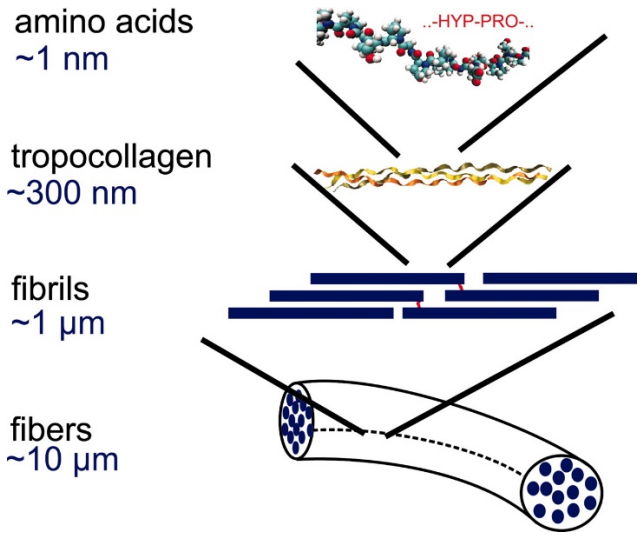

FIGURE 2.10: STRUCTURE OF COLLAGEN FIBERS UP TO NANOSCALE (AMINO ACIDS). HYP REPRESENTS HYDROXYPROLINE AND PRO PROLINE (IMAGE COPYRIGHT 2006 NATIONAL ACADEMY OF SCIENCES) [112]

In the literature, the most common method for the determination of hydroxyproline in a sample is by first oxidizing the hydroxyproline to a pyrrole related compound, then performing condensation of the intermediate by using a p-dimethylaminobenzaldehyde (pDAB) assay[113]. Neuman and Logan published a simple method utilizing the pDAB assay that allows for the amount of hydroxyproline to be determined from the optical density of the mixture related to a standard curve[114]. The oxidation step in this procedure results in a product that forms an intense red color when combined with pDAB[114]. The key distinguishing factor of the Neuman and

Logan method is that the oxidizer used is hydrogen peroxide[111]. The main issue with this method is that the results can be skewed by the interference of Tyrosine within the protein hydrolysates[114]. This was remedied by the introduction of an alternate system developed by Stegemann and Stalder that utilizes chloramine-T as the oxidation agent instead of hydrogen peroxide and shows little to no interference from related compounds, especially Tyrosine[115]. A direct comparison of the two different methods of oxidation showed lower percentages of hydroxyproline in protein using hydrogen peroxide as compared to the usage of chloramine-T[111]. Because of this, a chloramine-T oxidation method such as Stegemann and Stalder's should be used when determining the quantity of hydroxyproline in a tissue sample.

2.6. Histological analysis of cartilage and meniscus

Histology is an important component of OA disease assessment that allows tissues to be analyzed and compared using various staining techniques and scoring systems. Histology is the examination of normal cells using a microscope and it can be paired with histopathology, the examination of diseased cells and tissues, in order to determine the state of a specimen as compared to its normal, healthy form[116]. The method for preparing a histological sample is well established but the many variations in the stain used for the coloration step of the process are of interest for examining certain aspects of the sample[117].

2.6.1. Staining in histology

Staining of a histological sample is performed in order to identify specific components within a tissue, for example collagen, proteoglycans, or GAGs. The most commonly used stains for visualizing proteoglycans and GAGs are Hematoxylin and Eosin (H&E), Toluidine Blue, and Safranin O[116,118,119]. The gold standard is H&E, which results in a pinkish cartilage matrix with a blue aspect in the areas of high proteoglycan content (Figure 2.11A)[118,120]. Safranin O is a cationic dye with a staining intensity directly proportional to the amount of proteoglycan in normal cartilage[118,119]. It colors the cartilage matrix orange to red, the nuclei black, bone green, and the cytoplasm grey green (Figure 2.11B)[118,119,121]. In some instances of articular cartilage disease, the tissue degradation is supplemented with a change in the quantity or distribution of GAG[119]. Safranin O is therefore

used to demonstrate the changes that may be occurring in diseased cartilage. Unfortunately, where very low levels of GAG exist (for example in severely damaged tissue), the staining may not be detectable[119]. In situations of minimal GAG, monoclonal antibodies can be used as a more sensitive alternative to dyes[119]. These antibodies have a high affinity for specific epitopes to GAG, which allows for GAG molecules to be detected even at very low levels[119]. These antibodies can also amplify the staining reaction, which allows for the detection of proteoglycans within the diseased tissue where safranin O reactions appear negative[119]. Alternatively, another cationic dye stain Toluidine Blue can be used for the detection of proteoglycans and GAGs. Due to the fact that it has a higher affinity for the sulfur contained in the cartilage, it results in a more intense staining response as compared to safranin O[118,119]. It will stain the cartilage matrix and nuclei deep purple and the cytoplasm and other elements of the tissue shades of light blue[118,122]. With aid from the aforementioned staining techniques, the condition of proteoglycan and GAG structures within a tissue can be analyzed.

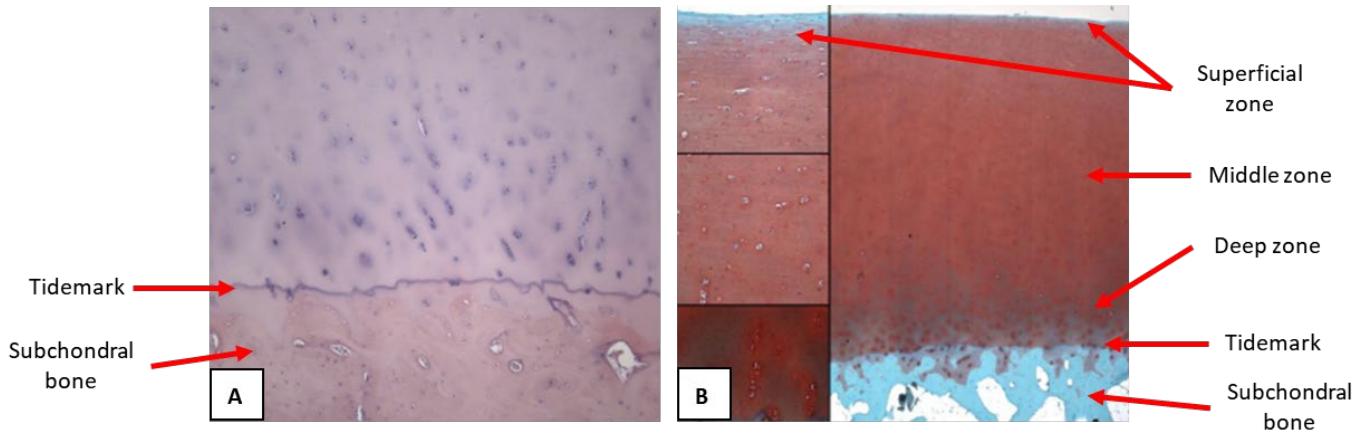

FIGURE 2.11: STAINING OF HUMAN KNEE ARTICULAR CARTILAGE WITH HEMATOXYLIN AND EOSIN (A) AND SAFRANIN O (B). MODIFIED FROM PAULI *ET AL*. REPRODCUED WITH PERMISSION FROM ORIGINAL PUBLISHER [123]

In order to gain a more comprehensive analysis of the level of degeneration in a tissue sample, it is also important to analyze the collagen within the tissue, which can be done using two different staining methods: Picrosirius Red (Figure 2.12) and Goldner's Trichrome (Figure 2.13). Samples stained using the Picrosirius Red method are observed using polarized light microscopy with the larger collagen fibers appearing bright yellow or orange and the thinner fibers showing as green [118,124]. A Trichrome stain will show a section with a nucleus

stained with hematoxylin and the cell cytoplasm and connective tissues stained with different colors [125]. More specifically, Goldner's Trichrome demonstrates the chondrocyte cytoplasm as red, the nucleus black, the collagen matrix green, and bone as well as calcified cartilage as green also [118] . Once the sample is stained, information can be attained about its level of degeneration and general condition.

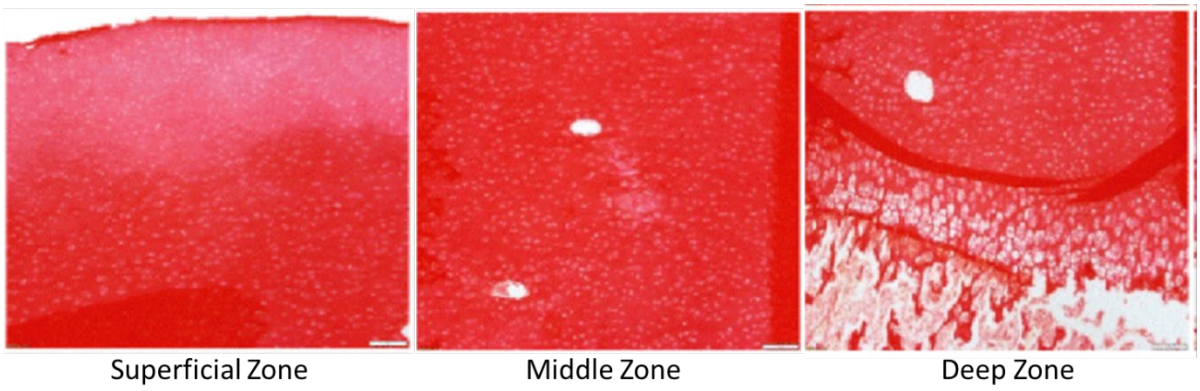

FIGURE 2.12: PICROSIRIUS RED STAINED PORCINE FEMEROPATELLAR ARTICULAR CARTILAGE. IMAGES FROM PUBLIC ACCESS ARTICLE[126]

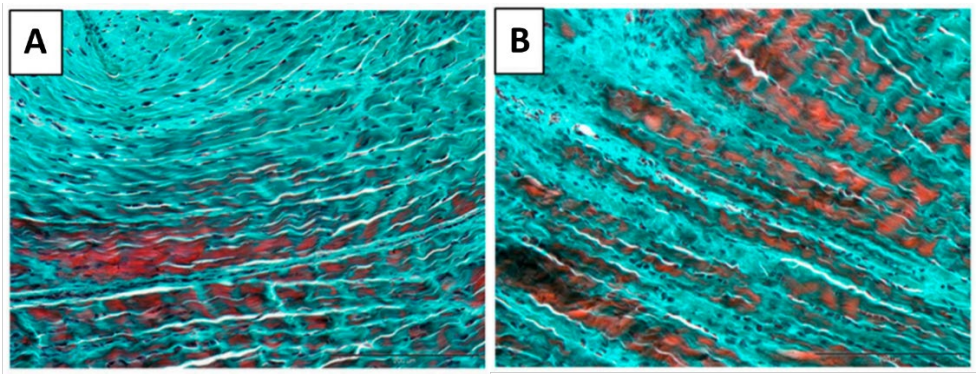

FIGURE 2.13: GOLDNER'S TRICHROME STAINED CANINE MENISCI (A SHOWS HEALTHY MENISCUS AND B COMPRESSED MENISCUS). IMAGES FROM PUBLIC ACCESS ARTICLE[127]

2.6.2. Histological scoring

Histological scoring is important for determining the current state of tissue degeneration in a way that makes it easy to compare different tissues damage based on their "score" or ordinal value. Historically, three systems have been used for scoring cartilage histology samples: the Collins macroscopic assessment grading system, the Mankin or Histologic Histochemical Grading System (HHGS), and the Osteoarthritis Research Society

International (OARSI) system[128,129]. The Collins system of 1949 was the first attempt to develop a cartilage scoring system with the Mankin method replacing it in 1971[129]. The OARSI system was then proposed in 2006 in order to address the pitfalls of both previous systems (Table 2.4)[128]. The OARSI system consists of a grade component reflecting the depth of lesions (Figure 2.14 and Figure 2.15) and a stage component representing the extent of disease across the tissue (percentage of surface involvement)[128].

TABLE 2.4: DESCRIPTION OF CARTILAGE SCORING SYSTEMS

Name	Basis	Score Value	Components	Drawbacks
Collins macroscopic assessment grading system[128]	Knee tissues removed at surgery or autopsy	I-IV	- Surface texture - Size of lesions - Any existing bony changes	- Arbitrary - Misrepresentation of fixed stages in disease
Mankin system[123,128,129]	Femoral heads removed at arthroplasty	0-14	- Cartilage structure - Cell distribution and density - Safranin O staining - Integrity of tidemark	- Not representative of early or mild cases of OA[130] - Lacks staging component [130] - No definition for how joint surface denuded of cartilage should be scored [131]
OARSI system[128]	Information not provided	0-24	- Grade (progression of OA into cartilage tissue) - Stage (horizontal extent of damage to the tissue)	- Subjective system with potential for inter-user differences

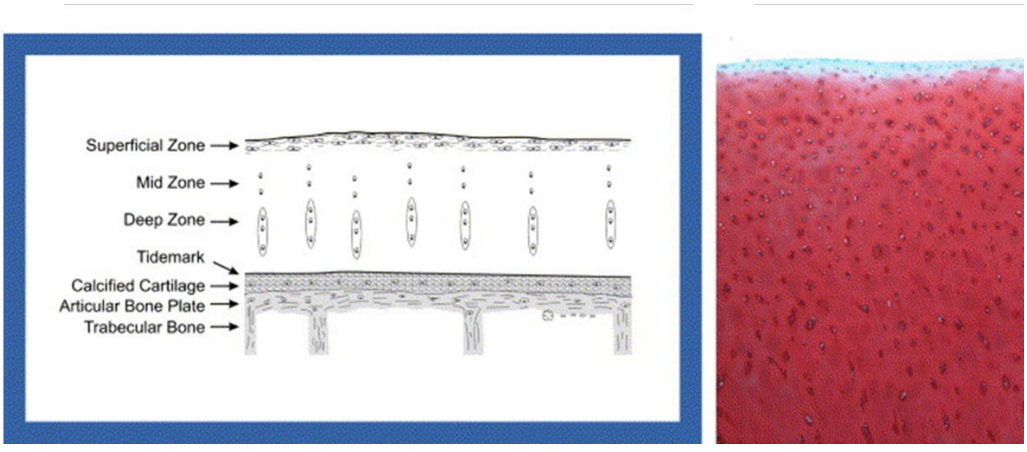

FIGURE 2.14: NORMAL ARTICULAR CARTILAGE (GRADE 0). SAFRANIN O STAINED 5X. REPRODUCED WITH PERMISSION FROM ORIGINAL PUBLISHER[128]

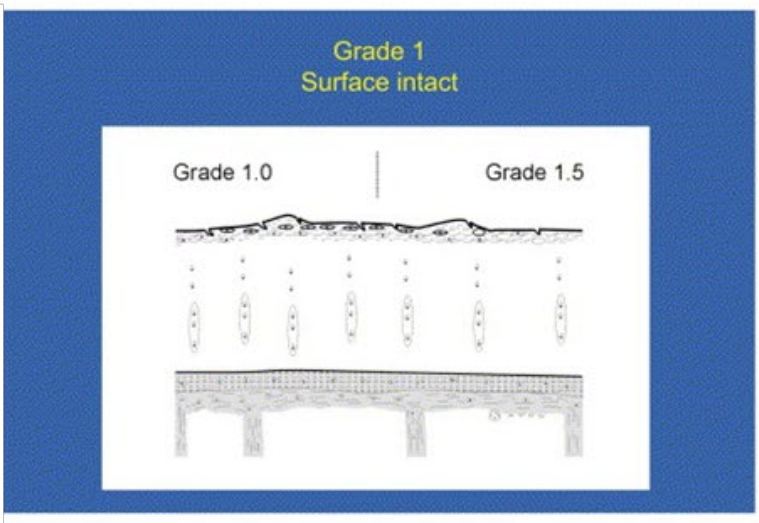
Grade 1
Surface intact
Grade 1.0
Grade 1.5

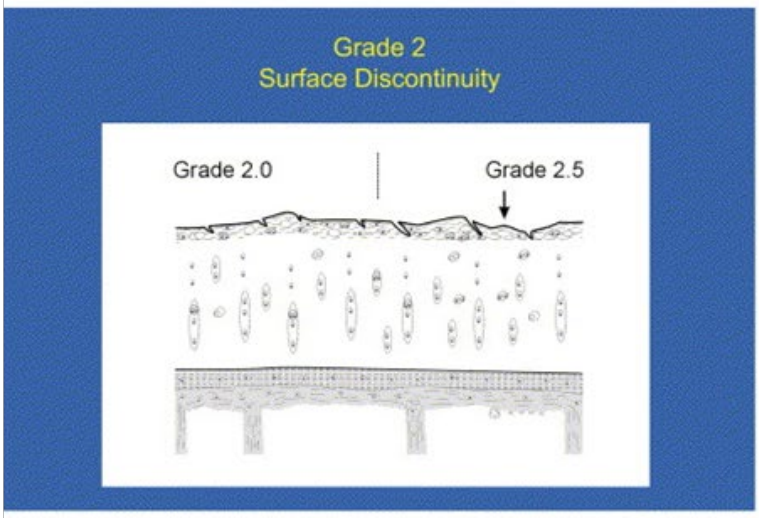
Grade 2
Surface Discontinuity
Grade 2.0
Grade 2.5

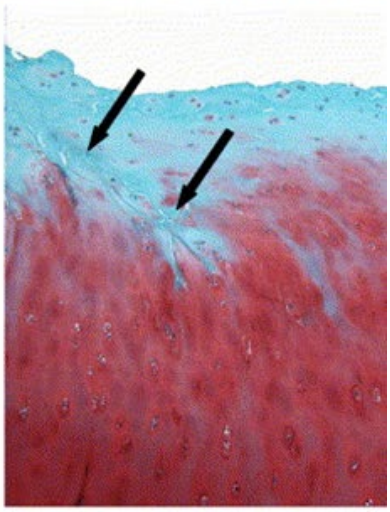

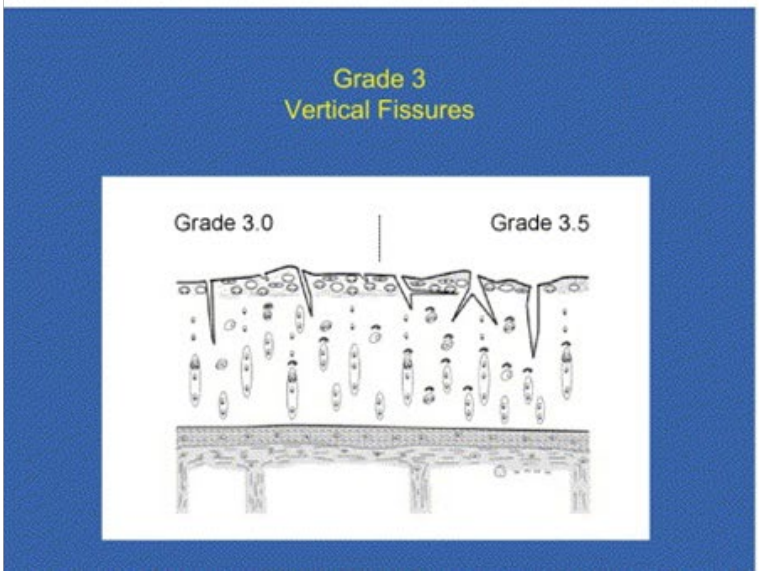
Grade 3
Vertical Fissures
Grade 3.0
Grade 3.5

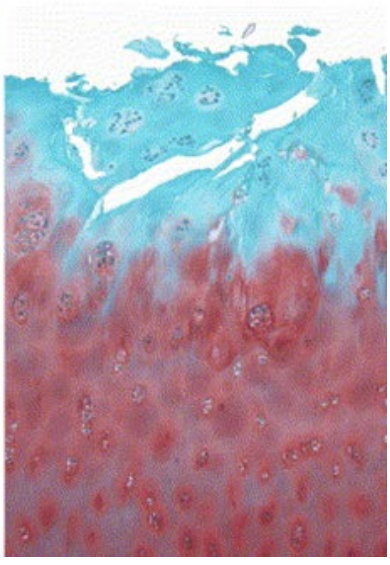

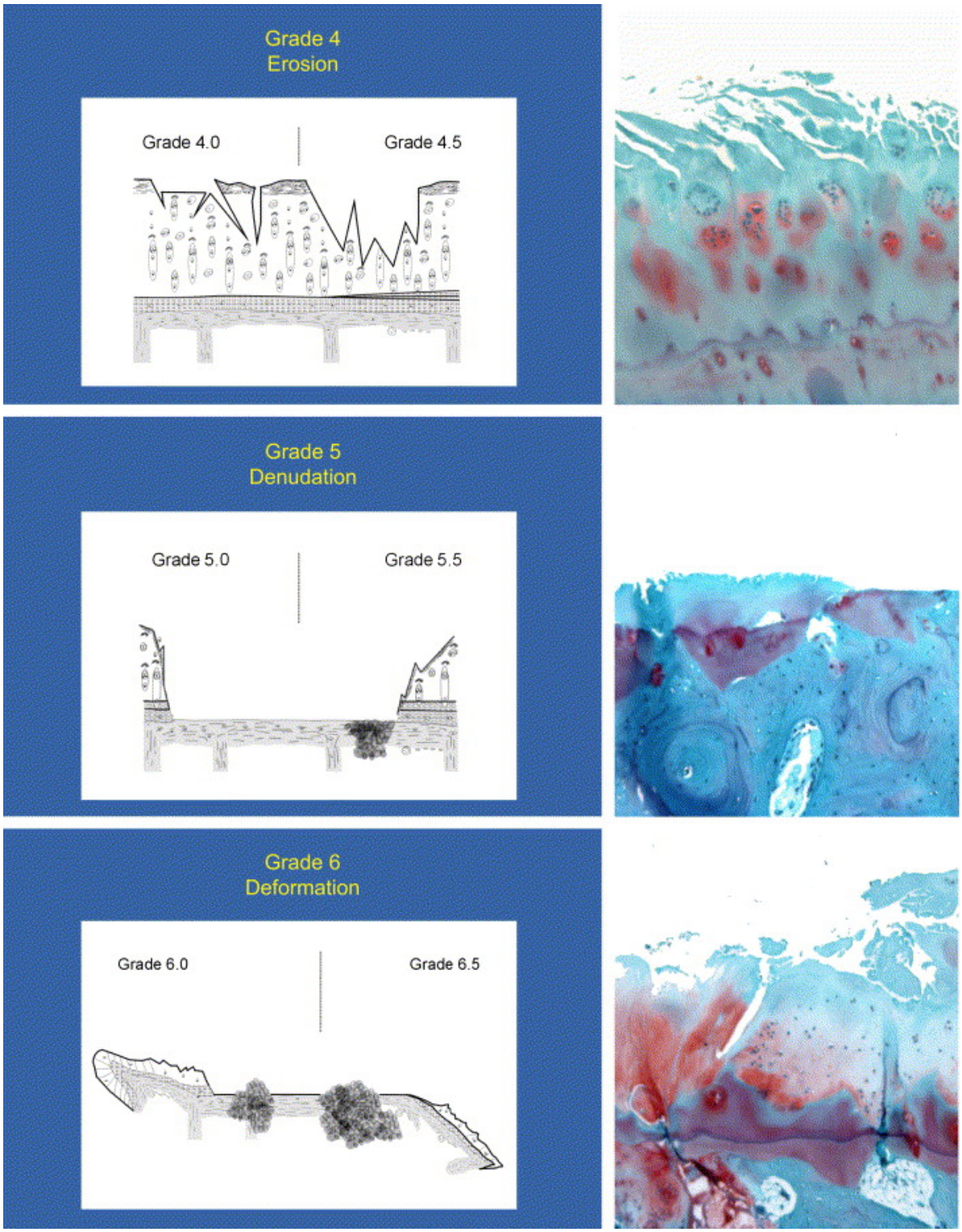

FIGURE 2.15: EXAMPLES OF OARSI GRADES 1-6. BRIEFLY, GRADE 1: SURFACE INTACT WITH SUPERFICIAL FIBRILLATION, GRADE 2: SURFACE DISCONTINUITY, FIBRILLATION EXTENDS FURTHER THROUGH THE SUPERFICIAL ZONE, GRADE 3: FISSURES EXTENDING TO MID ZONE, GRADE 4: EROSION, GRADE 5: DENUDATION, GRADE 6: DEFORMATION. SAFRANIN O STAINED, 5X. REPRODUCED WITH PERMISSION FROM ORIGINAL PUBLISHER[128]

From Table 2.4, it is clear that all three methods have similarities but that each consecutive system seeks to improve upon the major drawbacks of its predecessor. Many studies have sought to compare the Mankin and OARSI methods to determine which is superior. All studies find both to be highly reliable with reproducible results but frequently the OARSI method is preferred for being easier to use for inexperienced observers[123,130–133].

Histological scoring of meniscus samples is not as common but there have been some publications with methods for scoring certain meniscal features. Raunest *et al* developed a system based on the information presented about "interarticular cartilage" (the tissue category which meniscus falls under) in Bailey's Textbook of Histology[134,135]. This system labels samples as Stage 0 to Stage 3 with Stage 3 being the most severely degenerated and bases the assignment on the cellularity and matrix organization of the sample[134]. Other studies use a system with scores ranging from 0 to 6, which also focus on cellularity and matrix morphology as well as cell types and organization of the collagen[136,137]. Two more studies provide Grades between 0 and 3, again focusing mainly on changes to cell morphology and matrix organization, with one of them (Meister *et al*) also assessing the level of safranin O staining in order to attempt to quantify the proteoglycan content of the meniscus samples[138,139]. Despite all these methods, the most comprehensive meniscus histological scoring system to date was developed by Pauli *et al* in 2011[140]. This system utilizes four specific criteria associated with changes caused by age and disease: tissue surface condition on the femoral and tibial sides as well as the inner border (Figure 2.16), cellularity (Figure 2.17), matrix and collagen fiber organization (Figure 2.18), and safranin O staining intensity (Figure 2.19); resulting in a possible score of 0-18 which can be converted into a Grade of 1-4 with 4 being the most severely degenerated[140]. With this system, it is possible to reproducibly score meniscus histology samples and compare them with others to quantitatively assess the effects of aging and osteoarthritis.

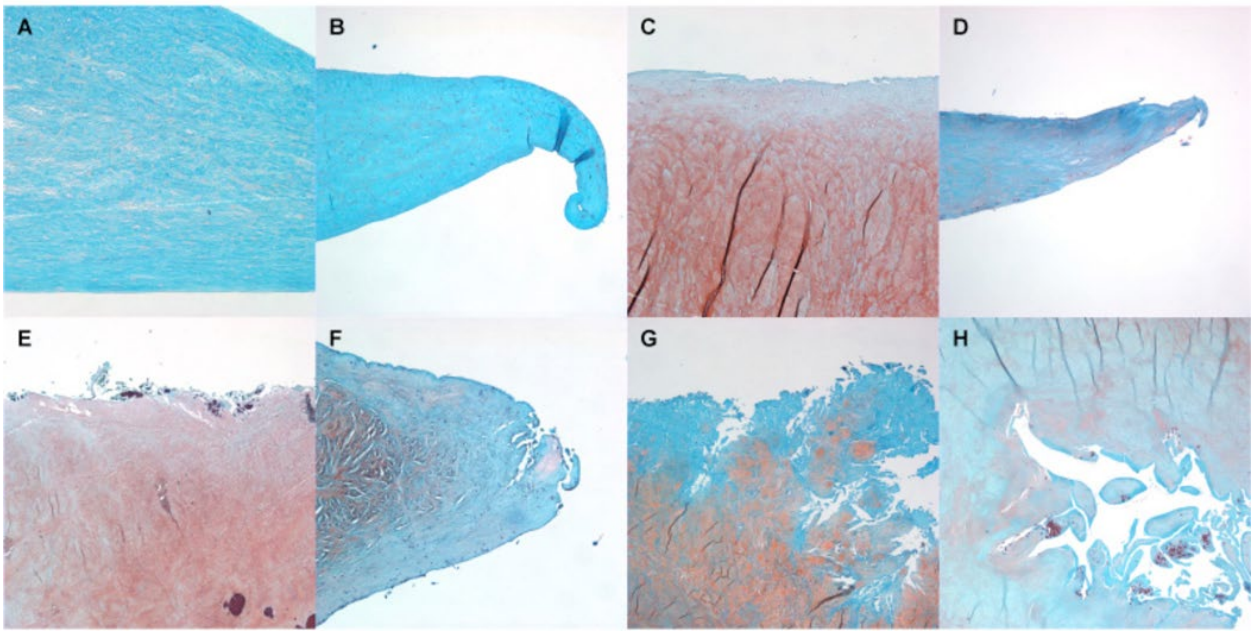

FIGURE 2.16: PAULI MENISCUS HISTOLOGY SCORING SYSTEM SURFACE INTEGRITY COMPONENT. (A,B) NORMAL MENISCUS - SCORE 0, (C,D) MILD CHANGES, SLIGHT FIBRILLATION - SCORE 1, (E,F) MODERATE FIBRILLATION AND SOME CLEFTS - SCORE 2, (G,H) SEVERE DAMAGE – SCORE 3. SAFRANIN O/FAST GREEN STAINED 4X. REPRODUCED WITH PERMISSION FROM ORIGINAL PUBLISHER[140]

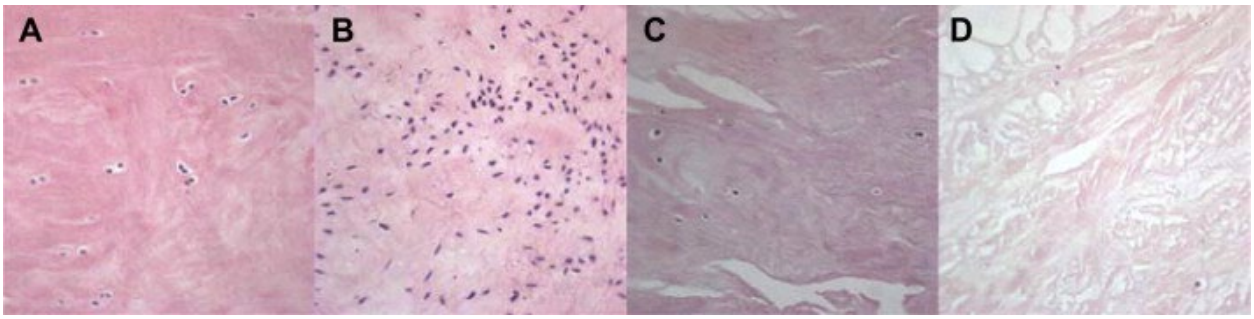

FIGURE 2.17: PAULI MENISCUS HISTOLOGY SCORING SYSTEM CELLULARITY COMPONENT. A) NORMAL CELLS – SCORE 0, B) DIFFUSE HYPERCELLULARITY – SCORE 1, C) HYPO- TO A-CELLULAR REGIONS – SCORE 2, D) HYPOCELLULARITY – SCORE 3. H&E 40X. REPRODUCED WITH PERMISSION FROM ORIGINAL PUBLISHER[140]

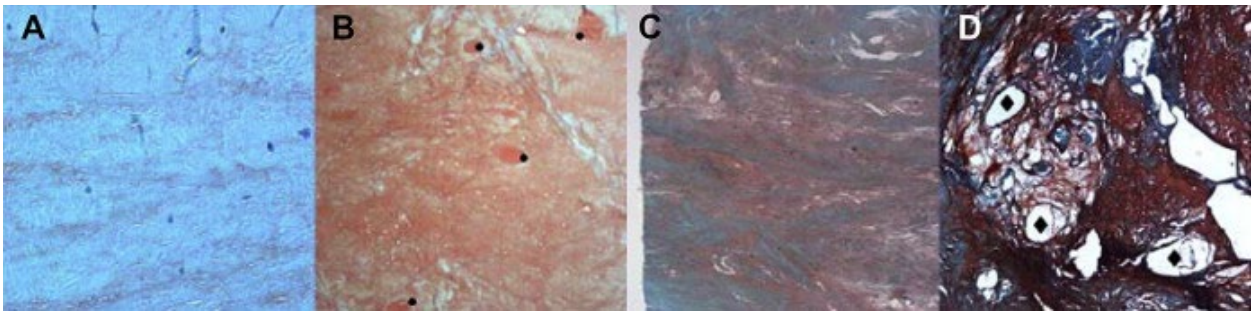

FIGURE 2.18: PAULI MENISCUS HISTOLOGY SCORING SYSTEM MATRIX AND COLLAGEN FIBER ORGANIZATION COMPONENT. A) NORMAL APPEARANCE – SCORE 0, B) DIFFUSE FOCI OF DEGENERATED EXTRACELLULAR MATRIX – SCORE 1, C) BANDS OR CONFLUENT FOCI OF DEGENERATED EXTRACELLULAR MATRIX, COLLAGEN FIBERS DISORGANIZED – SCORE 2, D) FIBROCARTILAGINOUS SEPARATION, UNORGANIZED COLLAGEN FIBERS – SCORE 3. SAFRANIN O/FAST GREEN 4X. REPRODUCED WITH PERMISSION FROM ORIGINAL PUBLISHER[140]

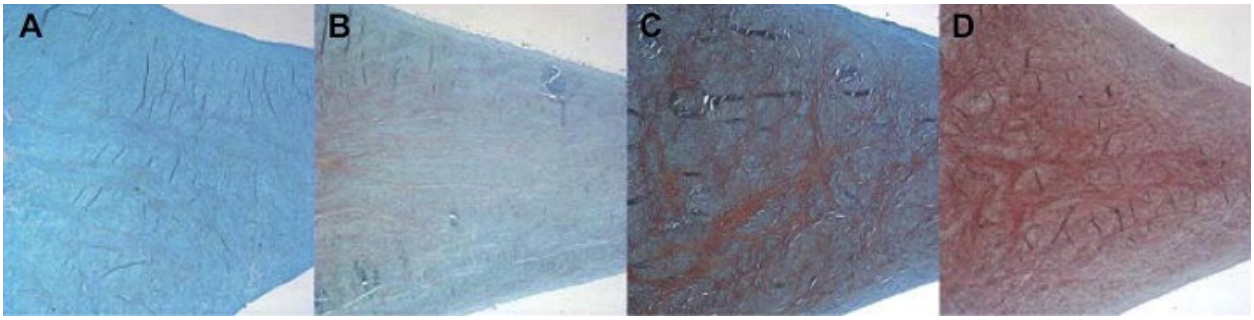

FIGURE 2.19: PAULI MENISCUS HISTOLOGY SCORING SYSTEM SAFRANIN O STAINING INTENSITY COMPONENT. A) NO STAIN – SCORE 0, B) SLIGHT INTENSITY – SCORE 1, C) MODERATE STAINING – SCORE 2, D) STRONG STAINING INTENSITY – SCORE 3. SAFRANIN O/FAST GREEN 4X. REPRODUCED WITH PERMISSION FROM ORIGINAL PUBLISHER[140]

2.7. Validation of qMRI metrics in the literature

As has been mentioned in other sections of this background, various studies have been conducted to validate qMRI metrics using mechanical (Table 2.5), biochemical (Table 2.6), and histological (Table 2.7) properties of the tissues as the reference standards. This section provides a summary of the literature on this topic. The following scheme was used to determine the strength of relationship based on the correlation coefficient: 0-0.19 = very weak, 0.2-0.39 = weak, 0.4-0.59 = moderate, 0.6-0.79 = strong, and 0.8-1 = very strong[141]. Only significant ($P<0.05$) correlations are discussed in this section, unless otherwise stated.

Several studies in the literature assessed and found correlations between the elastic, dynamic, and shear moduli and the qMRI parameters T_1, $T_{1\rho}$, and T_2 relaxation times (Table 2.5). T_1 relaxation time was found to decrease with an increase in elastic modulus ($r = -0.71$, $P<0.01$) and dynamic modulus ($r = -0.68$, $P<0.01$) in

tibial cartilage (both being strong correlations) [142] as well as decrease with increasing dynamic modulus (r = -0.24, P<0.05) at a weak correlation level in a combination of patellar, femoral, and tibial cartilage samples [143]. It was more common in the studies to compare tissue properties to $T_{1\rho}$ and T_2. In tibial cartilage, $T_{1\rho}$ was found to decrease with increasing elastic modulus at strong and very strong correlation levels, and $T_{1\rho}$ also decreased with increasing dynamic modulus at strong correlation levels [142]. In meniscus, weak correlations were found showing $T_{1\rho}$ to increase with decreasing elastic and shear modulus, and a moderate correlation showed $T_{1\rho}$ increased with decreasing dynamic modulus[16]. In the studies assessing T_2, the variable was often split into the T_2 relaxation time of the surface and that of the bulk sample. In patellar cartilage, weak to strong correlations were reported with T_2 and elastic and dynamic modulus in both the surface and bulk samples[143–145]. One study found a strong correlation between T_2 and elastic modulus in tibial cartilage[142] and in the meniscus, Son *et al* reported moderate correlations between T_2 and elastic, dynamic, and shear modulus[16]. Based on the results of these studies combined, there is clearly a relationship between the qMRI parameters and mechanical properties of both cartilage and meniscus. qMRI metrics more representative of the bound pool responsible for the mechanical strength of the tissue, such as the parameters obtained with qMT, could provide further and possibly stronger relationships to the mechanical properties.

TABLE 2.5: QMRI VALIDATION AGAINST TISSUE MECHANICAL PROPERTIES IN THE LITERATURE

Study	Tissue	Property	T_1	$T_{1\rho}$	T_2
Keenan *et al* 2015[108]	Human cadaveric patellae cartilage	Elastic Modulus		r = 0.16 healthy and r = 0.12 for all	r = -0.09 healthy and -0.09 for all
Kurkijarvi *et al* 2004[143]	Human cadaver (patella, femur, and tibia) cartilage	Elastic Modulus at Equilibrium	r = -0.12 to -0.55 (none significant)		T_2 bulk r = -0.27* for all regions and r = -0.76** for patella r = 0.21 to -0.43 (remaining) T_2 surface r = -0.01 to -0.51 (none significant)

Study	Tissue	Property	T_1	$T_{1\rho}$	T_2	
		Dynamic Modulus	r = -0.24* for all regions r = -0.22 to -0.60 (remaining)		T_2 bulk r = -0.59* for patella r = 0.02 to 0.48 (remaining) T_2 surface r = -0.11 to 0.44 (none significant)	
Lammentausta *et al* 2006[145]	Human cadaveric patellae cartilage				**1.5T**	**9.4T**
		Elastic Modulus			T_2 bulk Med r = -0.58** Lat r = -0.25 All r = -0.40** T_2 surface Med r = -0.69** Lat r = -0.44** All r = -0.55**	T_2 bulk Med r = -0.48** Lat r = -0.38* All r = -0.43** T_2 surface Med r = -0.39* Lat r = -0.34* All r = -0.37**
		Dynamic Modulus			T_2 bulk Med r = -0.59** Lat r = -0.33* All r = -0.45** T_2 surface Med r = -0.75** Lat r = -0.52** All r = -0.62**	T_2 bulk Med r = -0.50** Lat r = -0.41* All r = -0.45** T_2 surface Med r = -0.39* Lat r = -0.36* All r = -0.38**
Lammentausta *et al* 2007[144]	Human cadaveric patellae cartilage				**1.5T**	**9.4T**
		Elastic Modulus			T_2 bulk r = -0.40** T_2 surface r = -0.54**	None significant
		Dynamic Modulus			T_2 bulk r = -0.46** T_2 surface r = -0.62**	T_2 bulk r = -0.28* T_2 surface r = -0.24*
Rautiainen *et al* 2015[142]	Human cadaveric tibia cartilage	Elastic Modulus	r = -0.71**	r = -0.64* @ 1000HZ r = -0.81** @500Hz r = -0.80** @250Hz r = -0.67** @125Hz	r = -0.65*	

Study	Tissue	Property	T_1	$T_{1\rho}$	T_2
		Dynamic Modulus	r = -0.68**	r = -0.68** @ 1000HZ r = -0.76** @500Hz r = -0.72** @250Hz r = -0.62* @125Hz	r = -0.49
Son *et al* 2013[16]	Human TKA menisci	Elastic Modulus		ρ = -0.58**	ρ = -0.50**
		Dynamic Modulus		ρ = -0.62**	ρ = -0.57**
		Shear Modulus		ρ = -0.57**	ρ = -0.48**

r = Pearson correlation coefficient
ρ = Spearman correlation coefficient
* P < 0.05
** P < 0.01

In studies comparing qMRI parameters to the biochemical properties of cartilage and meniscus (Table 2.6), significant correlations were found between T_1, $T_{1\rho}$, and T_2 relaxation times and the contents of water, collagen, and proteoglycan (sometimes in the form of sGAGs or GAGs). In all the papers reviewed for this project, only two looked into the relationship between T_1 relaxation time and the biochemical tissue properties, and neither found any significant relationships[74,142]. Significant relationships were found between $T_{1\rho}$ and the proteoglycan content of bovine patellar cartilage through analysis of the coefficient of determination (R^2) in two studies[74,110]. Another significant moderate correlation was found between $T_{1\rho}$ and the GAG content in TKA patient cartilage[109]. In patellar cartilage, Keenan *et al* found weak correlations between sGAG content and $T_{1\rho}$ at a spin lock frequency of 500 Hz as well as T_2, but no significant correlations were observed between either parameter and the collagen content. This was a common trend, with none of the other cartilage studies finding any significant (or strong) correlations between any of the biochemistry properties and T_2 relaxation time[74,109,142]. qMT parameters, which are a direct measure of these macromolecules, could provide a greater quantity of

stronger correlations to the biochemistry properties of cartilage. In the single meniscus study included, weak and very weak correlations were found between sGAG content per wet mass and the $T_{1\rho}$ and T_2 relaxation times respectively[16]; this is not surprising given the low GAG content of the meniscus. This study also reported strong correlations between the collagen per wet mass and water content and the $T_{1\rho}$ and T_2 relaxation times as well as a moderate correlation between water content and T_2. Overall, there are a range of results in the literature with the correlations observed between qMRI parameters and the biochemical properties being generally weaker than correlations with the mechanical properties. These studies show potential in their relationships for the biochemical properties to be related to qMRI parameters. Perhaps qMT, which is more specific to the macromolecules of the tissue, will provide stronger correlations to biochemistry.

TABLE 2.6: QMRI VALIDATION AGAINST TISSUE BIOCHEMICAL PROPERTIES IN THE LITERATURE

Study	Tissue	Property	T_1	$T_{1\rho}$	T_2
Keenan *et al* 2015[108]	Human cadaveric patellae cartilage	sGAG/wet weight		<u>Healthy</u> r = 0.34* @ 500Hz r = 0.28 @ 1000Hz <u>All</u> r = 0.26* @ 500Hz r = 0.22 @ 1000Hz	Healthy: r = 0.31* All: r = 0.14
		Collagen/wet weight		<u>Healthy</u> r = 0.0 @ 500Hz r = -0.01 @ 1000Hz <u>All</u> r = 0.18 @ 500Hz r = -0.20 @ 1000Hz	Healthy: r = 0.07 All: r = 0.05
Rautiainen *et al* 2015[142]	Human cadaveric tibia cartilage	Water content	r = 0.45	r = 0.66 @ 1000Hz r = 0.60* @ 500Hz r = 0.59* @ 250Hz r = 0.48 @ 125Hz	r = 0.31
Li *et al* 2011[109]	Human TKA cartilage	GAG content		ρ = 0.45**	ρ = 0.24
		Collagen content		None significant	None significant
Akella *et al* 2001[110]	Bovine patellar cartilage	Proteoglycan content		R^2 = 0.987	

Study	Tissue	Property	T_1	$T_{1\rho}$	T_2
Wheaton *et al* 2005[74]	Bovine patellar cartilage	Proteoglycan content	None significant	$R^2 = 0.926$	None significant
Son *et al* 2013[16]	Human TKA menisci	sGAG/dry mass		ρ = -0.084	ρ = 0.096
		sGAG/wet mass		ρ = -0.37**	ρ = -0.16*
		Collagen/dry mass		ρ = -0.13	ρ = -0.27*
		Collagen/wet mass		ρ = -0.65**	ρ = -0.63**
		Water content		ρ = 0.65**	ρ = 0.55**

r = Pearson correlation coefficient
ρ = Spearman correlation coefficient
R^2 = regression analysis coefficient of determination
* $P < 0.05$
** $P < 0.01$

Four studies in the literature quantified relationships between the histology scores of cartilage and meniscus and their T_1, $T_{1\rho}$, and T_2 relaxation times, but only one found significant correlations (Table 2.7). When analyzing the Mankin histological score for cartilage, Li *et al* found no significant correlations with either $T_{1\rho}$ or T_2 relaxation times[109] while David-Vaudey *et al* found T_2 differences between the various Mankin grades to be significant except for grade 1 (healthy)[146]. In the study assessing OARSI cartilage histology score, strong correlations were found between OARSI score and $T_{1\rho}$ at spin lock frequencies 1000, 500, and 125 Hz and a very strong correlation was found at a frequency of 250 Hz[142]. A moderate correlation between OARSI score and T_2 was also reported[142]. Only one study was found to assess menisci histology using the scoring system developed by Pauli *et al* [140] and it actually looked into T_2*; no significant correlations were found. Based on the range of results in the existing literature, it is unclear if the histology score is correlated to qMRI parameters in

cartilage or meniscus. However, there are far less studies that quantify these relationships with histology than there are for the mechanical and biochemical properties, which provides motivation for continued work to more confidently determine if correlations exist.

TABLE 2.7: QMRI VALIDATION AGAINST HISTOLOGICAL SCORE IN THE LITERATURE

Study	Tissue	Property	T_1	$T_{1\rho}$	T_2	T_2*
Rautiainen *et al* 2015[142]	Human TKA cartilage	OARSI histology score[128]	r = 0.64*	r = 0.63* @ 1000Hz r = 0.78** @ 500Hz r = 0.80** @ 250Hz r = 0.68** @ 125Hz	r = 0.59*	
Li *et al* 2011[109]	Human TKA cartilage	Mankin histology score[129]		None significant	None significant	
David-Vaudey *et al* 2004[146]	Human cadaver and TKA cartilage	Mankin histology score[129]			T_2 differences between grades always significant (P=0.05) except for grade 1	
Williams *et al* 2012[71]	Human cadaver menisci	Pauli histology score[140]				Med ρ = 0.62 Lat ρ = 0.10

r = Pearson correlation coefficient
ρ = Spearman correlation coefficient
* P < 0.05
** P < 0.01

The main takeaway from the literature is that there is evidence of significant relationships between several of the tissue properties and the qMRI parameters of cartilage and meniscus. These include correlations between T_1 relaxation time and elastic modulus, dynamic modulus, and OARSI histology score; $T_{1\rho}$ relaxation time and elastic modulus, dynamic modulus, shear modulus, proteoglycan content, collagen content, water content, and OARSI histology score; and T_2 relaxation time and elastic modulus, dynamic modulus, shear modulus, proteoglycan content, collagen content, water content, OARSI, and Mankin histology score. The strength of

significant correlations observed across studies varies, but overall, the findings are promising and support the idea of qMRI parameters being representative of tissue structure and function.

2.7.1. Validation of qMT metrics in the literature

Far fewer studies have assessed the relationships between cartilage and meniscus tissue properties and the qMT parameters than the more typical qMRI metrics discussed above. In cartilage, only one study quantified qMT relationships, finding moderate correlations between bound pool fraction and proteoglycan content ($r=0.64$, $p<0.01$) and weak to moderate correlations between k and T_1 and collagen content ($r=0.37$, $p=0.06$ and $r=-0.493$, $p<0.05$ respectively)[18]. In the meniscus, one study quantified relationships between the qMT parameters and the mechanical properties and found a significant weak correlation between aggregate modulus and T_{2b} ($\rho=-0.336$, $p<0.01$)[141]. Further work must be done in both cartilage and meniscus to better understand the relationships between qMT parameters and the mechanical, biochemical, and histological properties of these tissues.

2.8. Gaps in the literature

Although some work has been done to study how articular cartilage and meniscus are affected by and change with OA, there are still major gaps in the literature that are important to fill for a more comprehensive understanding of the disease. One of these gaps is a study that investigates the relationship between the mechanical, biochemical, and histological properties of articular cartilage and meniscus and the qMT parameters of the tissues. Studies on the qMT properties of knee articular cartilage in general are limited, but those in existence have only looked into correlations between the biochemical content of the tissue and the qMT parameters in three tibial and one patellar cadaver knee specimens[18] or the difference in qMT parameters in healthy and OA patellar cartilage[19]; none have assessed the histological state or the mechanical properties. Alternatively, in the meniscus only the mechanical properties have been compared to qMT, and not the biochemical or histological properties[141]. As has been outlined throughout the background, all three of these categories of tissue properties provide valuable information and unique insights into the condition of the

tissue. Combining all three types of properties would give a more complete picture of the structure and function of the tissue. *The TKA and cadaver meniscus studies in this project will contribute valuable information to the field by providing more data on qMT properties in both cartilage and meniscus as well as assessing correlations between these parameters and the mechanical, biochemical, and histological properties of the tissues*.

Another major gap this project will fill has been touched on previously; the fact that there currently only exists two studies on qMT in the meniscus[20,141]. The meniscus is an important tissue for knee function and so the ability to observe the changes it undergoes during OA is key to understanding the disease process. qMT is an excellent option for doing this because it is non-invasive – allowing many populations to be studied (healthy and diseased) – and it is predicted to be more sensitive than traditional MRI to the macromolecules that make up meniscus and hence are affected by OA. *In this project, both healthy (cadaver) and diseased (TKA) populations are being studied which will not only contribute to the minimal literature on qMT in the meniscus but will also provide valuable comparisons between qMT parameters in healthy and more diseased menisci*.

The last main literature gap this research will fill is the comparison of *in vivo* (within living human subjects) to *ex situ* (removed from the body) qMT parameters in both knee articular cartilage and meniscus. Currently, in the literature, there exists a comparison between the *in situ* (within cadaver human subjects) and *ex situ* qMT parameters in the meniscus only[20]. This study found changes in the qMT parameters from *in situ* to *ex situ*, which proves the importance of more research being done to determine and perhaps quantify the effects of different environments on the qMT parameters. *This study will contribute to the understanding of the change in qMT parameters from in vivo to ex situ conditions*.

In summary, this project seeks to contribute to the field of OA research ***by validating qMT MRI as a non-invasive method of assessing the structure and function of cartilage and meniscus in the knee***. Potential uses of this could be in early diagnosis of OA, monitoring of disease progression, and studying the efficacy of proposed treatments. As OA continues to impact individuals worldwide, it is important for researchers to focus

their efforts on identifying OA early on and having objective tools for testing treatments that aim to slow down or stop the disease altogether.

3. General Methodology

For both the cadaver and TKA studies, similar methodologies were used; this chapter describes the general project methodology. The topics covered in this section include qMT image acquisition, image processing, biochemical content analysis, and histology.

3.1. qMT image acquisition

For both the TKA and cadaver studies, scanning took place at 3T (MAGNETOM Skyra, Siemens, Erlangen, Germany) using an in-house spoiled gradient recalled echo (SPGR) sequence developed by Lumeng Cui with pulsed off-resonance saturation for MT contrast and an 18-channel flexible receive coil. The protocol included 10 MT-SPGR scans (five offset frequencies: 433, 1087, 2732, 6862, 17235 Hz, at two flip angles: 142˚ and 426˚). Two of the parameters selected for these scans differed slightly between studies (Table 3.1), although these differences resulted in minor impacts on the outputs. The changes were made in order to minimize the scan time for the *in vivo* study. In the cadaver study, three scans were performed without an MT pulse to monitor drift from potential scanner heating at the beginning, middle, and end of the sequence. Upon analysis of these results, no evidence of scanner heating was observed, so only one MT disabled scan was required as a reference for the TKA study and it was acquired at the midway point of the experiment. Further details about the qMT scanning protocol can be found in Appendix A: qMT scanning protocols.

TABLE 3.1: SCANNING PARAMETERS FOR THE CADAVER AND TKA STUDIES

Parameter	Cadaver Study	TKA Study
Field of view (FOV)	160 x 160 mm^2	160 x 160 mm^2
TR/TE	48/3	26/3
Matrix size	256 x 256	256 x 256
Slice thickness	3 mm	3 mm
Constant flip angle (α)	10°	13°

T_1 relaxation maps, obtained with driven equilibrium single pulse observation of T_1 (DESPOT1)[147], were acquired for qMT-modeling. Four scans were acquired at constant flip angles (α= 5˚, 10˚, 20˚, and 30˚) using a

spoiled gradient recalled echo (SPGR) sequence with FOV = 160 x 160 mm^2, TR/TE = 26/3.22 ms, 256 x 256 matrix, and 3 mm slice thickness.

It was also necessary to obtain B_1 maps in order to correct for any field inhomogeneities that may impact the qMT parameter fitting, these were acquired using a standard double angle technique[148]. Parameters for these scans were constant flip angles α = 60 and 120˚, FOV = 160 x 160 mm^2, TR/TE = 6000/3.58 ms, 256 x 256 matrix, and 3 mm slice thickness. Details of the scanning protocols for these sequences can also be found in Appendix A: qMT scanning protocols. B_0 correction was not performed because of the small variation in B_0 across the tissue.

3.2. Image processing

This section describes the process of obtaining the qMT parameters of interest from the MR images collected. The steps involved were image segmentation to obtain binary masks of the tissue, determination of the qMT parameters across the entire tissue, and finally model registration to find the qMT parameters at specific locations.

3.2.1. Image segmentation for binary masks

In order to obtain the qMT parameters of the soft tissue from the MR images of the knee, it was first necessary to locate the articular cartilage and menisci in each slice of the scan data. For this, a packaged image processing software (Analyze 14.0, Mayo Clinic, Rochester, USA) was utilized to manually create binary masks of the cartilage (Figure 3.1A) and meniscus (Figure 3.2A) (independently) by selecting each pixel containing the targeted tissue in every slice. It was also necessary for the registration process to obtain a mask of just the top surface of the tissues (Figure 3.1B and Figure 3.2B).

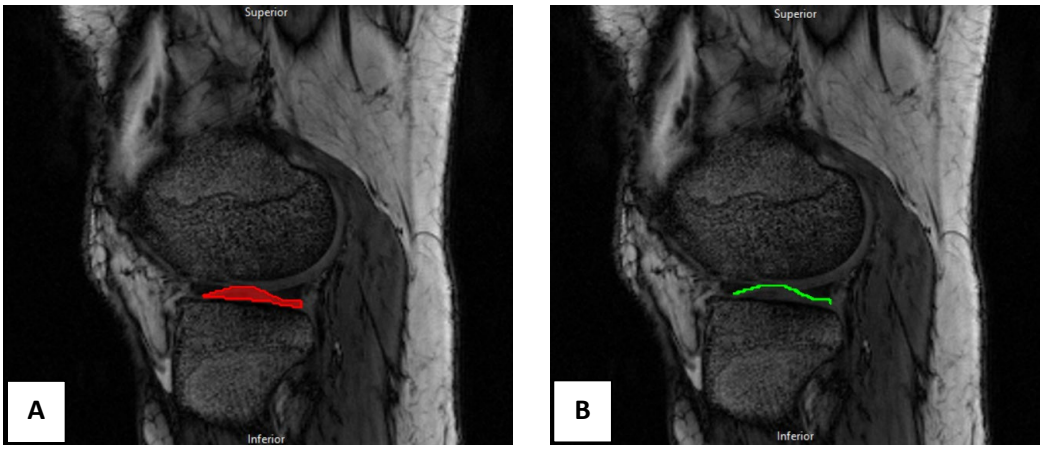

FIGURE 3.1: A) BINARY MASK OF CARTILAGE CREATED USING ANALYZE 14.0 OVERLAID ONTO THE CORRESPONDING MR IMAGE SLICE. B) BINARY MASK OF JUST THE TOP SURFACE OF THE CARTILAGE FOR THE SAME SLICE.

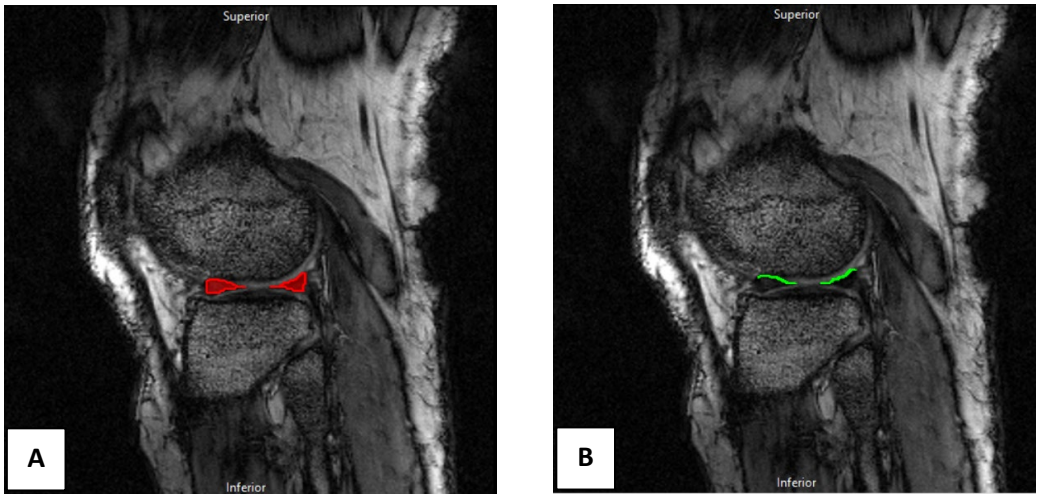

FIGURE 3.2: A) BINARY MASK OF MENISCUS CREATED USING ANALYZE 14.0 OVERLAID ONTO THE CORRESPONDING MR IMAGE SLICE. B) BINARY MASK OF JUST THE TOP SURFACE OF THE MENISCUS FOR THE SAME SLICE.

3.2.2. Determining qMT parameters from MRI data

In order to extract the qMT parameters of interest from the acquired MRI scans, the following steps were carried out. First, T_1 was determined with the DESPOT1 technique[147] by using multiple flip angles and constant TR from a series of SPGR images. The following signal model was fit:

$$\frac{SI_{SPGR}}{\sin\alpha} = \frac{SI_{SPGR}}{\tan\alpha}E_1 + M_{leq}(1 - E_1)$$

$$E_1 = \exp\left(-\frac{TR}{T_1}\right)$$

Where SI_{SPGR} = signal intensity, α = flip angle, and M_{leq} = a factor that is proportional to the equilibrium T_1. When $SI_{SPGR}/\sin\alpha$ is plotted versus $SI_{SPGR}/\tan\alpha$, T_1 can be calculated from the slope of the line:

$$T_1 = \frac{TR}{\ln(slope)}$$

Next, qMT parameter maps of the T_{1f}, T_{2f}, T_{2b}, k, and f were modeled by fitting the ten MT contrast images to the following Gaussian line shape [20,149] (Figure 3.3):

$$R = \omega^2 \sqrt{\frac{\pi}{2}} T_{2b} \left(e^{\frac{(-2\pi \Delta f T_{2b})^2}{2}} \right)$$

Where R = magnetization loss rate, ω = MT flip angle, and Δf = offset frequency. A Gaussian lineshape was chosen for this data because it has been shown to result in better fits (improvement of 30% in residual sum of squares as compared to a Super-Lorentzian lineshape) [149]. It was also assumed that T_{1b} = 1s to improve fitting, this has been shown to have negligible effects on the modeling [75]. The qMT parameters were then obtained by fitting the data to the two pool model[20] with in-house functions developed by Lumeng Cui (Matlab, MathWorks, Natick, MA, USA).

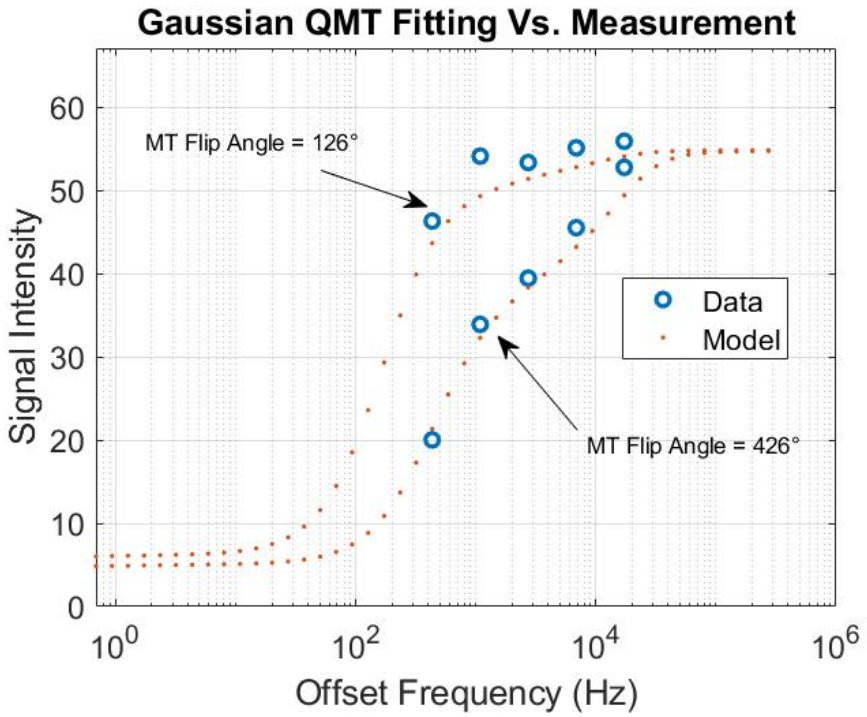

FIGURE 3.3: GAUSSIAN LINESHAPE FIT FOR *IN VIVO* CARTILAGE. THE UPPER DATA HAS MT FLIP ANGLE = 126°, AND LOWER DATA HAS MT FLIP ANGLE = 426°

For the correction of B_1 field inhomogeneities, a standard double angle technique was implemented to generate an adjustment factor which was applied to each individual voxel [148]. From these combined steps, the qMT parameters at any location in the Analyze segmented tissue mask could be determined.

3.2.3. Model registration

The registration component was necessary in order to determine the location of the samples with respect to the cartilage and meniscus MRI segmentation, and therefore qMT data. This required 3D models of the mechanical testing and MRI surfaces, segmentation masks, and 3D cylinders representing the sample locations, which were already created by another M.Sc. student in our group (Brennan Berryman) for the cadaver study and were created by me for the TKA study (explanation located in section 5.2.7). Registration was then accomplished using a custom MATLAB code developed by Brennan Berryman but with modifications for the specific data. This code first registered the mechanical testing surface model and the tissue sample (cylinder or block) model to the MRI surface model using an Iterative Closest Points function which translated and

rotated the mechanical surface and tissue sample models to be in line with the MRI surface model (MATLAB, MathWorks, Natick, MA, USA) (Figure 3.4A). This transformed cylinder model was then further transformed to the MRI tissue model space (not the MRI surface extracted from Analyze but the masks representative of the specific tissue locations on each slice of the MR images) via homogeneous transformation matrix (Figure 3.4B). From this, the overlap of the sample and the full MRI mask was known (Figure 3.5) and the average of each qMT parameter within the overlapping region was calculated.

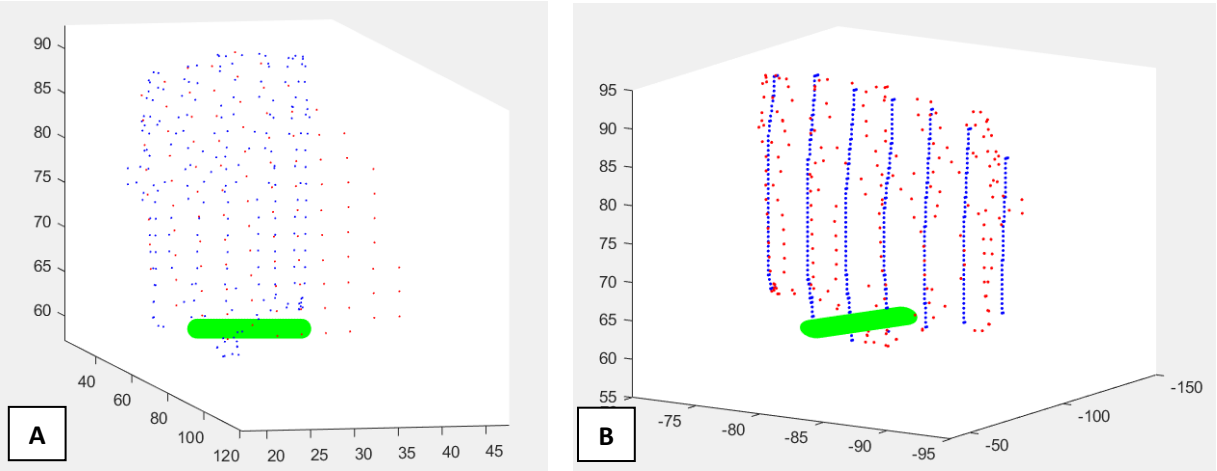

FIGURE 3.4: MATLAB REGISTRATION FIGURES. A) MACH-1 SURFACE AND SAMPLE CYLINDER REGISTERED TO ANALYZE SURFACE B) TRANSFORMED CYLINDER REGISTERED TO THE MRI MASK

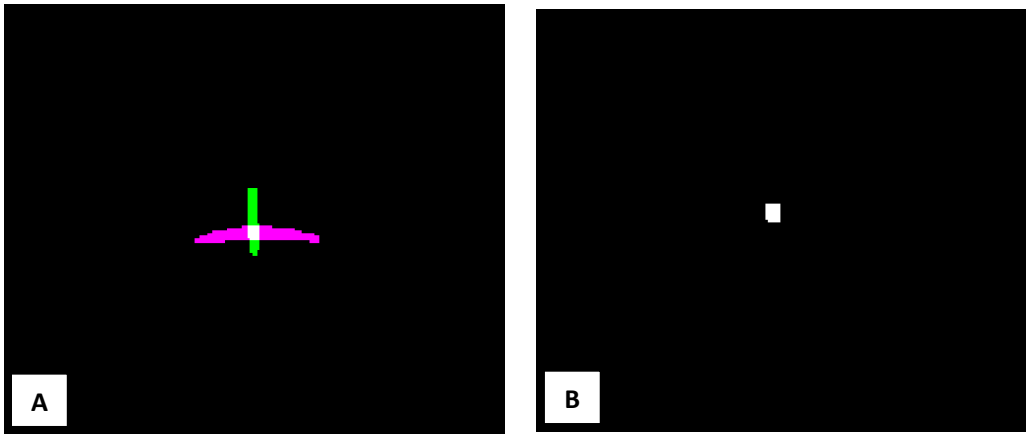

FIGURE 3.5: A) SINGLE SLICE SHOWING THE CARTILAGE MASK OVERLAPPED WITH THE CYLINDER B) REGION OF OVERLAP BETWEEN THE CARTILAGE AND CYLINDER

3.3. Biochemical content analysis

Proteoglycan and collagen content were quantified using sulfated GAG and hydroxyproline assays, respectively. This section discusses these procedures in greater detail.

3.3.1. Proteinase K digestion

Prior to performing the assays, all samples were weighed then vacuum dried (CentriVap Concentrator, Labconco, Kansas City, MO, USA) and weighed again for calculating water content. In order to prepare the samples to be assayed, dried solid samples were digested into a liquid using specific dilutions of a 10 mg/mL proteinase K stock solution made with a 0.1 M ammonium acetate solution. Dilutions were determined by assuming 1 mg of proteinase K would digest 80 mg of cartilage and 20 mg of meniscus; the dry weight of the largest sample in an assay run was used for this calculation. Samples were placed in a water bath at 60 ˚C overnight and then heated at 100˚C for five minutes to deactivate the remaining proteinase K. After this, samples were frozen until the assays were able to be performed.

3.3.2. Quantification of proteoglycan in the tissues

For the quantification of proteoglycan in the tissue samples, a dimethylmethylene blue (DMMB) assay for detection of sGAGs was used. As mentioned in the literature review section, there are no assays for directly measuring proteoglycan, and so the sGAG content is the best measure available. The DMMB dye was made by first dissolving 8 mg of 1:9-dimethylmethylene blue zinc chloride double salt (341088, Sigma-Aldrich, St. Louis, MO, USA) in 5 mL of 100% ethanol. This was then added to a separate mixture of 475 mL of deionized water, 1.52 g of glycine, and 1.185 g of NaCl and the pH was brought to 3.0 using HCl and NaOH. Standards for the assay were prepared by using chondroitin sulfate C from shark cartilage (C4384, Sigma-Aldrich, St. Louis, MO, USA). To create the standard curve, the standard stock solution (prepared at a concentration of 2 mg/mL in water) was serially diluted with 0.1 M ammonium acetate to get final standard concentrations of 50, 25, 12.5, 6.25, 3.125, 1.56, 0.78, and 0 µg/mL. The proteinase k digested tissue samples were then diluted 1:20, and the DMMB dye added to each sample in a 96 well plate. Absorbances were read at a wavelength of 525 nm, which

was chosen based on data presented by Farndale *et al* showing the greatest optical density in response to the chondroitin sulphate/DMMB reaction to occur at 525 nm [101]. A commercial system was used to obtain and save these measurements (Gen5, BioTek, Winooski, VT, USA). The concentration of sGAG in each sample was then determined using its absorbance and the equation of the line of the standard curve.

3.3.3. Quantification of collagen in the tissues

In order to determine the collagen content of the tissue samples, an assay kit (MAK008, Sigma-Aldrich, St. Louis, MO, USA) for the detection of hydroxyproline was used. The first step in the assay was hydrolysis. One hundred microliters of each digested sample were added to 100 µL of concentrated hydrochloric acid in pressure-tight polypropylene vials with polytetrafluoroethylene (PTFE) lined caps and immersed in an oil bath for three hours at a temperature of 120˚C. After this, samples were diluted 1:20, and the remaining kit steps were followed. This involved adding a chloramine T/oxidation buffer mixture to the samples followed by a diluted 4-dimethylaminobenzaldehyde reagent which resulted in a colorimetric product that was read using the commercial plate reader (Gen5, BioTek, Winooski, VT, USA) at 560 nm. The hydroxyproline concentrations of each sample were then determined by using the standard curve and a collagen to hydroxyproline mass ratio of 8 was assumed for quantifying the collagen [16].

3.4. Histology

Cartilage and meniscus samples were prepared for histological analysis and scoring according to established protocols[118]. This section discusses the general procedures utilized in further detail. More specific methods for the sample preparation can be found in section 4.2.2 for the cadaver study, and section 5.2.6 for the TKA study. All histology steps were completed in the histology core facility at the University of Saskatchewan with guidance and support from histologist Dr. Adi Manek.

3.4.1. Sample fixation, processing, and paraffin embedding

The most important step in the histological process was the first, sample fixation. Fixation allowed the tissues to be preserved by providing support to the macromolecules present and preventing decay. For this step, samples were first placed in individual histocasettes. These histocasettes were immersed in 10% neutral buffered formalin (NBF) and left to soak for 72 hours. After the three days, the tissues were transferred to 70% ethanol for 24 hours and then moved into fresh 70% ethanol for at least another 24 hours. During each step of fixation, the edges of the jars were sealed with flexible wax film (Parafilm) to prevent any evaporation. The volume of NBF and ethanol used was at least 20 mL per 1 g of samples.

The second part of the fixation was processing, which was completed in an automated tissue processor (RVG/1 Histology Tissue Processor, Belair Instrument Co. Inc., Springfield, NJ, USA) (Figure 3.6). This part was necessary to dehydrate the tissues and replace the spaces occupied by water with wax to allow sections to be cut while keeping the natural structure of the tissue. Essentially, the tissues are placed in a machine where they are exposed to a series of solutions that dehydrate, clear, and infiltrate the tissue.

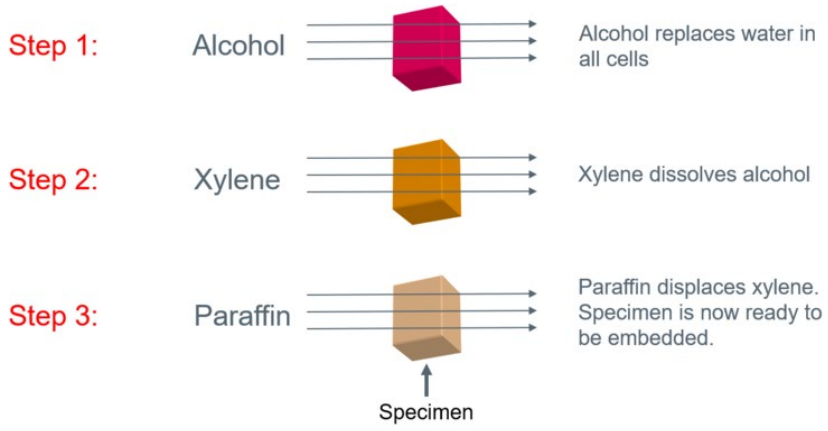

FIGURE 3.6: DESCRIPTION OF STEPS INVOLVED IN AUTOMATIC TISSUE PROCESSING FOR HISTOLOGY (IMAGE COPYRIGHT 2020 LEICA BIOSYSTEMS DIVISION OF LEICA MICROSYSTEMS, INC.)[150]

After samples were fixed and processed, they were embedded in paraffin at an embedding station (Tissue Tek, Sakura Finetek, Inc., St. Torrence, CA, USA). This step resulted in tissues being encased in a block of paraffin (Figure 3.7). After wax hardening, these blocks could be sectioned in order to obtain slides of tissue specimens.

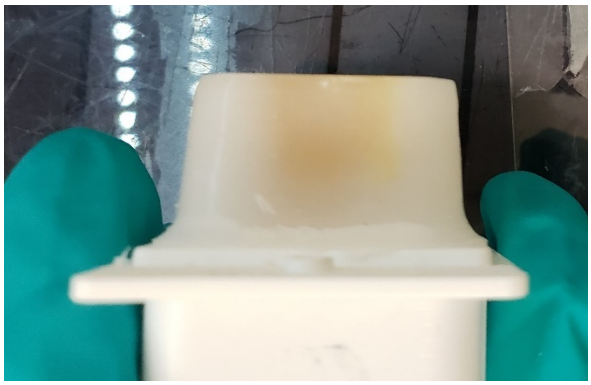

FIGURE 3.7: TISSUE SAMPLE EMBEDDED IN PARAFFIN FOR HISTOLOGICAL SECTIONING

3.4.2. Sectioning and staining

After paraffin embedding, the tissue blocks were cut into 5 µm thick sections using an automated microtome (Microm 350S, Epredia, Kalamazoo, MI, USA). These sections were mounted onto Superfrost Plus slides (charge adheres tissues better) and dried overnight and then were ready to be stained.

All slides were stained using a Safranin O/Fast Green protocol modified from Schmitz *et al*, (Table 3.2)[118]. This resulted in the cartilage matrix appearing orange to red, nuclei black, and cytoplasm grey green.

TABLE 3.2: SAFRANIN O/FAST GREEN STAINING PROTOCOL MODIFIED FROM SCHMITZ ET AL

Step	Solution slides immersed in	Amount of time	Step	Solution slides immersed in	Amount of time
1	Xylene – 1	4 minutes	**10**	Fast Green	5 minutes
2	Xylene – 2	4 minutes	**11**	1% Acetic Acid	10-15 seconds
3	Xylene – 3	4 minutes	**12**	Safranin O	5 minutes
4	95% Alcohol	1 minute	**13**	Absolute Alcohol – 1	5 minutes
5	95% Alcohol	1 minute	**14**	Absolute Alcohol – 2	5 minutes
6	70 % Alcohol	1 minute	**15**	Absolute Alcohol – 3	5 minutes
7	Tap Water	1 minute	**16**	Absolute Alcohol/Xylene	5 minutes
8	Weigert's Hematoxylin Working Solution	10 minutes	**17**	Xylene – 1	5 minutes
9	Running Tap Water	10 minutes	**18**	Xylene – 2	5 minutes

3.4.3. Scoring

The last step in the histological analysis was scoring of the stained tissue slides. For the cartilage samples, a modified version of the OARSI scoring system described by Pritzker *et al* was utilized [128]. Subgrades were used but, similarly to a study by Waldstein *et al* which also harvested cylindrical plug samples, OARSI grade 6 was not assessed as this would require observing the entire joint compartment for deformation and the formation of osteophytes [132]. Furthermore, grade 5 was also excluded because no subchondral bone was present in the sections. Stage was determined from the horizontal extent of damage across the plug that was present on the section. The final score for each sample was determined by multiplying the grade by the stage and resulted in a number between 1 and 18. The full OARSI scoring system allows for scores from 1-24.

For the menisci samples, the scoring system presented by Pauli *et al* was used with some modifications to account for the type of samples taken (plugs rather than radial pieces for the TKA study and radial pieces with potential holes for the cadaver study) [140]. For the surface category, the inner border evaluation was excluded resulting in possible total scores of 0-15 rather than the usual 0-18. The grades were also modified due to this so that G1 represented a score from 0-3, G2 from 4-7, G3 from 8-11, and G4 from 12-15.

4. Validation of qMT MRI in Cadaver Menisci

4.1. Introduction to the cadaver study

The cadaver study was carried out first with the objective to evaluate qMT MRI as a non-invasive marker of healthy menisci tissue content (biochemical properties) and structure (histology score) in cadaver knees. There is very limited research on qMT in the meniscus, with currently only two studies existing in the literature (Simard[20] and Berryman[141]). The Simard study established the first reported qMT values for healthy meniscus but did not assess correlations between these values and any tissue properties. The Berryman study found a correlation between aggregate modulus and T_{2b}, illustrating that qMT could be a valuable imaging technique for understanding the function of the meniscus; but no study has compared the qMT parameters to the biochemical or histological properties of the tissue. My study elucidates relationships between the qMT metrics and the structure and composition of meniscus as well as providing important information about the baseline qMT parameters expected in healthy meniscus. Baseline data in healthy menisci is essential before disease related changes in the parameters can be understood.

4.2. Methods specific to the cadaver study

The methodology for the cadaver study (Figure 4.1) included a qMT MRI scan of intact cadaver knees, sample retrieval, biochemical content analysis, histology scoring, image processing, and statistical analysis. This section serves to outline the differences in the methods for the cadaver study specifically, general methodologies have been omitted for brevity but can be found in chapter 3: General Methodology.

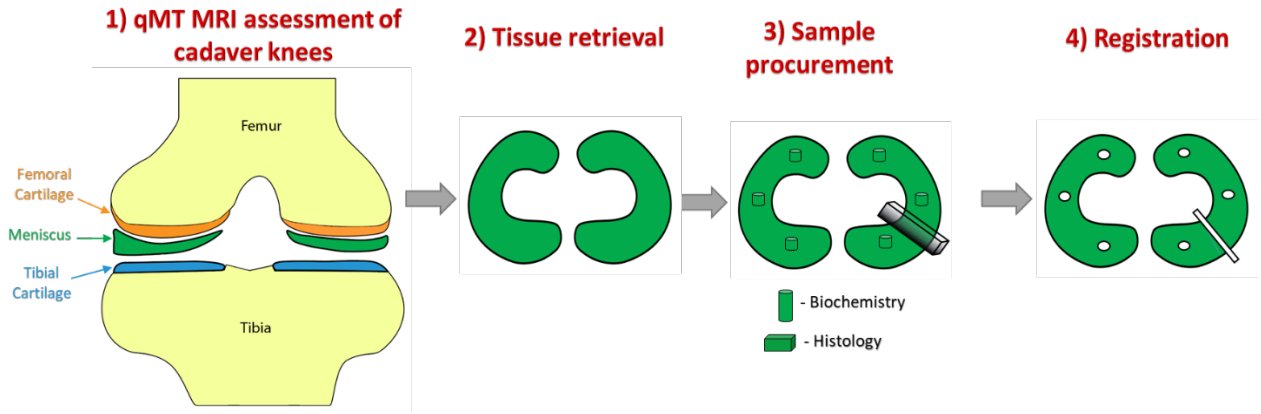

FIGURE 4.1: METHODOLOGY FOR THE CADAVER STUDY. THIS STUDY INCLUDED QMT MRI SCANNING OF THE WHOLE CADAVER KNEE, DISSECTION FOR TISSUE RETRIEVAL AND SAMPLE PROCUREMENT, BIOCHEMISTRY AND HISTOLOGY, AND THEN REGISTRATION

4.2.1. Specimens

For this study, the medial and lateral menisci from six different fresh frozen cadaver knees (12 menisci in total) with no history of surgery or injury were obtained from Science Care Inc., Phoenix, AZ. Of the six knees, three were male and 3 were female with a mean age of 70.3 ± 9.3 years and all knees were from different people. The specimens were approved for use in this study by the University of Saskatchewan Biomedical Research Ethics Board (Appendix H: Cadaver Study Ethics Certificate).

4.2.2. Sample retrieval for biochemistry and histology

After scanning, fellow MSc student Brennan Berryman opened the knees and removed the femur and surrounding tissues with a scalpel, leaving the menisci exposed but still attached to the tibia. In order to procure the biochemistry samples, Brennan used a 4 mm biopsy punch to obtain as many core samples along the menisci as possible. From these cores, he cut approximately 2 mm from the center for his own project (mechanical testing) and the outsides were stored in PBS with protease inhibitors (5 mM ethylenediaminetetraacetic acid and 5 mM benzamidine HCl) and frozen for around two months for future biochemical testing. After these cores were taken, Brennan placed gauze soaked in the PBS with protease

inhibitors over top of the menisci; and the tibial plateaus with attached menisci were also frozen for about 2 months until I could perform the histology sample retrieval. Various studies have proven that a single freeze-thaw cycle does not significantly alter the mechanical or biochemical properties of articular cartilage[151,152], and Peters *et al* also showed that canine femoral cartilage samples can undergo up to three freeze-thaw cycles without any statistically significant changes to the mechanical properties of the tissue[153]. This enforces that the two freeze-thaw cycles utilized in this project likely did not significantly alter the tissue properties.

The remaining sample retrieval was performed by me. To obtain the histology samples, the tibial plateaus with attached menisci were thawed, and the menisci were removed with a scalpel by cutting the collateral ligaments and then dissecting carefully around the edges. No magnification was used for this process. Both medial and lateral menisci were then cut into seven roughly equal pieces. The second, fourth, and sixth pieces (from either top or bottom) were taken for histological analysis representing the anterior, central, and posterior regions of the menisci (Figure 4.2). These regions were recorded for future registration of the histology scores to the qMT parameters. The tissue dye was used to mark the topmost corner of the posterior facing side of each piece for orientation during the paraffin embedding and sectioning steps. These radial sections were then placed in labelled histocasettes and the fixation step began immediately.

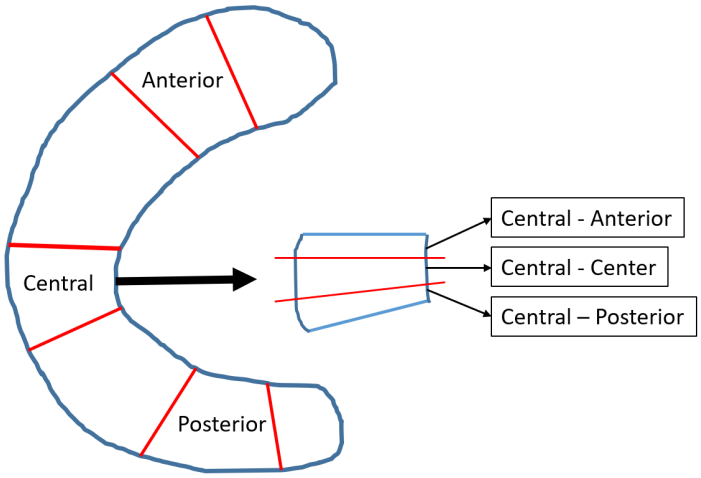

FIGURE 4.2: DEPICTION OF HISTOLOGY BLOCKS TAKEN FROM CADAVER MENISCI AND THE REGIONS REPRESENTED IN SECTIONS TAKEN FROM EACH BLOCK

4.2.3. Histology

The sample fixation and processing steps were described in the general methodology section (3.4.1. Sample fixation, processing, and paraffin embedding). During paraffin embedding, the same procedures were followed with special care being taken to note the orientation of the tissues for sectioning. When sectioning, several sections were taken throughout the blocks to represent the anterior, central, and posterior regions of each of the blocks (Figure 4.2). Once again, these regions were noted exclusively for registration purposes.

4.2.4. Image processing

Minor modifications were made in the image processing pipeline to accommodate the cadaver data. Binary masks of the menisci and models of the biochemistry sample cylinders had already been created for another study by Brennan Berryman, so these were utilized. In order to identify the location of the histological slices within the menisci, a block shape rather than a cylinder was custom drawn in packaged software (Fusion 360, Autodesk, San Rafael, USA). These shapes were created by visual inspection to resemble the blocks taken from each meniscus for histology. A photograph of the dissected meniscus was displayed beside the surface model and reference points such as cylindrical sample holes and unique shape characteristics were utilized to create the virtual blocks (Figure 4.3). To represent the three regions of each block, the overall shape was split into three roughly equal sections. Using these block models along with the cylinders, binary masks, and analyze surfaces already existing, the average and standard deviation of each qMT parameter was determined at each sample location within the specimens using the MATLAB registration code (Figure 4.4).

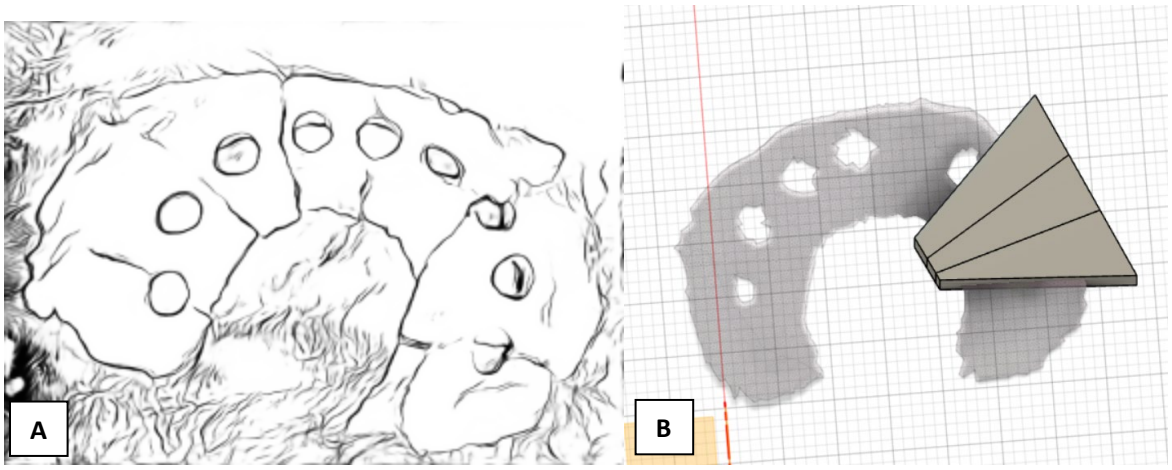

FIGURE 4.3: A) MODIFIED PHOTOGRAPH OF MENISCUS DISSECTED INTO BLOCKS FOR HISTOLOGY (SCIENCE CARE DOES NOT PERMIT PUBLICATION OF PICTURES OF CADAVER SPECIMENS. B) IMAGE OF BLOCKS CREATED IN FUSION 360 TO REPRESENT THE LOCATIONS OF THE HISTOLOGY SAMPLES TAKEN. THE BLOCKS WERE ALSO SPLIT INTO 3 REGIONS, THE ANTERIOR, CENTRAL, AND POSTERIOR PORTIONS OF EACH BLOCK.

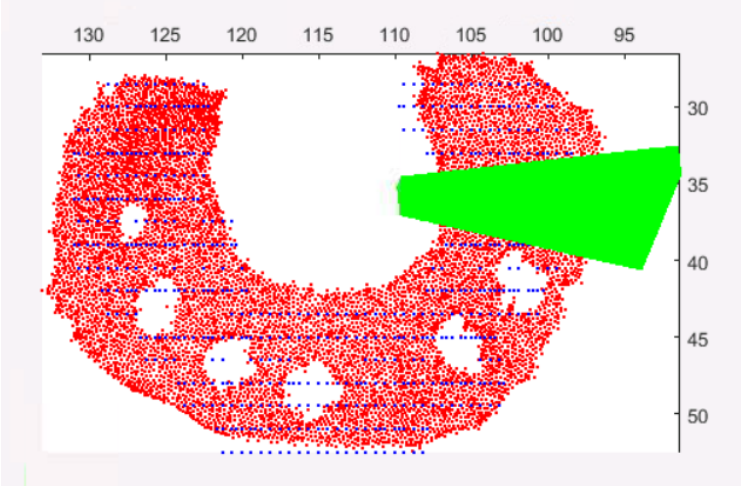

FIGURE 4.4: RESULTING FIGURE FROM REGISTRATION CODE RUN ON CADAVER HISTOLOGY BLOCKS. RED REPRESENTS THE SURFACE MODEL, BLUE THE ANALYZE SURFACE, AND GREEN THE HISTOLOGY BLOCK. THE AVERAGE SHAPE MATCH ERROR FOR ALL 6 CADAVER KNEE REGISTRATIONS WAS 0.676 ± 0.056 MM. NOT ALL DATA POINTS WILL NECESSARILY EXIST IN BOTH SURFACE AND ANALYZE MODELS

4.2.5. Statistical analysis specific to the cadaver study

Descriptive statistics (mean and standard deviations) were first determined for the qMT parameters and biochemistry and histology results then Pearson product moment and Spearman's rho correlations were assessed between the qMT parameters and tissue properties using a packaged software (SPSS, IBM Corp., Armonk, NY). Pearson correlations were used for the continuous variables (biochemical properties) while

Spearman's rho was determined for the histological values due to it being ordinal data. Correlations were considered significant if they had a p-value less than 0.05 and adhered to the following classifications based on the correlation coefficient: 0-0.19 = very weak, 0.2-0.39 = weak, 0.4-0.59 = moderate, 0.6-0.79 = strong, and 0.8-1 = very strong. Although many samples were taken from each specimen, individual samples were considered their own measurement as variation throughout the surfaces was to be expected. For the cadaver study, the qMT parameters were split into distinct categories (biochemistry and histology medial and lateral) to allow the statistical analysis to be separated into more specific groups to get a more comprehensive understanding of any correlations present. It also allowed for investigations to be made into the differences in properties between medial and lateral menisci.

4.3. Results of the cadaver study

From the six cadaver knees, 71 biochemistry samples were analyzed for sGAG content (40 from medial menisci and 31 from lateral), 70 were analyzed for collagen content (39 from medial and 31 from lateral), and 161 histology samples were scored (79 from lateral and 82 from medial) (Table 4.1).

TABLE 4.1: BREAKDOWN OF NUMBER OF SAMPLES TAKEN FROM EACH KNEE FOR HISTOLOGY AND BIOCHEMISTRY

Knee #	Histology Samples			Biochemistry Samples		
	Medial	Lateral	Total	Medial	Lateral	Total
1	22	23	45	4	5	9
2	20	19	39	5	4	9
3	15	9	24	7 (6 for Collagen)	4	11 (10 for Collagen)
4	9	10	19	7	8	15
5	9	9	18	8	5	13
6	7	9	16	9	5	14

4.3.1. qMT imaging parameter results

qMT parameters were estimated for the whole meniscus and all relevant regions (Table 4.2). The standard deviations in this table represent the between sample standard deviations. Overall, there appeared to be a range of values within the tissues (Figure 4.5), with T_1obs being around 680 ms and T_{1f} around 620 ms. The combined average value of T_{2f} was 5.66 ms, with T_{2b} trending much faster at 15.90 µs. Bound pool fraction hovered around 23% in all groups and k_f was around 3 s^{-1}.

TABLE 4.2: QMT PARAMETER RESULTS FOR THE CADAVER STUDY

	T_1 obs (ms)		T_{1f} (ms)		T_{2f} (ms)		T_{2b} (μs)		f (%)		k_f (s^{-1})	
	Mean	Std. Dev.	Mean	Std. Dev.	Mean	Std. Dev.	Mean	Std. Dev	Mean	Std. Dev	Mean	Std. Dev
All knees	681.31	15.43	619.45	17.36	5.66	1.25	15.90	0.56	22.16	1.20	2.80	0.33
Histology samples	663.29	84.94	590.06	111.51	5.45	2.18	15.97	0.96	22.92	3.57	2.91	0.93
Histology - lateral samples	697.43	68.24	622.41	112.21	6.18	1.65	16.07	0.87	22.12	3.67	2.79	1.03
Histology - medial samples	629.79	86.37	558.31	101.23	4.74	2.39	15.87	1.02	23.71	3.28	3.04	0.80
Biochemistry samples	661.63	77.09	592.88	93.81	5.62	2.16	16.16	1.00	23.36	3.62	3.01	0.94
Biochemistry - lateral samples	674.06	73.24	605.94	92.68	5.85	1.53	16.32	0.90	23.35	4.07	2.99	0.95
Biochemistry - medial samples	651.99	78.61	582.76	93.42	5.44	2.54	16.04	1.06	23.37	3.23	3.03	0.93

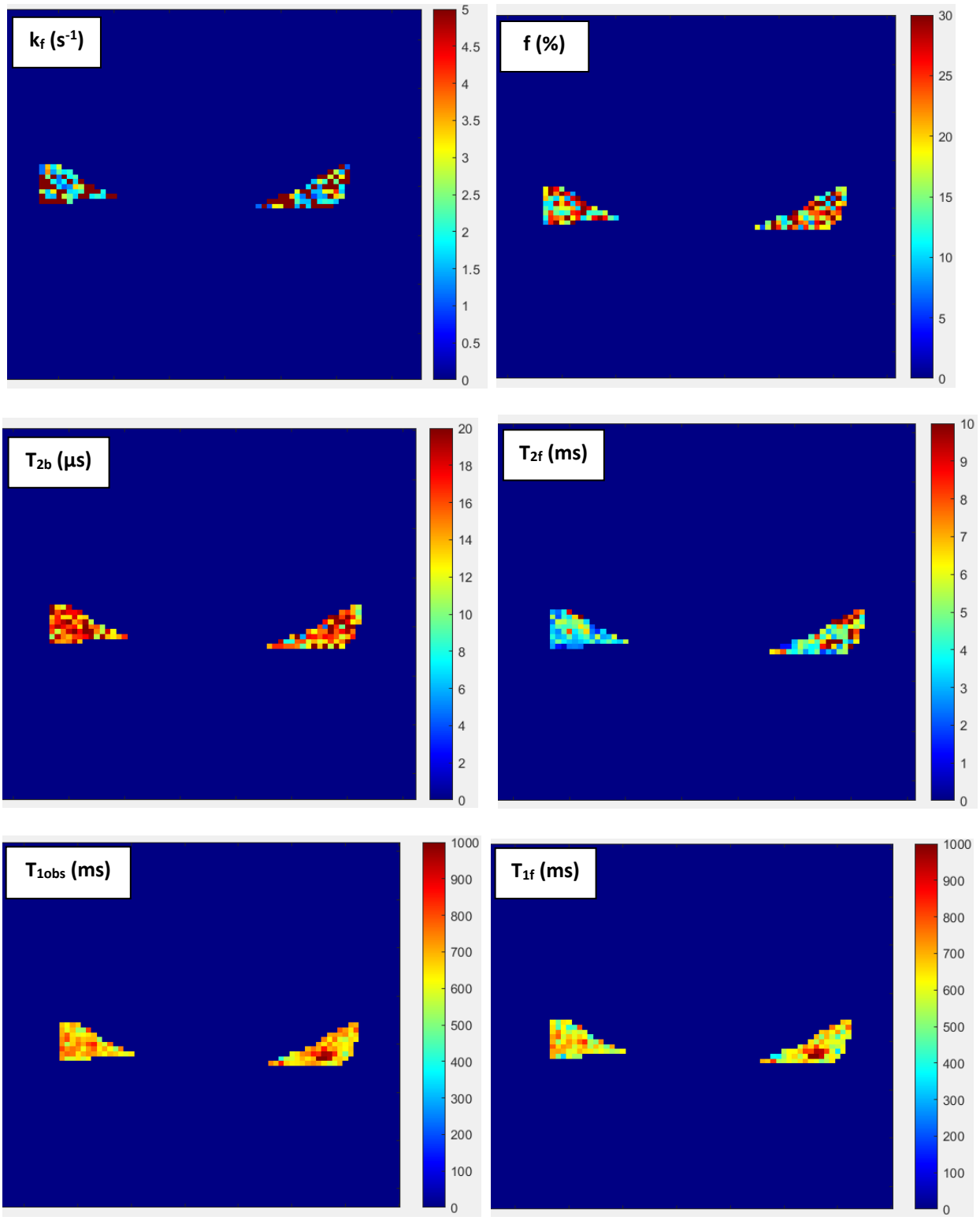

FIGURE 4.5: COLOR MAPS REPRESENTING THE RANGES OF QMT VALUES ACROSS A SINGLE SLICE OF HUMAN CADAVER MENISCI

4.3.2. Biochemistry results

On average, the amounts of both sGAG and collagen in the medial menisci trended lower than the lateral side (Table 4.3). The mean sGAG content in the combined samples was 2.29 ± 0.894 % when normalized by dry mass, and 0.564 ± 0.238 % by wet mass. The amount of collagen per dry mass was over 100% for medial, lateral, and both combined which was unexpected but the percentage of collagen per wet mass was 26.1 ± 6.18 %.

TABLE 4.3: AVERAGE BIOCHEMISTRY RESULTS FOR THE CADAVER STUDY

	Both sides combined (N=71)		Medial (N=40)		Lateral (N=31)	
	Mean	Standard deviation	Mean	Standard deviation	Mean	Standard deviation
Liquid content (%)	75.5	3.44	75.5	3.69	75.4	3.23
Solid content (%)	24.5	3.44	24.5	3.69	24.6	3.23
sGAG per dry mass (%)	2.29	0.894	2.15	0.779	2.40	0.962
sGAG per wet mass (%)	0.564	0.238	0.530	0.208	0.591	0.256
Collagen per dry mass (%)	107	23.2	104	18.8	110	26.0
Collagen per wet mass (%)	26.1	6.18	25.3	5.31	26.8	6.74

4.3.3. Histology results

For the 161 histology samples graded, the majority of the samples were grade 2 (67% of medial samples and 52% of lateral) and no grade 4 scores were present (Figure 4.6)[140]. Trends in the histology results showed that the medial side had a slightly higher frequency of grade 3 samples and the lateral side seemed to have a higher percentage of grade 1 samples. Examples of grade 1-3 samples are shown in Figure 4.7.

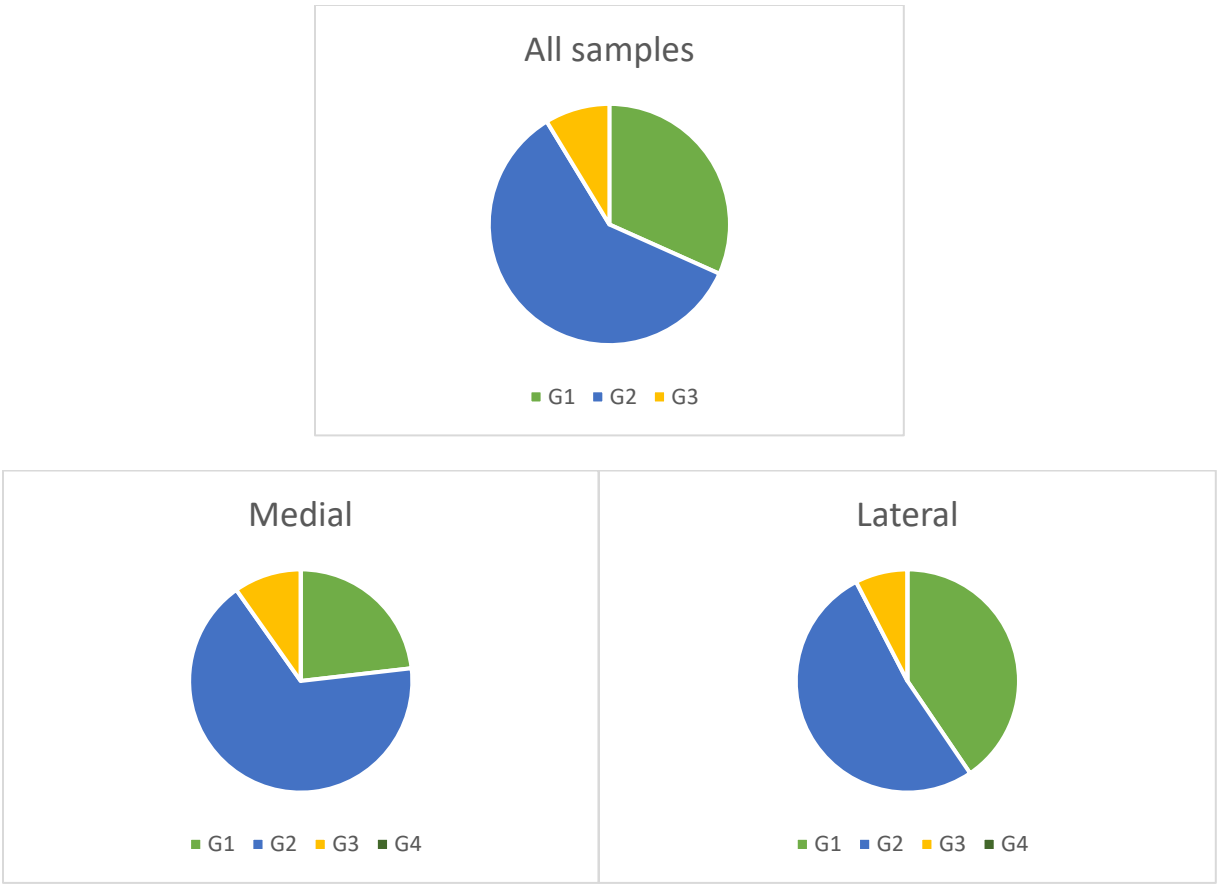

FIGURE 4.6: DISTRIBUTION OF HISTOLOGY SCORES IN ALL, MEDIAL, AND LATERAL SAMPLES FOR THE CADAVER STUDY. G1 = NORMAL TISSUE, G2 = MILD DEGENERATION, G3 = MODERATE DEGENERATION, G4 = SEVERE DEGENERATION

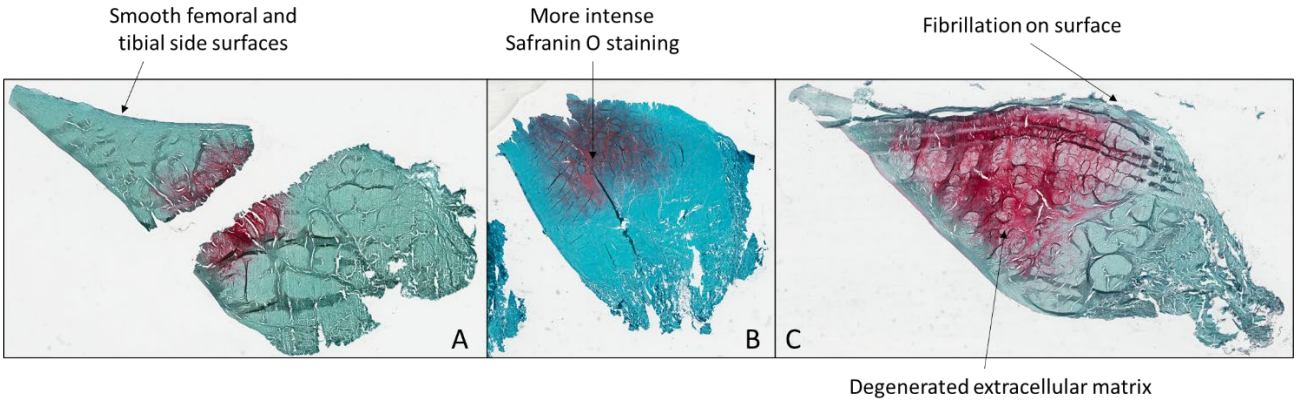

FIGURE 4.7: EXAMPLES OF EACH GRADE OF HISTOLOGY SAMPLE OBSERVED IN THE CADAVER STUDY A. GRADE 1, B. GRADE 2, C. GRADE 3

4.3.4. Biochemistry correlation analysis

In the medial side samples, correlations were stronger overall, as compared to the lateral side and the whole meniscus (Table 4.4). Sixty-six of the proteoglycan (sGAG) samples and 65 collagen samples had corresponding qMT data. Thirty-seven of these were from medial menisci (36 for collagen) and 29 were from lateral menisci. From the medial results it was shown that as the collagen per both wet and dry mass increased, so did the T_1obs, T_{1f}, and T_{2f}; with all cases having moderate correlations (Table 4.4b). Increasing collagen per dry mass also resulted in increased T_{2b} ($r=0.415$, $p<0.05$), and the same trend was observed between collagen per wet mass and T_{2b} ($r=0.356$, $p<0.05$). In these medial samples there were no significant correlations between any of the qMT parameters and the sGAG in the tissue, and there were also no significant correlations observed with the liquid or solid content.

TABLE 4.4: PEARSON CORRELATION COEFFICIENTS AND SIGNIFICANCE VALUES FOR BIOCHEMICAL PROPERTIES AND THE QMT PARAMETERS USING A) ALL BIOCHEMISTRY SAMPLES TAKEN FROM THE CADAVER MENISCI, B) ONLY SAMPLES TAKEN FROM MEDIAL MENISCI, AND C) ONLY SAMPLES TAKEN FROM LATERAL MENISCI

A. Combined		T_1 obs (ms)	T_{1f} (ms)	T_{2f} (ms)	T_{2b} (μs)	f (%)	k_f (s^{-1})
Liquid content (%) (N = 66)	Pearson Correlation	0.077	0.096	0.102	0.010	-.248*	-0.070
	Sig. (2-tailed)	0.539	0.444	0.417	0.939	0.045	0.576
Solid content (%) (N=66)	Pearson Correlation	-0.077	-0.096	-0.102	-0.010	.248*	0.070
	Sig. (2-tailed)	0.539	0.444	0.417	0.939	0.045	0.576
sGAG per dry mass (%) (N=66)	Pearson Correlation	-0.020	-0.031	-0.195	-0.137	0.107	0.112
	Sig. (2-tailed)	0.871	0.804	0.117	0.271	0.391	0.372
sGAG per wet mass (%) (N=66)	Pearson Correlation	-0.063	-0.079	-0.238	-0.150	0.186	0.134
	Sig. (2-tailed)	0.613	0.527	0.054	0.230	0.136	0.282
Collagen per dry mass (%) (N=65)	Pearson Correlation	.423**	.413**	.510**	0.235	-0.188	-0.218
	Sig. (2-tailed)	0.000	0.001	0.000	0.059	0.133	0.081
Collagen per wet mass (%) (N=65)	Pearson Correlation	.342**	.318**	.424**	0.237	0.000	-0.137
	Sig. (2-tailed)	0.005	0.010	0.000	0.057	1.000	0.277

** Correlation is significant at the 0.01 level	**Correlation legend**	Very weak (0-0.19)	Weak (0.2-0.39)
* Correlation is significant at the 0.05 level	Moderate (0.4-0.59)	Strong (0.6-0.79)	Very strong (0.8-1)

B. Medial		T_1 obs (ms)	T_{1f} (ms)	T_{2f} (ms)	T_{2b} (µs)	f (%)	k_f (s^{-1})
Liquid content (%) (N=37)	Pearson Correlation	-0.013	-0.022	0.081	0.157	-0.095	0.114
	Sig. (2-tailed)	0.938	0.899	0.634	0.354	0.578	0.502
Solid content (%) (N=37)	Pearson Correlation	0.013	0.022	-0.081	-0.157	0.095	-0.114
	Sig. (2-tailed)	0.938	0.899	0.634	0.354	0.578	0.502
sGAG per dry mass (%) (N=37)	Pearson Correlation	0.080	0.070	-0.273	-0.243	-0.002	-0.024
	Sig. (2-tailed)	0.637	0.682	0.101	0.148	0.991	0.887
sGAG per wet mass (%) (N=37)	Pearson Correlation	0.067	0.060	-0.288	-0.264	0.027	-0.047
	Sig. (2-tailed)	0.693	0.725	0.084	0.114	0.874	0.781
Collagen per dry mass (%) (N=36)	Pearson Correlation	.493**	.477**	.585**	.415*	-0.162	-0.251
	Sig. (2-tailed)	0.002	0.003	0.000	0.012	0.346	0.141
Collagen per wet mass (%) (N=36)	Pearson Correlation	.470**	.456**	.527**	.356*	-0.060	-0.260
	Sig. (2-tailed)	0.004	0.005	0.001	0.033	0.727	0.126

** Correlation is significant at the 0.01 level	**Correlation legend**	Very weak (0-0.19)	Weak (0.2-0.39)
* Correlation is significant at the 0.05 level	Moderate (0.4-0.59)	Strong (0.6-0.79)	Very strong (0.8-1)

C. Lateral		T_1 obs (ms)	T_{1f} (ms)	T_{2f} (ms)	T_{2b} (µs)	f (%)	k_f (s^{-1})
Liquid content (%) (N=29)	Pearson Correlation	0.183	0.226	0.156	-0.196	-.380*	-0.266
	Sig. (2-tailed)	0.342	0.239	0.420	0.308	0.042	0.163
Solid content (%) (N=29)	Pearson Correlation	-0.183	-0.226	-0.156	0.196	.380*	0.266
	Sig. (2-tailed)	0.342	0.239	0.420	0.308	0.042	0.163
sGAG per dry mass (%) (N=29)	Pearson Correlation	-0.146	-0.155	0.053	0.136	0.245	0.309
	Sig. (2-tailed)	0.448	0.422	0.784	0.483	0.201	0.103
sGAG per wet mass (%) (N=29)	Pearson Correlation	-0.246	-0.271	-0.075	0.135	.391*	.404*
	Sig. (2-tailed)	0.198	0.156	0.698	0.485	0.036	0.030
Collagen per dry mass (%) (N=29)	Pearson Correlation	0.357	0.358	0.355	-0.052	-0.245	-0.189
	Sig. (2-tailed)	0.057	0.056	0.059	0.788	0.200	0.325
Collagen per wet mass (%) (N=29)	Pearson Correlation	0.177	0.143	0.214	0.099	0.070	0.033
	Sig. (2-tailed)	0.359	0.458	0.266	0.610	0.717	0.863

** Correlation is significant at the 0.01 level	**Correlation legend**	Very weak (0-0.19)	Weak (0.2-0.39)
* Correlation is significant at the 0.05 level	Moderate (0.4-0.59)	Strong (0.6-0.79)	Very strong (0.8-1)

For the combined meniscus cores samples, increases in the collagen per dry mass resulted in simultaneous increases of T_1obs, T_{1f}, and T_{2f}; with all three correlations being moderate (r=0.423, p<0.01, r=0.413, p<0.01, and r=0.510, p<0.01 respectively) (Figure 4.8 and Table 4.4a). Similarly, as the collagen per wet mass increased, the T_{2f} (moderate correlation r=0.424, p<0.01) along with T_1obs and T_{1f} (weak correlations r=0.342, p<0.01 and r=0.318, p<0.01 respectively) increased as well (Table 4.4a). As liquid content increased, f decreased, and unsurprisingly, as solid content increased, so did f; however, in both cases the correlations were weak (r=-0.248, p<0.05, and r=0.248, p<0.05, respectively) (Table 4.4a). Figures of significant correlations for the combined data can be found in Appendix I: Significant correlations for combined cadaver data. No significant correlations were found between any of the qMT parameters and the sGAG content of the tissue.

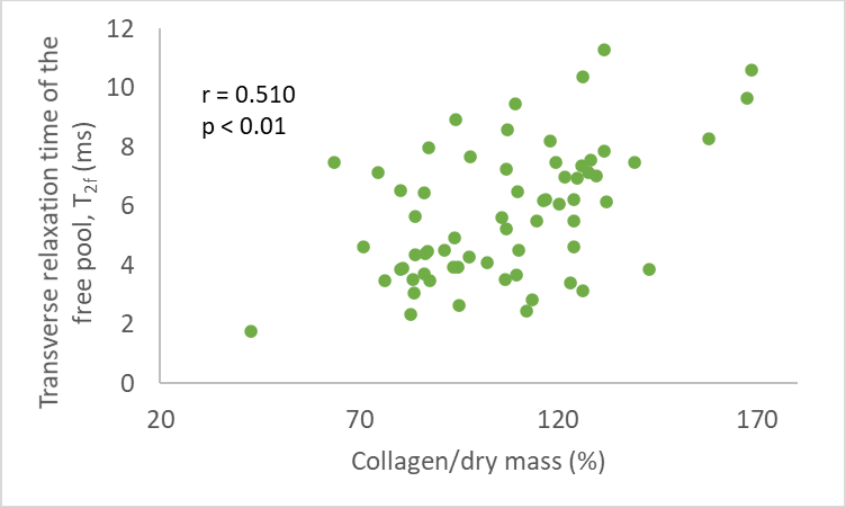

FIGURE 4.8: CORRELATION BETWEEN THE TRANSVERSE RELAXATION TIME OF THE FREE POOL AND THE PERCENTAGE OF COLLAGEN PER DRY MASS IN HUMAN CADAVER MENISCI

For the lateral side samples (Table 4.4c), the significant correlations observed were quite different than the medial. An increase in the solid content was accompanied by an increase in f (r=0.380, p<0.05), while increasing liquid content showed decreasing f (r=-0.380, p<0.05). Interestingly, in the lateral samples no significant correlations were seen with any of the qMT parameters and the collagen content, but a moderate correlation was found between the sGAG per wet mass and k_f (r=0.404, p<0.05), and a weak correlation between the sGAG per wet mass and f (r=0.391, p<0.05), where in both cases the parameters increased simultaneously.

4.3.5. Histology correlation analysis

As histology score increased, qMT parameters T_1obs, T_{1f}, T_{2f} and T_{2b} decreased, although the correlations were weak (ρ=-0.245, $p<0.05$; ρ=-0.232, $p<0.05$; ρ=-0.277, $p<0.01$; ρ=-0.207, $p<0.05$; respectively) (Table 4.5a) (figures shown in Appendix I: Significant correlations for combined cadaver data). Correlation coefficients were determined for the 100 histology samples with corresponding qMT data, 50 of which were from lateral menisci and 50 from medial. When analyzing just the medial side samples stronger correlations were seen but only between the total score and T_1obs, T_{1f}, and T_{2f}. No significant correlations were present when the lateral side samples were analyzed independently.

TABLE 4.5: SPEARMAN'S RHO CORRELATION COEFFICIENTS AND SIGNIFICANCE VALUES FOR HISTOLOGICAL SCORES AND THE QMT PARAMETERS USING A) ALL SAMPLES OBTAINED, B) ONLY SAMPLES FROM MEDIAL MENISCI, AND C) ONLY SAMPLES FROM LATERAL MENISCI

A. Combined (N=100)		**T_1 obs (ms)**	**T_{1f} (ms)**	**T_{2f} (ms)**	**T_{2b} (µs)**	**f (%)**	**k_f (s^{-1})**
Total Score	Correlation Coefficient	-.245*	-.232*	-.277**	-.207*	0.041	0.008
	Sig. (2-tailed)	0.014	0.020	0.005	0.038	0.689	0.934
B. Medial (N=50)		**T_1 obs (ms)**	**T_{1f} (ms)**	**T_{2f} (ms)**	**T_{2b} (µs)**	**f (%)**	**k_f (s^{-1})**
Total Score	Correlation Coefficient	-.346*	-.330*	-.319*	-0.210	0.018	0.079
	Sig. (2-tailed)	0.014	0.019	0.024	0.143	0.900	0.584
C. Lateral (N=50)		**T_1 obs (ms)**	**T_{1f} (ms)**	**T_{2f} (ms)**	**T_{2b} (µs)**	**f (%)**	**k_f (s^{-1})**
Total Score	Correlation Coefficient	-0.203	-0.179	-0.268	-0.180	0.040	-0.152
	Sig. (2-tailed)	0.157	0.214	0.060	0.212	0.785	0.293

** Correlation is significant at the 0.01 level	**Correlation legend**	Very weak (0-0.19)	Weak (0.2-0.39)
* Correlation is significant at the 0.05 level	Moderate (0.4-0.59)	Strong (0.6-0.79)	Very strong (0.8-1)

4.4. Cadaver study discussion

The key findings of this study were the qMT parameters of the meniscus, which had strong similarities to previously reported values, and the moderate to weak correlations observed between several tissue properties and qMT parameters. There were also observations made about the connections between the biochemistry and histology results.

4.4.1. qMT parameter analysis – comparison to literature

The results of the qMT property analysis showed similarities to the literature for most of the parameters (Table 4.6). The specimens used in the Berryman study[141] were the same as mine but the qMT results he presented were from the midsection of the menisci samples, whereas mine were from the whole plug, and so slight variation is seen. However, logically all parameter results I found were very similar to the Berryman midsection results. In comparison to the study conducted by Simard[20], the T_1obs, f, and k_f were all within a reasonable range; but the T_{2b} and T_{1f} were somewhat different. This could be due to the fact that Simard used a super-Lorentzian lineshape while a Gaussian lineshape was utilized in this study. Furthermore, their scanning sequence was slightly different as they used a GE scanner which implemented a Fermi MT sensitizing pre-pulse versus the Gaussian pulse utilized with our Siemens scanner.

TABLE 4.6: QMT VALUES IN MENISCUS – COMPARISON TO LITERATURE

Study:	**Berryman*[141]**	**Simard[20]**			**Current**		
		Lateral	**Medial**	**Both**	**Lateral****	**Medial****	**Both**
f (%)	23.53 (4.25)	21.86 (2.51)	26.76 (2.82)	23.36 (2.41)	23.35 (4.07)	23.37 (3.23)	22.16 (1.20)
k_f (s^{-1})	3.03 (1.19)	2.26 (0.59)	2.67 (0.64)	2.38 (0.35)	2.99 (0.95)	3.03 (0.93)	2.80 (0.33)
T_1obs (ms)	666.6 (83.9)	698.6 (120.0)	611.6 (85.9)	663.9 (90.9)	674.1 (73.2)	652.0 (78.6)	681.3 (15.4)
T_{1f} (ms)	598.1 (104.3)	783.1 (177.3)	661.0 (166.6)	736.2 (156.0)	605.9 (92.7)	582.8 (93.4)	619.5 (17.4)
T_{2b} (µs)	16.1 (1.47)	5.74 (0.74)	5.50 (0.95)	5.65 (0.81)	16.3 (0.9)	16.0 (1.1)	15.9 (0.6)
* Values reported are those found using a Gaussian lineshape. ** Medial and lateral values reported in this table are from the biochemistry samples. Standard deviations shown in brackets.							

For the bound pool fraction f, the results are logical as the meniscus is composed of about 72% water[28]; so it makes sense that the fraction of hydrogen atoms attached to the bound pool (or macromolecules) would be around 22%. Little variation was found between the f of medial and lateral menisci and the values obtained also aligned with the literature [20,141]. In the Simard study, there was slightly more variation, with a higher f in

the medial (26.76%) versus the lateral (21.86%) menisci [20]. That study also assessed cadaver knees with no history of knee injury, and so it is clear that a larger variety of tissue health is needed to understand the changes of f with damage to the meniscus.

With k_f, it is unclear what results would be expected because the physical implications of the parameter are difficult to interpret, but there seems to be linkages between it and proteoglycan content. k_f is the rate of magnetization being exchanged between the bound and free pools. This exchange can occur by two mechanisms: 1) chemical exchange between the pools and 2) magnetization exchange due to proximity of protons between pools. We cannot distinguish between these mechanisms. Therefore, it is not known whether this value would change with diminishing proteoglycan and collagen or if it would be unaffected. For example, although the bound pool may become smaller, reducing the first mechanism of exchange, the increased number of hydrogen atoms in the free pool could still be exchanging magnetization with the bound pool via the second mechanism. Sritanyaratana *et al* found k_f to be significantly lower in the patellar cartilage of OA patients (6.13 s^{-1}) compared to asymptomatic volunteers (7.22 s^{-1})[19]. These values are higher than mine (2.80 s^{-1}) but this often occurs with variation in data acquisition and processing methods[154]. Due to the fact that a study conducted by Lin *et al* [155] reported decreases in k_f after trypsin induced proteoglycan degradation in bovine nasal cartilage, Sritanyaratana *et al* hypothesized that their results may have been due to the proteoglycan loss associated with early OA[19]. My results also support this theory as I observed a moderate correlation between the k_f and sGAG/wet mass in my lateral samples ($r=0.404$, $p<0.05$), showing that as the sGAG content increases, potentially so does the k_f, and therefore k_f would decrease with reduced sGAG. This also makes some sense on a physical level, where if the bound pool size is reduced, so may be the potential for it to exchange magnetization with the free pool hence resulting in a decrease of k_f. Further work must be done to more fully understand the nature of this parameter, but preliminary results seem to indicate that k_f is related to proteoglycan content of the tissue.

4.4.2. Correlations between tissue properties and qMT parameters

Weak and moderate correlations were found between the qMT values and the biochemical properties of the meniscus (Table 4.4). A key finding in this analysis was the correlation observed between f and the solid and liquid contents. This correlation speaks to the fact that my results make sense, because f is a direct product of the amount of solid versus liquid in the sample. I would have expected the correlations to be stronger because of this, but a larger range of both qMT and biochemical values (resulting from a greater range of tissue health in the samples) would be necessary to fully understand this relationship.

The correlations in the medial and lateral samples combined proved to be slightly weaker than when the samples were split into medial and lateral. Interestingly, in the combined samples, the strongest correlations (which were at a moderate level) were all between qMT parameters and the amount of collagen. There were no significant (or stronger than "very weak") correlations between any of the qMT parameters and sGAG. It is possible that the lower concentration of proteoglycan in meniscus compared to cartilage may impact these correlations, i.e., there is too little dynamic range for the tools used to capture any relationship. This is evidenced by the fact that other qMRI metrics ($T_{1\rho}$ relaxation time – which is not a qMT measure but a common qMRI parameter) have been shown to be strongly correlated to the proteoglycan content in cartilage[110,156]. However, in the study by Son *et al* on the meniscus (which also assessed qMRI metrics but not qMT), the same trend was observed as my study with no significant correlations being found between either T_2 or $T_{1\rho}$ relaxation times and sGAG [16]. The Son study also reported strong correlations between the collagen per wet mass and both T_2 and $T_{1\rho}$, a weak correlation between collagen per dry mass and T_2, and a moderate and strong correlation between water content and T_2 and $T_{1\rho}$ respectively [16]. The meniscus has a higher percentage of collagen than cartilage so it makes sense that any relationships between the biochemical content and the qMT parameters would be through collagen. Due to the composition of meniscus, it is likely that the collagen or water content and not proteoglycan content will govern any relationships observed.

When the biochemical correlation analysis was separated into medial and lateral samples, a greater number of stronger correlations were found in both sides as compared to the combined analysis. In the medial side samples, moderate correlations were observed between both the collagen per dry and wet mass and all of the qMT parameters except f and k_f (one weak correlation between collagen per wet mass and T_{2b}). In the lateral side, the only correlations were observed between liquid and solid content and f, and sGAG per wet mass and f and k_f. The medial and lateral samples are completely opposite, which is quite interesting and may have something to do with the fact that generally the lateral side is expected to be in better condition than the medial; potentially showing that more damaged tissue has different correlations than healthier tissue.

In the histology correlation analysis (Table 4.5), more relationships were observed in the combined samples than the separate, and no significant relationships were seen in the lateral samples. The medial side samples had the strongest correlations, which were at a weak level, between the total histological score and T_1obs, T_{1f}, and T_{2f}. No correlations were found between f or k_f and the histology scores. The only other study to compare histology score to qMRI parameters in the meniscus was done by Williams *et al* and they looked at T_2* relaxation times. They found no significant correlations between T_2* and histology score in either medial or lateral menisci, but they acknowledge their small sample size (N=8 medial and N=8 lateral) may have contributed to this outcome[71]. They did notice an increase in T_2* relaxation time in more degenerated samples in the medial side, which could indicate that a larger sample size might produce significant relationships[71]. This is further supported by the results of my study. Although I was able to obtain the qMT parameters and histological score of 100 independent samples (50 medial and 50 lateral), these samples came from only 6 knees (N=6 medial and N=6 lateral) with a limited range of tissue health. I did find weak correlations, but perhaps a larger and more diverse sample set would have resulted in stronger relationships between the histology score and the qMT parameters.

4.4.3. Connections between biochemistry and histology results

From the histology results in Figure 4.6 it can be confirmed that overall, the tissue samples were quite healthy (mostly grade 2 and 1) with a small percentage being moderately degenerated (8.7% grade 3 in both lateral and medial combined). A slightly higher percentage was grade 2 and 3 (more degenerated) in the medial side samples than in the lateral, which aligns with what would be expected based on known typical patterns of OA degeneration[157,158], but the differences are small and there were only six knees so this is speculative. It is also worth mentioning that I was not blinded to the location the sample was taken from during the scoring process, which could have potentially introduced some bias.

The biochemistry results aligned with expectations based on the literature (Table 4.7) except for the collagen per dry mass amount, which was likely overestimated due to an oversimplification of the collagen to hydroxyproline mass ratio. The collagen per dry mass of my samples was 107%, which is illogical and should be around 75% [29]. This may be due to the quantification of hydroxyproline instead of collagen and assumption of a collagen to hydroxyproline mass ratio of 8. This ratio was adopted from the Son *et al* paper which also analyzed meniscal biochemistry[16]. In this paper however, the menisci utilized were from TKA patients experiencing end stage OA unlike the relatively healthy cadaver menisci from my study. Collagen content is known to decrease with OA/degeneration[51,159] thus decreasing the amount of hydroxyproline as well; so perhaps the collagen to hydroxyproline mass ratio of 8 is not appropriate for healthy populations, and ultimately overestimates the amount of collagen present in these samples. Another factor that may have impacted these values is the increase in hydroxyproline within the collagen after hydrolysis of the protein. After correcting for the water added during hydrolysis, the hydroxyproline quantity in the various collagen types change as follows: type I increases from 11.3 to 13.1%, type II from 12.9 to 51.0%, type III 15.0 to 17.4%, and type IV 14.3 to 16.6% [160]. Based on the compositional information provided by Fox e*t al* [29], the majority of collagen in the meniscus is type I (90%) with variable amounts of type II, III, and V (for the sake of this argument, I will assume 5% type II and 5% type III, excluding type V for consistency because information on its change with hydrolysis is not available in the same reference). Considering the corrected values for the free

hydroxyproline post hydrolyzation, the hydroxyproline percentage in meniscus would actually be around 13.4%. Furthermore, Makris *et al* breaks the composition down further, stating that the red-red zone contains 80% type I collagen and less than 1% each of types II, III, IV, V, and XVIII and in the white-white zone it is 40% type I and 60% type II [28]. This shows the complexity of the relationship between the hydroxyproline and collagen and how it varies throughout the meniscus as well as throughout the various collagen types. Therefore, the collagen to mass ratio of 8 used by Son *et al,* which equates to 12.5% hydroxyproline (1 hydroxyproline ÷ 8 collagen), may be oversimplifying the conditions and likely overestimating the collagen. Changing the mass ratio to 7 in my data resulted in an average collagen per dry mass percentage of 92%, a ratio of 9 gave 119%, and a ratio of 6 gave 79%. This illustrates how big an impact modifying this ratio can have on the results. Based on this sensitivity analysis and the values reported in the literature (Table 4.7), perhaps a collagen to mass ratio of 6.5 or 7 may be more suitable, but it also depends on which meniscal zone the samples are taken from. My study does not have enough data to perform a region-specific ratio correction, but this is something that should be considered for future work involving the quantification of collagen through hydroxyproline. It is also important to note that modifying this ratio has no effect on the strength of correlations, it only changes the absolute values of the collagen content.

TABLE 4.7: BIOCHEMISTRY VALUES IN MENISCUS - COMPARISON TO LITERATURE FOR CADAVER STUDY

Parameter	Value from literature	My result
Liquid content (%)	72[29], 70-75[51]	75.5
sGAG/dry mass (%)	1-2[29], 0.5-3*[27]	2.29
sGAG/wet mass (%)	0.6-0.8*[51]	0.564
Collagen/dry mass (%)	75[29],80-90*[27], 69-80[161]	107
Collagen/wet mass (%)	20-22[29,51]	26.1
*Value not stated, estimated from figure		

It is difficult in this specific study to confirm any relationships between biochemistry and histology because of the nature of the samples taken, and the small range of tissue health. The histology blocks were quite large (one seventh of the size of the meniscus) and often encompassed several of the biochemical plugs. Several sections were taken from each block but the exact location on the meniscus was difficult to discern and so only

estimates could be made as to their relation to the biochemistry samples. Table 4.8 shows eight samples with their biochemical content related to their histological score, four of which are relatively healthy (histological grades 1 and 2) with the remaining being more degenerated (grades 2 and 3). From this table, it can be seen that there are some noticeable differences between the two groups. The more damaged group has slightly higher liquid contents and overall lower amounts of both sGAG and collagen when compared to the healthy group. Although this does align with what would be expected, a more precise system for equating the different sample type locations would be beneficial to ensure a relationship between diminishing biochemical properties and higher histological scores exists and would also allow the quantification of this relationship.

TABLE 4.8: COMPARISON BETWEEN HISTOLOGY AND BIOCHEMISTRY RESULTS FOR A SMALL SAMPLING OF DATA WITH DIFFERING TISSUE HEALTH

Biochemistry Sample Label*	Corresponding Histology Block*	Histology Score	Liquid content (%)	Percentage of sGAG per dry weight (%)	Percentage of sGAG per wet weight (%)	Percentage of collagen per dry weight (%)	Percentage of collagen per wet weight (%)
K1M2	K1MP	G3	80.6	1.68	0.326	113	22.0
K1M5	K1MA	G2/G3	71.1	1.59	0.458	42.9	12.4
K2M3	K2MP	G2/G3	79.4	1.30	0.267	109	22.6
K2L4	K2LA	G3	83.4	0.752	0.125	124	20.6
K3L4	K3LA	G1/G2	73.9	1.78	0.464	132	34.4
K4M3	K4MP	G1	79.6	1.94	0.396	118	24.0
K5M8	K5MA	G1	71.7	3.00	0.846	112	31.6
K6L4	K6LA	G1	69.5	1.10	0.335	93.9	28.7

Red grouping represents more histologically damaged samples (grades 2 and 3) while green block represents healthier samples (grades 1 and 2).
*Sample labelling is as follows: Kx is knee number x, M/L is medial or lateral, biochemistry – last number is the sample number taken from that specimen, histology – A=anterior, P=posterior

4.5. Limitations of the cadaver study

The largest limitation of this study was the relatively homogeneous nature of the specimens. This limited the range of results in all the qMT parameters and tissue properties, and likely reduced the strength and quantity of correlations. A larger variety of tissue health could elucidate further relationships. However, this work establishes a healthy baseline dataset which is essential as research progresses to diseased tissues.

Another limitation was the nature of the histology sample procurement. Due to the fact that the histology samples were large radial blocks, many sections could be taken representing the condition of the entire cross-section of tissue. Unfortunately, the close proximity of the slices may have led to some of the histology results being correlated to each other and therefore not being as independent as desired. Furthermore, it was also difficult to directly connect the histology results to the biochemistry, which was a secondary outcome of my work. However, the primary goal was to investigate relationships between the biochemistry and histology results and the qMT parameters of the tissue. My methodology allowed for this to be accomplished and therefore the results obtained are still valuable.

4.6. Cadaver study conclusion

My study is the first to compare the biochemical and histological properties to the qMT parameters in the meniscus. My correlations align with the only other study in meniscus to compare biochemical properties and qMRI [16] and I found stronger relationships between histological score and qMT parameters than the only other meniscus study to compare histology to qMRI [71]. These findings show the potential value of qMT parameters in assessing tissue content and structure, but further work must be done to include a larger spectrum of tissue health and validate the relationships observed in this study.

5. qMT MRI of Articular Cartilage and Meniscus in Total Knee Arthroplasty Patients

5.1. Introduction to the TKA study

The TKA study assessed a population experiencing end stage OA; the objective of this part of my project was to evaluate qMT MRI as a non-invasive marker of articular cartilage and meniscus tissue content (biochemical properties), structure (histology score), and function (mechanical properties) in an end stage OA population (TKA patients) and to compare qMT results between *in vivo* and *ex situ* scanning environments.

Logistically, it is much easier to image specimens *ex situ* than *in vivo* as patient recruitment, movement, and scanning time do not limit acquisition or image quality. However, it is unknown how the qMT parameter values change in these different environments. This is necessary to determine in order to understand the applicability of *ex situ* or *in situ* results to *in vivo* situations. Only one other study in the literature compared *in situ* to *ex situ* meniscus qMT parameters, and they found significant variations in most parameters[20]. None of the cartilage qMT studies performed any scanning environment comparisons, which is a major gap in the literature that my project begins to fill.

There is also limited information on qMT in both cartilage and meniscus of the knee in general. Only two meniscus qMT studies have been published[20,141], and only three with reported qMT parameters in cartilage[18–20]. Of these cartilage studies, only one compares the qMT parameters of asymptomatic participants to OA patients and it is patellar cartilage being assessed[19]. The Simard and Stikov studies include tibial cartilage qMT values in healthy populations with the scanning environments being *in situ* and *ex situ,* respectively. Knowledge about qMT parameters in OA tibial cartilage as well as meniscus is currently lacking. This is why my project is necessary, to begin to understand the qMT parameters of damaged tissue.

It is important to reiterate that this study is incomplete due to impacts caused by the global COVID-19 pandemic. The intended participant size for this study was originally 10 or more patients, but only 2 were able

to be recruited before the pandemic began. Preliminary results have been provided but this project requires more data in order to confirm the relationships observed with the limited sample size.

5.2. Methods specific to the TKA study

The TKA project involved acquiring meniscal and tibial cartilage tissue for mechanical testing, histology and biochemistry (Figure 5.1). Prior to TKA surgery, patients were scanned using the custom qMT MRI protocol outlined in section 3.1 (qMT image acquisition) and after surgery, tibial plateaus with menisci attached were retrieved and scanned using the same protocol (excised tissue). Mechanical indentation testing was performed, then small samples were procured from the tissue specimens for histological and biochemical testing. Finally, the mechanical, histological and biochemical data were registered to the image data so that relationships could be studied. This section describes the specifics of patient recruitment, specimen retrieval, *ex situ* scanning, the process of procuring samples for biochemistry and histology, mechanical testing using the Mach-1, creation of 3D surface models for registration, and the statistical methods used in this study. All other methods can be found in section 3. General Methodology.

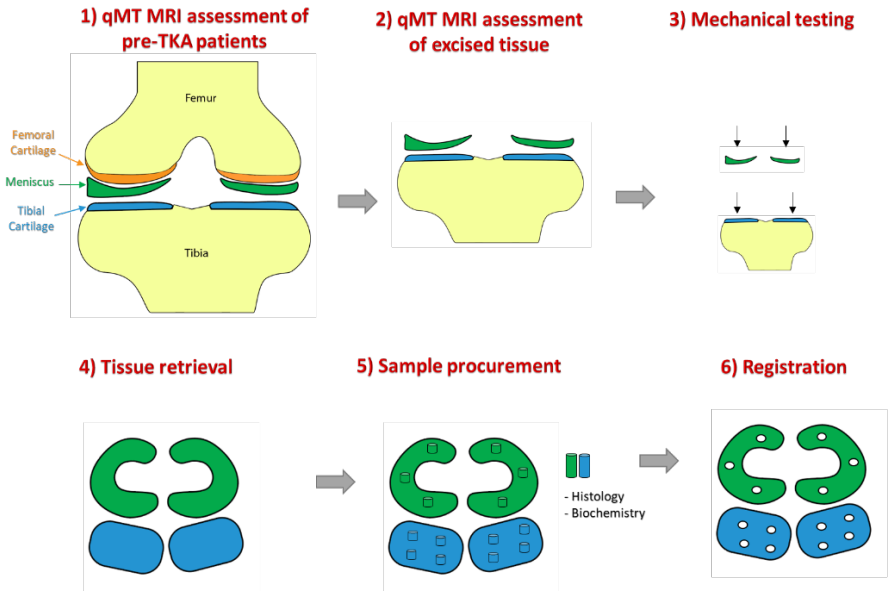

FIGURE 5.1: OVERALL TKA STUDY METHODOLOGY. ***(1) PRIOR TO TKA, PATIENTS UNDERWENT MRI ASSESSMENT. (2) AFTER SURGERY, EXCISED TIBIAL PLATEAUS WITH ATTACHED MENISCI WERE SCANNED AGAIN. (3) MECHANICAL TESTING. (4) TISSUE RETRIEVAL. (5) SMALL SAMPLES WERE PROCURED FROM THE TISSUE SPECIMENS FOR TESTING. (6) REGISTRATION OF MECHANICAL, HISTOLOGICAL, AND BIOCHEMICAL VALUES TO LOCATION OF SAMPLES FOLLOWED.***

5.2.1. Patient recruitment

The participants recruited for this study were undergoing TKA for treatment of end stage OA. They were recruited through Dr. William Dust's orthopedic clinic. Only patients living within Saskatoon and surrounding municipalities were included for feasibility purposes. From this criterion, eight potential participants were approached during a pre-assessment appointment scheduled a few weeks before the surgery. To be eligible, participants had to be receiving TKA surgery for treatment of OA and could not have any contraindications for MRI (listed in Appendix B: MRI screening form). Of the eight, two were eligible and agreed to take part in the study. The study protocol was approved by the University of Saskatchewan Biomedical Research Ethics Board (Appendix F: TKA Study Ethics Certificate) and both participants provided informed consent (Appendix C: Consent form).

5.2.2. *In vivo* participant qMT MRI scanning

For the TKA study, the pre-surgery MRI scan was carried out on the 3T MRI scanner (MAGNETOM Skyra, Siemens, Erlangen, Germany) at Royal University Hospital in Saskatoon using the sequence outlined in section 3.1 (qMT image acquisition) and at the time of scanning, patients were given a demographic questionnaire (Appendix D: Participant demographic survey) and a Knee Injury and Osteoarthritis Score (KOOS) survey (Appendix E: KOOS pain survey) to complete. Participants were scanned in a feet-first supine position with a standard knee coil positioned by an MRI technologist.

5.2.3. Specimen retrieval

The patient's tibial plateau with any present menisci were removed as a part of the standard surgical procedure; these specimens would usually be disposed of as surgical waste. One tibial plateau had both medial and lateral menisci attached and the other had only the lateral (it is believed the medial meniscus had been removed in a previous meniscectomy surgery). Specimens were placed in a jar containing phosphate buffered saline (PBS) with protease inhibitors (5 mM benzamidine hydrochloride and 5 mM ethylenediamine tetraacetic acid) immediately after removal and refrigerated as soon as possible (within 12 hours of removal).

5.2.4. *Ex Situ* specimen qMT MRI scanning

After specimens were retrieved from Dr. Dust, they were promptly prepared to be scanned (within approximately less than 8 hours) using a 3T MRI scanner (MAGNETOM Skyra, Siemens, Erlangen, Germany) *ex situ*. A custom designed, MRI safe sample holder was utilized for this. Specimens were first fixed to a hockey puck using ethyl cyanoacrylate adhesive (Gorilla Glue, Maine Wood Concepts, Sharonville, OH, USA). A hockey puck was used because it provided a stiff underlying surface that would not interfere with the mechanical testing results, and it was also MRI compatible (no metal components). The hockey puck had been previously secured to the lid of a wide mouth 16 oz plastic jar that had three nylon bolts protruding from it for attachment to the Mach-1 mechanical testing system (discussed in section 5.2.5.Mechanical testing) (Figure 5.2). The plastic container was filled with perfluorooctyl bromide (CAS# 423-55-2, Exfluor Research Corporation, Round Rock, TX, USA) and the lid with the specimen attached was sealed. Perfluorooctyl bromide is a fluid without hydrogen, hence providing no signal on MRI. Specimens were immersed in perfluorooctyl bromide in order to minimize susceptibility artifacts caused by the tissue-air interface without affecting the dynamic range of the tissue signal in the image. Fluids containing hydrogen, such as PBS, would appear very bright on the images and make it difficult to delineate tissues with similar contrasts during segmentation. Furthermore, the mechanical properties of both cartilage and meniscus are known to change depending on the concentration of PBS the samples are stored and tested in, so even using PBS would result in changes to the properties of the tissue[162,163]. Perfluorooctyl bromide was chosen because the benefit of improved contrast for segmentation outweighed the drawback of not scanning in a liquid more representative of the original synovial fluid present. After preparation, the container was refrigerated until scanning later the same day.

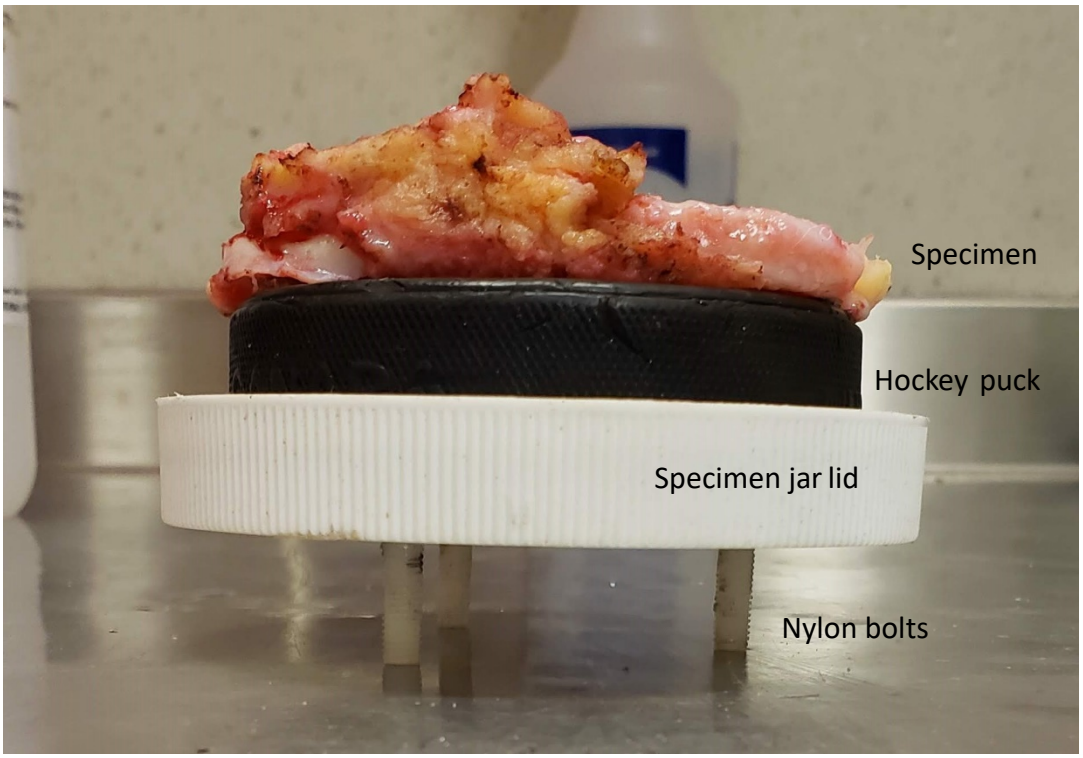

FIGURE 5.2: SPECIMEN SET-UP FOR MRI SCANNING OF TKA SAMPLES

For imaging, the qMT MRI protocol (section 3.1) was repeated exactly using a standard knee coil. In order to reduce the magic angle effect, specimens were oriented perpendicular to the main magnetic field, just as if they were still in the body and being scanned in a foot-first, supine position. After scanning, perfluorooctyl bromide was drained and tissues were stored in PBS and refrigerated until mechanical testing.

5.2.5. Mechanical testing using the Mach-1

Indentation testing was carried out using a commercial, soft tissue testing system (Mach-1, Biomomentum Inc, Laval, QC) (Figure 5.3). This apparatus is a multi-axis mechanical tester developed initially for articular cartilage testing; it is capable of testing small specimens (dimensions from microns to a few centimeters) that allows for the characterization of several biological tissue mechanical properties[164,165]. It is able to perform tension, shear, compression, and torsion tests on cartilage and other soft tissues as well as automatically map the corresponding mechanical properties along the full tissue surface[165]. The motion controller paired with motion software moves the stage up and down, front to back, and left to right in order to position the specimen

appropriately for testing. Specimens can be loaded into the pictured testing chamber for indentation testing (Figure 5.3) and a spherical indenter attached, or a confined compression chamber can be attached. The Indenter can be lowered to an ideal spot on the testing frame to allow the specimen to fit. For thickness testing, the spherical indenter can be removed and replaced with an attachment which connects to a needle. This equipment has been used previously for mechanical testing of both cartilage and meniscus [166–168].

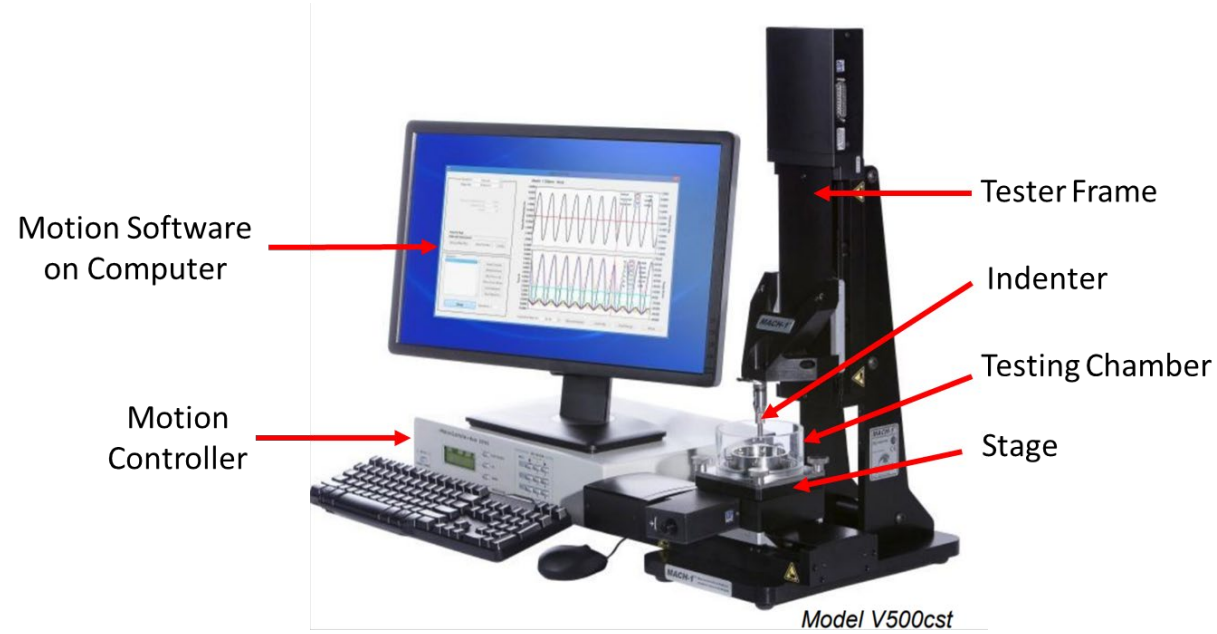

FIGURE 5.3: MACH-1 MECHANICAL TESTING SYSTEM SET-UP (MACH-1, BIOMOMENTUM, LAVAL, QC, CANADA). IMAGE COPYRIGHT 2013 BIOMOMENTUM.

For cartilage and meniscus testing, the samples had to be secured to the mechanical testing system. For cartilage testing, the menisci were carefully removed from the tibial plateau by using a scalpel to detach the collateral ligaments and dissect the edges. No magnification was used but care was taken to prevent inadvertent cuts to the surfaces, although some minor nicks may have occurred during dissection or surgery. Detached menisci were stored in PBS and the remaining specimen (still fixed to a hockey puck and plastic container lid) was attached to the testing platform by nylon nuts secured around the nylon bolts. For meniscus testing, the tibial plateau was removed from the hockey puck and replaced by the menisci specimens. Superglue (Gorilla Glue, Maine Wood Concepts, Sharonville, OH, USA) was used around the edges of the

bottom of the menisci to adhere them to the puck. The testing platform was then screwed onto the base of the testing chamber and the plastic liquid retainment lid was attached (Figure 5.4). The entire chamber was secured onto the Mach-1 tester and the standard operating procedures were followed for calibration and testing (summarized in Appendix G: Mach-1 Indentation Testing SOP).

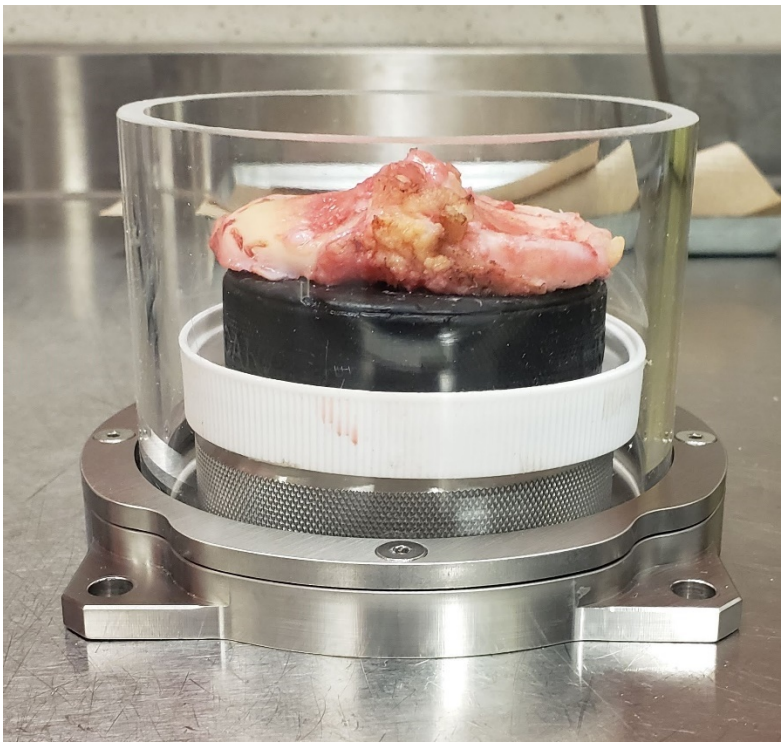

FIGURE 5.4: SPECIMEN IN MACH-1 TESTING CHAMBER FOR CARTILAGE MECHANICAL TESTING

The first step was to specify the points on the specimen at which data would be collected. This was done by using the built-in mapping software. This software allowed a grid to be superimposed over an image of the sample's surface, and discrete points over the entire surface to be selected for analysis (Figure 5.5). A boundary was manually specified along the outside of the sample (black line) and testing points manually selected on the tissue. Any points of denuded cartilage (i.e., just bone) were excluded from data collection. When the data points were selected and their locations saved, the indentation test was performed.

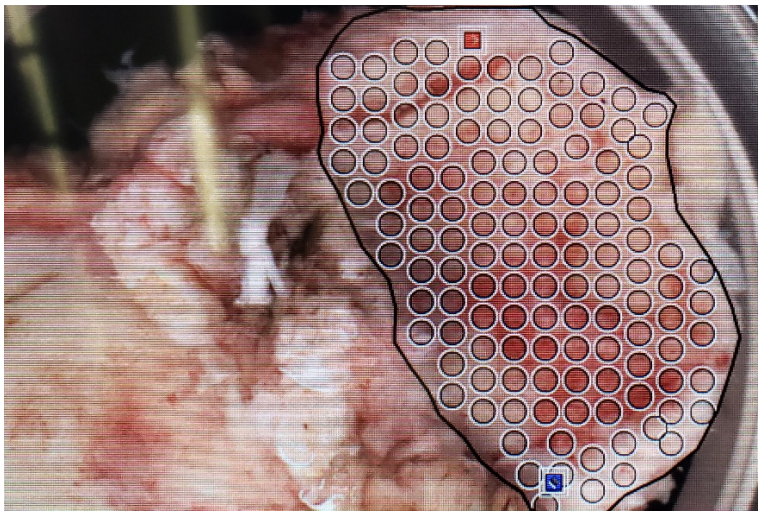

FIGURE 5.5: SAMPLES SELECTED FOR ANALYSIS USING THE MACH-1 MAPPING TOOLBOX SOFTWARE

In order to calculate mechanical properties of the tissue both indentation and thickness data were required. This was accomplished in two separate tests, indentation and thickness. The indentation test utilized a 2 mm diameter spherical indenter to compress the tissue at a constant rate until a specified displacement was reached (Table 5.1). While the tissue was being compressed, the force experienced by the indenter was recorded.

TABLE 5.1: MACH-1 PARAMETERS SPECIFIED FOR TISSUE INDENTATION TESTING

Parameter:	**Value*:**	**Parameter description:**
Z-contact velocity	0.2 mm/s	Velocity of the vertical stage while indenter finds tissue surface
Contact criteria	0.03145 N	Force required to assume contact (the point at which the indenter reaches the tissue surface)
Stage limit	30 mm	Vertical distance the stage will travel before it aborts the test due to not being able to find the surface
Scanning grid	0.2 mm	Horizontal distance indenter will move from the original point of interest in order to map the surroundings and determine the angle of the surface
Indentation amplitude	0.2 mm	Displacement that is applied to the point of contact
Indentation velocity	0.1 mm/s	How fast the displacement is applied
Relaxation time	5 s	Amount of time given for the sample to relax after displacement is reached
Gap distance from surface	0.2 mm	The indentation is started at this specified distance above the tissue. This allows the exact moment of contact to be captured
* Values in this table were selected based on recommendations from Biomomentum from previous studies they had carried out on similar tissues[167,169]		

After the indentation test was performed, thickness data had to be collected for each point. The thickness test was very similar to the indentation experiment except instead of the spherical indenter, a needle was used. In this test, the stage moved the needle downwards at a constant velocity and stopped when a set maximum load was reached (Table 5.2). This maximum load was the point at which the needle had fully penetrated the cartilage or meniscus and reached the underlying subchondral bone or hockey puck. Throughout the test, the vertical position of the needle and the force it was experiencing was measured so that the point at which it first contacted the tissue and subsequently reached the hard-underlying surface could be used to determine tissue thickness by the product analysis software.

TABLE 5.2: MACH-1 PARAMETERS SPECIFIED FOR TISSUE THICKNESS TESTING

Parameter:	**Value chosen*:**	**Parameter description:**
Contact criteria	5.0014 N	Force required to assume contact with underlying bone or surface below tissue
Stage Velocity	0.2 mm/s	Speed at which stage (and therefore needle) is moved vertically downwards
Stage Limit	30 mm	Vertical distance the stage will travel before it aborts the test due to not being able to find the surface
Stage repositioning	2X load resolution	This setting controls the position that the stage is brought back to before moving on to the next data point. 2X load resolution brings the stage back to the location at which the change in load was twice the resolution of the load cell (where the surface of the tissue was detected)
* Values in this table were selected based on recommendations from Biomomentum from previous studies they had carried out on similar tissues[167,169]		

In order to extract the mechanical properties from the raw indentation and thickness data, the product analysis software was used. Firstly, the surface angles for each data point were recorded from the indentation test data. This parameter was determined by the software based on the locations of four test points around each data point (scanning grid). Next, the vertical thickness of each data point was determined and then the tissue thickness was calculated using $tissue\ thickness = vertical\ thickness \times \cos(surface\ angle)$. Lastly, the mechanical properties were calculated by fitting the indentation test results, thickness results, and prescribed

parameters (Table 5.3) to the Hayes elastic model[88]. This gave the instantaneous modulus (IM) and elastic fit mean squared error for each data point.

TABLE 5.3: PARAMETERS CHOSEN FOR MACH-1 INDENTATION ANALYSIS

Parameter:	**Value:**
Indenter radius	0.5 mm
Poisson ratio	0.5
Position at contact is	The following value = 0.2 * The position of the left cursor in the analysis program. This is where the curve fit starts.
Sample thickness is	The following value = (varies) * Thickness was input for each specific point (from thickness test analysis)
Curve fit is up to	Delta position (mm) = 0.1 * The position of the right cursor in the analysis program. This is the length of the curve fit.

5.2.6. Sample retrieval for biochemistry and histology

Core samples were retrieved to be used in the biochemical and histological analyses. Locations of samples were strategically selected to include regions that appeared more and less damaged; and as many samples were obtained as could reasonably be extracted (Figure 5.6). For histology, a 6 mm biopsy punch was used to excise cylindrical samples (excluding bone in the case of cartilage). The use of cylindrical samples rather than radial pieces did not impact the scoring method, except for the exclusion of the inner border criteria. All cylindrical histology samples were marked with a small amount of tissue dye (Thermo Scientific Mark-It tissue dye, Catalog No. 22-050-459, Waltham, MA, USA) to identify the orientation of the sample (marked on femoral facing side). A 2 mm biopsy punch was then used to extract the biochemistry samples as close to the histology sample as possible. Samples were stored in vials containing PBS and frozen until processing. The locations of the samples were recorded and photographed with the mechanical testing system's built-in camera. The mechanical testing system's mapping toolbox was also used to identify the locations of samples for registration purposes.

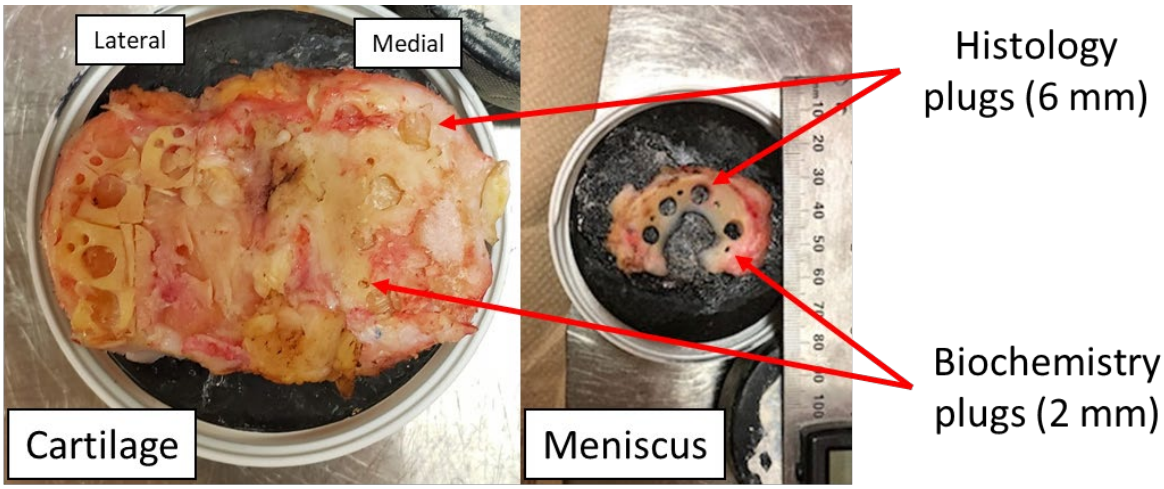

FIGURE 5.6: CARTILAGE SURFACE (LEFT) AND LATERAL MENISCUS SURFACE (RIGHT) AFTER SAMPLES REMOVED FOR BIOCHEMISTRY AND HISTOLOGY. ON THE CARTILAGE SURFACE, TAN COLORED TISSUE IS THE CARTILAGE WHILE THE PINK AND RED AREAS ARE SUBCHONDRAL BONE. PINK AREAS OF THE MENISCUS ARE THE SURROUNDING LIGAMENTS.

5.2.7. Creation of surface and sample models

In order to determine the qMT parameters at the sample locations, 3D models of the tissue surface, segmentation masks, and sample cylinders were required. For the model of the tissue surface, the XYZ data was obtained from the mechanical testing system. Custom software (MATLAB, MathWorks, Natick, MA, USA) was developed to find the point at which the needle contacted the tissue surface during the thickness test for each data point. This was determined by finding the point at which the change in force was greater than 0.03 N (Figure 5.7), which gave the vertical location of the point at which the needle contacted the tissue surface, effectively representing the top surface of the tissue. The X&Y coordinates at each of these points was also known, and so the 3D location of each point was compiled into a list. This list, representing the locations of each of the data points collected during the mechanical testing, was imported into SolidWorks (Dassault Systèmes, Vélizy-Villacoublay, France) and the scan to 3D add on was utilized in order to convert the 3D point cloud into a mesh body representative of the surface of the tissue.

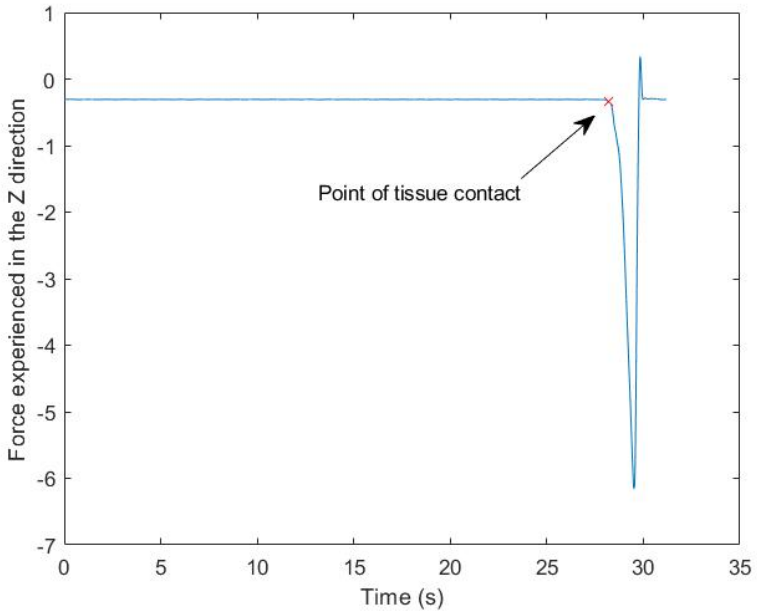

FIGURE 5.7: PLOT OF THE FORCE EXPERIENCED IN THE Z DIRECTION BY THE MACH-1 INDENTER OVER TIME FOR FINDING THE POINT OF CONTACT OF THE INDENTER WITH THE TISSUE. THE UNITS OF THE FORCE IN THIS FIGURE DO NOT HAVE MEANING BUT REPRESENT THE FORCE EXPERIENCED IN NEWTONS.

This mesh body was imported into modeling software Fusion 360 (Autodesk, San Rafael, USA) and overlaid on the 3D point cloud. The overlay allowed for more accurate knowledge of the location of the data points along the surface. Based on the positions of these points on the surface and the fact that the biochemistry and histology sample locations were known in relation to the mechanical testing points (specimens photographed after sample retrieval in the mechanical testing system), virtual cylinders of appropriate size (6 mm diameter for histology and 2 mm diameter for biochemistry) were constructed and made long enough to ensure they would go through the entire thickness of the tissue at each sample location. These cylinders were then imported into another modeling software (Geomagic, Geomagic, Morrisville, USA) to increase the number of points in the cylinder to help with subsequent registration.

Lastly, it was necessary to obtain a surface model of the cartilage and meniscus segmentation. This was achieved using only the image processing software (Analyze 14.0, Mayo Clinic, Rochester, USA). After all the models had been created, it was possible to move on to the registration step. Prior to registration in this study,

the qMT parameters were filtered. Details of this are included in Appendix J: qMT parameter filtering prior to registration for the TKA study.

5.2.8. Statistical analysis specific to the TKA study

Descriptive statistics (means, standard deviations, and grade frequencies for histology) were determined for all qMT parameters and tissue properties, Wilcoxon signed ranks tests were performed to compare the *in vivo* qMT results to the *ex situ,* Pearson's product moment correlation coefficients were determined for the correlations between the qMT parameters and the biochemistry and mechanical properties, and Spearman's rho for the qMT to histology score relationships (Table 5.4). The correlation analysis was divided into several groups and where possible within these groups, the data was further separated into the medial and lateral sides. Correlations were determined between the qMT parameters and the corresponding tissue properties in the following groups: cartilage mechanical property samples, meniscus mechanical property samples, cartilage biochemistry content samples, meniscus biochemistry content samples, cartilage histology samples, meniscus histology samples, and the average value for each property across each individual surface (N=7). Although the last correlation listed combined meniscus and cartilage surfaces into the same analysis, the goal was to investigate overall relationships between the qMT parameters and tissue properties.

TABLE 5.4: LIST OF STATISTICAL METHODS USED TO PERFORM THE VARIOUS ANALYSES IN THE TKA STUDY

Analysis	Statistical Method
Comparison of qMT results *in vivo* to *ex situ*	Wilcoxon Signed Ranks Test
Correlations between mechanical properties and qMT parameters	Pearson product moment correlation
Correlations between biochemical properties and qMT parameters	Pearson product moment correlation
Correlations between histology results and qMT parameters	Spearman's rho correlation
Correlations between average surface tissue properties and qMT parameters (N=7 surfaces)	Pearson product moment + Spearman's rho corelations

5.3. Results of the TKA study

In total, seven tissue surfaces from two knees were analyzed for this study: 4 tibial cartilage (2 medial and 2 lateral) and 3 menisci (1 medial and 2 lateral). Sample sizes for the tissue property tests varied for each surface and depended on the condition and shape of each region (Table 5.5).

TABLE 5.5: NUMBER OF SAMPLES FOR EACH KNEE AND SIDE FOR THE TISSUE PROPERTY TESTS PERFORMED IN THE TKA STUDY

		Knee 1			Knee 2		
	Sample type	**Medial**	**Lateral**	**Total**	**Medial**	**Lateral**	**Total**
Cartilage	Mechanical	77	95	172	54	64	118
	Thickness	100	105	205	60	73	133
	Biochemical	6	7	13	4	4	8
	Histology	5	7	12	4	4	8
Meniscus	Mechanical		20	20	9	17	26
	Thickness		22	22	9	19	28
	Biochemical		4	4	2	3	5
	Histology		4	4	2	3	5

5.3.1. qMT imaging parameters *in vivo* versus *ex situ*

Upon statistical comparison of the seven *in vivo* to *ex situ* global surface qMT results from the two knees, significant differences between groups were found for T_1obs, T_{1f}, T_{2f}, and T_{2b}, but not for f or k_f (Table 5.6). Differences were especially pronounced for T1f and T2f (Figure 5.8). In cartilage, T_1obs varied from an average of 1126 ms *in vivo* to 721 ms *ex situ*, T_{1f} from 1211 ms to 632 ms, T_{2f} from 29.5 ms to 4.9 ms, and T_{2b} from 6.60 µs to 5.48 µs. In meniscus, T_1obs varied from 1058 ms *in vivo* to 798 ms *ex situ*, T_{1f} from 1085 ms to 743 ms, T_{2f} from 17.9 ms to 6.6 ms, and T_{2b} from 8.53 µs to 5.05 µs. Values generally trended higher in the medial side than lateral for T1obs, T2f, T2f, and T2b, as well as the f and kf of cartilage, but the f and kf of meniscus trended higher in the lateral side than the medial. Full results are located in Appendix K: qMT imaging results of the TKA study – *in vivo* and *ex situ*.

TABLE 5.6: WILCOXON SIGNED RANKS TEST RESULTS FOR COMPARISON OF THE *IN VIVO* TO *EX SITU* QMT PARAMETER RESULTS

	T_1obs	T_{1f}	T_{2f}	T_{2b}	f	k_f
Z*	-2.366	-2.366	-2.366	-2.028	-0.676	-1.859
Asymp. Sig. (2-tailed)	0.018	0.018	0.018	0.043	0.499	0.063
*Based on positive ranks						

FIGURE 5.8: BAR GRAPHS COMPARING *IN VIVO* TO *EX SITU* QMT PARAMETERS ACROSS SURFACES FOR THE TKA STUDY

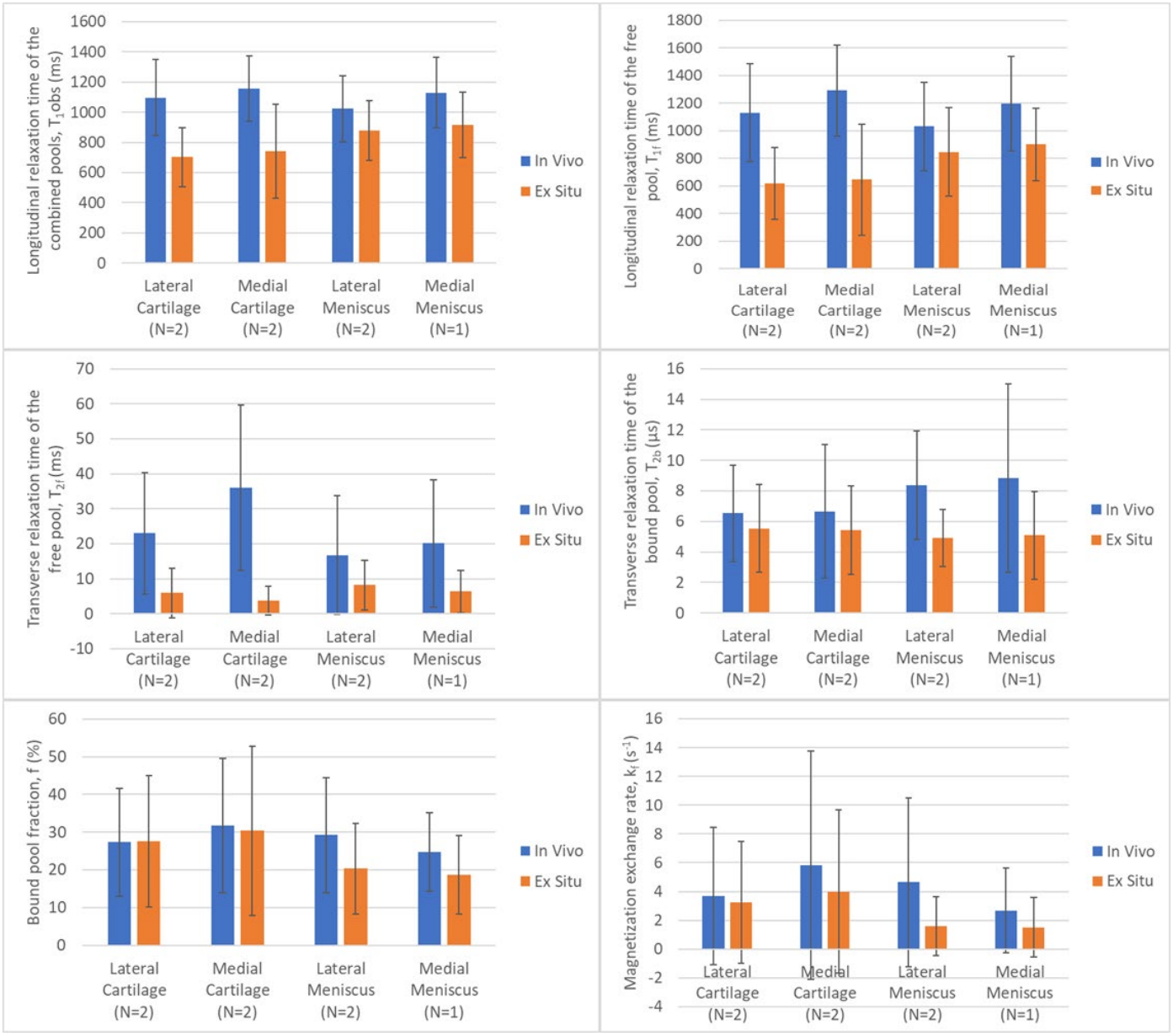

5.3.2. Mechanical testing results

Properties determined for the cartilage and meniscus TKA samples in the mechanical testing were the instantaneous modulus and tissue thickness. These results were correlated to the qMT parameters using Pearson product moment correlation coefficients.

5.3.2.1. Instantaneous modulus results

Instantaneous modulus values in the cartilage ranged from 0.29-1.35 MPa and trended higher than those in the meniscus (0.12-0.23 MPa). In the cartilage samples, values trended higher in the lateral side than the medial (Table 5.7). In knee two, the lateral instantaneous modulus (0.49 ± 0.65 MPa) was very close to that of the medial (0.44 ± 0.51 MPa); while in knee one, the lateral (1.35 ± 1.94 MPa) appeared much higher than the medial side (0.29 ± 0.37 MPa). For the menisci, the results were relatively close for all surfaces; but similar to the cartilage, the lateral side had higher trending values than the medial. The highest values were seen in the lateral meniscus of knee two (0.23 ± 0.26 MPa) and the lowest in the medial meniscus of knee two (0.12 ± 0.08 MPa). The elastic fit mean squared error (a dimensionless number representing the error on the fitting of the stress-relaxation curve) was relatively small in all surfaces, indicating the Hayes model[88] is a good fit for the data. Thickness results are located in Appendix L: Thickness testing results for the TKA study.

TABLE 5.7: AVERAGE MECHANICAL PROPERTY RESULTS FOR THE TKA STUDY

Cartilage						
Side	Knee	Instantaneous Modulus		Elastic fit mean squared error		N
		Mean (MPa)	Standard deviation	Mean	Standard deviation	
Lateral	1	1.35	1.94	0.83	1.55	95
	2	0.49	0.65	0.17	0.34	64
Medial	1	0.29	0.37	0.05	0.12	77
	2	0.44	0.51	0.08	0.19	54
Meniscus						
Side	Knee	Instantaneous Modulus		Elastic fit mean squared error		N
		Mean (MPa)	Standard deviation	Mean	Standard deviation	
Lateral	1	0.17	0.11	0.01	0.01	20
	2	0.23	0.26	0.01	0.01	17
Medial	1					
	2	0.12	0.08	0.01	0.00	9

A color map showing the distribution of the instantaneous modulus over one surface is shown in Figure 5.9. This map shows that the instantaneous modulus is lower in the middle part of the tibia, which is where direct contact between the femur and tibial cartilage occurs; and higher near the outside where the meniscus covers the cartilage and absorbs some of the load. Maps of the remaining knees (including thickness distribution) can be found in Appendix M: Mechanical testing results color maps for TKA study.

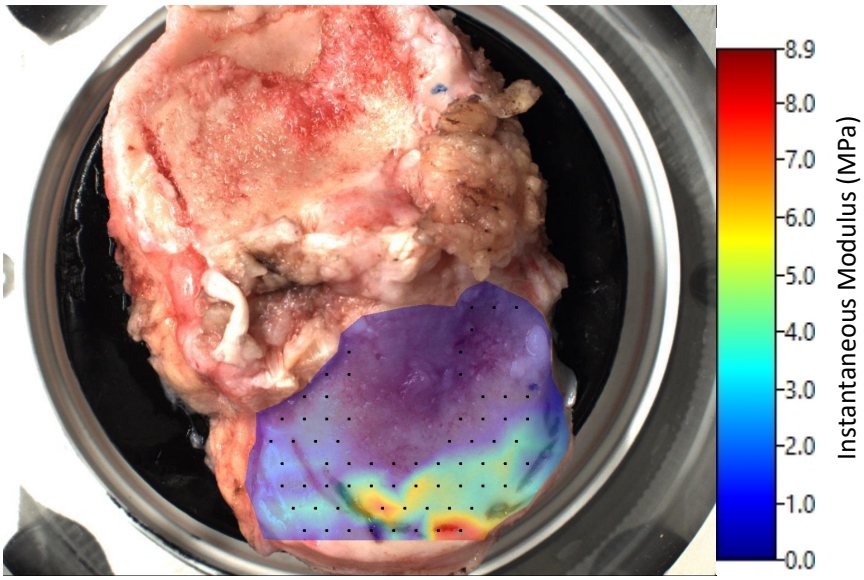

FIGURE 5.9: COLOR MAP SHOWING VARIATION OF INSTANTANEOUS MODULUS VALUES ACROSS THE SURFACE OF THE LATERAL CARTILAGE OF KNEE 1

5.3.2.2. Instantaneous modulus correlations to qMT parameters

In the lateral *in vivo* cartilage, as the instantaneous modulus increased, there was a decrease in the T_1obs ($r = -0.218$, $p < 0.05$), T_{1f} ($r = -0.221$, $p < 0.05$), and T_{2f} ($r = -0.233$, $p < 0.05$), all of which showed weak correlations. No significant correlations were found between these properties and any of the qMT parameters in either the combined or medial sides (Appendix N: Correlation coefficient tables for the TKA study Table N.1).

In the *ex situ* meniscus samples, one moderate correlation was found: as instantaneous modulus decreased, T_{2f} increased ($r = -0.563$, $p < 0.05$). Correlations with qMT parameters and the thickness results can be found in Appendix N: Correlation coefficient tables for the TKA study.

5.3.3. Biochemistry results

Average water content in the articular cartilage samples was 80.0%, with the medial side (80.8%) being about the same as the lateral (79.3%) (Table 5.8). While the sGAG amounts trended much higher in the medial side than the lateral (14.0 ± 6.93 % vs 9.54 ± 3.33 % respectively, for sGAG/dry mass), the opposite was observed for collagen, where the data trend indicated higher amounts in the lateral side (62.3 ± 23.5 % in medial and 65.7 ± 27.0 % in lateral for collagen/dry mass).

The meniscus samples followed the same trends as cartilage (Table 5.8). The liquid content again appeared to be higher in the medial side (80.8 ± 1.12 % vs 76.9 ± 4.98 % in the lateral side). For the sGAG content, the medial side also showed a trending higher concentration at 4.81 ± 0.156 % sGAG/dry mass than the lateral side (3.08 ± 1.20 %). The most interesting finding however was the collagen per dry mass results. In the medial side, the average amount of collagen per dry mass was 57.8 ± 0.901 % but in the lateral side, it trended much higher at 84.8 ± 20.4 %. It is also important to note however that there were only two samples available to assess from the medial side as opposed to the seven lateral samples, which may not give a complete picture of the medial versus lateral meniscus comparison.

TABLE 5.8: AVERAGE BIOCHEMISTRY RESULTS FOR THE TKA STUDY

	Cartilage						Meniscus					
	Both sides combined (N=21)		Medial (N=10)		Lateral (N=11)		Both sides combined (N=9)		Medial (N=2)		Lateral (N=7)	
	Mean	Standard deviation	Mean	Standard deviation	Mean	Standard deviation	Mean	Standard deviation	Mean	Standard deviation	Mean	Standard deviation
Liquid content (%)	80.0	4.00	80.8	3.44	79.3	4.31	77.7	4.71	80.8	1.12	76.9	4.98
Solid content (%)	20.0	4.00	19.2	3.44	20.73	4.31	22.3	4.71	19.2	1.12	23.1	4.98
sGAG per dry mass (%)	11.7	5.80	14.0	6.93	9.54	3.33	3.47	1.28	4.81	0.156	3.08	1.20
sGAG per wet mass (%)	2.26	0.91	2.54	0.938	2.00	0.795	0.769	0.327	0.926	0.0836	0.725	0.356
Collagen per dry mass (%)	64.1	25.5	62.3	23.5	65.7	27.0	78.8	21.2	57.8	0.901	84.8	20.4
Collagen per wet mass (%)	13.7	6.45	13.3	4.69	14.1	7.69	15.4	5.46	11.1	0.819	16.6	5.60

5.3.3.1. Biochemistry property correlations to qMT parameters

In the *in vivo* lateral cartilage, very strong, significant correlations were found between the T_{1f} and both the liquid and solid contents (correlation coefficients were equal, with correlations between liquid content being positive and solid content being negative) (Figure 5.10) (Table N.3 Correlation coefficient tables for the TKA study). A correlation analysis could not be performed for the *in vivo* medial or either *ex situ* surfaces because there were only three samples with both qMT and biochemistry results in these regions (N=3), but scatterplots showing trends are located in Appendix O: Correlation scatterplots for TKA data with N=3 and N=2 sample sizes: Figure O.1, Figure O.2, and Figure O.3.

FIGURE 5.10: VERY STRONG CORRELATION BETWEEN T_{1F} AND LIQUID CONTENT FOR *IN VIVO* LATERAL CARTILAGE

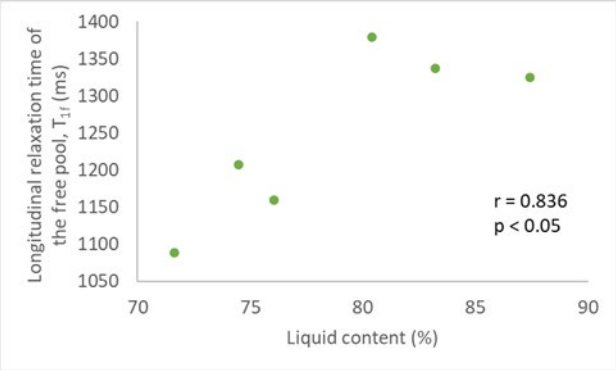

For the meniscus, the *in vivo* analysis included six samples and four very strong significant correlations were found (Appendix N: Correlation coefficient tables for the TKA study Table N.4). As liquid content increased, and solid content decreased, k_f was found to decrease ($r = -0.890$, $p < 0.05$ and $r = 0.890$, $p < 0.05$ respectively). With increasing T_{2b}, sGAG per dry mass increased ($r = 0.869$, $p < 0.05$) along with sGAG per wet mass ($r = 0.846$, $p < 0.05$). The *ex situ* only had two samples with corresponding qMT data and so a correlation analysis could not be performed. Scatterplots indicating potential trends in this data are shown in Appendix O: Correlation scatterplots for TKA data with N=3 and N=2 sample sizes Figure O.4.

5.3.4. Histology results

In general, the histology samples for the full articular cartilage displayed severe damage, with the majority being above a grade and score of 3 (G3S3) (Table 5.9). The medial side samples have no instances of any scores less damaged than G3S4 while the lateral group has 44% of their samples in the G0 and G1 range. Despite this, most of the samples on the lateral side were severely damaged with scores in the G4.5 range and one instance of G3.5S4. Examples of each grade are shown in Figure 5.11.

TABLE 5.9: CARTILAGE HISTOLOGY RESULTS FOR THE TKA STUDY

Combined (N=20)							
Grade	Stage					Frequency (N)	Percentage (%)
	S0	S1	S2	S3	S4		
G0	3	0	0	0	0	3	15
G1	0	1	0	0	0	1	5
G2	0	0	0	0	0	0	0
G3	0	0	0	0	1	1	5
G3.5	0	0	0	0	3	3	15
G4	0	0	0	1	1	2	10
G4.5	0	0	0	3	7	10	50

* Grade is the progression of OA into the cartilage (normal cartilage = G0)[128]
* Stage is the horizontal extent of joint involvement (no disease activity = S0)[128]

Medial (N=9)								Lateral (N=11)							
Grade	Stage					Frequency (N)	Percentage (%)	Grade	Stage					Frequency (N)	Percentage (%)
	S0	S1	S2	S3	S4				S0	S1	S2	S3	S4		
G0	0	0	0	0	0	0	0	G0	3	0	0	0	0	3	33
G1	0	0	0	0	0	0	0	G1	0	1	0	0	0	1	11
G2	0	0	0	0	0	0	0	G2	0	0	0	0	0	0	0
G3	0	0	0	0	1	1	11	G3	0	0	0	0	0	0	0
G3.5	0	0	0	0	2	2	22	G3.5	0	0	0	0	1	1	11
G4	0	0	0	1	1	2	22	G4	0	0	0	0	0	0	0
G4.5	0	0	0	2	2	4	44	G4.5	0	0	0	1	5	6	67

* Grade is the progression of OA into the cartilage (normal cartilage = G0)[128]
* Stage is the horizontal extent of joint involvement (no disease activity = S0)[128]

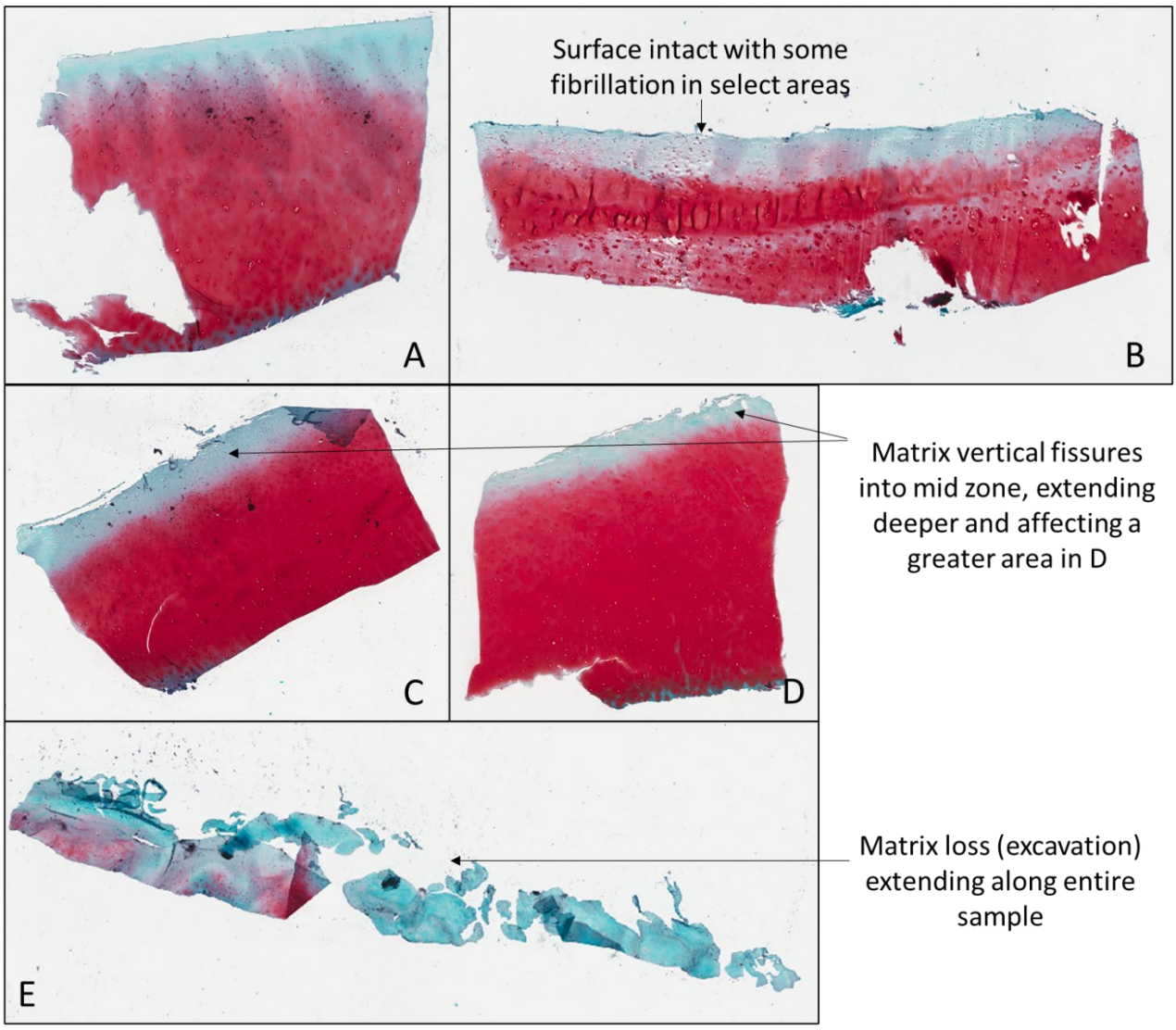

FIGURE 5.11: EXAMPLES OF STAINED CARTILAGE SLIDES FOR THE TKA STUDY. A) GRADE 0 STAGE 0 B) GRADE 1 STAGE 1 C) GRADE 3.5 STAGE 4 D) GRADE 4.5 STAGE 3 E) GRADE 4.5 STAGE 4. ALL SIDES SHOW THE FEMORAL SIDE OR TOP SURFACE OF THE CARTILAGE AT THE TOP OF THE IMAGE. THE CUT OUT PORTIONS IN A AND B SHOULD BE IGNORED BECAUSE THEY WERE BY-PRODUCTS OF SAMPLE EXTRACTION AND DO NOT INFLUENCE THE SCORING.

Counterintuitively, most of the meniscus histology samples overall fell into grades 1 and 2, which is typically representative of less damaged tissue (Figure 5.12). These came from the lateral samples with six being G2 and only one being G0. Less surprisingly, 100% of the medial samples fell into the G4 category. Once again it is important to note that there were only two medial samples and seven lateral samples assessed. Examples of each grade observed are shown in Figure 5.13.

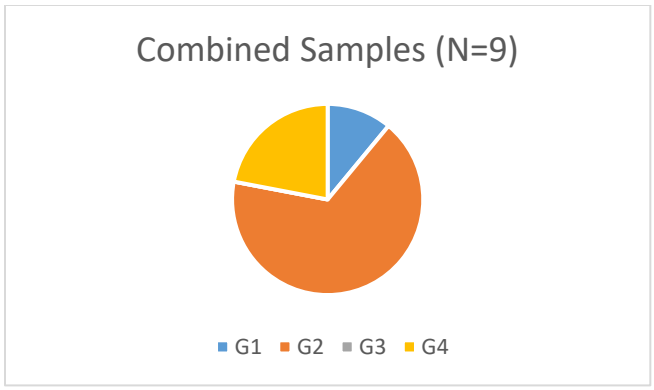

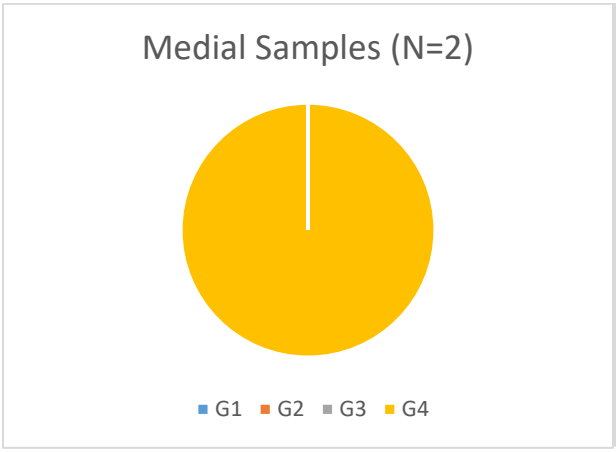

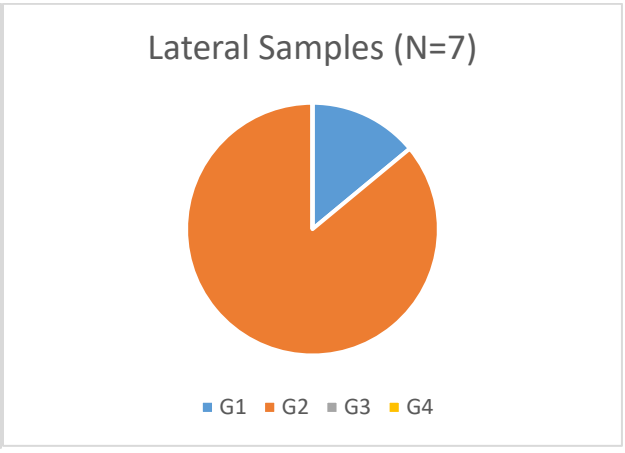

FIGURE 5.12: MENISCUS HISTOLOGY RESULTS FOR THE TKA STUDY. G1 = NORMAL TISSUE, G2 = MILD DEGENERATION, G3 = MODERATE DEGENERATION, G4 = SEVERE DEGENERATION

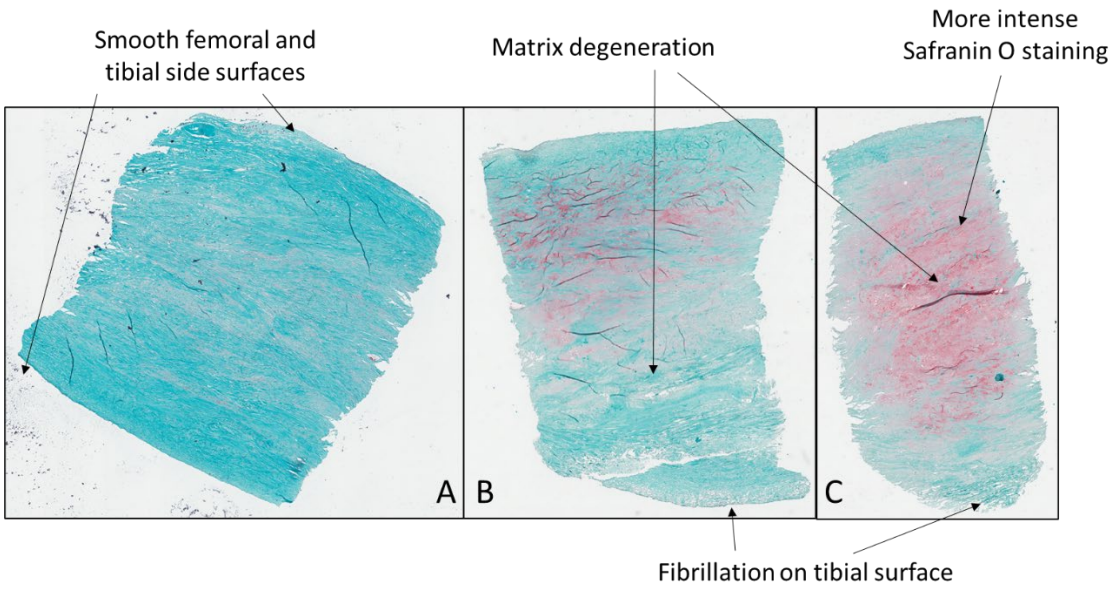

FIGURE 5.13: EXAMPLES OF STAINED MENISCUS SLIDES FOR THE TKA STUDY A) GRADE 1 B) GRADE 2 C) GRADE 4

5.3.4.1. Histology score correlations to qMT parameters

In the cartilage samples, three significant correlations were found between increasing histology score and increasing bound pool fraction in the whole plate samples *in vivo* (ρ=0.670, p<0.05) and medial surfaces *in vivo* (ρ=1.000 p<0.01), as well as between decreasing histology score and increasing T_{2b} in the *ex situ* lateral samples (Figure 5.14C), all of which were strong or very strong. These values are reported in Appendix N: Correlation coefficient tables for the TKA study Table N.5.

FIGURE 5.14: SIGNIFICANT CORRELATIONS FOR TKA CARTILAGE HISTOLOGY CORRELATION ANALYSIS A: *IN VIVO* COMBINED SURFACES, B: *IN VIVO* MEDIAL SURFACES, AND C: *EX SITU* LATERAL SURFACES

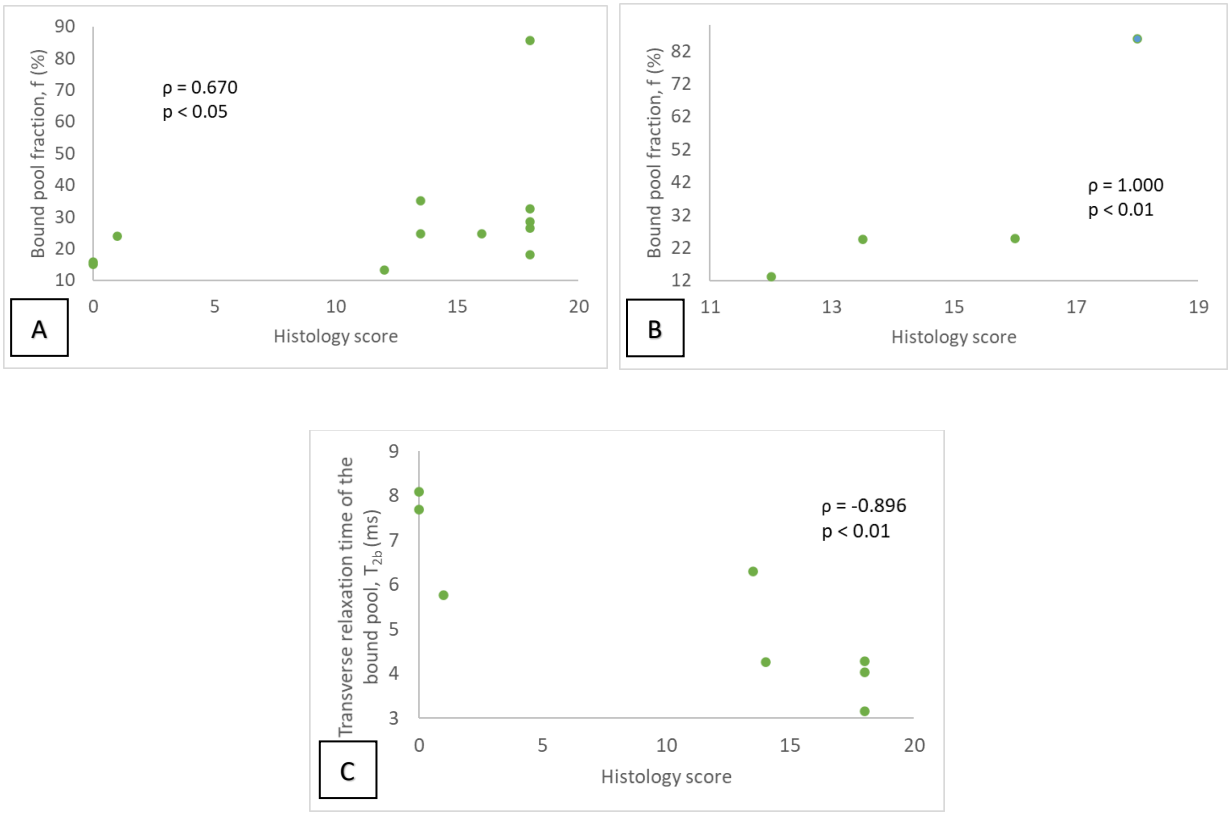

For the meniscus, only lateral samples had corresponding qMT data and no significant correlations were found in the *in vivo* samples (Appendix N: Correlation coefficient tables for the TKA study Table N.6). The excised samples had a sample size of only two and so a correlation analysis could not be performed but scatter plots for each qMT parameter are displayed in Appendix O: Correlation scatterplots for TKA data with N=3 and N=2 sample sizes Figure O.5.

5.3.5. Combined tissue correlation

Several strong and very strong significant correlations were found between various tissue properties and three of the qMT parameters (T_1obs, T_{1f}, and T_{2f}) in the seven *in vivo* surfaces Appendix N: Correlation coefficient tables for the TKA study Table N.7. The strongest of these were the correlations with the liquid content (Figure 5.15A-C). The same correlations were also observed with the solid content, but the relationships were negative (increases in the qMT parameters were associated with decreases in the solid content). There were also very strong correlations between the three aforementioned qMT parameters and sGAG content (Figure 5.15D-G), as well as between the histology score and T_{2f} (Figure 5.15H). It was found that as the collagen per dry mass increased, both T_1obs and T_{1f} decreased ($r=-0.788$, $p<0.05$ and $r=-0.780$, $p<0.05$ respectively). No significant correlations were found between any of the other tissue properties and T_{2b}, f, or k_f. There were also no significant correlations found in the analysis of the seven *ex situ* surfaces.

FIGURE 5.15: VERY STRONG SIGNIFICANT CORRELATIONS FOR TKA STUDY *IN VIVO* SURFACES. RED DATA POINTS ARE FROM MENISCUS, GREEN FROM ARTICULAR CARTILAGE. A-C) CORRELATIONS BETWEEN T_{1}OBS, T_{1F}, AND T_{2F} (RESPECTIVELY) AND LIQUID CONTENT, D-F) CORRELATIONS BETWEEN T_{1}OBS, T_{1F}, AND T_{2F} (RESPECTIVELY) AND SGAG/DRY MASS, F) CORRELATION BETWEEN T_{2F} AND SGAG/WET MASS, AND H) CORRELATION BETWEEN T_{2F} AND HISTOLOGY SCORE

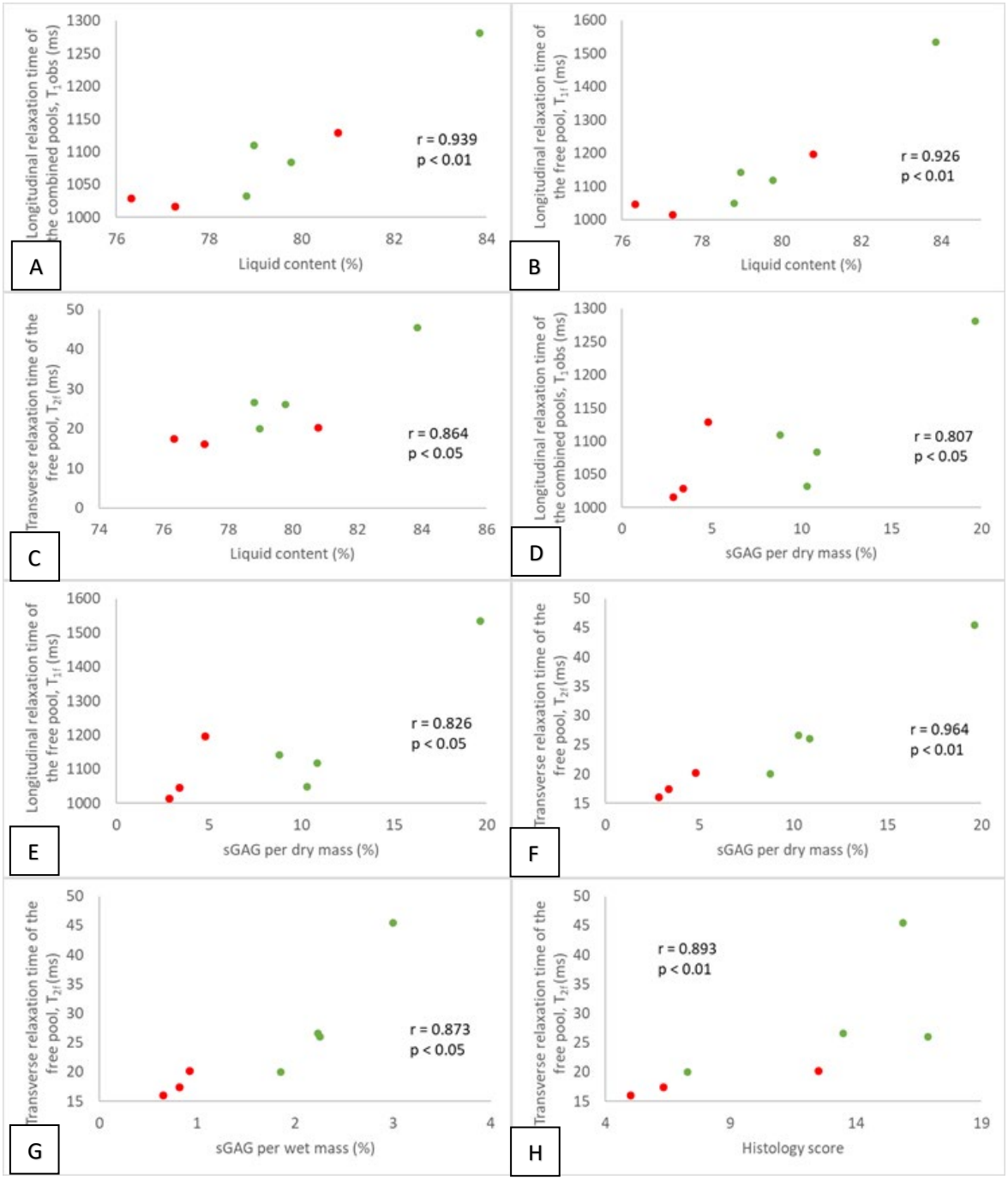

5.4. Discussion of the TKA study

Although the overall sample size was limited (N=2 knees with N=7 surfaces assessed), significant differences in T_1obs, T_{1f}, T_{2f}, and T_{2b} were found from *in vivo* to *ex situ* and several relationships were observed between the qMT parameters and the various tissue properties, with T_{1f} seeming to show up in these correlations most frequently. In some cases, only trends could be assessed due to the limited sample sizes, but initial findings reinforce the potential for qMT parameters to be correlated to physical properties of cartilage and meniscus. Furthermore, the analysis of both cartilage and meniscus resulted in valuable contributions to the limited literature on qMT in these tissue types, especially in damaged tissue.

5.4.1. Comparison of *in vivo* to *ex situ* results

T_1obs, T_{1f}, T_{2f}, and T_{2b} were all found to significantly differ between *in vivo* and *ex situ* environments (Table 5.6 and Figure 5.8), providing evidence that *ex situ* qMT parameters appear to not be representative of those *in vivo*. T_1obs, T_{1f}, and T_{2f} were lower in all groups of both cartilage and meniscus in the *ex situ* scans (Table K.1 and Table K.2). The T_{2b} values were slightly lower *ex situ* as well, although the decrease was not as large as for the other three. Both the f and k_f averages appeared to remain about the same between both groups.

So why are there generally decreases in T_1obs, T_{1f}, T_{2f}, and T_{2b} from *in vivo* to *ex situ*? And why do the f and k_f values seem to roughly stay the same with only slight decreases? The answers to both questions may lie in the change in hydration between the two environments. When you take the tissue out of the body, some of the water (in the form of synovial fluid for example) is inevitably released. Longer T_2 times are thought to be correlated to damaged tissue due to the disorganized collagen increasing water mobility and leading to a decrease in spin-spin interactions[16]. If there is less water in the tissue, then more spin-spin interactions could occur and result in reduced T_2 relaxation times; and greater spin-lattice interactions could reduce the T_1 relaxation times as well. This theory also explains the slight reduction in the bound pool fraction and magnetization exchange rate. Since it is unlikely that the amount of bound macromolecules changed between the *in vivo* and *ex situ* cases, the decrease in these parameters is likely due to the loss in water. Furthermore,

after removal, my tissues were stored in PBS, which is chemically different than synovial fluid and may have further altered the excised tissue hydration and affected the qMT results.

The Simard study[20] assessed differences between *in situ* and *ex situ* qMT parameters (f, k_f, T_{1f}, T_1obs, and T_{2b}) in cadaver menisci and they found the opposite trend in their results (Table 5.10). They found large increases in T_1obs and T_{1f} along with a slight increase in T_{2b} from *in situ* to *ex situ*. Their average f and k_f values over both lateral and medial menisci decreased slightly but were relatively close together. These results contradict my study, and it is unclear what is driving the differences. Some explanation could lie within the different environments studied. My study assesses *in vivo* versus *ex situ,* while Simard compares cadaver *in situ* to *ex situ. In vivo* scanning is more difficult than either *ex situ* or *in situ* because a living subject is involved, and artifacts caused by participant motion are possible. This can cause errors in the registration process and could impact the parameter results. Ideally, we would study all three conditions in the same knees but logistically this would be nearly impossible. There simply is not enough information on the significantly differing conditions to fully understand what change of values is to be expected in the different environments. Future studies should include the assessment of qMT parameters in as many conditions as possible in order to begin to establish common trends.

TABLE 5.10: COMPARISON OF TKA STUDY MENISCUS QMT RESULTS TO VALUES FROM THE LITERATURE

Study:	Berryman[141] * (*in situ*)	Simard[20] (*in situ*)			Simard[20] (*ex situ*)**			Current (*in vivo*)			Current (*ex situ*)		
		Lateral	Medial	Both	Lateral	Medial	Both	Lateral	Medial	Both	Lateral	Medial	Both
f (%)	23.53 (4.25)	21.86 (2.51)	26.76 (2.82)	23.36 (2.41)	17.88 (6.5)	19.75 (7.5)	18.81 (7)	29.25 (15.27)	24.78 (10.45)	27.76 (13.67)	27.34 (12.09)	18.64 (12.79)	24.44 (12.32)
k_f (s^{-1})	3.03 (1.19)	2.26 (0.59)	2.67 (0.64)	2.38 (0.35)	1.86 (1.23)	2.04 (1.48)	1.95 (1.35)	4.64 (5.85)	2.67 (2.94)	3.99 (4.88)	2.42 (2.06)	1.52 (2.08)	2.12 (2.07)
T_1obs (ms)	666.6 (83.9)	698.6 (120.0)	611.6 (85.9)	663.9 (90.9)	1090.0 (287.5)	975.0 (212.5)	1032.5 (250)	1022.3 (218.3)	1128.9 (232.6)	1057.8 (223.1)	739.6 (198.4)	916.2 (217.9)	798.4 (204.9)
T_{1f} (ms)	598.1 (104.3)	783.1 (177.3)	661.0 (166.6)	736.2 (156.0)	1363.8 (412.5)	1122.5 (237.5)	1243.1 (325)	1030.1 (320.5)	1196.1 (341.1)	1085.4 (327.4)	663.9 (252.7)	900.5 (264.4)	742.8 (256.6)
T_{2b} (μs)	16.1 (1.47)	5.74 (0.74)	5.50 (0.95)	5.65 (0.81)	6.11 (2.13)	6.23 (2.5)	6.17 (2.31)	8.38 (3.56)	8.83 (6.16)	8.53 (4.43)	5.03 (1.88)	5.08 (2.89)	5.05 (2.22)

* Values reported are those found using a Gaussian lineshape.
** Values estimated from figures (not directly reported). Standard deviations also estimated from figures.
Blue shaded are *in situ* and green shaded are *ex situ*, white is *in vivo.*
Standard deviations are shown in brackets.

The changes within the T_1obs, T_{1f}, T_{2f}, T_{2b}, f, and k_f from *in vivo* to *ex vivo* to *ex situ* environments shown in this study indicate that caution should be used comparing qMT parameters between them. Based on these findings, it is clear that *ex situ* results cannot be assumed to be representative of the *in vivo* situation. Perhaps when more work has been done, some sort of equation or factor can be established for predicting the qMT parameters in different conditions. Until then, however, it is clear that *ex situ* qMT parameters are substantially different from those *in vivo*.

5.4.2. Correlations between qMT parameters and the TKA tissue properties

One of the main objectives of this study was to establish relationships between the tissue properties and the qMT parameters of osteoarthritic meniscus and cartilage. This was accomplished and several significant correlations were discovered between the qMT metrics and the mechanical, histology, and biochemical properties of both tissue types. Despite the limitation of small sample sizes, valuable relationships were still identified, showing the potential value of qMT imaging for determining tissue properties.

5.4.2.1. Mechanical properties

The correlation analysis performed between the qMT parameters and the instantaneous modulus of both cartilage and meniscus resulted in several weak correlations with various qMT parameters (Appendix N: Correlation coefficient tables for the TKA study Table N.1). Based on a visual inspection of the specimens, there appeared to be regions of healthy to damaged tissue, which translated into a range of instantaneous modulus results. Correlations with the instantaneous modulus were only present in the lateral side samples and they were with T_1obs, T_{1f}, and T_{2f}. Although there are no studies comparing qMT parameters to the mechanical tissue properties in cartilage, several studies have found correlations between the dynamic modulus and T_1, $T_{1\rho}$, and T_2 [142–145]. Rautiainen *et al* found strong and very strong negative correlations with dynamic modulus and all three qMRI parameters, Kurkijarvi *et al* found weak to strong negative correlations between dynamic modulus and T_1 and T_2, and Lammentausta *et al* (2005 and 2007) found weak to strong negative correlations between dynamic modulus and T_2. I found weak negative correlations, which fits in with the literature and

shows increasing modulus results in a decrease in specific qMRI parameters. Furthermore, the findings in the literature paired with my results indicate that T_1obs, T_{1f}, T_{2f}, and T_{2b} may be more indicative of the cartilage mechanical properties than f or k_f. k_f especially does not show to be related to any of the mechanical properties.

In the meniscus, only in the *ex situ* data moderate correlations were found between T_{2f} and instantaneous modulus. The strength of these correlations could be due to the damaged nature of the tissue and level of variability within the data. These findings line up with the significant correlations observed between elastic, dynamic, and shear modulus and T_2 by Son *et al*[16] in human TKA menisci in unconfined compression. The T_{2f} value obtained in my study is very similar to the T_2 found by Son *et al*, so the fact I also found a correlation between it and instantaneous modulus is promising. In the Berryman study[141], the only significant correlation observed was between the aggregate modulus and T_{2b}, but only when using a Super-Lorentzian qMT lineshape. The Berryman study differs in that it studies a cadaveric "healthy population" and uses a confined compression mechanical test versus the indentation testing method used in my study, which could be driving the differences in the correlations observed. However, the results of my study and their differences from the Berryman study show the need for further research in order to validate these correlations and expected parameters.

The presence of correlations between the mechanical properties and the qMT parameters in both cartilage and meniscus indicate that some of the qMT parameters are associated with the function of the tissue. This is an important discovery and first step in possibly quantifying these relationships in the future.

5.4.2.2. Biochemical properties

Several strong to very strong significant correlations and trending relationships (for sample sizes of three or less) were observed between various qMT parameters and the biochemical tissue properties, especially with the liquid and sGAG contents (Appendix N: Correlation coefficient tables for the TKA study and Appendix O: Correlation scatterplots for TKA data with N=3 and N=2 sample sizes). Once again, T_{1f} seemed to be the most commonly involved qMT parameter. Currently only one study has assessed qMT parameters in comparison to the biochemical tissue properties of cartilage in the literature (Stikov[18]). The Stikov findings of significant

correlations between proteoglycan and the bound pool fraction in the tibial cartilage ($r=0.7$, $p<0.05$) were consistent with my results, but I did not find the correlations they reported between proteoglycan and the k_f and T_1 in the tibial cartilage. This is not surprising as my sample sizes were so small, limiting the potential for relationships to be observed. More data is required to fully understand which biochemical properties are related to the qMT parameters of cartilage.

In the meniscus, the correlations observed were with k_f and T_{2b} *in vivo* (Table N.4). These parameters had connections to the liquid and solid content, sGAG, and collagen content. No other studies have compared the qMT parameters to any tissue properties of the meniscus, but Son *et al*[16] did find significant correlations between T_2 and sGAG/wet mass ($\rho= -0.16$, $p<0.05$), collagen/dry mass ($\rho=-0.27$, $p<0.01$), collagen/wet mass ($\rho=-0.63$, $p<0.01$), and water content ($\rho=0.55$, $p<0.01$) in human TKA menisci.

These findings show the potential of the biochemical properties of both cartilage and meniscus to be related to the qMT parameters of the tissue, but a larger sample size is required to validate the relationships observed and uncover other relationships.

5.4.2.3. Histology score

The results of the histology correlation analysis showed fewer but stronger correlations than the other tissue properties, and one very strong correlation was found between the score and T_{2f} in the combined surface analysis. In the cartilage (Table N.5) *in vivo* samples, the OARSI score was strongly correlated with f in the combined samples and very strongly correlated with f in the medial samples. *Ex situ,* the only significant correlation was between the OARSI score and T_{2b} and it was very strong. In the literature, Rautiainen *et al*[142] found correlations between the OARSI score and T_2 as well (T_2 is a qMRI metric not qMT but it is most closely related to the T_{2b} relaxation time in my study). The fact that these correlations are seen with the T_{2b} and f suggests there is a relationship between the tissue structure and the bound pool. This makes sense because the bound pool would be the biggest contributor to the organization of the tissue, and the histology score would logically impact the free pool less than the bound. It is odd however, that the correlations were not

observed between the same parameters *in vivo* and *ex situ*. This could be due to the differing hydration affecting the qMT parameters in either environment, but it is difficult to ascertain with such a small sample size. A larger number of samples may provide further insights into the relationships between cartilage qMT parameters and histology score.

In the meniscus, no significant (or stronger than weak) correlations were found between the histology score and any of the qMT parameters. This is consistent with the Williams study[71] which assessed relationships between the Pauli histology score of the meniscus and T_2* values and found no significant relationships. However, they did find that T_2* values tended to be lower in menisci with lower histology scores and higher in torn or degenerate menisci. Furthermore, Eijgenraam *et al* found T_2 relaxation time to be strongly correlated to the Pauli score of TKA menisci (r_s = 0.84, CI 95% 0.64-0.93)[170]. These findings in the literature are encouraging, and with a larger sample size my study may elucidate relationships between the histology score and the qMT properties of damaged meniscus.

5.4.3. Comparison of qMT parameters to literature

Despite the differences in environments, tissue locations (femoral/tibial/patellar cartilage and meniscus), and tissue health present between my results and those presented in the literature, comparisons can and should be made to provide overall context to the current state of the field.

5.4.3.1. Cartilage

The Sritanyaratana *et al*[19] study assessed the qMT parameters of asymptomatic volunteers and OA patients *in vivo*, and therefore is an excellent comparison to my study (Table 5.11). Their reported OA T_{2b} value (6.80 µs) corresponded to the results from my study, especially when compared to the medial side (6.65 µs); and similarly, the k_f (6.13 s^{-1}) corresponded to my medial side result (5.82 s^{-1}) as well. The f values reported in the Sritanyaratana study (12.46% asymptomatic and 12.80% OA) did not align with my results (29.52% in combined samples), they were much lower. Their MRI protocol and post-processing method was different than mine, which may have accounted for the differences in f. It is important to remember that these two studies are

comparing two different cartilage plates (the patellar cartilage vs the tibial cartilage) and the tissue in my study was more damaged as it was from end-stage OA, TKA patients. More studies assessing tibial cartilage are required to determine the expected qMT parameters in damaged tissue.

TABLE 5.11: COMPARISON OF TKA STUDY CARTILAGE QMT RESULTS TO VALUES FROM THE LITERATURE

Study:	Simard[20] (*in situ*)				Sritanyaratana[19] (*in vivo* patella)		Stikov[18]* (*ex situ*)	Current (*in vivo*)			Current (*ex situ*)		
	Tibial	Femoral	Patellar	Whole	Asymp-tomatic	OA	Tibia	Lateral	Medial	Both	Lateral	Medial	Both
f (%)	16.24 (1.23)	15.47 (0.68)	12.99 (0.68)	15.19 (0.61)	12.46 (0.89)	12.80 (0.78)	25	27.31 (14.26)	31.73 (17.77)	29.52 (16.02)	27.58 (17.45)	30.33 (22.38)	28.96 (19.91)
k_f (s^{-1})	2.87 (0.58)	3.11 (0.78)	2.82 (0.64)	3.00 (0.69)	7.22 (0.95)	6.13 (0.83)	1.8	3.67 (4.78)	5.82 (7.93)	4.75 (6.35)	3.24 (4.25)	4.00 (5.67)	3.62 (4.96)
T_1obs (ms)	763 (128.9)	805.1 (128.9)	904.5 (143.9)	813.3 (117.2)			900	1096.6 (253.0)	1156.7 (215.1)	1126.6 (234.1)	702.1 (197.1)	739.7 (311.1)	720.9 (254.1)
T_{1f} (ms)	815.8 (189.5)	881.5 (191.3)	977.4 (225.5)	882.8 (186.2)				1130.2 (354.3)	1291.6 (329.1)	1210.9 (341.7)	618.4 (258.9)	646.2 (402.3)	632.3 (330.6)
T_{2b} (µs)	4.97 (0.42)	5.37 (0.36)	5.56 (0.20)	5.30 (0.17)	6.49 (0.13)	6.80 (0.14)		6.54 (3.15)	6.65 (4.37)	6.60 (3.76)	5.54 (2.87)	5.42 (2.92)	5.48 (2.89)

* Values estimated from figures (not directly reported). Standard deviations were not reported, so could not be included.
Blue shaded are *in vivo* results and green shaded are *ex situ.*
Standard deviations are shown in brackets.

The Simard study assessed the cartilage of healthy intact cadaver knees (*in situ*), and despite using a Super-Lorentzian lineshape (I used a Gaussian), and having a different approach to qMT parameter fitting, comparisons between our findings are valuable for understanding how these differences may impact the results. Overall, my results aligned reasonably well with Simard's however in all parameters, the Simard results were closer to my *ex situ* values than *in vivo*. This is to be expected because the Simard menisci are no longer part of the complex living body environment (and they had been frozen) so it makes sense that their properties would more closely align with the removed cartilage. Differences between our studies are likely a result of the differing tissue healths and approach used for the qMT fitting.

Lastly, my *ex situ* findings can be directly compared to the Stikov study[18]. The Stikov study only assessed f, k_f, and T_1obs, but commonalities could be seen between all three and my results. The most similar value was f (25%), which was especially close to my f result in the lateral side (27.58%). The k_f reported in Stikov (1.8 s^{-1}) was slightly lower than my results, and once again was closer to the lateral side (3.24 s^{-1}). The T_1obs (900 ms) was higher than both lateral (702.1 ms) and medial (739.7 ms), but the fact that the Stikov study utilized a Super-Lorentzian lineshape as opposed to the Gaussian lineshape used in mine likely accounts for some of these differences, as does the difference in acquisition sequence, MT pulse, and fitting protocol. Furthermore, the specimens used in the Stikov study were from human cadaver knees, but no information is available on their health, which also could be influencing their results.

This detailed comparison of my results with those reported in the literature has ultimately shown several commonalities: similar trends have been observed in the more damaged samples[19] and *ex situ* results have proven to align quite well with previous studies[18]. It is difficult to confirm any direct linkages between my *in vivo* results and those currently presented in the literature[19] due to the different cartilage plates, and differing environments (comparison to *in situ* results)[20] but these preliminary findings are encouraging.

5.4.3.2. Meniscus

My study is the first to perform qMT on the meniscus *in vivo*, but valuable comparisons can be made between my results and the *in situ* results existing in the literature (Table 5.10). The average k_f from both sides combined (3.99 s^{-1}) in my study was the highest amongst all studies and aligned most closely with the *in situ* k_f value found in the Berryman study (3.03 s^{-1}). The f value (27.76%) followed this same trend, being the highest and most in agreement with the Berryman *in situ* f (23.53%), but it also seemed to match the Simard *in situ* f (23.36%). The remaining *in vivo* parameters with existing values in the literature (T_1obs, T_{1f}, and T_{2b}) more closely resembled the Simard e*x situ* results than either of the Simard or Berryman *in situ* values. These similarities to the Berryman study are not surprising because the qMT analysis pipeline used was the same as mine. The similarities seen with the Simard study are encouraging because they show potential consistency in the qMT results across differing methods of parameter fitting, but further work should be done to more fully understand the effects of different fitting methods on the final qMT results.

My *ex situ* results were quite different from the Simard study, which is the only other work in the literature on *ex situ* meniscus qMT. For f, my medial side result (18.64%) did line up with the Simard medial (19.75%) as well as both side (18.81%) results, but the lateral side (27.34%) was much higher. k_f in my study (2.12 s^{-1}) was slightly higher than Simard (1.95 s^{-1}) but was within the Simard value's standard deviation (±1.35 s^{-1}). The greatest differences were seen in T_1obs and T_{1f}. The results I found for these two parameters were much lower than what the Simard study reported, and my T_{2b} was slightly lower as well. This was quite unexpected, due to the fact that my samples came from TKA patients and thus would be expected to have higher T_1 and T_2 values than a healthier population[142,156]. However, the Simard study used a Super-Lorentzian lineshape for the qMT fitting while I utilized a Gaussian lineshape, which could potentially explain the differences in the T_{1f} and T_{2b}. It is possible that these differing lineshapes may have a greater effect on the data *ex situ* and that is driving the differences between my results and those presented by Simard. A previous qMT study in the brain found that *in vitro,* a Super-Lorentzian lineshape gave the best fit while *in vivo,* a Gaussian lineshape was better [149]. The Berryman study on *in situ* specimens compared results obtained using a Super-Lorentzian lineshape to a

Gaussian and it was found that Gaussian gave the best fit (r^2=0.9054 Gaussian and r^2=0.8876 Super-Lorentzian), but resulted in a higher T_{2b} value than was observed with the Super-Lorentzian[141]. Furthermore, other parameters did not greatly differ, but each parameter was slightly different when using either lineshape[141]. This shows the possible sensitivity of T_{2b} in particular to the lineshape used for parameter fitting; and as is a common theme in this work, there are simply not enough publications (especially using similar conditions to mine) to confidently determine what is normal and to be expected of the results.

5.5. Limitations of the TKA study

The greatest limitation of this study was the small sample size. Only two participants, with seven total surfaces could be assessed (due to constraints caused by the COVID-19 global pandemic), which resulted in less samples being taken than originally intended for this project. This low sample size may have impacted the outcomes of the correlation analysis. Although each sample point was considered individually, the reality of the situation was that all data points came from one of two participants, possibly introducing a bias in the relationships observed. Additional participants will be recruited for this study as COVID-19 regulations allow and additional data may elucidate the preliminary relationships observed here.

Another limitation specific to the TKA study was the long scan time. The time required for the scanning protocol used was just under an hour, and for TKA patients with severe pain caused by OA, sitting still for this long is very difficult. Because of this, movement within some of the scans was present, potentially leading to motion artifacts and errors in the segmentation. Future work in our group to optimize the protocol and minimize the scan time is necessary in order to reduce the likelihood of movement; but with this specific cohort, elimination of all movement is likely impossible.

5.6. Conclusion of the TKA study

The results of my study indicate that qMT parameters vary from *in vivo* to *ex situ* environments, and the correlations found show that the qMT parameters are related to the instantaneous modulus and thickness of

cartilage and meniscus to varying degrees. The correlations and linear trends observed between the qMT parameters and the biochemical and histology properties show promising preliminary relationships, but the small sample sizes for these analyses caused by the COVID-19 pandemic are the major limiting factors. More data is necessary to validate these findings, but the results of my study provide motivation and justification for continued work in this field.

6. Integrated discussion

This chapter is an integrated discussion incorporating the findings from both the cadaver and the TKA studies. Included is a brief comparison of the meniscus qMT parameters found in the healthy population to the diseased, an analysis of the differences between the medial and lateral side qMT parameters observed in both studies, and a discussion of the strengths and limitations of this project overall.

6.1. qMT parameters of meniscus in healthy versus diseased knees

The combination of the cadaver and TKA studies allowed for valuable information to be obtained about the qMT parameters of a healthy as well as a diseased population. It also provided a unique opportunity to compare the differing tissue health stages. The purpose of the cadaver study was to assess meniscus, as information on qMT in the meniscus is lacking in the literature, but it also allowed direct tissue comparisons to be made between the cadaver qMT results and the TKA meniscus *ex situ*. Comparisons of the results of these two environments (*in situ* and *ex situ*) were chosen because they were free of motion artifact and more closely resembled each other's physical condition than either to *in vivo*.

Clear differences are present between the healthy and TKA meniscus groups for all qMT parameters, with T_1obs, T_{1f}, and T_{2f} all being higher in the TKA group and T_{2b}, f, and k_f being lower (Figure 6.1). T_1obs, T_{1f}, and T_{2f} all show the expected trend with higher values in the damaged as opposed to healthy population[16,142,156]. The T_{2b} results comparison was surprising; it was expected for the T_{2b} to be higher in the TKA samples, but the results showed a much higher T_{2b} in the healthy samples. It is unclear exactly why this was observed, but the reasoning could lie in the unknown effects of changes to the cartilage and meniscus macromolecules with damage on T_{2b} or the difference in scanning environment (*in situ* versus *ex situ*). As discussed in section 5.4.1 (Comparison of *in vivo* to *ex situ* results), the different tissue conditions have varying hydration (further compounded by immersion in synovial fluid versus PBS), which likely affects the parameter outcomes. It was also unknown if the TKA patients had primary (idiopathic) or secondary (post-traumatic) OA, which could also

account for these findings. The bound pool fraction was slightly higher in healthy samples, which aligns with the expectation that the damaged samples would have diminished macromolecules and therefore a reduced f. Further to this point, the k_f values also decreased from healthy to diseased, displaying a similar trend possibly explained by the reduced macromolecules not being able to as effectively transfer magnetization to the free pool. This trend was also discovered in the Sritanyaratana study[19] on patellar cartilage, which observed significant reduction in k_f from healthy to OA patients.

FIGURE 6.1: BAR GRAPHS COMPARING THE CADAVER MENISCUS TO *EX SITU* TKA MENISCUS AND CARTILAGE QMT RESULTS. CADAVER RESULTS ARE TAKEN FROM THE QMT PARAMETERS OF THE CORRESPONDING BIOCHEMISTRY SAMPLES.

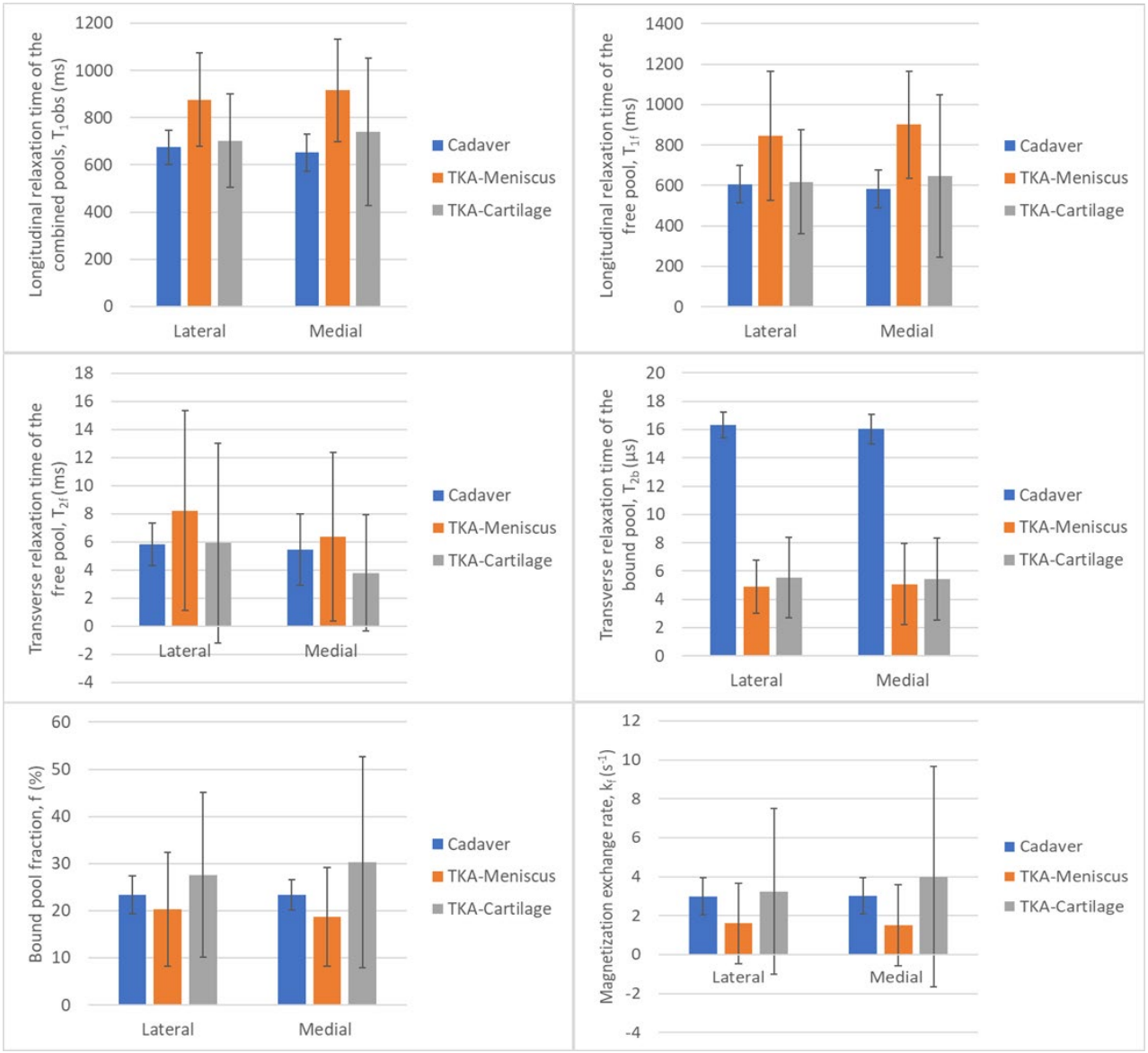

Upon comparison of the meniscus results to the TKA cartilage, some interesting findings were present. The T_1obs, T_{1f}, and T_{2f} values of damaged cartilage were very close to but slightly higher than those of healthy menisci, and all three parameters were higher in the TKA menisci than cartilage. The only exception to this was the T_{2f} in the medial TKA cartilage, which was lower than that of both the cadaver and TKA menisci. These are surprising findings because typically in the literature, higher T_1 and T_2 relaxation times are associated with more damaged tissue and cartilage usually has higher T_1 and T_2 values than meniscus[15,156,171]. Therefore, it would be expected that the TKA cartilage would have the highest T_1 and T_2 relaxation times followed by TKA meniscus, and then healthy meniscus. The T_{2b} results partially followed this trend, with higher values in the TKA cartilage than TKA menisci, but it is interesting and unexpected that the results for the cadaver menisci are so much higher than either group of TKA data. Because the cadaver data was taken *in situ*, it is not possible to know if the same patterns would have occurred *ex situ*. The only way to verify these findings and confirm expected relationships would be to image healthy cadaver menisci *ex situ* and compare the findings to the TKA data from this study.

The remaining parameters resulted in fewer surprises, partially due to the lack of existing information available for comparison. The bound pool fraction and magnetization exchange rates followed similar patterns whereby cartilage had the highest values, and they were reduced in the meniscus from healthy to OA. These trends suggest that damaged cartilage *ex situ* has a higher fraction of bound pool (i.e., macromolecules) than damaged meniscus *ex situ* as well as healthy meniscus *in situ*. The biochemistry results of my project showed the cadaver menisci samples to have the highest quantity of collagen followed by TKA meniscus and then TKA cartilage, while sGAG content was the highest in TKA cartilage, followed by TKA meniscus and then cadaver meniscus. The sGAG findings were unexpected, but the increase in proteoglycan from healthy to damaged menisci could have been due to relative changes in the water to macromolecule ratio or an artifact of the biochemistry procedures. This trend should be further assessed in future studies. Perhaps these results, combined with the trends observed in the bound pool fraction, indicate f is more associated with sGAG than with collagen content. This theory is further solidified by the results of the cadaver correlation analysis, which found a weak

correlation between sGAG and f and a moderate correlation between sGAG and k_f, and no significant correlations between either f or k_f and collagen. This theory could not be validated in the TKA study because the sample sizes for the biochemistry results with corresponding qMT data were too small to perform a correlation analysis, but this relationship should be further explored in future research.

In conclusion, these are interesting findings that may indicate damaged cartilage could have similar qMT values to healthy meniscus. Further research must be carried out with consistent tissue environments in order to more confidently establish these relationships.

6.2. Medial versus lateral qMT parameters in healthy and diseased knees

In both the cadaver and TKA studies there were interesting and somewhat unexpected trends observed in the medial compared to lateral side qMT results. In the cadaver study, differences in sides for all qMT parameters were very small (Figure 6.1). The medial side had similar but slightly lower T_1obs, T_{1f}, T_{2f}, and T_{2b} values, which is unexpected because it would be assumed that the medial side would have values indicative of more damaged tissue due to the fact that these are older knees (mean age 70.3 years) that may be on the path to developing OA, which is more common in the medial compartment of the knee[157,158]. In a study by Mittal *et al* it was found that the T_1 and T_2 relaxation times of both cartilage and menisci were significantly higher in OA patients (1089 ms and 55 ms respectively in cartilage and 1007 ms and 30 ms respectively in meniscus) than healthy volunteers (907 ms and 46 ms respectively in cartilage and 803 ms and 22 ms respectively in meniscus)[156]. This trend was also observed by Rautiainen *et al* who found increases with both T_1 (1390.4 ms healthy to 1565.7 ms OA) and T_2 (20.0 ms healthy to 32.0 ms OA) relaxation times in patellar cartilage with OARSI scores greater than 1.5 (indicating OA) [142]. T_1 and T_2 relaxation times are expected to increase with damage, because the disorganized and diminished collagen and proteoglycan contents result in increased water mobility, effectively reducing spin-spin and spin-lattice interactions [16]. These studies exemplify what would be expected of damaged tissue, and what is predicted to occur from lateral to medial menisci, but this pattern was not observed in my results. This expected trend is seen for T_1obs, T_{1f}, and T_{2b} in both the *in vivo* (Figure 5.8) and *ex situ* cartilage and

meniscus of the TKA study, with higher values for all three parameters in the medial side (except for T_{2b} *ex situ* cartilage). Interestingly, the T_{2f} values also displayed unexpected results. *In vivo*, the values followed the predicted pattern, being higher in the medial side, but *ex situ* the opposite was observed. It is unclear why this occurred and because it contradicts the *in vivo* situation, it should only be taken as a cautionary finding. It is also important to note that differences in these values are very small, and there were a limited number of tissue plates (seven in total) available for analysis. Both f and k_f also displayed some odd results when comparing medial to lateral. In cartilage, the values increased from lateral to medial, but in meniscus they decreased. This phenomenon is present in both *in vivo* and *ex situ* samples and may be indicating that f and k_f present differently in cartilage and meniscus with regards to their changes with damage.

Based on all these observations, it appears that with most of the parameters, healthy samples result in qMT values indicative of healthier tissue in the medial side compared to lateral, while damaged samples indicate a less healthy medial side versus lateral. This however, is speculative and based on limited sample sizes in both studies so in order to confirm this, more information is required. These preliminary findings encourage further investigation into this matter.

6.3.Strengths and limitations

The greatest strength of this work was the comprehensive nature of the comparison of the qMT parameters to the tissue properties. Correlations were assessed between the six main qMT parameters (T_1obs, T_{1f}, T_{2f}, T_{2b}, f, and k_f) and the mechanical, biochemical, and histological properties (representing the tissue function, composition, and structure respectively) of both cartilage and meniscus. This was the first study to do this in either cartilage or meniscus; further, very few studies across all qMRI have carried out such a comprehensive assessment[16,108,109,142]. Another strength of this project was the range of tissue health assessed for the meniscus. The combination of the cadaver and TKA studies allowed for differences in qMT parameters between healthy and osteoarthritic menisci to be uncovered. This is important because only two other qMT studies currently exist in the literature about the meniscus[20,141], neither of which asses an OA population, and so my

study begins to fill this gap in the field. The flip side of this is the extremes of the health observed in the cadaver versus OA specimens. The relative uniformity of the results may have reduced the dynamic range of values seen in the individual studies, which likely limited the strength of the correlations observed. Future work should assess varying degrees of tissue health all in the same study.

Another limiting factor in this project was the differing tissue environments between the cadaver and TKA studies. The fact that the cadaver specimens were scanned *in situ* and the TKA *in vivo* and *ex situ* gave a lot of very valuable information about the differing tissue conditions, but it also made it challenging to directly relate the results between groups.

There also could have been some inconsistencies with the freezing and thawing and storage of samples. The cadaver study biochemical samples and whole menisci prior to histology sample retrieval were handled by another student, and so slightly different storage and freezing methods from those that I used may have been implemented. For the TKA study, time between the various testing was kept as short as possible but I was not always able to accomplish the same timing for both knees; this is due to the surgical scheduling and resulting specimen pick-up scheduling. For the future work conducted to continue the TKA project there should be a focus on maintaining similar conditions and time frames for each knee involved, and a record should be kept of timing and freezing cycles for each specimen.

Another limitation was the fact that all the tissue property analysis methods were developed and performed by me for the first time in our group. This could have introduced errors, especially in the beginning and troubleshooting phases of the protocol development that may not have been present with more practice. More specifically, a limitation of the histology component of the project was that I was inexperienced in the scoring methods for both cartilage and meniscus and was basing the scores I assigned off of only the scoring guides. This could have resulted in some errors in the initial histology scores I reported. For future work, a second round of scoring should be carried out by the same grader to assess the intra-rater reliability as well as by another grader to assess the inter-rater reliability of the histology results. Also, the Mach-1 system was new to

our lab and equipment and protocol set-up was my responsibility. When testing meniscus, I secured the specimen to the hockey puck using superglue around the edges, but some movement was still possible, which may have impacted the mechanical results obtained.

For the registration component of the project, the manual segmentation performed for both studies was susceptible to errors that could have led to inaccuracies in the qMT parameter result locations; however, all segmentation was reviewed by a segmenter with 18 years of experience (Prof. McWalter). Furthermore, the registration was also limited by the cylinders and blocks I created and positioned using photographs and visual reference points. Future work should focus on developing a less human centered method for creating and locating the surfaces and cylinders used in the registration code.

7. Conclusion

The main objectives of this research were to establish relationships between qMT parameters and the mechanical, biochemical, and histological properties of human knee articular cartilage and meniscus in a healthy as well as diseased population, as well as compare the qMT parameters obtained *in vivo* to those *ex situ*. This objective was accomplished and by carrying out this research, several important contributions have been made to the scientific community.

1. Significant correlations have been found in cadaver meniscus between liquid and solid content and f; collagen and T_1obs, T_{1f}, T_{2f}, and T_{2b}; sGAG and f and k_f; and histology score and T_1obs, T_{1f}, T_{2f}, and T_{2b}. In TKA cartilage, significant correlations were observed between instantaneous modulus and T_1obs, T_{1f}, and T_{2f}; liquid and solid content and T_{1f}; and histology score and T_{2b} and f. In TKA meniscus significant correlations were uncovered between instantaneous modulus and T_{2f}; liquid and solid content and k_f; sGAG and T_{2b}; and collagen and k_f. This has contributed evidence to support the use of qMT imaging in determining the functional state of these tissues and the level of OA. Potential uses of this include diagnosis of early OA, assessment of the progression of OA over time, and the evaluation of treatments in order to determine their effectiveness.
2. Further knowledge about the effects of OA on the tissue properties of menisci has been presented. Proteoglycan content seems to remain unaffected while water content increases, and collagen content decreases with disease. T_1obs, T_{1f}, and T_{2f} all show increases with OA, while T_{2b}, f, and k_f show small decreases. The information obtained about the qMT parameters of menisci is especially valuable as prior to this research, there was an absence of such data for damaged menisci in the literature.
3. Comparisons between qMT parameters *in vivo* and *ex situ* have been made in order to determine if correlations between tissue properties and qMT values discovered in previous studies are applicable to *in vivo* situations as well. This has also provided insight into whether qMT is a viable imaging modality for

predicting *in vivo* tissue properties. It has been determined that *ex situ* qMT results are not the same as *in vivo*, but further research may be able to discover relationships between these values.

Overall, this research contributes quantitative information about the tissue properties and qMT parameters of cartilage and menisci in OA patients as well as menisci in relatively healthy populations, which aids in establishing expected values for these populations. The relationships determined between the various properties and parameters assessed highlight the potential of qMT for predicting the state of the tissue non-invasively. In order to more clearly understand and quantify these relationships, more work must be done. Future research in this field should compare the qMT parameters of differing degrees of damaged tissue in the same environment – i.e., all *in vivo* or all *ex situ*. This uniformity is imperative to begin to establish expectations of qMT values in both cartilage and meniscus by removing doubts caused by the differing conditions. Additionally, future studies should include both cartilage and meniscus as was done in my project instead of just one tissue independently to more fully understand the effects of OA on the knee. The meniscus plays a very important role in knee function and further work should be done to determine if the meniscus is impacted more severely than cartilage is by OA. Having a tool that can simultaneously, non-invasively and objectively assess articular cartilage and meniscus health and function will allow us to further understand the etiology of OA throughout the disease process and evaluate the efficacy of treatment strategies that aim to arrest the onset and progression of the disease.

References

1. Infographic on OA as a Serious Disease | Osteoarthritis Research Society International (OARSI). https://oarsi.org/research/infographic-oa-serious-disease. Accessed May 26, 2021.

2. Eckstein F, Glaser C. Measuring cartilage morphology with quantitative magnetic resonance imaging. *Semin Musculoskelet Radiol*. 2004;8(4):329-353. doi:10.1055/s-2004-861579

3. Litwic A, Edwards MH, Dennison EM, Cooper C. Epidemiology and burden of osteoarthritis. *Br Med Bull*. 2013;105(1):185-199. doi:10.1093/bmb/lds038

4. Hutton CW. Osteoarthritis: the cause not result of joint failure? *Ann Rheum Dis*. 1989;48(11):958-961.

5. Sandell LJ, Aigner T. Articular cartilage and changes in arthritis. An introduction: cell biology of osteoarthritis. *Arthritis Res*. 2001;3(2):107. doi:10.1186/ar148

6. Lawrence RC, Felson DT, Helmick CG, et al. Estimates of the prevalence of arthritis and other rheumatic conditions in the United States. Part II. *Arthritis Rheum*. 2008;58(1):26-35. doi:10.1002/art.23176

7. Bombardier C, Hawker G, Mosher D. *The Impact of Arthritis in Canada: Today and over the next 30 Years*.; 2011.

8. Sharif B, Kopec J, Bansback N, et al. Projecting the direct cost burden of osteoarthritis in Canada using a microsimulation model. *Osteoarthr Cartil*. 2015;23(10):1654-1663. doi:10.1016/j.joca.2015.05.029

9. Altman RD. Classification of disease: Osteoarthritis. *Semin Arthritis Rheum*. 1991;20(6):40-47. doi:10.1016/0049-0172(91)90026-V

10. Bijlsma JWJ, Knahr K. Strategies for the prevention and management of osteoarthritis of the hip and knee. *Best Pract Res Clin Rheumatol*. 2007;21(1):59-76. doi:10.1016/j.berh.2006.08.013

11. Loeser RF, Goldring SR, Scanzello CR, Goldring MB. Osteoarthritis: A disease of the joint as an organ. *Arthritis Rheum*. 2012;64(6):1697-1707. doi:10.1002/art.34453

12. Braun HJ, Gold GE. Diagnosis of osteoarthritis: Imaging. *Bone*. 2012;51(2):278-288. doi:10.1016/J.BONE.2011.11.019

13. Dunn TC, Lu Y, Jin H, Ries MD, Majumdar S. T2 Relaxation Time of Cartilage at MR Imaging: Comparison with Severity of Knee Osteoarthritis. *Radiology*. 2004;232(2):592-598. doi:10.1148/radiol.2322030976

14. Wang L, Chang G, Xu J, et al. T1rho MRI of menisci and cartilage in patients with osteoarthritis at 3T. *Eur J Radiol*. 2012;81(9):2329-2336. doi:10.1016/j.ejrad.2011.07.017

15. Rauscher I, Stahl R, Cheng J, et al. Meniscal measurements of T1rho and T2 at MR imaging in healthy subjects and patients with osteoarthritis. *Radiology*. 2008;249(2):591-600. doi:10.1148/radiol.2492071870

16. Son M, Goodman SB, Chen W, Hargreaves BA, Gold GE, Levenston ME. Regional variation in T1ρ and T2 times in osteoarthritic human menisci: correlation with mechanical properties and matrix composition. *Osteoarthr Cartil*. 2013;21(6):796-805. doi:10.1016/j.joca.2013.03.002

17. Sled JG, Pike GB. Quantitative Interpretation of Magnetization Transfer in Spoiled Gradient Echo MRI Sequences. *J Magn Reson*. 2000;145(1):24-36. doi:10.1006/jmre.2000.2059

18. Stikov N, Keenan KE, Pauly JM, Smith RL, Dougherty RF, Gold GE. Cross-relaxation imaging of human articular cartilage. *Magn Reson Med*. 2011;66(3):725-734. doi:10.1002/mrm.22865

19. Sritanyaratana N, Samsonov A, Mossahebi P, Wilson JJ, Block WF, Kijowski R. Cross-relaxation imaging of human patellar cartilage in vivo at 3.0T. *Osteoarthr Cartil*. 2014;22(10):1568-1576. doi:10.1016/j.joca.2014.06.004

20. Simard M. *Quantitative Magnetization Transfer Evaluation of the Knee Joint in Magnetic Resonance Imaging*.; 2016.

21. Sophia Fox AJ, Bedi A, Rodeo SA. The basic science of articular cartilage: structure, composition, and function. *Sports Health*. 2009;1(6):461-468. doi:10.1177/1941738109350438

22. McDevitt CA. Biochemistry of articular cartilage. Nature of proteoglycans and collagen of articular cartilage and their role in ageing and in osteoarthrosis. *Ann Rheum Dis*. 1973;32(4):364-378.

23. Woo SLY, Lee TQ, Gomez MA, Sato S, Field FP. Temperature dependent behavior of the canine medial collateral ligament. *J Biomech Eng*. 1987;109(1):68-71. doi:10.1115/1.3138645

24. Hardingham T, Bayliss M. Proteoglycans of articular cartilage: changes in aging and in joint disease. *Semin Arthritis Rheum*. 1990;20(3 Suppl 1):12-33.

25. Mow VC, Huiskes R. *Basic Orthopaedic Biomechanics and Mechano-Biology*. Lippincott Williams & Wilkins; 2005.

26. Mansour JM. Biomechanics of cartilage. July 2013:69-83.

27. Sanchez-Adams J, Willard VP, Athanasiou KA. Regional variation in the mechanical role of knee meniscus glycosaminoglycans. *J Appl Physiol*. 2011;111(6):1590-1596. doi:10.1152/japplphysiol.00848.2011

28. Makris EA, Hadidi P, Athanasiou KA. The knee meniscus: Structure–function, pathophysiology, current repair techniques, and prospects for regeneration. *Biomaterials*. 2011;32(30):7411-7431. doi:10.1016/J.BIOMATERIALS.2011.06.037

29. Fox AJS, Bedi A, Rodeo SA. The Basic Science of Human Knee Menisci. *Sport Heal A Multidiscip Approach*. 2011;4(4):340-351. doi:10.1177/1941738111429419

30. McDevitt CA, Webber RJ. The Ultrastructure and Biochemistry of Meniscal Cartilage. *Clin Orthop Relat Res*. 1990;NA;(252):8???18. doi:10.1097/00003086-199003000-00003

31. Verdonk PCM, Forsyth RG, Wang J, et al. Characterisation of human knee meniscus cell phenotype. *Osteoarthr Cartil*. 2005;13(7):548-560. doi:10.1016/J.JOCA.2005.01.010

32. Ghadially FN, Lalonde JM, Wedge JH. Ultrastructure of normal and torn menisci of the human knee joint. *J Anat*. 1983;136(Pt 4):773-791.

33. Ghosh P, Taylor TKF. The Knee Joint Meniscus. *Clin Orthop Relat Res*. 1987;NA;(224):52???63. doi:10.1097/00003086-198711000-00008

34. Noyes FR, Barber-Westin SD. Repair of complex and avascular meniscal tears and meniscal transplantation. *J Bone Joint Surg Am*. 2010;92(4):1012-1029.

35. Bullough PG, Munuera L, Murphy J, Weinstein AM. The strength of the menisci of the knee as it relates to their fine structure. Bullough PG, ed. *J Bone Joint Surg Br*. 1970;52(3):564-567. doi:10.1302/0301-620X.52B3.564

36. Hunter DJ, Zhang YQ, Niu JB, et al. The association of meniscal pathologic changes with cartilage loss in symptomatic knee osteoarthritis. *Arthritis Rheum*. 2006;54(3):795-801. doi:10.1002/art.21724

37. Neogi T, Zhang Y. Epidemiology of OA. 2012. doi:10.1016/j.rdc.2012.10.004

38. HAQ SA, DAVATCHI F. Osteoarthritis of the knees in the COPCORD world. *Int J Rheum Dis*. 2011;14(2):122-129. doi:10.1111/j.1756-185X.2011.01615.x

39. Hollander AP, Heathfield TF, Webber C, et al. Increased damage to type II collagen in osteoarthritic articular cartilage detected by a new immunoassay. *J Clin Invest*. 1994;93(4):1722-1732. doi:10.1172/JCI117156

40. Venn M, Maroudas A. Chemical composition and swelling of normal and osteoarthrotic femoral head cartilage I. Chemical composition. *Ann Rheum Dis*. 1977;36:121-129. doi:10.1136/ard.36.2.121

41. Jones G, Ding C, Scott F, Glisson M, Cicuttini F. Early radiographic osteoarthritis is associated with substantial changes in cartilage volume and tibial bone surface area in both males and females. *Osteoarthr Cartil*. 2004;12(2):169-174. doi:10.1016/j.joca.2003.08.010

42. Mäkelä JTA, Han SK, Herzog W, Korhonen RK. Very early osteoarthritis changes sensitively fluid flow properties of articular cartilage. *J Biomech*. 2015;48(12):3369-3376. doi:10.1016/j.jbiomech.2015.06.010

43. Englund M, Roemer FW, Hayashi D, Crema MD, Guermazi A. Meniscus pathology, osteoarthritis and the treatment controversy. *Nat Rev Rheumatol*. 2012;8(7):412-419. doi:10.1038/nrrheum.2012.69

44. Xu D, Hansson M, Klein S, et al. Association between meniscus volume and development of knee osteoarthritis. *Osteoarthr Cartil*. 2019;27:S272-S273. doi:10.1016/j.joca.2019.02.650

45. Bloecker K, Wirth W, Guermazi A, Hitzl W, Hunter DJ, Eckstein F. Longitudinal change in quantitative meniscus measurements in knee osteoarthritis—data from the Osteoarthritis Initiative. *Eur Radiol*. 2015;25(10):2960-2968. doi:10.1007/s00330-015-3710-7

46. Englund M, Guermazi A, Lohmander SL. The Role of the Meniscus in Knee Osteoarthritis: a Cause or Consequence? *Radiol Clin North Am*. 2009;47(4):703-712. doi:10.1016/j.rcl.2009.03.003

47. Muzaffar N, Kirmani O, Ahsan M, Ahmad S. Meniscal Extrusion in the Knee: Should only 3 mm Extrusion be Considered Significant? An Assessment by MRI and Arthroscopy. *Malaysian Orthop J*. 2015;9(2):17. doi:10.5704/MOJ.1507.013

48. Roos H, Adalberth T, Dahlberg L, Lohmander LS. Osteoarthritis of the knee after injury to the anterior cruciate ligament or meniscus: the influence of time and age. *Osteoarthr Cartil*. 1995;3(4):261-267. doi:10.1016/S1063-4584(05)80017-2

49. Karachalios T, Zibis A, Papanagiotou P, Karantanas AH, Malizos KN, Roidis N. MR imaging findings in early osteoarthritis of the knee. *Eur J Radiol*. 2004;50(3):225-230. doi:10.1016/j.ejrad.2004.01.018

50. Emmanuel K, Quinn E, Niu J, et al. Quantitative measures of meniscus extrusion predict incident radiographic knee osteoarthritis - data from the Osteoarthritis Initiative. *Osteoarthr Cartil*. 2016;24(2):262-269. doi:10.1016/j.joca.2015.08.003

51. Herwig J, Egner E, Buddecke E. *Chemical Changes of Human Knee Joint Menisci in Various Stages of Degeneration*. Vol 43.; 1984.

52. Altman R, Asch E, Bloch D, et al. Development of criteria for the classification and reporting of osteoarthritis: Classification of osteoarthritis of the knee. *Arthritis Rheum*. 1986;29(8):1039-1049. doi:10.1002/art.1780290816

53. Altman RD, Gold GE. Atlas of individual radiographic features in osteoarthritis, revised. *Osteoarthr Cartil*.

2007;15:A1-A56. doi:10.1016/j.joca.2006.11.009

54. Kellgren JH, Lawrence JS. Radiological Assessment of Osteo-Arthrosis. *Ann Rheum Dis*. 1957;16(4):494-502. doi:10.1136/ard.16.4.494

55. Guermazi A, Hayashi D, Roemer F, et al. Severe radiographic knee osteoarthritis – does Kellgren and Lawrence grade 4 represent end stage disease? – the MOST study. *Osteoarthr Cartil*. 2015;23(9):1499-1505. doi:10.1016/J.JOCA.2015.04.018

56. Altman R, Alarcon G, Appelrouth D, et al. The American College of Rheumatology criteria for the classification and reporting of osteoarthritis of the hand. *Arthritis Rheum*. 1990;33(11):1601-1610. doi:10.1002/art.1780331101

57. Diseases and Conditions Osteoarthritis.

58. Riddle DL, Jiranek WA, Hayes CW. Use of a validated algorithm to judge the appropriateness of total knee arthroplasty in the United States: A multicenter longitudinal cohort study. *Arthritis Rheumatol*. 2014;66(8):2134-2143. doi:10.1002/art.38685

59. Carr AJ, Robertsson O, Graves S, et al. Knee replacement. *Lancet*. 2012;379(9823):1331-1340. doi:10.1016/S0140-6736(11)60752-6

60. *Hip and Knee Replacements in Canada, 2017–2018: Canadian Joint Replacement Registry Annual Report*.; 2019.

61. Jacobs MA, Ibrahim TS, Ouwerkerk R. MR Imaging: Brief Overview and Emerging Applications. *RadioGraphics*. 2007;27(4):1213-1229. doi:10.1148/rg.274065115

62. Carr MW, Grey ML. Magnetic resonance imaging: overview, risks, and safety measures. *Am J Nurs*. 2002;102(12):26-33.

63. Currie S, Hoggard N, Craven IJ, Hadjivassiliou M, Wilkinson ID. Understanding MRI: basic MR physics for physicians. *Postgrad Med J*. 2013;89(1050):209-223. doi:10.1136/postgradmedj-2012-131342

64. MRI Physics | Body MRI Research Group (BMR) | Stanford Medicine.

65. Elster AD. k-space - Questions and Answers in MRI. http://mriquestions.com/what-is-k-space.html. Accessed May 28, 2021.

66. Hashemi RH, Bradley WG, Lisanti CJ. *MRI : The Basics* .; 2018. https://primo-pmtna02.hosted.exlibrisgroup.com/primo-explore/fulldisplay?docid=USaskIII.b43939910&context=L&vid=USASK&lang=en_US&search_scope=UofS&adaptor=Local Search Engine&isFrbr=true&tab=default_tab&query=any,contains,MRI the basics&mode=Basic. Accessed May 28, 2021.

67. Pierpaoli C. Quantitative brain MRI. *Top Magn Reson Imaging*. 2010;21(2):63. doi:10.1097/RMR.0b013e31821e56f8

68. Bitar R, Leung G, Perng R, et al. MR pulse sequences: What every radiologist wants to know but is afraid to ask. *Radiographics*. 2006;26(2):513-537. doi:10.1148/rg.262055063

69. Nieminen MT, Rieppo J, Töyräs J, et al. T2 relaxation reveals spatial collagen architecture in articular cartilage: A comparative quantitative MRI and polarized light microscopic study. *Magn Reson Med*. 2001;46(3):487-493. doi:10.1002/mrm.1218

70. Raya JG, Ruiz A, Ferizi U. Revisiting the experimental base of compositional biomarkers: A meta-analysis

study. In: *ISMRM*. ; 2017.

71. Williams A, Qian Y, Golla S, Chu CR. UTE-T2* mapping detects sub-clinical meniscus injury after anterior cruciate ligament tear. *Osteoarthr Cartil*. 2012;20(6):486-494. doi:10.1016/j.joca.2012.01.009

72. Ravinder Reddy Regatte 1, Sarma V S Akella, Arijitt Borthakur RR. Proton spin-lock ratio imaging for quantitation of glycosaminoglycans in articular cartilage. *J Magn Reson Imaging*. 2003;17(1):114-121. doi:10.1002/jmri.10228

73. Duvvuri U, Reddy R, Patel SD, Kaufman JH, Kneeland JB, Leigh JS. T(1ρ)-relaxation in articular cartilage: Effects of enzymatic degradation. *Magn Reson Med*. 1997;38(6):863-867. doi:10.1002/mrm.1910380602

74. Wheaton AJ, Dodge GR, Borthakur A, Kneeland JB, Schumacher HR, Reddy R. Detection of changes in articular cartilage proteoglycan by T1ρ magnetic resonance imaging. *J Orthop Res*. 2005;23(1):102-108. doi:10.1016/j.orthres.2004.06.015

75. Sled JG, Pike GB. Quantitative imaging of magnetization transfer exchange and relaxation properties in vivo using MRI. *Magn Reson Med*. 2001;46(5):923-931.

76. Henkelman RM, Stanisz GJ, Graham SJ. Magnetization transfer in MRI: a review. *NMR Biomed*. 2001;14:57-64. doi:10.1002/nbm.683

77. Athanasiou KA, Rosenwasser MP, Buckwalter JA, Malinin TI, Mow VC. Interspecies comparisons of in situ intrinsic mechanical properties of distal femoral cartilage. *J Orthop Res*. 1991;9(3):330-340. doi:10.1002/jor.1100090304

78. Seitz AM, Galbusera F, Krais C, Ignatius A, Dürselen L. Stress-relaxation response of human menisci under confined compression conditions. *J Mech Behav Biomed Mater*. 2013;26:68-80. doi:10.1016/j.jmbbm.2013.05.027

79. Korhonen RK, Laasanen MS, Töyräs J, et al. Comparison of the equilibrium response of articular cartilage in unconfined compression, confined compression and indentation. *J Biomech*. 2002;35(7):903-909.

80. Armstrong CG, Lai WM, Mow VC. An analysis of the unconfined compression of articular cartilage. *J Biomech Eng*. 1984;106(2):165-173.

81. LU XL, MOW VC. Biomechanics of Articular Cartilage and Determination of Material Properties. *Med Sci Sport Exerc*. 2008;40(2):193-199. doi:10.1249/mss.0b013e31815cb1fc

82. Lai JH, Levenston ME. Meniscus and cartilage exhibit distinct intra-tissue strain distributions under unconfined compression. *Osteoarthr Cartil*. 2010;18(10):1291-1299. doi:10.1016/J.JOCA.2010.05.020

83. Moyer JT, Priest R, Bouman T, Abraham AC, Donahue TLH. Indentation Properties and Glycosaminoglycan Content of Human Menisci in the Deep Zone. *Acta Biomater*. 2013;9(5):6624-6629. doi:10.1016/j.actbio.2012.12.033

84. Obeid EM, Adams MA, Newman JH. Mechanical properties of articular cartilage in knees with unicompartmental osteoarthritis. *J Bone Joint Surg Br*. 1994;76(2):315-319.

85. Töyräs J, Lyyra-Laitinen T, Niinimäki M, et al. Estimation of the Young's modulus of articular cartilage using an arthroscopic indentation instrument and ultrasonic measurement of tissue thickness. *J Biomech*. 2001;34(2):251-256.

86. Danso EK, Julkunen P, Korhonen RK. Poisson's ratio of bovine meniscus determined combining unconfined and confined compression. *J Biomech*. 2018;77:233-237. doi:10.1016/J.JBIOMECH.2018.07.001

87. Danso EK, Mäkelä JTA, Tanska P, et al. Characterization of site-specific biomechanical properties of human meniscus-Importance of collagen and fluid on mechanical nonlinearities. doi:10.1016/j.jbiomech.2015.01.048

88. Hayes WC, Keer LM, Herrmann G, Mockros LF. A mathematical analysis for indentation tests of articular cartilage. *J Biomech*. 1972;5(5):541-551. doi:10.1016/0021-9290(72)90010-3

89. Parsons JR, Black J. The viscoelastic shear behavior of normal rabbit articular cartilage. *J Biomech*. 1977;10(1):21-29. doi:10.1016/0021-9290(77)90026-4

90. Mow VC, Kuei SC, Lai WM, Armstrong CG. Biphasic creep and stress relaxation of articular cartilage in compression: Theory and experiments. *J Biomech Eng*. 1980;102(1):73-84. doi:10.1115/1.3138202

91. Lai WM, Hou JS, Mow VC. A triphasic theory for the swelling and deformation behaviors of articular cartilage. *J Biomech Eng*. 1991;113(3):245-258. doi:10.1115/1.2894880

92. Biomomentum. *Mach-1 Analysis-Extraction of Elastic Model Parameters Following an Automated Indentation Mapping*.; 2015.

93. Fischenich KM, Lewis J, Kindsfater KA, Bailey TS, Haut Donahue TL. Effects of degeneration on the compressive and tensile properties of human meniscus. *J Biomech*. 2015;48(8):1407-1411. doi:10.1016/j.jbiomech.2015.02.042

94. Bank RA, Soudry M, Maroudas A, Mizrahi J, TeKoppele JM. The increased swelling and instantaneous deformation of osteoarthritic cartilage is highly correlated with collagen degradation. *Arthritis Rheum*. 2000;43(10):2202-2210. doi:10.1002/1529-0131(200010)43:10<2202::AID-ANR7>3.0.CO;2-E

95. Ewers BJ, Weaver BT, Sevensma ET, Haut RC. Chronic changes in rabbit retro-patellar cartilage and subchondral bone after blunt impact loading of the patellofemoral joint. *J Orthop Res*. 2002;20(3):545-550. doi:10.1016/S0736-0266(01)00135-8

96. Abraham AC, Pauly HM, Haut Donahue TL. Deleterious effects of osteoarthritis on the structure and function of the meniscal enthesis. *Osteoarthr Cartil*. 2014;22(2):275-283. doi:10.1016/j.joca.2013.11.013

97. Björnsson S. Quantitation of Proteoglycans as Glycosaminoglycans in Biological Fluids Using an Alcian Blue Dot Blot Analysis. *Anal Biochem*. 1998;256(2):229-237. doi:10.1006/abio.1997.2494

98. Carroll GJ. Spectrophotometric measurement of proteoglycans in osteoarthritic synovial fluid. *Ann Rheum Dis*. 1987;46(5):375-379.

99. Gandhi NS, Mancera RL. The structure of glycosaminoglycans and their interactions with proteins. *Chem Biol Drug Des*. 2008;72(6):455-482. doi:10.1111/j.1747-0285.2008.00741.x

100. Taylor KB, Jeffree GM. A new basic metachromatic dye, 1:9-Dimethyl Methylene Blue. *Histochem J*. 1969;1(3):199-204. doi:10.1007/BF01081408

101. Farndale RW, Buttle DJ, Barrett AJ. Improved quantitation and discrimination of sulphated glycosaminoglycans by use of dimethylmethylene blue. *Biochim Biophys Acta*. 1986;883(2):173-177.

102. Enobakhare BO, Bader DL, Lee DA. Quantification of Sulfated Glycosaminoglycans in Chondrocyte/Alginate Cultures, by Use of 1,9-Dimethylmethylene Blue. *Anal Biochem*. 1996;243(1):189-191. doi:10.1006/abio.1996.0502

103. Whiteman P. The quantitative measurement of Alcian Blue-glycosaminoglycan complexes. *Biochem J*. 1973;131(2):343-350.

104. Panin G, Naia S, Dall'Amico R, et al. Simple spectrophotometric quantification of urinary excretion of glycosaminoglycan sulfates. *Clin Chem*. 1986;32(11):2073-2076.

105. Pennock CA. A review and selection of simple laboratory methods used for the study of glycosaminoglycan excretion and the diagnosis of the mucopolysaccharidoses. *J Clin Pathol*. 1976;29(2):111-123.

106. Volpi N, Maccari F. Detection of submicrogram quantities of glycosaminoglycans on agarose gels by sequential staining with toluidine blue and Stains-All. *Electrophoresis*. 2002;23(24):4060-4066. doi:10.1002/elps.200290021

107. Kubaski F, Osago H, Mason RW, et al. Glycosaminoglycans detection methods: Applications of mass spectrometry. *Mol Genet Metab*. 2017;120(1-2):67-77. doi:10.1016/j.ymgme.2016.09.005

108. Keenan KE, Besier TF, Pauly JM, et al. T1ρ Dispersion in Articular Cartilage: Relationship to Material Properties and Macromolecular Content. *Cartilage*. 2015;6(2):113-122. doi:10.1177/1947603515569529

109. Li X, Cheng J, Lin K, et al. Quantitative MRI using T1ρ and T2 in human osteoarthritic cartilage specimens: Correlation with biochemical measurements and histology. *Magn Reson Imaging*. 2011;29(3):324-334. doi:10.1016/j.mri.2010.09.004

110. Akella SVS, Regatte RR, Gougoutas AJ, et al. Proteoglycan-induced changes in T1ρ-relaxation of articular cartilage at 4T. *Magn Reson Med*. 2001;46(3):419-423. doi:10.1002/mrm.1208

111. Dahl O, Persson K. Hydroxyproline, methodological studies of analysis. *Acta Chem Scand*. 1963;17(9):2499-2503.

112. Buehler MJ. *Nature Designs Tough Collagen: Explaining the Nanostructure of Collagen Fibrils*.; 2006.

113. Bergman I, Loxley R. Two Improved and Simplified Methods for the Spectrophotometric Determination of Hydroxyproline. *Anal Chem*. 1963;35(12):1961-1965. doi:10.1021/ac60205a053

114. NEUMAN RE, LOGAN MA. The determination of hydroxyproline. *J Biol Chem*. 1950;184(1):299-306.

115. Stegemann H, Stalder K. Determination of hydroxyproline. *Clin Chim Acta*. 1967;18(2):267-273. doi:10.1016/0009-8981(67)90167-2

116. Cotter MB, Loda M. Introduction to Histology. In: *Pathology and Epidemiology of Cancer*. Cham: Springer International Publishing; 2017:11-26. doi:10.1007/978-3-319-35153-7_2

117. Gartner LP, Hiatt JL, Gartner LP. *Concise Histology*. Saunders/Elsevier; 2011.

118. Schmitz N, Laverty S, Kraus VB, Aigner T. Basic methods in histopathology of joint tissues. *Osteoarthr Cartil*. 2010;18:S113-S116. doi:10.1016/j.joca.2010.05.026

119. Camplejohn KL, Allard SA. Limitations of safranin "O" staining in proteoglycan-depleted cartilage demonstrated with monoclonal antibodies. *Histochemistry*. 1988;89(2):185-188. http://www.ncbi.nlm.nih.gov/pubmed/3135283. Accessed August 12, 2018.

120. Mayer P. No Title. *Mitth aus der Zool Stn zu Neapel*. 1896;12(303).

121. Kahveci Z, Zehra Minbay F, Cavusoglu I. Safranin O Staining Using a Microwave Oven. *Zehra Minbay Ilk Cavusoglu*. 2000;75(6):264-268. doi:10.3109/10520290009085130

122. Carson FL. Histotechnology: a Self-Instructional Text. In: 2nd ed. ; 1996:154-156.

123. Pauli C, Whiteside R, Heras FL, et al. Comparison of cartilage histopathology assessment systems on human

knee joints at all stages of osteoarthritis development. *Osteoarthr Cartil*. 2012;20(6):476-485. doi:10.1016/j.joca.2011.12.018

124. Junqueira LCU, Bignolas G, Brentani RR. *Picrosirius Staining plus Polarization Microscopy, a Specific Method for Collagen Detection in Tissue Sections*. Vol 11.; 1979.

125. Titford M. Progress in the Development of Microscopical Techniques for Diagnostic Pathology. *J Histotechnol*. 2009;32(1):9-19. doi:10.1179/

126. Gannon AR, Nagel T, Bell AP, Avery NC, Kelly DJ. Postnatal changes to the mechanical properties of articular cartilage are driven by the evolution of its Collagen network. *Eur Cells Mater*. 2015;29:105-123. doi:10.22203/eCM.v029a09

127. Polito U, Peretti GM, Giancamillo M Di, et al. Meniscus Matrix Remodeling in Response to Compressive Forces in Dogs. doi:10.3390/cells9020265

128. Pritzker KPH, Gay S, Jimenez SA, et al. Osteoarthritis cartilage histopathology: grading and staging. *Osteoarthr Cartil*. 2006;14(1):13-29. doi:10.1016/j.joca.2005.07.014

129. Mankin HJ, Lippiello L. Biochemical and metabolic abnormalities in articular cartilage from osteo-arthritic human hips. *J Bone Jt Surg*. 1970;52(3):424.

130. Custers RJH, Creemers LB, Verbout AJ, van Rijen MHP, Dhert WJA, Saris DBF. Reliability, reproducibility and variability of the traditional Histologic/Histochemical Grading System vs the new OARSI Osteoarthritis Cartilage Histopathology Assessment System. *Osteoarthr Cartil*. 2007;15(11):1241-1248. doi:10.1016/j.joca.2007.04.017

131. Pearson RG, Kurien T, Shu KSS, Scammell BE. Histopathology grading systems for characterisation of human knee osteoarthritis – reproducibility, variability, reliability, correlation, and validity. *Osteoarthr Cartil*. 2011;19(3):324-331. doi:10.1016/j.joca.2010.12.005

132. Waldstein W, Perino G, Gilbert SL, Maher SA, Windhager R, Boettner F. OARSI osteoarthritis cartilage histopathology assessment system: A biomechanical evaluation in the human knee. *J Orthop Res*. 2016;34(1):135-140. doi:10.1002/jor.23010

133. Rout R, McDonnell S, Benson R, et al. The histological features of Anteromedial Gonarthrosis — The comparison of two grading systems in a human phenotype of osteoarthritis. *Knee*. 2011;18(3):172-176. doi:10.1016/j.knee.2010.04.010

134. Raunest J, Hötzinger H, Bürrig KF. Magnetic resonance imaging (MRI) and arthroscopy in the detection of meniscal degenerations: Correlation of arthroscopy and MRI with histology findings. *Arthrosc J Arthrosc Relat Surg*. 1994;10(6):634-640. doi:10.1016/S0749-8063(05)80061-1

135. Copenhaver WM, Kelly ED, Wood RL. *Bailey's Textbook of Histology*. 17th ed. Baltimore: Williams & Wilkins; 1978.

136. Rodeo SA, Seneviratne A, Suzuki K, Felker K, Wickiewicz TL, Warren RF. Histological Analysis of Human Meniscal Allografts. *J Bone Jt Surgery-American Vol*. 2000;82(8):1071-1082. doi:10.2106/00004623-200008000-00002

137. Mesiha M, Zurakowski D, Soriano J, Nielson JH, Zarins B, Murray MM. Pathologic Characteristics of the Torn Human Meniscus. *Am J Sports Med*. 2007;35(1):103-112. doi:10.1177/0363546506293700

138. Krenn V, Kurz B, Krukemeyer MG, et al. [Histopathological degeneration score of fibrocartilage. Low-grade and high-grade meniscal degeneration]. *Z Rheumatol*. 2010;69(7):644-652. doi:10.1007/s00393-010-0609-

1

139. Meister K, Indelicato PA, Spanier S, Franklin J, Batts J. Histology of the Torn Meniscus: A Comparison of Histologic Differences in Meniscal Tissue between Tears in Anterior Cruciate LigamentIntact and Anterior Cruciate LigamentDeficient Knees. *Am J Sports Med*. 2004;32(6):1479-1483. doi:10.1177/0363546503262182

140. Pauli C, Grogan SP, Patil S, et al. Macroscopic and histopathologic analysis of human knee menisci in aging and osteoarthritis. *Osteoarthr Cartil*. 2011;19(9):1132-1141. doi:10.1016/j.joca.2011.05.008

141. Berryman B. Predicting Meniscus Mechanical Properties using Quantitative Magnetization Transfer Magnetic Resonance Imaging. 2020.

142. Rautiainen J, Nissi MJ, Salo EN, et al. Multiparametric MRI assessment of human articular cartilage degeneration: Correlation with quantitative histology and mechanical properties. *Magn Reson Med*. 2015;74(1):249-259. doi:10.1002/mrm.25401

143. Kurkijärvi JE, Nissi MJ, Kiviranta I, Jurvelin JS, Nieminen MT. Delayed gadolinium-enhanced MRI of cartilage (dGEMRIC) and T2 characteristics of human knee articular cartilage: Topographical variation and relationships to mechanical properties. *Magn Reson Med*. 2004;52(1):41-46. doi:10.1002/mrm.20104

144. Lammentausta E, Kiviranta P, Töyräs J, et al. Quantitative MRI of parallel changes of articular cartilage and underlying trabecular bone in degeneration. *Osteoarthr Cartil*. 2007;15(10):1149-1157. doi:10.1016/j.joca.2007.03.019

145. Lammentausta E, Kiviranta P, Nissi MJ, et al. T2 relaxation time and delayed gadolinium-enhanced MRI of cartilage (dGEMRIC) of human patellar cartilage at 1.5 T and 9.4 T: Relationships with tissue mechanical properties. *J Orthop Res*. 2006;24(3):366-374. doi:10.1002/jor.20041

146. David-Vaudey E, Ghosh S, Ries M, Majumdar S. T2 relaxation time measurements in osteoarthritis. *Magn Reson Imaging*. 2004;22(5):673-682. doi:10.1016/j.mri.2004.01.071

147. Deoni SCL, Peters TM, Rutt BK. High-resolutionT1 andT2 mapping of the brain in a clinically acceptable time with DESPOT1 and DESPOT2. *Magn Reson Med*. 2005;53(1). doi:10.1002/mrm.20314

148. Insko EK, Bolinger L. Mapping of the radiofrequency field. *J Magn Reson - Ser A*. 1993;103(1):82-85. doi:10.1006/jmra.1993.1133

149. Ramani A, Dalton C, Miller DH, Tofts PS, Barker GJ. Precise estimate of fundamental in-vivo MT parameters in human brain in clinically feasible times. *Magn Reson Imaging*. 2002;20(10):721-731. doi:10.1016/S0730-725X(02)00598-2

150. Lisowski A. *Science of Tissue Processing*.

151. Szarko M, Muldrew K, Bertram JE. Freeze-thaw treatment effects on the dynamic mechanical properties of articular cartilage. *BMC Musculoskelet Disord*. 2010;11(1):231. doi:10.1186/1471-2474-11-231

152. Qu C, Hirviniemi M, Tiitu V, Jurvelin JS, Töyräs J, Lammi MJ. Effects of Freeze-Thaw Cycle with and without Proteolysis Inhibitors and Cryopreservant on the Biochemical and Biomechanical Properties of Articular Cartilage. *Cartilage*. 2014;5(2):97-106. doi:10.1177/1947603513515998

153. Peters AE, Akhtar R, Comerford EJ, Bates KT. The effect of ageing and osteoarthritis on the mechanical properties of cartilage and bone in the human knee joint. *Sci Rep*. 2018;8(1). doi:10.1038/s41598-018-24258-6

154. Matzat SJ, McWalter EJ, Kogan F, Chen W, Gold GE. T2 Relaxation time quantitation differs between pulse sequences in articular cartilage. *J Magn Reson Imaging*. 2015;42(1):105-113. doi:10.1002/jmri.24757

155. Lin PC, Reiter DA, Spencer RG. Sensitivity and specificity of univariate MRI analysis of experimentally degraded cartilage. *Magn Reson Med*. 2009;62(5):1311-1318. doi:10.1002/mrm.22110

156. Mittal S, Pradhan G, Singh S, Batra R. T1 and T2 mapping of articular cartilage and menisci in early osteoarthritis of the knee using 3-Tesla magnetic resonance imaging. *Polish J Radiol*. 2019;84:549-564. doi:10.5114/pjr.2019.91375

157. Wise BL, Niu J, Yang M, et al. Patterns of compartment involvement in tibiofemoral osteoarthritis in men and women and in whites and African Americans. *Arthritis Care Res*. 2012;64(6):847-852. doi:10.1002/acr.21606

158. McAlindon TE, Snow S, Cooper C, Dieppe PA. Radiographic patterns of osteoarthritis of the knee joint in the community: The importance of the patellofemoral joint. *Ann Rheum Dis*. 1992;51(7):844-849. doi:10.1136/ard.51.7.844

159. López-Franco M, Gómez-Barrena E. Cellular and molecular meniscal changes in the degenerative knee: A review. *J Exp Orthop*. 2018;5(1). doi:10.1186/s40634-018-0126-8

160. Etherington DJ, Sims TJ. Detection and estimation of collagen. *J Sci Food Agric*. 1981;32(6):539-546. doi:10.1002/jsfa.2740320603

161. Cheung HS. Distribution of Type I, II, III and V in the Pepsin Solubilized Collagens in Bovine Menisci. *Connect Tissue Res*. 1987;16(4):343-356. doi:10.3109/03008208709005619

162. Baylon EG, Levenston ME. Osmotic Swelling Responses Are Conserved Across Cartilaginous Tissues With Varied Sulfated-Glycosaminoglycan Contents. *J Orthop Res*. 2020;38(4):785-792. doi:10.1002/JOR.24521

163. SH A, JB R, NG S, JL R. Swelling significantly affects the material properties of the menisci in compression. *J Biomech*. 2015;48(8):1485-1489. doi:10.1016/J.JBIOMECH.2015.02.001

164. Biomomentum. *Mach-1 Analysis User Manual*.; 2018.

165. 2015 OARSI World Congress General Information. *Osteoarthr Cartil*. 2015;23:A4-A6. doi:10.1016/j.joca.2015.02.028

166. Legrand C, Centonze P, Comblain F, Lambert C, Sanchez C, Henrotin Y. Study of the Evolution of the Osteoarthritis Pathology and the Mechanical Properties of Cartilage in a Spontaneous Osteoarthritis Model in the Dunkin-Hartley Guinea Pigs. *Osteoarthr Cartil*. 2017;25:S314-S315. doi:10.1016/j.joca.2017.02.526

167. Sim S, Lavoie J-F, Moreau A, Garon M, Quenneville E, Buschmann M. Novel technique to map the biomechanical properties of entire mice articular surfaces using indentation. *Osteoarthr Cartil*. 2014;22:S310-S311. doi:10.1016/j.joca.2014.02.576

168. Kolaczek S, Candidate M, Changoor A, Hurtig M, Gordon K, Getgood A. *Micro-CT Visualization and Indentation Properties of Whole Meniscus Following Mercury Exposure*.

169. Sim S, Chevrier A, Garon M, Quenneville E, Buschmann M. *Novel Technique to Map the Biomechanical Properties of Entire Articular Surfaces Using Indentation to Identify Early Osteoarthritis-like Regions*.; 2014.

170. Eijgenraam SM, Bovendeert FAT, Verschueren J, et al. T2 mapping of the meniscus is a biomarker for early osteoarthritis. *Eur Radiol*. 2019;29(10):5664-5672. doi:10.1007/s00330-019-06091-1

171. Baum T, Joseph GB, Karampinos DC, Jungmann PM, Link TM, Bauer JS. Cartilage and meniscal T2 relaxation

time as non-invasive biomarker for knee osteoarthritis and cartilage repair procedures. *Osteoarthr Cartil*. 2013;21(10):1474-1484. doi:10.1016/j.joca.2013.07.012

172. Adams ME, Billingham MEJ, Muir H. The glycosaminoglycans in menisci in experimental and natural osteoarthritis. *Arthritis Rheum*. 1983;26(1):69-76. doi:10.1002/art.1780260111

Appendix A: qMT scanning protocols

No.	Sequence	Orientation	Slices per slab	FOV read	FOV phase	Slice Thickness	TR	TE	Averages	Fat suppr.	MTC	Flip angle	Base resolution	Dimension	Contrast	Bandwidth	RF spoiling	Repetition for Steady-State
0	Localizer																	
1	GRE_Fatsat	Sagittal	36	108 mm	100%	3 mm	26 ms	3.22 ms	1	Fat sat.	Uncheck	13°	256	3D	1	630 (or highest	Check	489
2	QDESS	Sagittal	36	108 mm	100%	3 mm	26 ms	3.22 ms	1	None	Uncheck	13°	256	3D	1	630 (or highest	Check	489
3	MEDESS	Sagittal	36	108 mm	100%	3 mm	26 ms	3.22 ms	1	None	Uncheck	13°	256	3D	1	630 (or highest	Check	489
	T1 map (QMT) Begain	Sagittal	36	108 mm	100%	3 mm	26 ms	3.22 ms	1	None	Uncheck	Variable	256	3D	1	630 (or highest	Check	489
4																		
	No.	*MTC*	*Flip angle*	*No. of Repetition*														
	4.1	OFF	30°	489														
	4.2	OFF	5°	489														
	4.3	OFF	10°	489														
	4.4	OFF	20°	489														
	QMT	Sagittal	36	108 mm	100%	3 mm	26 ms	3.22 ms	1	None	Variable	13°	256	3D	1	630 (or highest	Check	Variable
5	Please make the following changes first, which are under special card ↓																	
	No.	*MTC*	*MT duration*	*MT flip angle*	*MT frequency*	*No. of Repetition*												
	5.1	ON	10.24 ms	142°	433 Hz	489												
	5.2	ON	10.24 ms	426°	433 Hz	489												
	5.3	ON	10.24 ms	142°	1087 Hz	489												
	5.4	ON	10.24 ms	426°	1087 Hz	489												
	5.5	ON	10.24 ms	142°	2732 Hz	489												
	5.6	OFF	10.24 ms	N/A	N/A	489												
	5.7	ON	10.24 ms	426°	2732 Hz	489												
	5.8	ON	10.24 ms	142°	6862 Hz	489												
	5.9	ON	10.24 ms	426°	6862 Hz	489												
	5.10	ON	10.24 ms	142°	17235 Hz	489												
	5.11	ON	10.24 ms	426°	17235 Hz	489												
	B1 map (QMT)	Sagittal	36	108 mm	100%	3 mm	6000 ms	3.58 ms (d	1	None	Uncheck	Variable	64	2D	1	260	Uncheck	489
6																		
	No.	*MTC*	*Flip angle*	*No. of Repetition*														
	6.1	OFF	60°	0														
	6.2	OFF	120°	0														

Appendix B: MRI screening form

Saskatoon Health Region

MRI PATIENT SAFETY SCREENING QUESTIONNAIRE

Site ☐ **RUH** ☐ **SCH** ☐ **SPH** ☐ **OP** ☐ **IP** ☐ **GA**

Patient Name_____ **MRN**_____

Booked date_____ time _____am/pm

Place Client I.D. sticker here if available

Office use only: Require physiological monitoring, sedation, analgesia, or direct nursing care? Y N
Meets NSF risk criteria and may require Serum Creatinine testing? See over. Y N

Y N N/A

☐ ☐ **Have you had a previous MRI examination? If yes. When? _____Where? _____**

☐ ☐ **Have you had any abdominal, chest or heart surgery or procedures?**
If yes: *Did you have a Colonoscopy or Gastroscopy?* If yes: Did they snare, biopsy, or clip anything in the bowel or stomach?__
Do you have: a cardiac pacemaker, pacemaker leads, coronary artery stent, vessel coils or filters, cardiac defibrillator, prosthetic heart valve, etc, implanted in your body? Please list/describe:_____

☐ ☐ **Have you had any head, neck, spine or brain surgery or procedures?**
If Yes: Do you have: Intracranial aneurysm clip, Cochlear implants, Intra ventricular drain, valve or VP shunt (adjustable?), brain stimulator, etc.? Please list/describe: _____

☐ ☐ **Have you had any orthopedic devices such as: metal rods, pins, screws, implanted in your body?**
If yes please list/describe _____

☐ ☐ **Have you had any other surgery or procedures?** Please list/describe: _____
If so: Did they use any metallic clips, sutures, staples, etc.? Y ☐ N ☐ _____

☐ ☐ **Do you have electronic pumps, electrodes, prosthesis, or other devices implanted or attached to or near your body?**
Example: IUD, diabetic pump, pain pump, ear (cochlear) or eye implant, etc. Please list/describe: _____

☐ ☐ **Have you ever had a known foreign body in your eye or felt something strike your eye during welding, grinding, metalworking, etc. and could not confirm that you or your physician removed it successfully?** If yes, explain:

☐ ☐ **Have you ever had any metal or shrapnel pierce/enter your body from a MVA, industrial accident, or war injury?**
If yes, explain_____

☐ ☐ **Are you claustrophobic?** If yes:

	Y	N	don't know
Will you require sedation for the procedure?	☐	☐	☐
Will you supply your own from your family doctor.?	☐	☐	

☐ ☐ **Are you experiencing significant pain which could make this test difficult for you?** Will you require an Analgesic (pain medication)? If yes, please take it 30 minutes before or have it available at your appointment time.

☐ ☐ ☐ **Can you walk?** *(Ambulatory, Cane, Walker, Walk with assistance, Wheelchair, need mechanical lift)*_____

☐ ☐ **Can you lay flat on your back without moving, with only a thin pillow for a minimum of 30 min?**_____

☐ ☐ **Do you have any dentures, hearing aides, or a wig?** If so, they must be removed prior to MRI scan.

☐ ☐ ☐ **Is there any chance that you might be pregnant?** If yes when is your due date? _____ or LMP_____

☐ ☐ **Do you have any body piercing(s) or Tattoos?** _____

☐ ☐ **Do you use any trans-dermal medication patches?**_____ If so, they must be removed prior to scanning.

For Breast MRI only: When did your last menstrual period begin? _____

What is your height? _____FT. IN. _____METRES **What is your weight?** _____LBS_____KG

Do you have any other concerns or comments about having an MRI scan? _____

_____

_____

This questionnaire was completed by (circle): patient, mother, father, sibling, guardian, nurse, other_____

(If completed in person) **Patient/Guardian signature** ***X***_____ Date _____

Technologist/Nurse signature_____Date_____

PHONE SCREENED OUTPATIENTS ONLY:

☐ ☐ ☐ *Do you know how to get here and where to park?*

Over

Word Form # 102676 11/12

102676

Patient Name_____ **MRN**_____

Place Client I.D. sticker here if available

For Gadolinium enhanced MRI examinations only----NSF RISK ASSESSMENT

Patients with significant renal (kidney) disease may be at an increased risk of developing NSF (Nephrogenic Systemic Fibrosis), a serious but rare condition resulting in fibrosis of the skin, muscles, and internal organs Exposure to .MRI contrast (Gadolinium) has been implicated in the development of NSF.

√ **Y**es or **N**o for the following:

	Y	N	
1	☐	☐	**Are you over the age of 60?**
2	☐	☐	**Do you have a history of renal (kidney) disease or serious injury to the kidneys?**
3	☐	☐	**Do you have a history of liver disease?**
4	☐	☐	**Are you diabetic?**
5	☐	☐	**Have you had an organ transplant?**
6	☐	☐	**Do you have a history of hypertension (high blood pressure)?**
7	☐	☐	**Have you ever been on kidney dialysis?**
8	☐	☐	**Do you have a history of vascular disease including stroke, heart attack, or peripheral vascular disease?**
9	☐	☐	**Have you had recent chemotherapy (within 60 days)?**

If you answered yes to any of the above you will need to have a **serum creatinine** level blood test obtained within a 3 months period prior to your gadolinium enhanced MRI. It will be important for that result to be available for the radiologist on the day of the MRI, to determine if it is safe to administer gadolinium. You may already have these results as part of a recent routine blood-test, and if so, we will access those results. If not we will arrange to have this done either at the hospital or a clinic of your choice. If you are already onsite we will arrange for this to be done here today before your MRI.

For Office Use Only: **LAB RESULTS**

Date of specimen collection _____

SerumCreatinine(umol/L)_____ **Reference range – adult male 60-104 umol/l**
Reference range—adult female 45-90 umol/l

eGFR (mL/min/1.73m^2)_____

Word Form # 102676 11/12 102676

Appendix C: Consent form

UNIVERSITY OF SASKATCHEWAN

PARTICIPANT INFORMATION AND CONSENT FORM

STUDY TITLE:

Validation of a Non-Invasive MRI Imaging Tool to Assess the Structure and Function of Osteoarthritic Articular Cartilage and Meniscus

PRINCIPAL INVESTIGATOR (PI):
Emily McWalter, PhD
Assistant Professor, Department of Mechanical Engineering
University of Saskatchewan
57 Campus Drive, Saskatoon, SK, S7N 5A9
phone: (306) 966-5298
email: emily.mcwalter@usask.ca

SUB-INVESTIGATORS
Ives Levesque, PhD
Ives.levesque@mcgill.ca
Medical Physics Unit
McGill University

William Dust, MD
william.dust@usask.ca
College of Medicine
University of Saskatchewan

Brian Eames, PhD
b.frank@usask.ca
College of Medicine
University of Saskatchewan

Haron Obaid
haron.obaid@usask.ca
College of Medicine
University of Saskatchewan

STUDENT RESEARCHERS
Kirstin Olsen

kdo068@mail.usask.ca

Lumeng Cui

lumeng.cui@usask.ca

SPONSOR:
The Arthritis Society of Canada

INTRODUCTION
You are invited to take part in this research study because you are undergoing a total knee replacement for the treatment of osteoarthritis.

Your participation is voluntary. It is up to you to decide whether or not you wish to take part. If you wish to participate, you will be asked to sign this form. If you do decide to take part in this study, you are still free to withdraw at any time and without giving any reasons for your decision.

If you do not wish to participate, you will not lose the benefit of any medical care to which you are entitled or are presently receiving. It will not affect your relationship with any of the researchers or with your surgeon Dr. Dust.

Please take time to read the following information carefully. You can ask the study principal investigator or staff to explain any information that you do not clearly understand. You may ask as many questions as you need. Please feel free to discuss this with your family, friends or family physician before you decide.

WHO IS CONDUCTING THE STUDY?
The study is being conducted by Dr. McWalter, her co-investigators, and her students at the University of Saskatchewan. The sponsor of this study, The Arthritis Society of Canada, will reimburse Dr. McWalter and the University of Saskatchewan for the costs of undertaking this study. However, neither the institution nor any of the investigators or staff will receive any direct financial benefit from conducting this study.

WHY IS THIS STUDY BEING DONE?
This study is being done because we are in need of more validated and robust research tools to measure osteoarthritis in its early stages, before the damage to the joint is too severe. This research tool can then be used to study the disease in its early stages, monitor disease progression, and develop and evaluate new treatment methods.

WHO CAN PARTICIPATE IN THE STUDY?
You are eligible to participate in this study if you are scheduled to undergo a total knee replacement surgery for treatment of osteoarthritis.

You may not participate in this study if you have any contraindications for magnetic resonance imaging (MRI) including but not limited to a cardiac pacemaker, implanted metal, pregnancy, a history of metal work or potential metal fragments within the eye, and severe claustrophobia that would interfere with your ability to have your legs inserted into the MRI bore (diameter 60 cm).

The goal is to recruit 30 individuals to participate in this study.

WHAT DOES THE STUDY INVOLVE?
If you decide to take part in this study, it involves one visit to the Royal University Hospital (RUH) scheduled before your total knee replacement surgery. This visit will take about 2.5 hours. During this visit you will be asked to complete a questionnaire about you (e.g. date of birth, height, weight, knee pain, physical activity levels) and you will have an imaging scan completed. The Magnetic Resonance Imaging (MRI) test involves a series of scans of your knee and will take about two hours in total.

This study will assess various characteristics of the tissue obtained from you and other participants during your knee replacement surgery. No special modifications to your surgery are required in order for us to obtain these tissue samples, we would simply be collecting the articular cartilage and meniscus tissue considered to be surgical waste after your surgery is complete. These tissues will be scanned in the MRI and then various tests will be performed on them (histological, biochemical, and mechanical analysis) to determine several tissue properties that describe the health and function of the tissue. Your tissue will only be used for this specific study and will be discarded after a length of time required for study completion and publication.

Each participant will fill out a questionnaire immediately before MRI scanning in a private room near the MRI center in RUH asking basic information (sex, height, weight, date of birth, knee pain, physical activity

levels etc.). This form should take approximately 30 minutes to fill out. This information will be used to identify any potential bias in the data; for example, results of a group of all young individuals may differ from those of a group of older individuals.

Each participant will also undergo one MRI of the knee(s) being operated on prior to surgery. This MRI exam will consist of a series of scans of your knee that will last approximately two hours. The MRI exam will take place at Royal University Hospital. After your surgery has been completed we will also be scanning the removed tissues which you will not be present for.

Information from your health record, limited to that related to osteoarthritis and knee replacement surgery, such as degree of tissue damage and X-rays prior to surgery will be acquired.

Not including the time it will take for your surgeon to perform your knee replacement, your total commitment to this study will not be more than 2.5 hours.

Participation in the study will involve extra requirements outside the standard of care (i.e. in addition to having the total knee replacement surgery). These extra requirements are:

1. Filling out a questionnaire that asks about your sex, height, weight, date of birth, knee pain, physical activity levels.
2. Having an extra MRI scan that will take just over one hour.
3. Collection of tissue that would normally be discarded after surgery. The tissue will be kept and tested. These tests will look at the health of your tissue including biochemical content, structure and mechanical function.

OPTION OF HAVING DATA STORED IN A RESEARCH DATABASE

The researchers are creating a database of MRI data that may be used to answer additional research questions in the future. The purpose of this is to use the research data to its fullest extent in the long term. For example, a larger study of patients with osteoarthritis of the knee may need to be compared to a group of individuals with healthy knees; instead of collecting data from osteoarthritis patients again, we could use the data collected for the present study. Examples of other potential studies that may be conducted include further knee osteoarthritis, anterior cruciate ligament injury (ACL), meniscus injury, changes in tissue health with age, and changes in tissue health with exercise. Your tissue samples will not be included in this database, it is for MR images (pictures) only.

Having your information included in this database is optional and does not impact your participation in the present study. The data will be stored until the lead investigator, Dr. Emily McWalter, either retires or leaves the University of Saskatchewan at which point it will be destroyed. The database will consist of only de-identified data, this means that your name will not be included in the database. Information such as the study you participated in and your MRI scans, age, height, sex, weight will be included. The database will be password protected on an encrypted computer. Only Dr. McWalter's research team and collaborators at the University of Saskatchewan will have access to the database. Prior to using your data in any subsequent research studies, approval by the University of Saskatchewan Research Ethics Board will be obtained but you will not be contacted to reaffirm consent.

WHAT ARE THE BENEFITS OF PARTICIPATING IN THIS STUDY?

If you choose to participate in this study, there will not be direct benefits to you. It is hoped the information gained from this study can be used in the future to benefit other people with knee injury or disease. Once the study is complete, a summary of the aggregate study results and published data will be provided to you

via PDF attachment in an email from Dr. Emily McWalter. If you do not have email, a paper copy will be mailed.

The study may lead to the development of commercial products but there are no plans to share with you any financial profits resulting from the use of your samples or data.

WHAT ARE THE POSSIBLE RISKS AND DISCOMFORTS?
To date, there are no known long-term health risks associated with having a MRI procedure. For the MRI you will be moved into the round tunnel of the scanner. Some individuals feel claustrophobic in the MRI scanner, however, in this study you will move into the scanner 'feet first' and so your head will be on the edge or outside of the tunnel. The extended length of your MRI session could result in you becoming uncomfortable lying still during the scan or a brief elevation in your body temperature. The MRI technologist or researcher operating the system will visually monitor you throughout the procedure and will communicate with you via a two-way telecom system throughout the MRI exam. The MRI exam can be stopped at any time if you are uncomfortable.

Despite the many safeguards in place to protect your personal information, as with any data, there is a risk that data can be released either inadvertently or by cyber-attack. In a case of a data breach, you will be contacted and the course of action to protect you and your data will be communicated.

WHAT HAPPENS IF I DECIDE TO WITHDRAW?
Your participation in this research is voluntary. You may withdraw from this study at any time. You do not have to provide a reason. Your future medical care will not be affected.

If you choose to enter the study and then decide to withdraw at a later time, all data collected about you during your enrolment will be retained for analysis.

WHAT HAPPENS IF SOMETHING GOES WRONG?
In the case of a medical emergency related to the study or during the MRI scan, necessary medical treatment will be made available at no cost to you. By signing this document, you do not waive any of your legal rights against the sponsor, investigators or anyone else.

WHAT HAPPENS AFTER THE COMPLETION OF THE STUDY?
The results of the study in the form of a brief summary and/or published aggregate data will be sent to you via PDF attachment in an email after the completion of the entire project from the Principal Investigator Dr. Emily McWalter. If you do not have email, a paper copy will be mailed to you.

WHAT WILL THE STUDY COST ME?
You will not be charged for any research-related procedures. You will not be paid for participating in this study. Parking costs will be covered for the 2.5 hour visit to the MRI center in RUH. The research assistant (Kirstin Olsen) will accompany you to the parking payment machines in the RUH lobby and pay the parking fee.

WILL MY PARTICIPATION BE KEPT CONFIDENTIAL?
In Saskatchewan, the Health Information Protection Act (HIPA) defines how the privacy of your personal health information must be maintained so that your privacy will be respected. Your name will not be attached to any information, nor mentioned in any study report, nor be made available to anyone except the research team. A key that associates your name with a study ID will be stored securely (in a password protected file on an encrypted computer under the supervision of the principal investigator) and will only be accessible by research team members. A study ID is a code using numbers and not any personal

information or initials that links the collected data (MRI and tissue) to you. Data collected by the study team will be retained for a minimum of 5 years after the final results are published. There is also a possibility that de-identified MRI scans (i.e. your MRI scans without any of your personal information attached to it) will be securely transported to a researcher at McGill University for further research purposes. Tissue samples collected during surgery will be securely stored and labelled using a study ID, not your name, for the duration of the study and will be disposed of two years after the results have been published. It is the intention of the research team to publish results of this research in scientific journals and to present the findings at related conferences and workshops, but your identity will not be revealed. Research records identifying you may be inspected by the University of Saskatchewan Biomedical Research Ethics Board in the presence of the Principal Investigator for quality assurance and monitoring purposes. The MRI protocols used in this study consist of research sequences, therefore your MRI results will not be used by the study team or your doctors to guide medical decisions regarding your care. The MRI images will only be kept as part of your study data and will not become part of your medical record.

In the rare case that a team member cuts himself or herself while preparing the tissue obtained from your surgery, your personal health record may be accessed by the attending physician(s) if it is required to inform appropriate course of care. The information will only be accessed by the physician(s) and will only be shared with the team member who cut himself or herself if necessary.

WHO DO I CONTACT IF I HAVE QUESTIONS ABOUT THE STUDY?

If you have any questions or desire further information about this study before or during participation, you can contact Dr. Emily McWalter at *306-966-5298*.

If you have any concerns about your rights as a research participant and/or your experiences while participating in this study, contact the Chair of the University of Saskatchewan Research Ethics Board, at *306-966-2975(out of town calls 1-888-966-2975)*. The Research Ethics Board is a group of individuals (scientists, physicians, ethicists, lawyers and members of the community) that provide an independent review of human research studies. This study has been reviewed and approved on ethical grounds by the University of Saskatchewan Research Ethics Board.

UNIVERSITY OF SASKATCHEWAN

PARTICIPANT CONSENT TO PARTICIPATE

Study Title:

Validation of a Non-Invasive MRI Imaging Tool to Assess the Structure and Function of Osteoarthritic Articular Cartilage and Meniscus

- I have read (or someone has read to me) the information in this consent form.
- I understand the purpose and procedures and the possible risks and benefits of the study.
- I was given sufficient time to think about it.
- I had the opportunity to ask questions and have received satisfactory answers.
- I understand that I am free to withdraw from this study at any time for any reason and the decision to stop taking part will not affect my future relationships.
- I give permission to the use and disclosure of my de-identified information collected for the research purposes described in this form.
- I understand that by signing this document I do not waive any of my legal rights.
- I will be given a signed copy of this consent form.

I agree to allow the tissue that is taken for surgery to be used for research: Yes No

I agree to be contacted about research projects in the future. Yes No

I give permission for the data collected to be stored in a database and used for similar, related research studies not described in this form knowing that my identity will remain confidential.

Yes No

I agree to participate in this study:

Printed name of participant: _____ _____

Signature Date

Printed name of person obtaining consent: _____ _____

Signature Date

Appendix D: Participant demographic survey

Participant Information Form

Full name: _____

Email address: _____

Phone number: _____

Sex: _____

Date of birth: _____

Height: _____

Weight: _____

Knee being replaced: Left / Right (Please Circle One)

Dominant knee – which foot would you kick a ball with? : Left / Right (Please Circle One)

Frequency of activity: Rarely / 1-2 times per week / 3-4 times per week / 5+ times per week (Please Circle One)

Type of activities: Walking / Running / Cycling / Gym / Housework / Other: _____

_____ (Circle all that apply)

Appendix E: KOOS pain survey

KOOS KNEE SURVEY

Today's date: _____/_____/_____ Date of birth: _____/_____/_____

Name: _____

INSTRUCTIONS: This survey asks for your view about your knee. This information will help us keep track of how you feel about your knee and how well you are able to perform your usual activities.
Answer every question by ticking the appropriate box, only one box for each question. If you are unsure about how to answer a question, please give the best answer you can.

Symptoms
These questions should be answered thinking of your knee symptoms during the **last week**.

S1. Do you have swelling in your knee?

Never	Rarely	Sometimes	Often	Always
☐	☐	☐	☐	☐

S2. Do you feel grinding, hear clicking or any other type of noise when your knee moves?

Never	Rarely	Sometimes	Often	Always
☐	☐	☐	☐	☐

S3. Does your knee catch or hang up when moving?

Never	Rarely	Sometimes	Often	Always
☐	☐	☐	☐	☐

S4. Can you straighten your knee fully?

Always	Often	Sometimes	Rarely	Never
☐	☐	☐	☐	☐

S5. Can you bend your knee fully?

Always	Often	Sometimes	Rarely	Never
☐	☐	☐	☐	☐

Stiffness
The following questions concern the amount of joint stiffness you have experienced during the **last week** in your knee. Stiffness is a sensation of restriction or slowness in the ease with which you move your knee joint.

S6. How severe is your knee joint stiffness after first wakening in the morning?

None	Mild	Moderate	Severe	Extreme
☐	☐	☐	☐	☐

S7. How severe is your knee stiffness after sitting, lying or resting **later in the day**?

None	Mild	Moderate	Severe	Extreme
☐	☐	☐	☐	☐

Pain

P1. How often do you experience knee pain?

Never	Monthly	Weekly	Daily	Always
☐	☐	☐	☐	☐

What amount of knee pain have you experienced the **last week** during the following activities?

P2. Twisting/pivoting on your knee

None	Mild	Moderate	Severe	Extreme
☐	☐	☐	☐	☐

P3. Straightening knee fully

None	Mild	Moderate	Severe	Extreme
☐	☐	☐	☐	☐

P4. Bending knee fully

None	Mild	Moderate	Severe	Extreme
☐	☐	☐	☐	☐

P5. Walking on flat surface

None	Mild	Moderate	Severe	Extreme
☐	☐	☐	☐	☐

P6. Going up or down stairs

None	Mild	Moderate	Severe	Extreme
☐	☐	☐	☐	☐

P7. At night while in bed

None	Mild	Moderate	Severe	Extreme
☐	☐	☐	☐	☐

P8. Sitting or lying

None	Mild	Moderate	Severe	Extreme
☐	☐	☐	☐	☐

P9. Standing upright

None	Mild	Moderate	Severe	Extreme
☐	☐	☐	☐	☐

Function, daily living

The following questions concern your physical function. By this we mean your ability to move around and to look after yourself. For each of the following activities please indicate the degree of difficulty you have experienced in the **last week** due to your knee.

A1. Descending stairs

None	Mild	Moderate	Severe	Extreme
☐	☐	☐	☐	☐

A2. Ascending stairs

None	Mild	Moderate	Severe	Extreme
☐	☐	☐	☐	☐

For each of the following activities please indicate the degree of difficulty you have experienced in the **last week** due to your knee.

A3. Rising from sitting

None	Mild	Moderate	Severe	Extreme
☐	☐	☐	☐	☐

A4. Standing

None	Mild	Moderate	Severe	Extreme
☐	☐	☐	☐	☐

A5. Bending to floor/pick up an object

None	Mild	Moderate	Severe	Extreme
☐	☐	☐	☐	☐

A6. Walking on flat surface

None	Mild	Moderate	Severe	Extreme
☐	☐	☐	☐	☐

A7. Getting in/out of car

None	Mild	Moderate	Severe	Extreme
☐	☐	☐	☐	☐

A8. Going shopping

None	Mild	Moderate	Severe	Extreme
☐	☐	☐	☐	☐

A9. Putting on socks/stockings

None	Mild	Moderate	Severe	Extreme
☐	☐	☐	☐	☐

A10. Rising from bed

None	Mild	Moderate	Severe	Extreme
☐	☐	☐	☐	☐

A11. Taking off socks/stockings

None	Mild	Moderate	Severe	Extreme
☐	☐	☐	☐	☐

A12. Lying in bed (turning over, maintaining knee position)

None	Mild	Moderate	Severe	Extreme
☐	☐	☐	☐	☐

A13. Getting in/out of bath

None	Mild	Moderate	Severe	Extreme
☐	☐	☐	☐	☐

A14. Sitting

None	Mild	Moderate	Severe	Extreme
☐	☐	☐	☐	☐

A15. Getting on/off toilet

None	Mild	Moderate	Severe	Extreme
☐	☐	☐	☐	☐

For each of the following activities please indicate the degree of difficulty you have experienced in the **last week** due to your knee.

A16. Heavy domestic duties (moving heavy boxes, scrubbing floors, etc)

None	Mild	Moderate	Severe	Extreme
☐	☐	☐	☐	☐

A17. Light domestic duties (cooking, dusting, etc)

None	Mild	Moderate	Severe	Extreme
☐	☐	☐	☐	☐

Function, sports and recreational activities

The following questions concern your physical function when being active on a higher level. The questions should be answered thinking of what degree of difficulty you have experienced during the **last week** due to your knee.

SP1. Squatting

None	Mild	Moderate	Severe	Extreme
☐	☐	☐	☐	☐

SP2. Running

None	Mild	Moderate	Severe	Extreme
☐	☐	☐	☐	☐

SP3. Jumping

None	Mild	Moderate	Severe	Extreme
☐	☐	☐	☐	☐

SP4. Twisting/pivoting on your injured knee

None	Mild	Moderate	Severe	Extreme
☐	☐	☐	☐	☐

SP5. Kneeling

None	Mild	Moderate	Severe	Extreme
☐	☐	☐	☐	☐

Quality of Life

Q1. How often are you aware of your knee problem?

Never	Monthly	Weekly	Daily	Constantly
☐	☐	☐	☐	☐

Q2. Have you modified your life style to avoid potentially damaging activities to your knee?

Not at all	Mildly	Moderately	Severely	Totally
☐	☐	☐	☐	☐

Q3. How much are you troubled with lack of confidence in your knee?

Not at all	Mildly	Moderately	Severely	Extremely
☐	☐	☐	☐	☐

Q4. In general, how much difficulty do you have with your knee?

None	Mild	Moderate	Severe	Extreme
☐	☐	☐	☐	☐

Thank you very much for completing all the questions in this questionnaire.

Appendix F: TKA Study Ethics Certificate

UNIVERSITY OF SASKATCHEWAN

Biomedical Research Ethics Board (Bio-REB) 09-May-2019

Certificate of Approval

Application ID: 1039

Principal Investigator: Emily McWalter Department: Department of Mechanical Engineering

Locations Where Research Activities are Conducted: ENG 2C50, HS B330, HS B109B, RUH MRI Centre, Canada

Student(s): Kirstin Olsen
Lumeng Cui

Funder(s): Arthritis Society

Sponsor:

Title: Validation of a Non-Invasive MRI Imaging Tool to Assess the Structure and Function of Osteoarthritic Articular Cartilage and Meniscus

Protocol Number:

Approved On: 08/05/2019

Expiry Date: 07/05/2020

Approval Of:

* Notice of Ethical Review Response, rec'd 04-May-2019
* Biomedical Application, Prospective, rec'd 04-May-2019
* Participant Information and Consent Form, v.2 (May2019)
* MRI Screening Form, rec'd 04-May-2019

Acknowledgment Of:

Review Type: Full Board

Meeting Date: 20/03/2019

IRB Registration Number: Not Applicable

CERTIFICATION

The University of Saskatchewan Biomedical Research Ethics Board (Bio-REB) has reviewed the above-named project.The project is acceptable on scientific and ethical grounds. The principal investigator has the responsibility for any other administrative or regulatory approvals that may pertain to this project, and for ensuring that the authorized project is carried out according to governing law. This approval is valid for the specified period provided there is no change to the approved project.

FIRST TIME REVIEW AND CONTINUING APPROVAL

The University of Saskatchewan Research Ethics Boards review above minimal risk projects at a full-board (face-to-face) meeting. If a project has been reviewed at a full board meeting, a subsequent project of the same protocol may be reviewed through the delegated review process. Any research classified as minimal risk is reviewed through the delegated (subcommittee) review process. The initial Certificate of Approval includes the approval period the REB has assigned to a study. The Status Report form must be submitted within one month prior to the assigned expiry date. The researcher shall indicate to the REB any specific requirements of the sponsoring organizations (e.g. requirement for full-board review and approval) for the continuing review process deemed necessary for that project.

REB ATTESTATION

In respect to clinical trials, the University of Saskatchewan Research Ethics Board complies with the membership requirements for Research Ethics Boards defined in Part 4 of the Natural Health Products Regulations and Part C Division 5 of the Food and Drug Regulations and carries out its functions in a manner consistent with Good Clinical Practices. Members of the Bio-REB who are named as investigators, do not participate in the discussion related to, nor vote on such studies when presented to the Bio-REB. This approval and the views of this REB have been documented in writing. The University of Saskatchewan Biomedical Research Ethics Board is constituted and operates in accordance with the current version of the Tri-Council Policy Statement: Ethical Conduct for Research Involving Humans (TCPS 2 2014).

Digitally Approved by Gordon McKay, Ph.D.
Chair, Biomedical Research Ethics Board
University of Saskatchewan

Appendix G: Mach-1 Indentation Testing SOP

Mach -1 Indentation Testing Steps

Written by Kirstin Olsen

Last Updated: January 31, 2020

First: Indentation Test Steps

1. Open Mach-1 motion software
    - Select CSS configuration
2. Turn on motion controller (at back of device above the power cord inlet)
3. Press start button on motion software
4. Calibrate the load cell
    - Click load cells button
    - Make sure proper load cell is selected
        - This can be checked by lightly touching the load cell area to see if there is a response on the motion screen of live force detection
    - Select calibrate button
    - Select calibration weight (big weight for 17 & 70 N load cell)
    - Follow prompts
    - Record calibration factor in book
5. Install prepped sample
    - Pick suitable height of plastic ring (the smaller size is the most ideal)
    - Put rubber circle around it and then put plastic ring retainer device into the metal bottom and tighten screws
    - Screw sample onto the sample holder component
        - Line up the sample so that it is in line with an edge (draw with sharpie where the middle of the sample holder platform is in line with the middle of the outer part when screwed in and then align the sample with this in mind)
    - Wipe outside with disinfectant and bring to Mach-1 machine
    - Make sure platform is covered with lab bench protective material to save hardware from possible spills.
    - Screw fixture containing sample into the base of the Mach-1
6. Install indenter carefully onto load cell
    - In the spherical indenter kit, there will be a bag labelled “tools”. Take out the larger metal piece and use the smaller tool to screw the desired indenter (several different sizes available) into this larger piece. Then screw this piece with the indenter attached into the load cell.
7. Take off camera cap and open mapping toolbox software
    - Click camera and start
    - Move stage using manual controls in Mach-1 motion window
    - Focus image by using controls on the actual camera
    - Center and focus sample

8. Place small red and blue marks on your sample, making sure they are spread out (opposite sides of sample)
9. Pick your sample locations and the blue and red reference points on your mapping toolbox
    - Go to edit – reference 1 (red) then select where on the image the red dot is located. Do the same for the blue dot
    - Go to edit – add boundary to set a boundary for the samples (when mechanical testing occurs it will not go outside of this area)
        - This is good for making sure the indenter never hits the platform and just stays on the sample
    - View – grid shows you a grid system for selecting your sample locations. You can change the grid size in edit – grid
    - Make sure edit – add position is selected before picking your points. Then you can click where you want it to sample. If you click ctrl, it will allow you to just hover over the points and it selects them for you
        - The order you click is the order it will sample them so pick points that are close together and follow a logical pattern to save time when performing the actual test
10. Save your position map and image of your sample
    - Go to file – create .map and then select the appropriate folder and file name
    - This will save a txt file with all your locations and an image (picture) of your sample
11. Perform a mapping calibration
    - Go to edit – calibration in the mapping toolbox software
    - Go back to the mach-1 motion software and manually move the indenter until it is over top of either the red or blue marker
    - Record the values of the x and y positions listed on the motion software (top right corner) in the proper location on the calibration window. Do both red and blue
    - Export to file – save with appropriate name in the proper location
12. Do a test scan function to make sure your points seem accurate
    - First manually lift indenter to above the plastic ring
    - Go to Mach-1 motion software and select scan in the function drop down menu
    - Click load X-Y and select the correct calibration file, the values should all load into the positions X-Y (mm) boxes
    - In the repetitions box enter the number of positions (given above) and make sure you click outside of the box after so there is no blinking cursor
    - Click execute and ok and watch the indenter to make sure it positions it moves to seem correct
13. Add PBS (phosphate buffered saline) to container
    - Must entirely cover specimen and tip of indenter
    - **********Watch for spills! If specimen holder was assembled incorrectly or plastic ring has been nudged spills are extremely likely. Make sure there is lab bench protective coverings over the machine hardware
14. Manually move the indenter to a height where it will clear any part of the sample on its path but is also low enough to take less time. This height will be the starting point of the indenter for all sample locations
15. Do the indentation tests
    - Click insert function in the sequence box
    - Change it to Normal Indentation by selecting this in the function drop down

- Select/change to all the proper values
- Click browse data files and name a file with the proper name for the indentation test in the current folder

  ***If you do not do this, data will not save!!
- Click execute and then ok

16. Wait for indentation test to finish
17. Manually raise indenter, carefully unscrew indenter component from the load cell and clean with ethanol disinfectant. Unscrew indenter from adapter and replace to correct locations.

Second: Thickness Test Steps

1. Install appropriately long needle (may need to choose a longer one for meniscus) onto the needle attachment then carefully remove needle casing and screw onto load cell
2. Lower the needle so that it is as close to the tissue surface as possible while still being able to clear all points along its path.
3. Perform thickness test
   - Replace the Normal Indentation function with a Find Contact function in the drop-down menu. Leave Scan before this.
   - Select appropriate parameters
   - Ensure you create a new data file path titled “Sample Name Thickness”
   - Execute the sequence as many times as there are samples (need thickness data for all points to do indentation analysis)
4. Wait for thickness test to finish
5. Manually raise indenter and remove/clean needle and needle attachment from the load cell carefully.
6. Remove sample set-up and do clean up
7. Turn off motion controller and close the motion software when test is complete

Third: Analysis Steps

1. Open mapping toolbox and create a new .map file with your positions and boundaries
   - File – open image and select correct image
   - File – import .map and select the map you made previously with references and sample points
   - If not already done, make a boundary around your sample (edit – add boundary)
   - Save this as filename – Results .map (file – create .map)
2. Open up your newly created .map file (in notepad)
3. Edit .map file to have your result headings
   - First you will have to assign a characterization, this is the row that says MAPPING many times. Put your cursor after last MAPPING and click tab then write your category. It should either be indentation or thickness, but you could also include other values such as histology scores and biochemistry values. Hit tab again and re write it again. You will need to do this for however many results columns you will be adding (depends on the test, four for indentation and two for thickness)

- You will also need to copy and paste the image file designation (row above characterization) for as many pieces of data you will add as well
- Next add in your headings. Click at the end of ScanY(mm) and click tab. Then type Instantaneous Modulus (MPa). Click tab – type Shear Modulus (MPa) – tab – type Elastic Fit Mean Squared Error () – tab – type Surface Angle (deg) – tab – Vertical Thickness (mm) – tab – Cartilage/Meniscus Thickness (mm)
- File save

4. Locate and open your results
    - Open the Mach-1 Analysis software
    - Click the little folder button beside the folder path box and select the folder that contains your data (the results you saved from your experiment using the Mach-1 motion software)
5. Get surface angle for each data point
    - Click on your indentation test results then click on the first "Normal Indentation"
    - In the bottom left corner, there is a box with test information. Scroll down in this box until the last block of information to record the Angle from Z-axis for each point
        - Make sure when you copy the angle that you choose the angle that says Yes for Surface Normal is Valid. If it does not say yes, it means that there was an error with the surface scan and the test failed at that point
6. Get thickness data for each point
    - Click on your thickness test results then click on the first "Find Contact"
    - Ensure your Y-axis is set to Fz, N and your X-axis is Position (z), mm
    - Select "Cursors" in the analysis drop down menu
    - To ensure accurate selection of points it is recommended to zoom in on the area of interest (with any of the tools to the right of the cross)
    - Use the cross tool on the right to move the cursors
        - The first vertical line should be moved to the point where the load starts to change
        - The second should be at the point of contact with the subchondral bone (this is the inflection point where the force suddenly rapidly increases)
    - Copy the Delta X (mm) value located in the results window and paste it into your .map file under the Vertical Thickness (mm) heading
    - For cartilage or meniscus thickness, calculate Vertical Thickness x cos(Surface Angle) and write it into your .map file
7. Get indentation data
    - Make sure your Y-axis is Normal Force, N and your x is Normal Position, mm
    - Click the analysis drop down and select "Elastic Model in Indentation"
    - Fill in all the proper inputs (indenter radius is half the size you used because they all state the diameter on their packaging)
    - You will see 3 buttons with diagrams on them on the bottom right above print, help, and about. Select the far left one (looks like a cross)
    - Move the first blue dot to align with where the curve begins to change. This will create a line of best fit, move this first dot until the best fit is achieved
    - Scroll down until you see the RESULTS. Copy and paste these into your .map file under the respective heading. The first normal indentation curve corresponds to the first point. The order to record the data is the same as you wrote the headings. In the map file click beside the last number entered and click tab then copy and paste then tab and so on. Data will not line up with the headings in the map file.

- When it comes to surface angle you actually get this at the bottom of the data information box on the left (angle from z-axis, deg)
- Keep moving down the list and entering your data as you go
- File save

Mach-1: Color Mapping Procedure

1. Open Analysis – MAP software
2. Select Open .map File button (top left)
3. Find the appropriate file (the one you made in the previous section) and click ok
4. Click on the .map file in the file list and then click on your property of interest in the characterizations list
5. Click mapping and then choose your reference image and press ok
6. At this point you should see your sample picture with a color map. Adjust your image using the various options then save image and scale.

Appendix H: Cadaver Study Ethics Certificate

UNIVERSITY OF SASKATCHEWAN

Biomedical Research Ethics Board (Bio-REB) 24-Jul-2020

Certificate of Re-Approval

Ethics Number: 16-158

Principal Investigator: Emily McWalter Department: Department of Mechanical Engineering

Locations Where Research Activities are Conducted: Canadian Light Source, Canada
College of Kinesiology, Canada
Royal University Hospital, Saskatoon, Canada

Student(s): Alvaro Espinosa Maldonado
Brennan Berryman
Chelsey Thorson
Ibukunoluwa Elebute
Kirstin Olsen
Lumeng Cui
Madeline Martel

Funder(s): Canada Foundation for Innovation
College of Engineering
Innovation Saskatchewan
Natural Sciences and Engineering Research Council of Canada
Office of the Vice-Provost, Faculty Relations

Sponsor:

Title: MRI and Mechanical Testing of Cadaver Knee Specimens

Protocol Number:

Approval Effective Date: 16/07/2020

Expiry Date: 16/07/2021

Acknowledgment Of:

Review Type: Delegated Review

IRB Registration Number:

* This study, inclusive of all previously approved documents, has been re-approved until the expiry date noted above

Application ID: 16-158 Principal Investigator: Emily McWalter 2 / 2

CERTIFICATION

The University of Saskatchewan Biomedical Research Ethics Board (Bio-REB) has reviewed the above-named project.The project is acceptable on scientific and ethical grounds. The principal investigator has the responsibility for any other administrative or regulatory approvals that may pertain to this project, and for ensuring that the authorized project is carried out according to governing law. This approval is valid for the specified period provided there is no change to the approved project.

FIRST TIME REVIEW AND CONTINUING APPROVAL

The University of Saskatchewan Research Ethics Boards review above minimal projects at a full-board (face-to-face) meeting. If a project has been reviewed at a full board meeting, a subsequent project of the same protocol may be reviewed through the delegated review process. Any research classified as minimal risk is reviewed through the delegated (subcommittee) review process. The initial Certificate of Approval includes the approval period the REB has assigned to a study. The Status Report form must be submitted within one month prior to the assigned expiry date. The researcher shall indicate to the REB any specific requirements of the sponsoring organizations (e.g. requirement for full-board review and approval) for the continuing review process deemed necessary for that project.

REB ATTESTATION

In respect to clinical trials, the University of Saskatchewan Research Ethics Board complies with the membership requirements for Research Ethics Boards defined in Part 4 of the Natural Health Products Regulations and Part C Division 5 of the Food and Drug Regulations and carries out its functions in a manner consistent with Good Clinical Practices. Members of the Bio-REB who are named as investigators, do not participate in the discussion related to, nor vote on such studies when presented to the Bio-REB. This approval and the views of this REB have been documented in writing. The University of Saskatchewan Biomedical Research Ethics Board is constituted and operates in accordance with the current version of the Tri-Council Policy Statement: Ethical Conduct for Research Involving Humans (TCPS 2 2018).

Digitally Approved by Dr. Gordon McKay, Ph.D.
Chair, Biomedical Research Ethics Board
University of Saskatchewan

Appendix I: Significant correlations for combined cadaver data

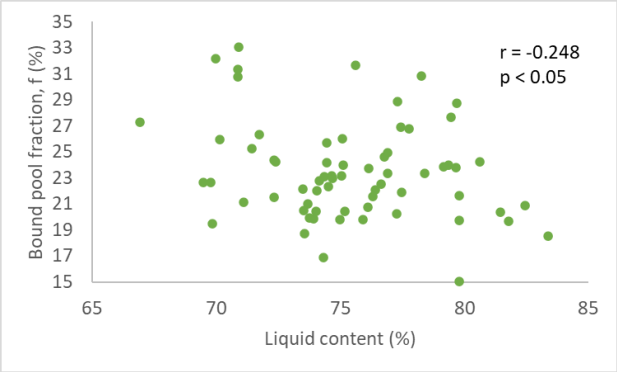

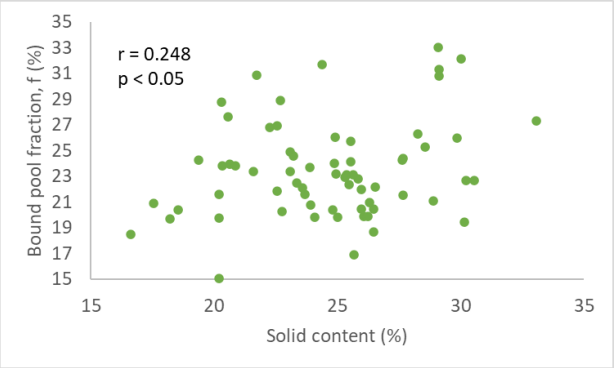

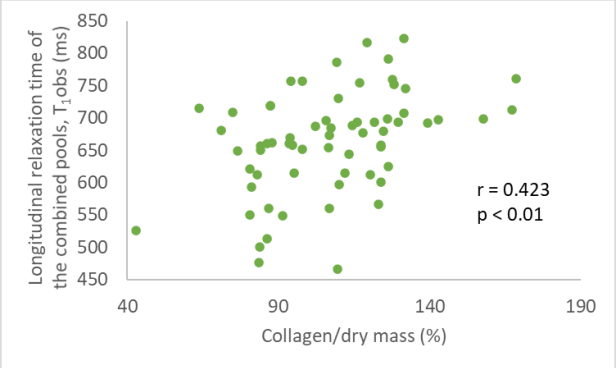

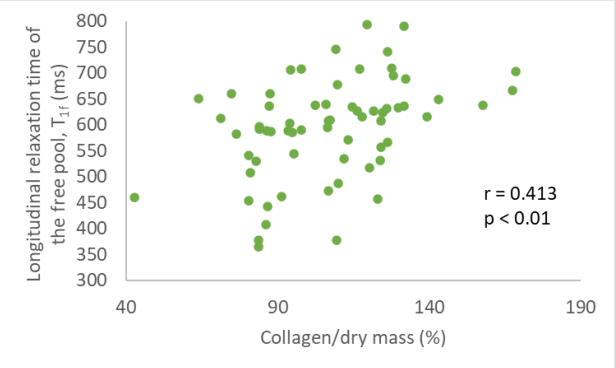

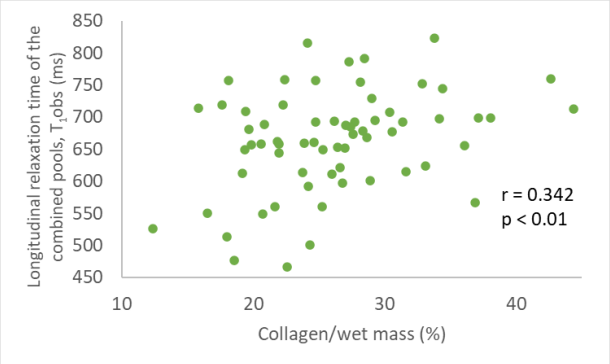

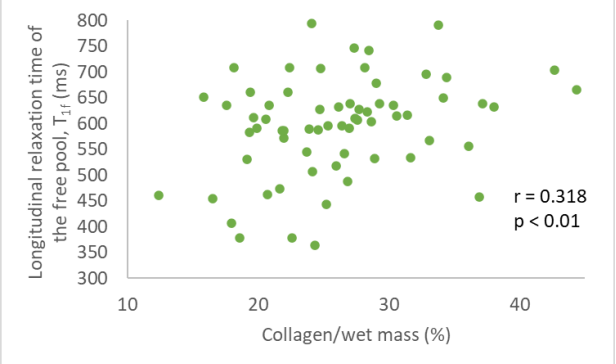

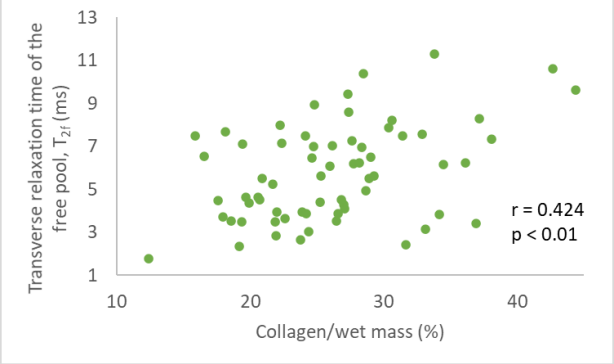

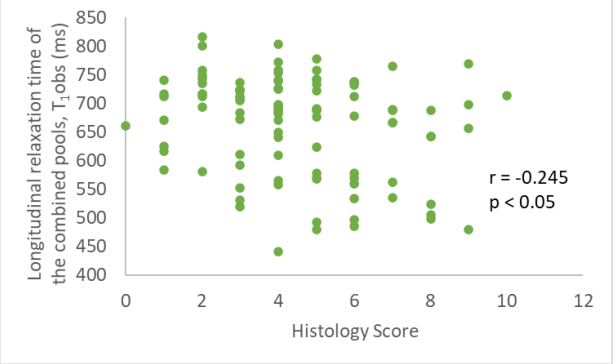

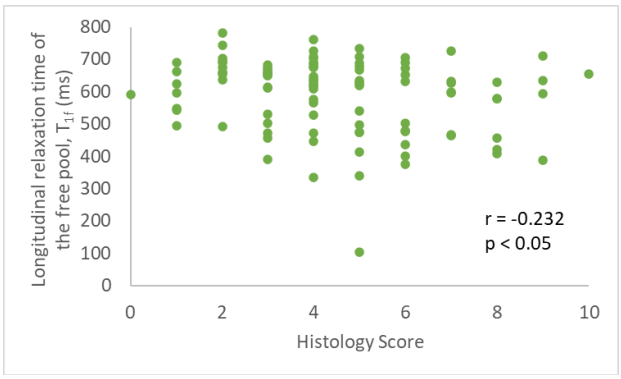
Longitudinal relaxation time of the free pool, T_{1f} (ms)
800
700
600
500
400
300
200
100
0
0
2
4
6
8
10
Histology Score
r = -0.232
p < 0.05

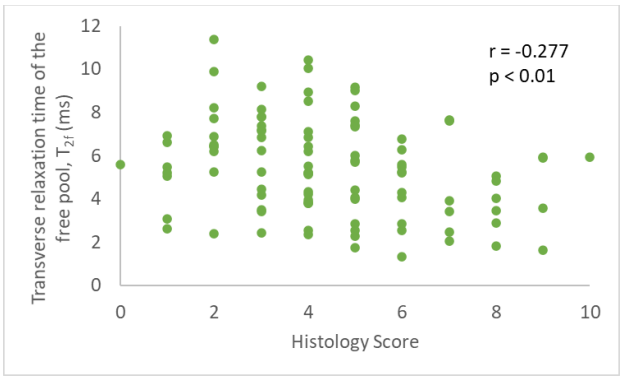
Transverse relaxation time of the free pool, T_{2f} (ms)
12
10
8
6
4
2
0
0
2
4
6
8
10
Histology Score
r = -0.277
p < 0.01

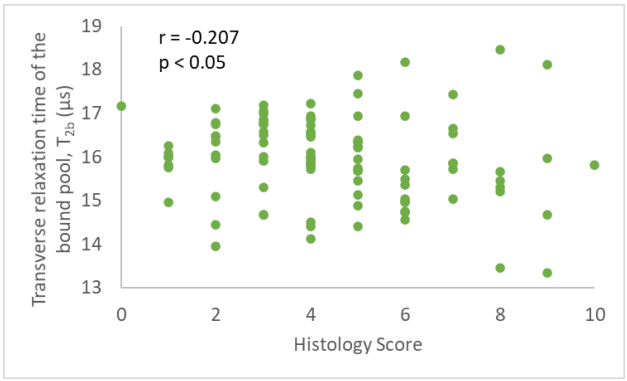
Transverse relaxation time of the bound pool, T_{2b} (µs)
19
18
17
16
15
14
13
0
2
4
6
8
10
Histology Score
r = -0.207
p < 0.05

Appendix J: qMT parameter filtering prior to registration for the TKA study

For the TKA study, the raw qMT data was filtered prior to registration to remove outliers. The acceptable ranges of values for each parameter (Table J.1) were chosen based on an assessment of the raw data as well as the ranges that the data fell within in the cadaver study.

TABLE J.1: QMT RAW DATA FILTERING RANGES FOR EACH PARAMETER IN THE TKA STUDY

Parameter	Range
T_1obs (ms)	0.1-2000
T_{1f} (ms)	0.1-2000
T_{2f} (ms)	0.1-100
T_{2b} (μs)	0.1-50
f (%)	0.1-100
k_f (s^{-1})	0.1-50

Appendix K: qMT imaging results of the TKA study – *in vivo* and *ex situ*

TABLE K.1: *IN VIVO* QMT PARAMETER RESULTS FOR THE TKA STUDY

Cartilage	T_1obs (ms)		T_{1f} (ms)		T_{2f} (ms)		T_{2b} (μs)		f (%)		k_f (s^{-1})	
	Mean	Std. Dev.	Mean	Std. Dev.	Mean	Std. Dev.	Mean	Std. Dev	Mean	Std. Dev	Mean	Std. Dev
Knee 1 Lateral Cartilage (N=373)	1110	273	1142	354	20.0	14.3	5.46	2.54	22.8	12.3	3.90	5.67
Knee 1 Medial Cartilage (N=293)	1032	190	1049	248	26.6	20.6	6.12	3.06	22.2	10.8	3.59	5.88
Knee 2 Lateral Cartilage (N=141)	1084	233	1119	355	26.0	20.4	7.62	3.76	31.9	16.2	3.44	3.88
Knee 2 Medial Cartilage (N=7)	1281	240	1534	411	45.5	26.5	7.19	5.67	41.3	24.8	8.05	9.98
Meniscus												
Knee 1 Lateral Meniscus (N=260)	1016	218	1014	320	16.1	17.2	6.90	2.44	32.6	14.3	5.57	6.14
Knee 2 Lateral Meniscus (N=660)	1028	219	1046	321	17.4	16.7	9.86	4.68	25.9	16.3	3.72	5.55
Knee 2 Medial Meniscus (N=145)	1129	233	1196	341	20.1	18.2	8.83	6.16	24.8	10.5	2.67	2.94

Sample sizes (N) in this table represent the number of voxels with signals averaged to arrive at the results presented.

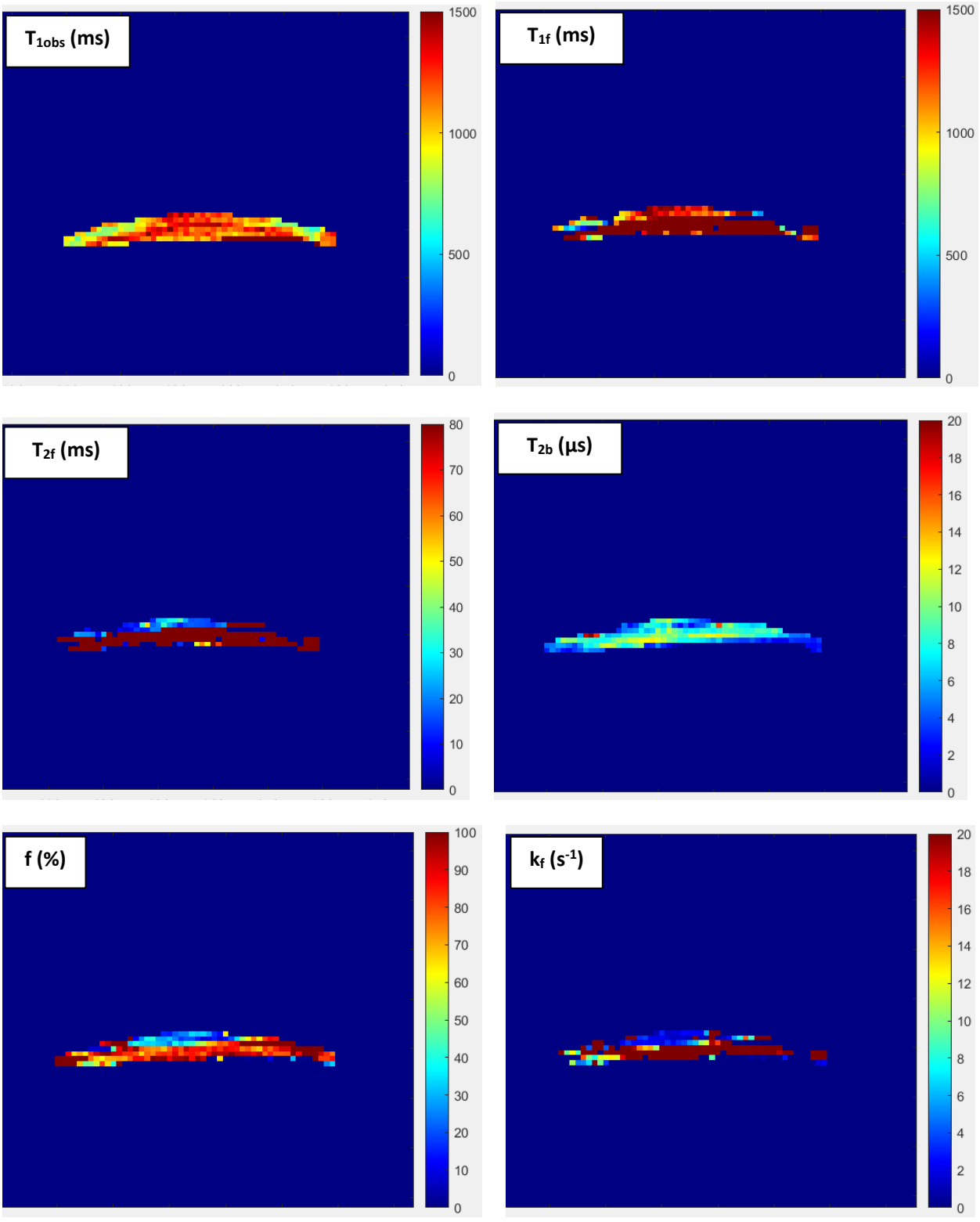

FIGURE K.1: QMT PARAMETER MAPS FOR A SINGLE SLICE OF *IN VIVO* CARTILAGE (KNEE 2 LATERAL)

TABLE K.2: EX SITU QMT PARAMETERS FOR THE TKA STUDY

Cartilage	T_1obs (ms)		T_{1f} (ms)		T_{2f} (ms)		T_{2b} (μs)		f (%)		k_f (s^{-1})	
	Mean	Std. Dev.	Mean	Std. Dev.	Mean	Std. Dev.	Mean	Std. Dev	Mean	Std Dev	Mean	Std. Dev
Knee 1 Lateral Cartilage (N=119)	805	257	729	341	10.7	13.9	6.29	3.46	26.8	21.2	3.93	6.25
Knee 1 Medial Cartilage (N=49)	783	275	707	360	4.7	4.7	5.86	3.18	27.0	19.9	3.73	6.22
Knee 2 Lateral Cartilage (N=24)	599	137	508	177	1.2	0.4	4.78	2.27	28.4	13.7	2.55	2.25
Knee 2 Medial Cartilage (N=25)	696	348	585	445	2.9	3.5	4.99	2.65	33.6	24.9	4.26	5.11
Meniscus												
Knee 1 Lateral Meniscus (N=233)	643	215	536	280	3.2	3.9	5.34	2.25	32.7	15.0	3.15	2.48
Knee 2 Lateral Meniscus (N=1859)	836	182	792	226	10.1	10.3	4.73	1.52	22.0	9.2	1.69	1.63
Knee 2 Medial Meniscus (N=317)	916	218	900	264	6.4	6.0	5.08	2.89	18.6	12.8	1.52	2.08

Sample sizes (N) in this table represent the number of voxels with signals averaged to arrive at the results presented.

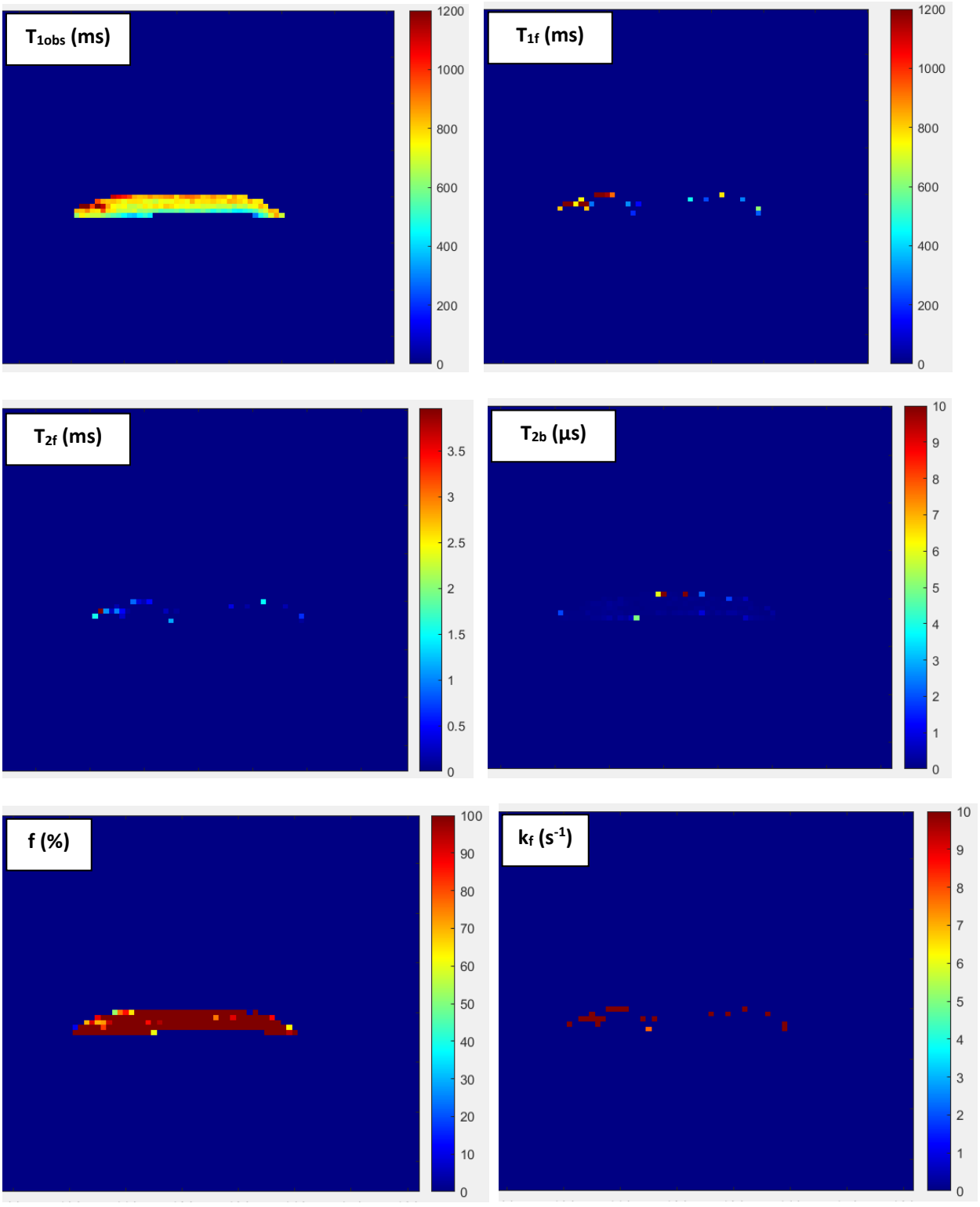

FIGURE K.2: QMT PARAMETER MAPS FOR A SINGLE SLICE OF *EX SITU* CARTILAGE (KNEE 2 LATERAL)

Appendix L: Thickness testing results for the TKA study

The average thicknesses ranged from 1.55-2.29 mm in cartilage and 2.09-3.39 mm in meniscus and were generally lower in regions that displayed higher instantaneous modulus (Table L.1). The medial cartilage of knee two, which had relatively low modulus values, was the thickest (2.28 ± 3.06 mm). The lateral cartilage in this knee was quite a bit thinner, at 1.95 ± 0.64 mm, and not far off from the thickness of knee one's lateral cartilage (1.75 ± 0.80 mm). The thickness of the medial cartilage in knee one was lower than the lateral, at 1.55 ± 0.78 mm. The thicknesses of the menisci samples were closer to predicted. Knee one had only a lateral meniscus (3.39 ± 0.87 mm) and in knee two, the lateral meniscus (2.90 ± 0.89 mm) had a greater thickness than the medial (2.09 ± 1.26 mm).

TABLE L.1: AVERAGE TISSUE THICKNESS FOR TKA STUDY SAMPLES

Cartilage					Meniscus				
Side	Knee	Mean thickness (mm)	Standard deviation	N	Side	Knee	Mean thickness (mm)	Standard deviation	N
Lateral	1	1.75	0.80	105	Lateral	1	3.39	0.87	22
	2	1.95	0.64	73		2	2.90	0.89	19
Medial	1	1.55	0.78	100	Medial	1			
	2	2.28	3.06	60		2	2.09	1.26	9

Appendix M: Mechanical testing results color maps for TKA study

Knee 1 lateral cartilage:

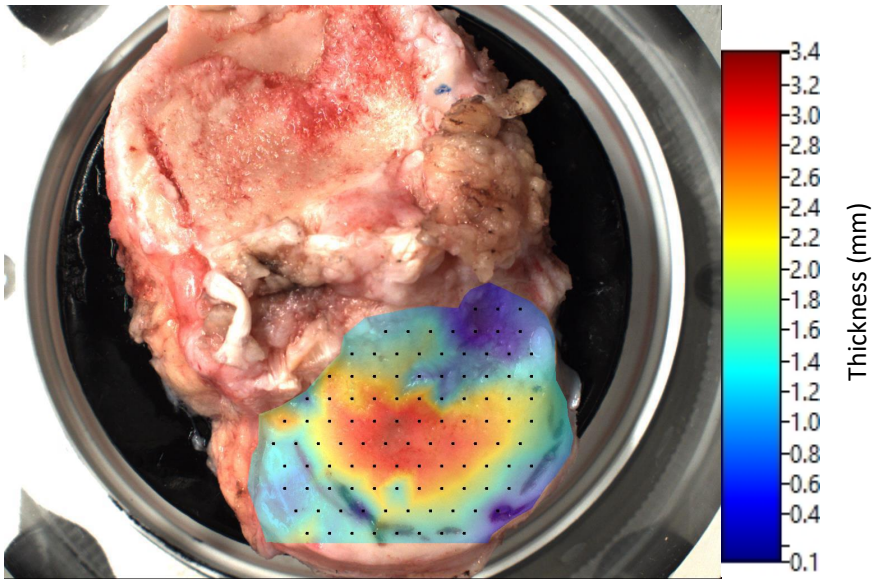

Knee 1 lateral meniscus:

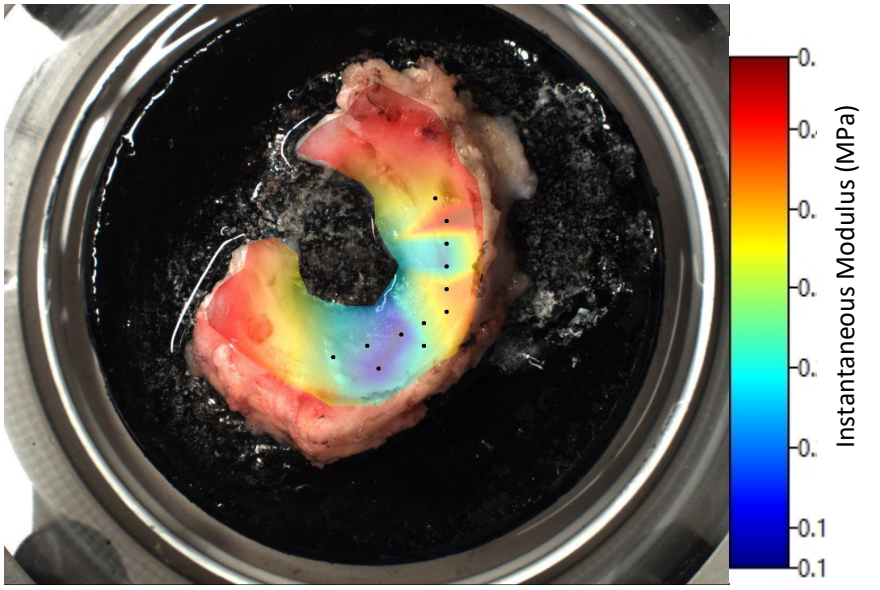

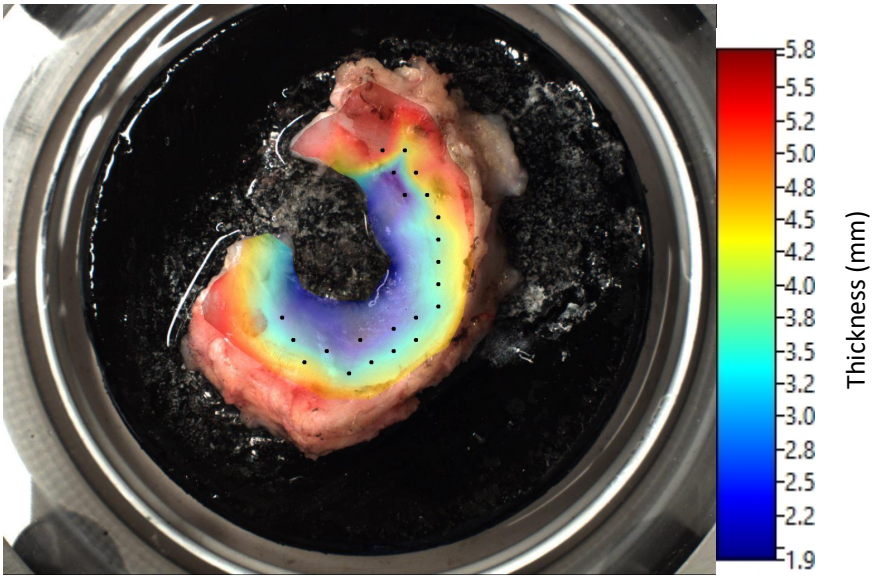

Knee 1 medial cartilage:

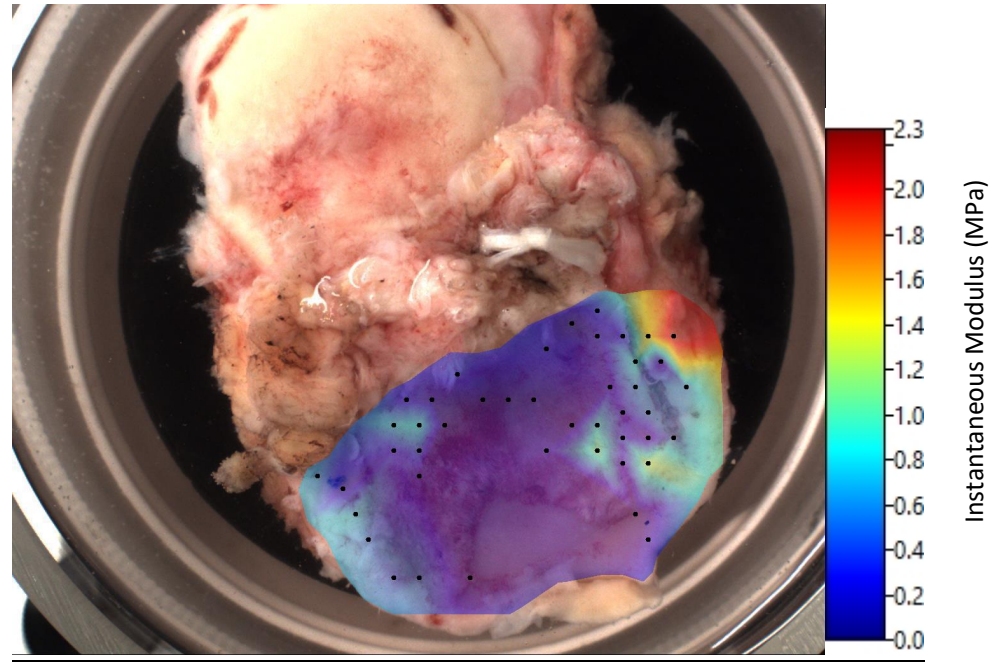

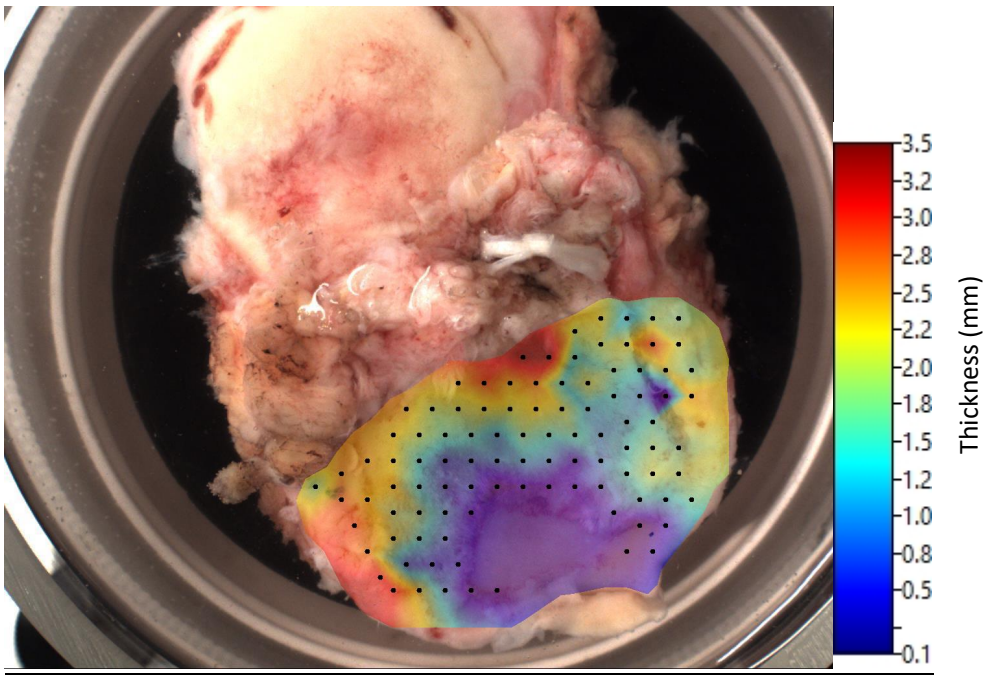

Knee 2 lateral cartilage:

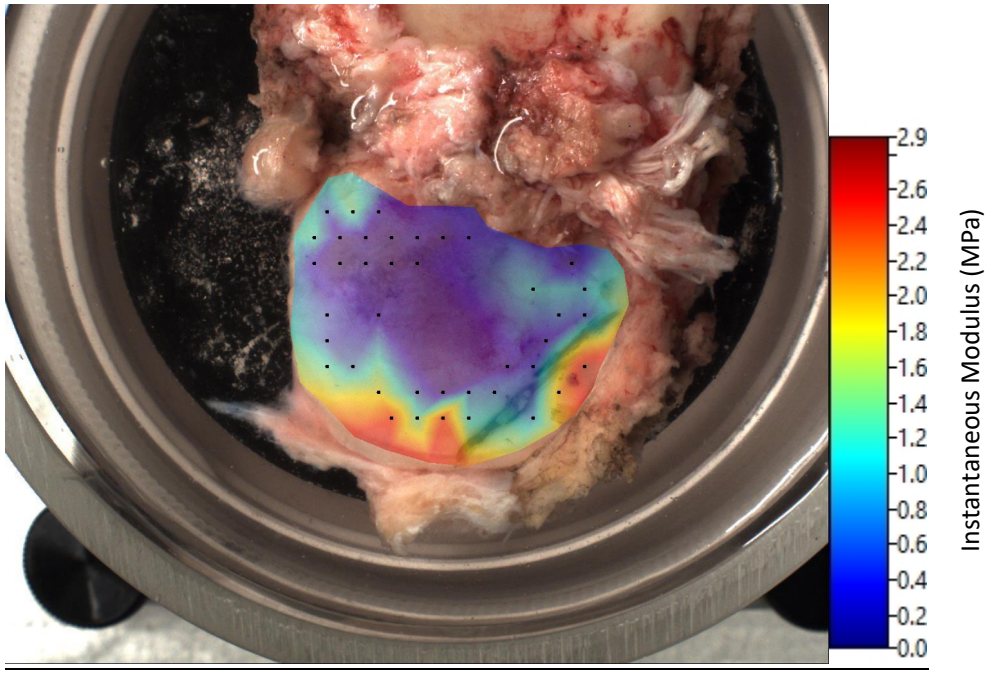

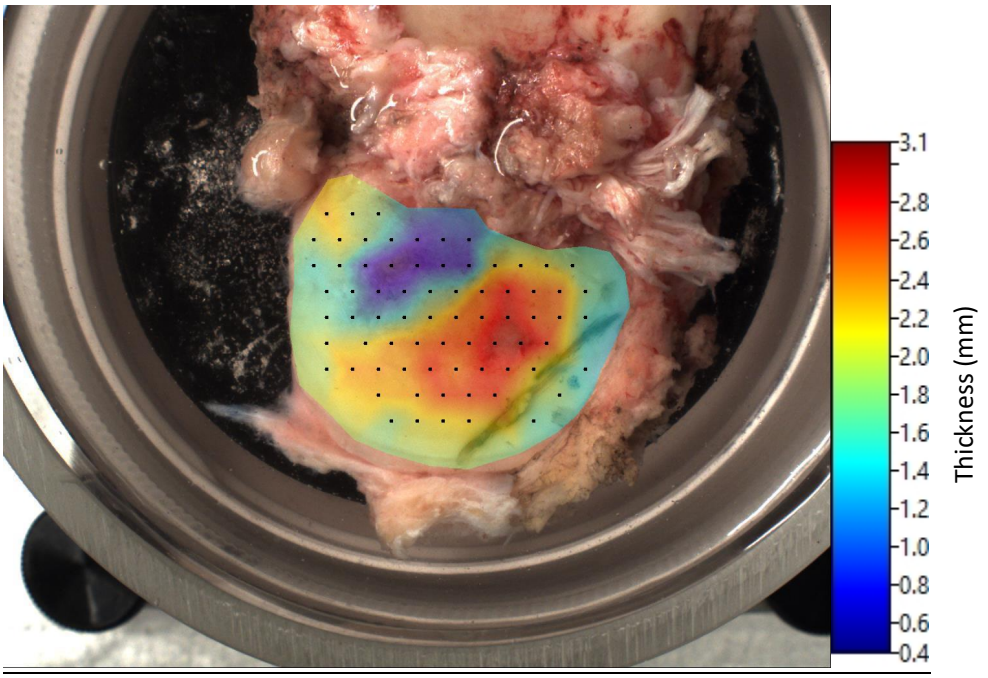

Knee 2 lateral meniscus:

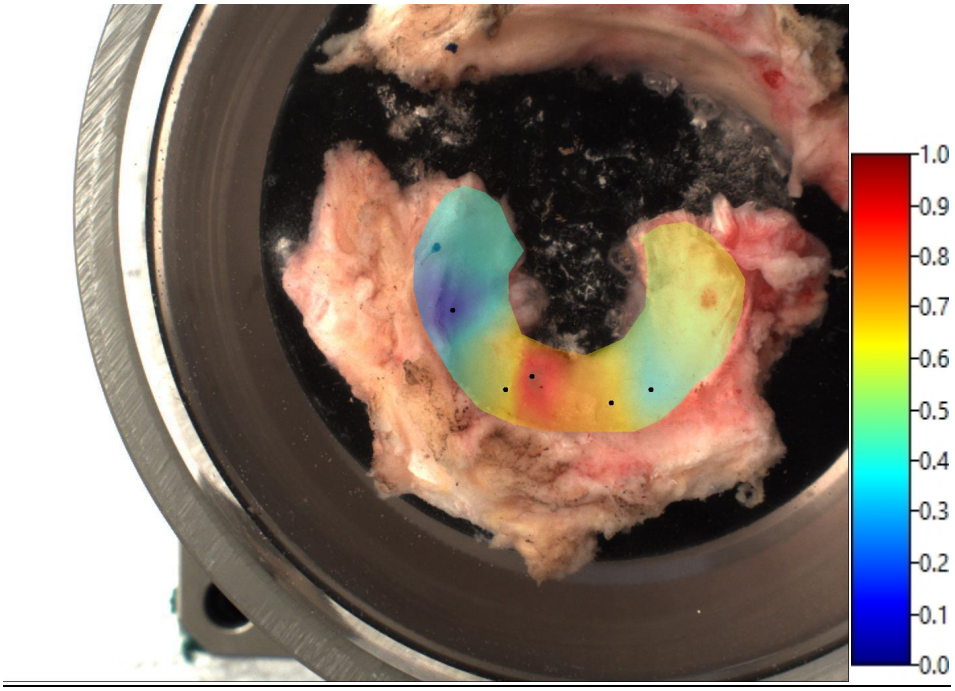

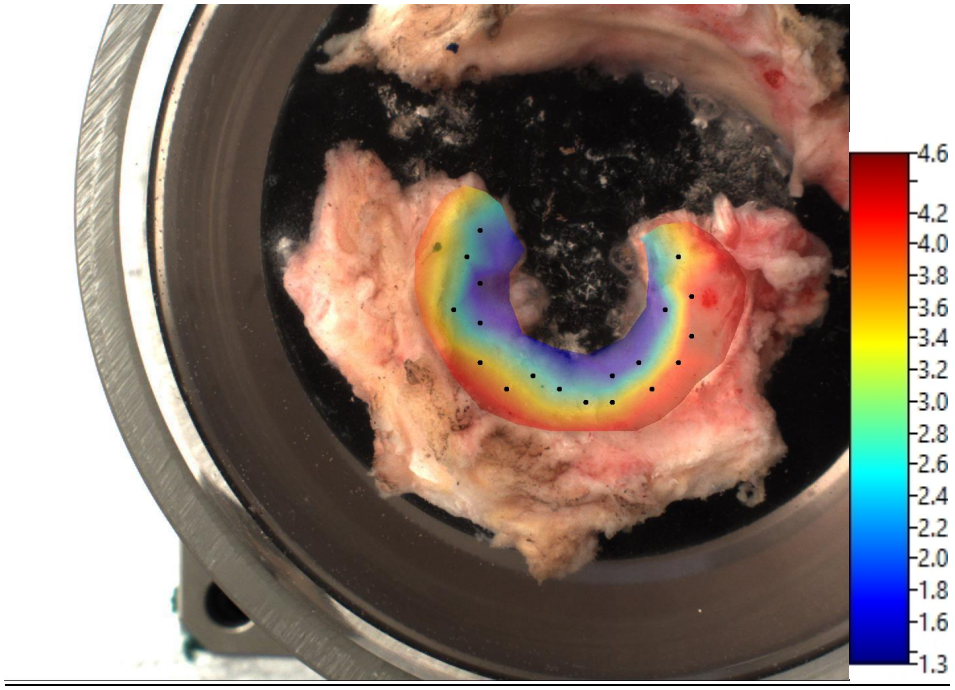

Knee 2 medial cartilage:

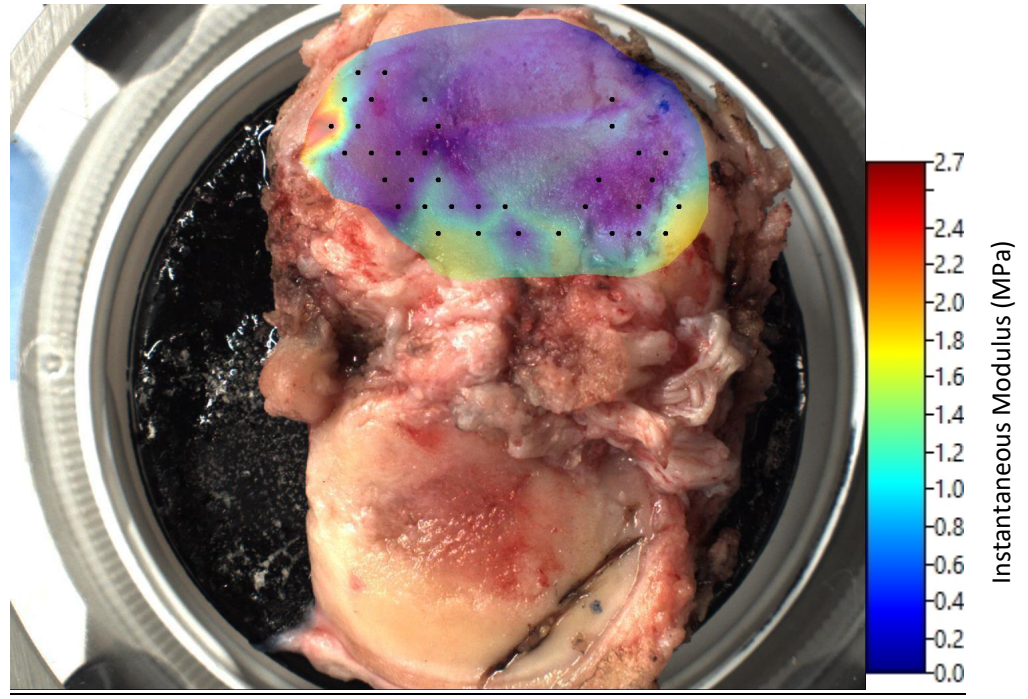

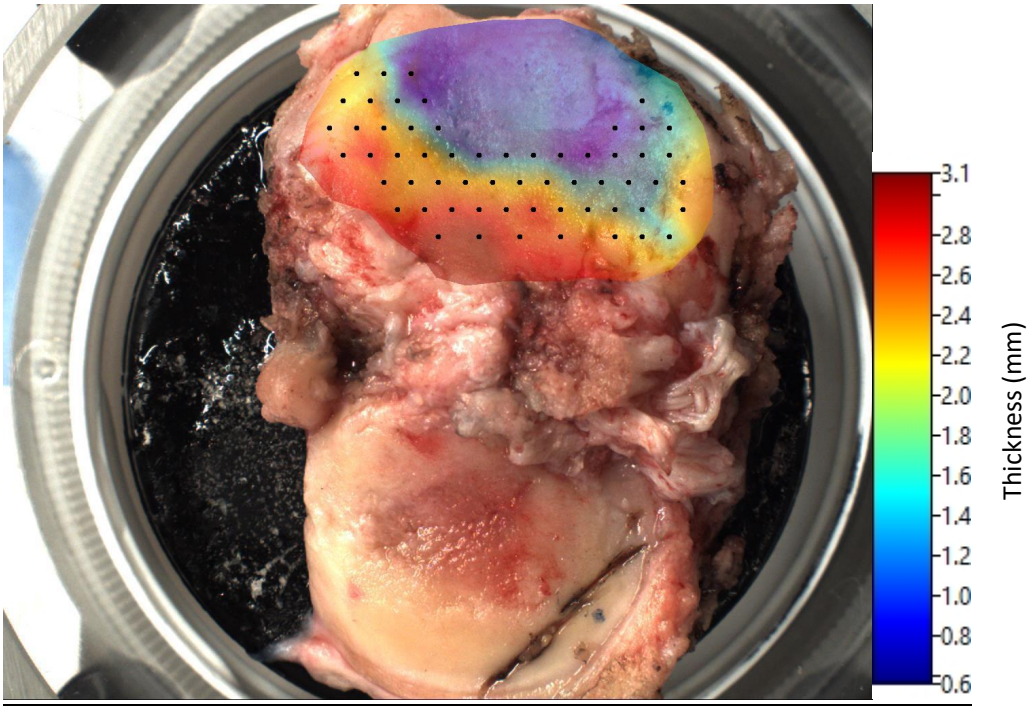

Knee 2 medial meniscus:

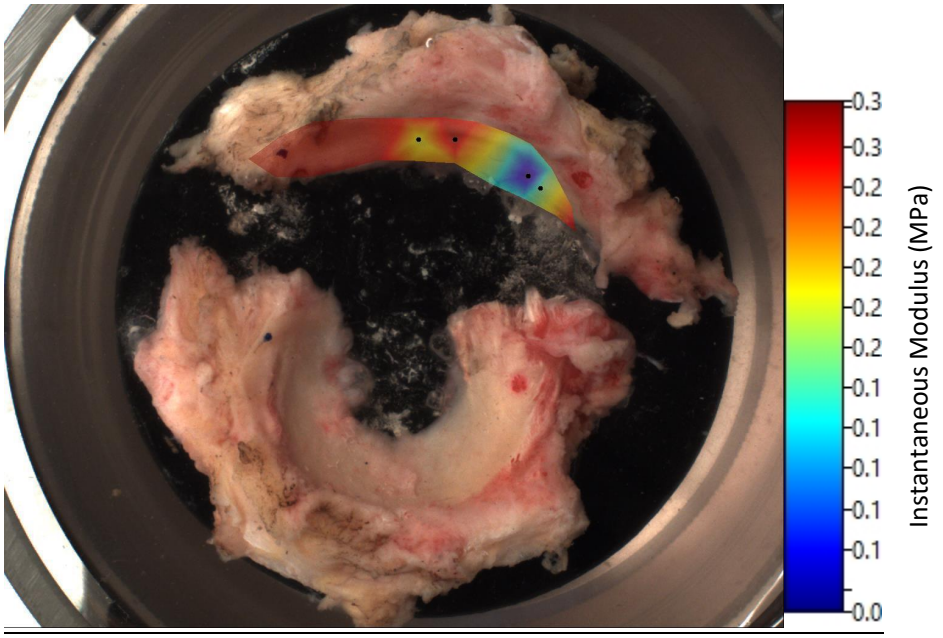

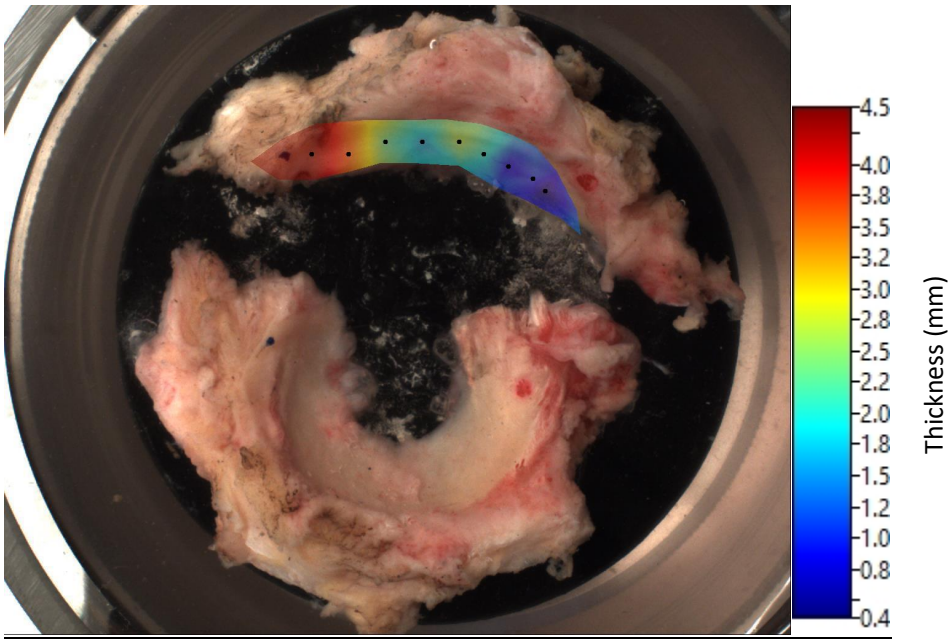

Appendix N: Correlation coefficient tables for the TKA study

TABLE N.1: PEARSON CORRELATION COEFFICIENTS WITH SIGNIFICANCE VALUES IN BRACKETS FOR A: *IN VIVO* AND B: *EX SITU* CARTILAGE QMT TO MECHANICAL PROPERTIES: ALL SAMPLES, MEDIAL SAMPLES, AND LATERAL SAMPLES

A. In Vivo		T_1 obs (ms)	T_{1f} (ms)	T_{2f} (ms)	T_{2b} (μs)	f (%)	k_f (s^{-1})
Instantaneous Modulus (MPa)	Combined (N=130)	-0.086 (0.329)	-0.095 (0.280)	-0.156 (0.076)	0.008 (0.928)	-0.148 (0.092)	-0.099 (0.261)
	Medial (N=44)	0.248 (0.104)	0.279 (0.067)	0.226 (0.141)	0.117 (0.449)	-0.130 (0.401)	-0.006 (0.968)
	Lateral (N=86)	-0.218* (0.044)	-0.221* (0.041)	-0.233* (0.030)	-0.067 (0.540)	-0.176 (0.105)	-0.058 (0.594)
Cartilage Thickness (mm)	Combined (N=146)	0.214** (0.010)	0.166* (0.045)	0.215** (0.009)	0.353** (<0.01)	-0.227** (0.006)	-0.142 (0.087)
	Medial (N=50)	0.324* (0.022)	0.315* (0.026)	0.393** (0.005)	0.282* (0.047)	-0.385** (0.006)	-0.126 (0.384)
	Lateral (N=96)	0.089 (0.390)	0.025 (0.809)	0.161 (0.117)	0.356** (<0.01)	-0.148 (0.151)	-0.046 (0.654)
B. Ex Situ		**T_1 obs (ms)**	**T_{1f} (ms)**	**T_{2f} (ms)**	**T_{2b} (μs)**	**f (%)**	**k_f (s^{-1})**
Instantaneous Modulus (MPa)	Combined (N=71)	0.122 (0.309)	0.138 (0.252)	-0.038 (0.756)	0.178 (0.137)	-0.172 (0.151)	-0.128 (0.286)
	Medial (N=31)	0.037 (0.841)	0.054 (0.775)	0.134 (0.472)	0.287 (0.117)	-0.040 (0.832)	-0.117 (0.532)
	Lateral (N=40)	0.210 (0.194)	0.220 (0.172)	-0.047 (0.775)	0.160 (0.323)	-0.253 (0.115)	-0.143 (0.380)
Cartilage Thickness (mm)	Combined (N=83)	-0.193 (0.081)	-0.187 (0.090)	-0.022 (0.840)	-0.136 (0.220)	0.197 (0.074)	0.001 (0.995)
	Medial (N=35)	-0.236 (0.172)	-0.180 (0.300)	0.058 (0.741)	-0.017 (0.921)	0.108 (0.538)	-0.162 (0.351)
	Lateral (N=48)	-0.166 (0.259)	-0.240 (0.100)	-0.158 (0.285)	-0.269 (0.065)	0.374** (0.009)	0.162 (0.271)

** Correlation is significant at the 0.01 level	**Correlation legend**	Very weak (0-0.19)	Weak (0.2-0.39)
* Correlation is significant at the 0.05 level	Moderate (0.4-0.59)	Strong (0.6-0.79)	Very strong (0.8-1)

TABLE N.2: PEARSON CORRELATION COEFFICIENTS WITH SIGNIFICANCE VALUES IN BRACKETS FOR A: *IN VIVO* AND B: *EX SITU* MENISCUS QMT TO MECHANICAL PROPERTIES

A. Lateral Meniscus In Vivo	T_1 obs (ms)	T_{1f} (ms)	T_{2f} (ms)	T_{2b} (μs)	f (%)	k_f (s^{-1})
Instantaneous Modulus (MPa) (N=32)	-0.208 (0.252)	-0.194 (0.286)	-0.227 (0.212)	0.064 (0.729)	-0.022 (0.903)	0.180 (0.325)
Meniscus Thickness (mm) (N=36)	-0.213 (0.212)	-0.143 (0.405)	-0.362* (0.030)	-0.108 (0.532)	0.384* (0.021)	0.374* (0.025)
B. Lateral Meniscus Ex Situ	**T_1 obs (ms)**	**T_{1f} (ms)**	**T_{2f} (ms)**	**T_{2b} (μs)**	**f (%)**	**k_f (s^{-1})**
Instantaneous Modulus (MPa) (N=14)	-0.417 (0.138)	-0.382 (0.177)	-0.563* (0.036)	0.514 (0.060)	-0.130 (0.658)	-0.318 (0.267)
Meniscus Thickness (mm) (N=16)	-0.235 (0.381)	-0.279 (0.295)	-0.224 (0.404)	-0.292 (0.272)	0.378 (0.149)	0.078 (0.774)

** Correlation is significant at the 0.01 level	**Correlation legend**	Very weak (0-0.19)	Weak (0.2-0.39)
* Correlation is significant at the 0.05 level	Moderate (0.4-0.59)	Strong (0.6-0.79)	Very strong (0.8-1)

TABLE N.3: PEARSON CORRELATION COEFFICIENTS WITH SIGNIFICANCE VALUES IN BRACKETS FOR A: *IN VIVO* AND B: *EX SITU* CARTILAGE QMT TO BIOCHEMISTRY: ALL SAMPLES, MEDIAL SAMPLES, AND LATERAL SAMPLES

A. In Vivo		T_1 obs (ms)	T_{1f} (ms)	T_{2f} (ms)	T_{2b} (μs)	f (%)	k_f (s^{-1})
Liquid content (%)	Combined (N=9)	0.284 (0.459)	0.368 (0.329)	0.003 (0.993)	0.201 (0.605)	0.309 (0.419)	0.006 (0.989)
	Lateral (N=6)	0.745 (0.089)	0.836* (0.038)	0.258 (0.622)	0.449 (0.372)	0.243 (0.643)	-0.457 (0.362)
Solid content (%)	Combined (N=9)	-0.284 (0.459)	-0.368 (0.329)	-0.003 (0.993)	-0.201 (0.605)	-0.309 (0.419)	-0.006 (0.989)
	Lateral (N=6)	-0.745 (0.089)	-0.836* (0.038)	-0.258 (0.622)	-0.449 (0.372)	-0.243 (0.643)	-0.457 (0.362)
sGAG per dry mass (%)	Combined (N=9)	-0.299 (0.434)	-0.308 (0.420)	0.164 (0.673)	0.043 (0.913)	-0.451 (0.223)	0.079 (0.840)
	Lateral (N=6)	0.456 (0.363)	0.290 (0.578)	-0.201 (0.703)	-0.275 (0.597)	-0.183 (0.729)	-0.233 (0.657)
sGAG per wet mass (%)	Combined (N=9)	-0.390 (0.300)	-0.423 (0.257)	0.191 (0.623)	-0.007 (0.987)	-0.521 (0.151)	0.049 (0.901)
	Lateral (N=6)	0.027 (0.960)	-0.148 (0.780)	-0.302 (0.560)	-0.465 (0.353)	-0.181 (0.731)	0.089 (0.866)
Collagen per dry mass (%)	Combined (N=9)	-0.196 (0.612)	-0.310 (0.416)	-0.347 (0.360)	-0.543 (0.131)	-0.295 (0.440)	0.104 (0.791)
	Lateral (N=6)	-0.546 (0.263)	-0.713 (0.112)	-0.632 (0.178)	-0.766 (0.076)	-0.352 (0.494)	0.658 (0.156)
Collagen per wet mass (%)	Combined (N=9)	-0.204 (0.599)	-0.315 (0.409)	-0.233 (0.546)	-0.442 (0.233)	-0.295 (0.441)	0.058 (0.883)
	Lateral (N=6)	-0.664 (0.151)	-0.808 (0.052)	-0.494 (0.320)	-0.667 (0.148)	-0.323 (0.533)	0.658 (0.155)
B. Ex Situ		T_1 obs (ms)	T_{1f} (ms)	T_{2f} (ms)	T_{2b} (μs)	f (%)	k_f (s^{-1})
Liquid content (%)	Combined (N=6)	0.386 (0.450)	0.419 (0.408)	0.148 (0.779)	-0.435 (0.388)	-0.427 (0.398)	-0.446 (0.375)
Solid content (%)	Combined (N=6)	-0.386 (0.450)	-0.419 (0.408)	-0.148 (0.779)	0.435 (0.388)	0.427 (0.398)	0.446 (0.375)
sGAG per dry mass (%)	Combined (N=6)	-0.537 (0.272)	-0.655 (0.158)	-0.492 (0.322)	-0.619 (0.190)	0.685 (0.134)	0.339 (0.511)
sGAG per wet mass (%)	Combined (N=6)	-0.517 (0.293)	-0.644 (0.168)	-0.331 (0.522)	-0.335 (0.517)	0.695 (0.125)	0.427 (0.398)
Collagen per dry mass (%)	Combined (N=6)	-0.604 (0.205)	-0.320 (0.537)	-0.434 (0.390)	0.722 (0.105)	-0.028 (0.958)	-0.436 (0.388)
Collagen per wet mass (%)	Combined (N=6)	-0.770 (0.073)	-0.535 (0.274)	-0.588 (0.219)	0.602 (0.206)	0.209 (0.691)	-0.262 (0.616)

** Correlation is significant at the 0.01 level	**Correlation legend**	Very weak (0-0.19)	Weak (0.2-0.39)
* Correlation is significant at the 0.05 level	Moderate (0.4-0.59)	Strong (0.6-0.79)	Very strong (0.8-1)

TABLE N.4: PEARSON CORRELATION COEFFICIENTS WITH SIGNIFICANCE VALUES IN BRACKETS FOR *IN VIVO* MENISCUS QMT TO BIOCHEMISTRY

Lateral Meniscus (N=6)***	T_1 obs (ms)	T_{1f} (ms)	T_{2f} (ms)	T_{2b} (μs)	f (%)	k_f (s^{-1})
Liquid content (%)	-0.351 (0.495)	-0.300 (0.564)	-0.790 (0.062)	-0.252 (0.631)	0.034 (0.948)	-0.890* (0.018)
Solid content (%)	0.351 (0.495)	0.300 (0.564)	0.790 (0.062)	0.252 (0.631)	-0.034 (0.948)	0.890* (0.018)
sGAG per dry mass (%)	0.223 (0.671)	0.239 (0.648)	0.399 (0.433)	0.869* (0.025)	-0.294 (0.572)	-0.114 (0.829)
sGAG per wet mass (%)	0.396 (0.437)	0.404 (0.427)	0.578 (0.229)	0.846* (0.034)	-0.391 (0.444)	0.063 (0.906)
Collagen per dry mass (%)	-0.161 (0.761)	-0.206 (0.695)	0.288 (0.580)	0.238 (0.650)	0.229 (0.662)	0.375 (0.464)
Collagen per wet mass (%)	0.197 (0.708)	0.144 (0.786)	0.700 (0.121)	0.239 (0.648)	0.083 (0.876)	0.820* (0.046)

** Correlation is significant at the 0.01 level	**Correlation legend**	Very weak (0-0.19)	Weak (0.2-0.39)
* Correlation is significant at the 0.05 level	Moderate (0.4-0.59)	Strong (0.6-0.79)	Very strong (0.8-1)

*** Correlations could only be found between the lateral menisci samples and the biochemical properties – no qMT data could be obtained from the medial meniscus samples

TABLE N.5: SPEARMAN'S RHO CORRELATION COEFFICIENTS WITH SIGNIFICANCE VALUES IN BRACKETS FOR A: *IN VIVO* AND B: *EX SITU* CARTILAGE QMT TO HISTOLOGICAL SCORE: ALL SAMPLES, MEDIAL SAMPLES, AND LATERAL SAMPLES

A. In Vivo		T_1 obs (ms)	T_{1f} (ms)	T_{2f} (ms)	T_{2b} (μs)	f (%)	k_f (s^{-1})
Score	Combined (N=12)	-0.127 (0.693)	-0.164 (0.611)	-0.306 (0.334)	-0.149 (0.643)	0.670* (0.017)	0.280 (0.378)
	Medial (N=4)	0.200 (0.800)	-0.400 (0.600)	-0.800 (0.200)	-0.800 (0.200)	1.000** (<0.01)	0.400 (0.600)
	Lateral (N=8)	-0.102 (0.810)	-0.013 (0.976)	-0.294 (0.480)	0.038 (0.928)	0.587 (0.126)	0.064 (0.881)
B. Ex Situ		T_1 obs (ms)	T_{1f} (ms)	T_{2f} (ms)	T_{2b} (μs)	f (%)	k_f (s^{-1})
Score	Combined (N=14)	-0.284 (0.325)	-0.309 (0.282)	-0.404 (0.152)	-0.532 (0.050)	0.253 (0.384)	0.192 (0.511)
	Medial (N=6)	0.145 (0.784)	0.232 (0.658)	-0.232 (0.658)	-0.232 (0.658)	-0.232 (0.658)	-0.029 (0.957)
	Lateral (N=8)	-0.602 (0.115)	-0.638 (0.089)	-0.687 (0.060)	-0.896** (0.003)	0.393 (0.336)	0.233 (0.578)

** Correlation is significant at the 0.01 level	**Correlation legend**	Very weak (0-0.19)	Weak (0.2-0.39)
* Correlation is significant at the 0.05 level	Moderate (0.4-0.59)	Strong (0.6-0.79)	Very strong (0.8-1)

TABLE N.6: SPEARMAN'S RHO CORRELATION COEFFICIENTS WITH SIGNIFICANCE VALUES IN BRACKETS FOR *IN VIVO* MENISCUS QMT TO HISTOLOGICAL SCORE

Lateral Meniscus (N=7)* **	**T_1 obs (ms)**	**T_{1f} (ms)**	**T_{2f} (ms)**	**T_{2b} (µs)**	**f (%)**	**k_f (s^{-1})**
Score	0.206 (0.658)	0.299 (0.514)	0.019 (0.968)	-0.168 (0.718)	0.112 (0.811)	-0.056 (0.905)

** Correlation is significant at the 0.01 level	**Correlation legend**	Very weak (0-0.19)	Weak (0.2-0.39)
* Correlation is significant at the 0.05 level	Moderate (0.4-0.59)	Strong (0.6-0.79)	Very strong (0.8-1)

*** Correlations could only be found between the lateral menisci samples and the biochemical properties – no qMT data could be obtained from the medial meniscus samples

TABLE N.7: CORRELATION COEFFICIENTS FOR COMBINED A. *IN VIVO* AND B. *EX SITU* SURFACES – COMPARISON OF QMT PARAMETERS TO ALL EVALUATED TISSUE PROPERTIES. ALL COEFFICIENTS REPORTED IN TABLE ARE PEARSON EXCEPT FOR HISTOLOGY SCORE WHICH IS SPEARMAN. SIGNIFICANCE VALUES IN BRACKETS.

A. In Vivo Surfaces (N=7)	T_1 obs (ms)	T_{1f} (ms)	T_{2f} (ms)	T_{2b} (µs)	f (%)	k_f (s^{-1})
Liquid content (%)	0.939** (0.002)	0.926** (0.003)	0.864* (0.012)	-0.170 (0.716)	0.575 (0.177)	0.513 (0.239)
Solid content (%)	-0.939** (0.002)	-0.926** (0.003)	-0.864* (0.012)	0.170 (0.716)	-0.575 (0.177)	-0.513 (0.239)
sGAG per dry mass (%)	0.807* (0.028)	0.826* (0.022)	0.964** (<0.01)	-0.371 (0.412)	0.585 (0.167)	0.628 (0.131)
sGAG per wet mass (%)	0.651 (0.113)	0.659 (0.108)	0.873* (0.010)	-0.478 (0.278)	0.412 (0.358)	0.455 (0.305)
Collagen per dry mass (%)	-0.788* (0.035)	-0.780* (0.039)	-0.737 (0.059)	-0.272 (0.555)	-0.495 (0.259)	-0.243 (0.599)
Collagen per wet mass (%)	-0.632 (0.128)	-0.636 (0.125)	-0.569 (0.182)	-0.536 (0.215)	-0.370 (0.414)	-0.098 (0.835)
Instantaneous Modulus (MPa)	0.197 (0.672)	0.108 (0.818)	0.033 (0.945)	-0.626 (0.133)	-0.199 (0.669)	0.000 (1.000)
Elastic Fit Mean Squared Error	0.109 (0.815)	0.010 (0.984)	-0.104 (0.824)	-0.610 (0.146)	-0.306 (0.505)	-0.106 (0.821)
Tissue Thickness (mm)	-0.260 (0.573)	-0.196 (0.674)	-0.319 (0.485)	0.430 (0.336)	0.376 (0.406)	0.331 (0.468)
Histology Score (Spearman's)	0.607 (0.148)	0.607 (0.148)	0.893** (0.007)	0.036 (0.939)	0.071 (0.879)	-0.286 (0.535)

B. Ex Situ Surfaces (N=7)	T_1 obs (ms)	T_{1f} (ms)	T_{2f} (ms)	T_{2b} (µs)	f (%)	k_f (s^{-1})
Liquid content (%)	-0.088 (0.851)	-0.120 (0.798)	-0.424 (0.343)	-0.111 (0.813)	0.274 (0.552)	0.389 (0.389)
Solid content (%)	0.088 (0.851)	0.120 (0.798)	0.424 (0.343)	0.111 (0.813)	-0.274 (0.552)	-0.389 (0.389)
sGAG per dry mass (%)	-0.338 (0.458)	-0.392 (0.385)	-0.413 (0.357)	0.007 (0.988)	0.537 (0.214)	0.678 (0.094)
sGAG per wet mass (%)	-0.364 (0.422)	-0.410 (0.361)	-0.394 (0.382)	0.127 (0.786)	0.496 (0.258)	0.696 (0.082)
Collagen per dry mass (%)	0.061 (0.896)	0.043 (0.927)	0.304 (0.507)	0.502 (0.251)	0.020 (0.966)	0.018 (0.970)
Collagen per wet mass (%)	-0.098 (0.835)	-0.132 (0.778)	0.132 (0.777)	0.648 (0.116)	0.238 (0.608)	0.267 (0.562)
Instantaneous Modulus (MPa)	-0.022 (0.962)	-0.068 (0.885)	0.428 (0.339)	0.660 (0.107)	0.154 (0.741)	0.518 (0.234)
Elastic Fit Mean Squared Error	0.062 (0.895)	0.022 (0.963)	0.493 (0.261)	0.706 (0.076)	0.058 (0.901)	0.434 (0.331)
Tissue Thickness (mm)	-0.229 (0.622)	-0.217 (0.640)	-0.041 (0.930)	-0.448 (0.313)	0.213 (0.646)	-0.287 (0.533)
Histology Score (Spearman's)	-0.357 (0.432)	-0.357 (0.432)	-0.607 (0.148)	-0.214 (0.645)	0.286 (0.535)	-0.536 (0.215)

** Correlation is significant at the 0.01 level	**Correlation legend**	Very weak (0-0.19)	Weak (0.2-0.39)
* Correlation is significant at the 0.05 level	Moderate (0.4-0.59)	Strong (0.6-0.79)	Very strong (0.8-1)

Appendix O: Correlation scatterplots for TKA data with N=3 and N=2 sample sizes

FIGURE O.1: RELATIONSHIPS BETWEEN QMT PARAMETERS AND BIOCHEMICAL PROPERTIES IN THE *IN VIVO* MEDIAL CARTILAGE SAMPLES

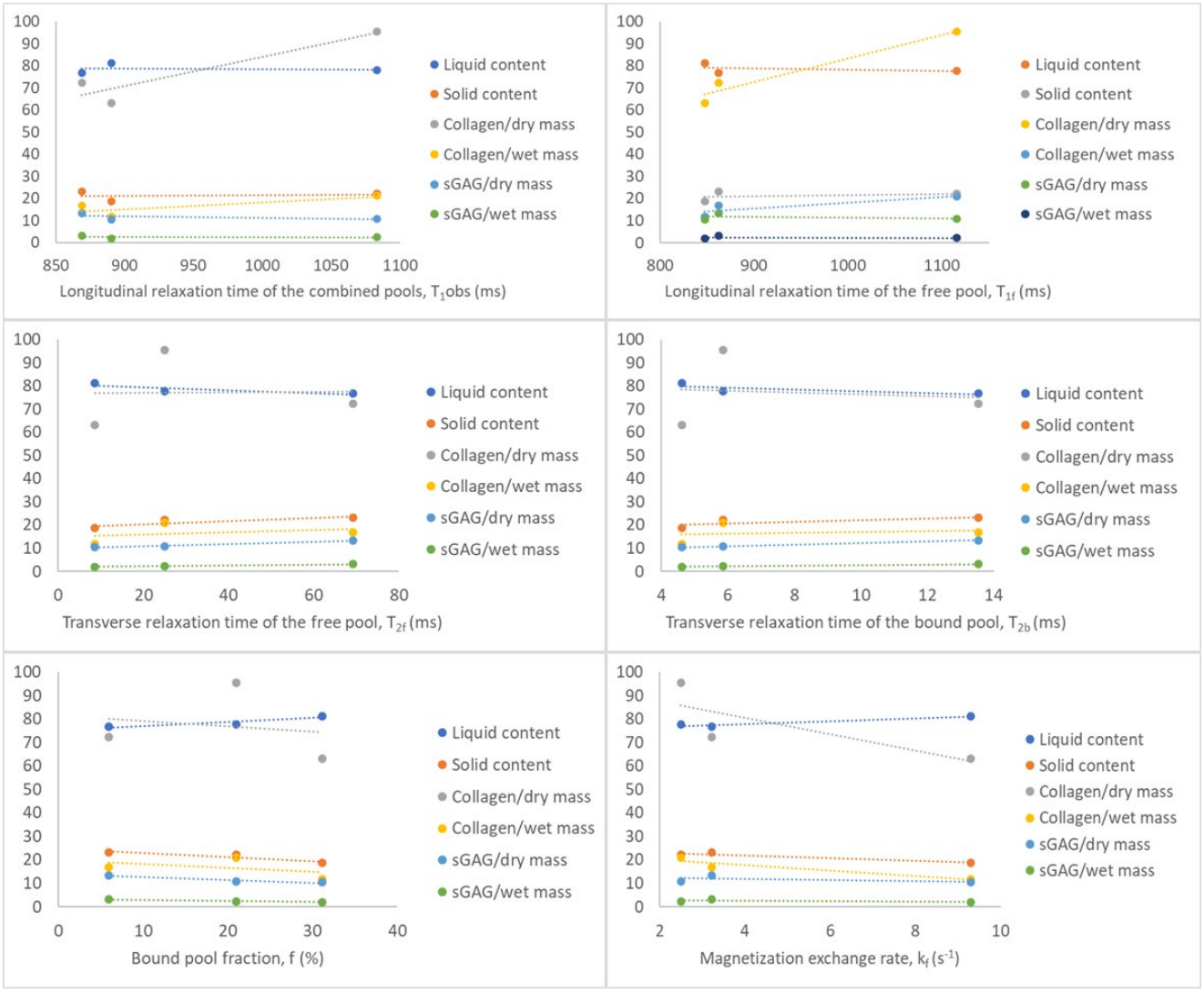

FIGURE O.2: RELATIONSHIPS BETWEEN QMT PARAMETERS AND BIOCHEMICAL PROPERTIES IN THE *EX SITU* MEDIAL CARTILAGE SAMPLES

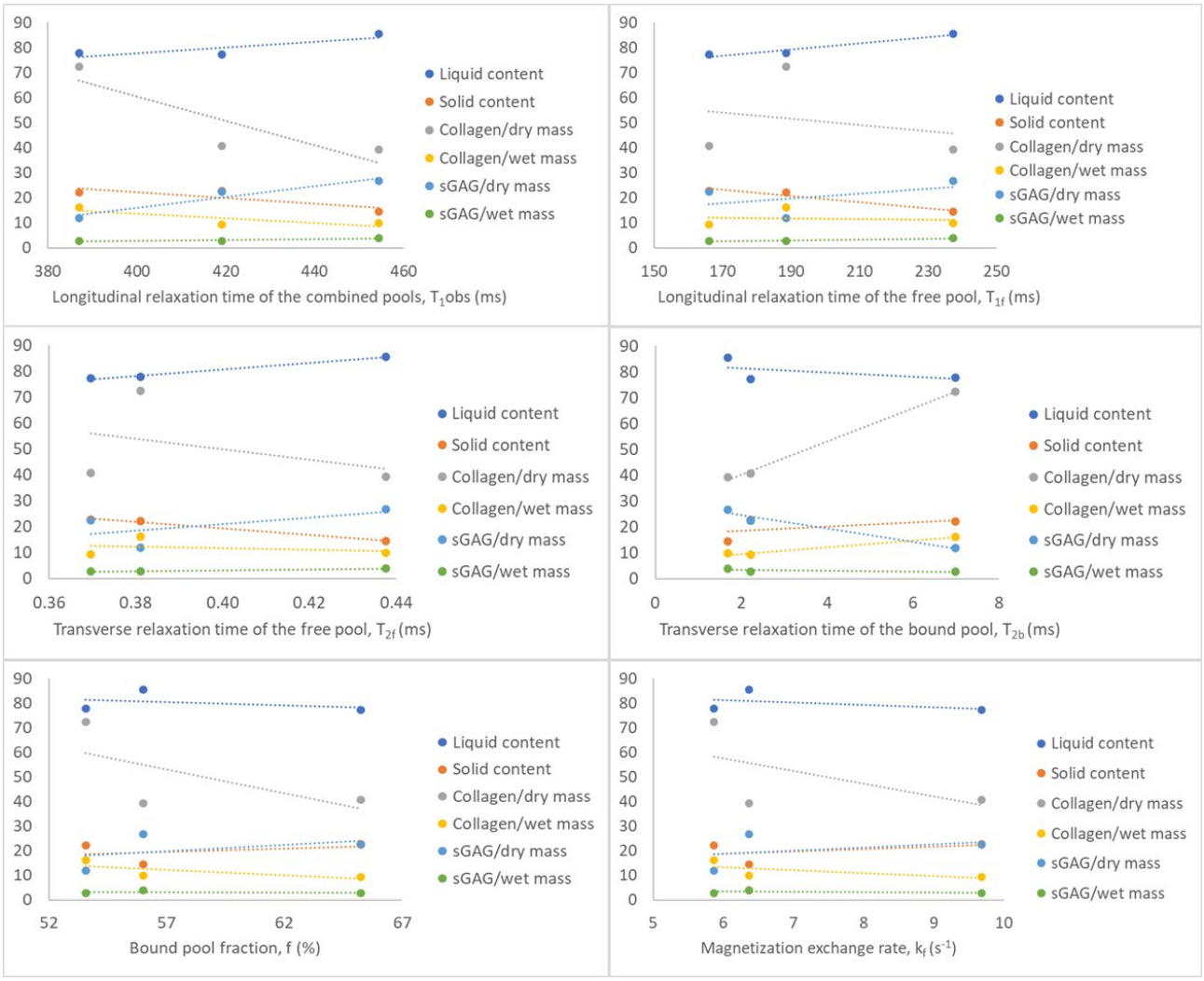

FIGURE O.3: RELATIONSHIPS BETWEEN QMT PARAMETERS AND BIOCHEMICAL PROPERTIES IN THE *EX SITU* LATERAL CARTILAGE SAMPLES

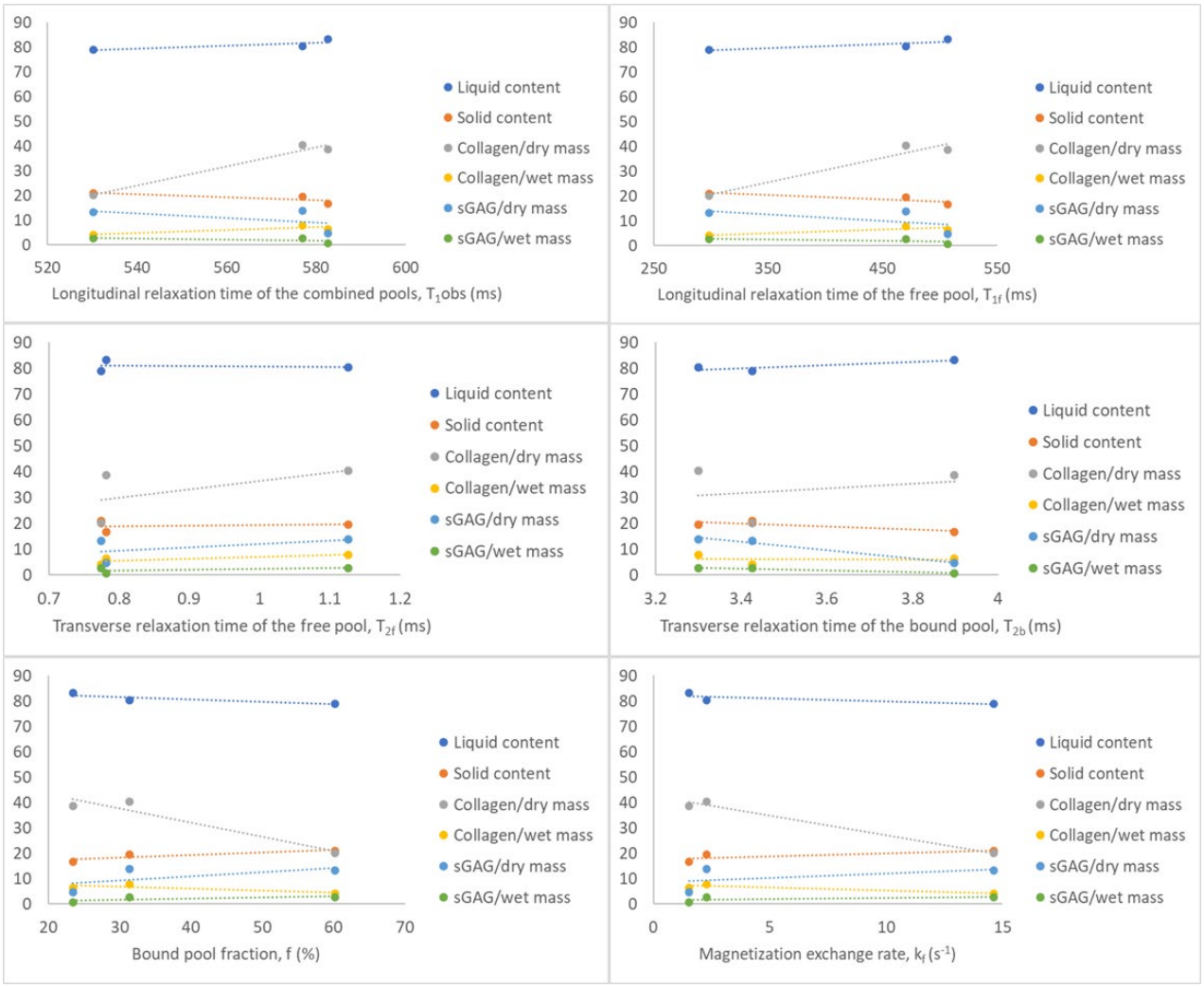

FIGURE O.4: RELATIONSHIPS BETWEEN QMT PARAMETERS AND BIOCHEMICAL PROPERTIES IN THE *EX SITU* MENISCUS SAMPLES

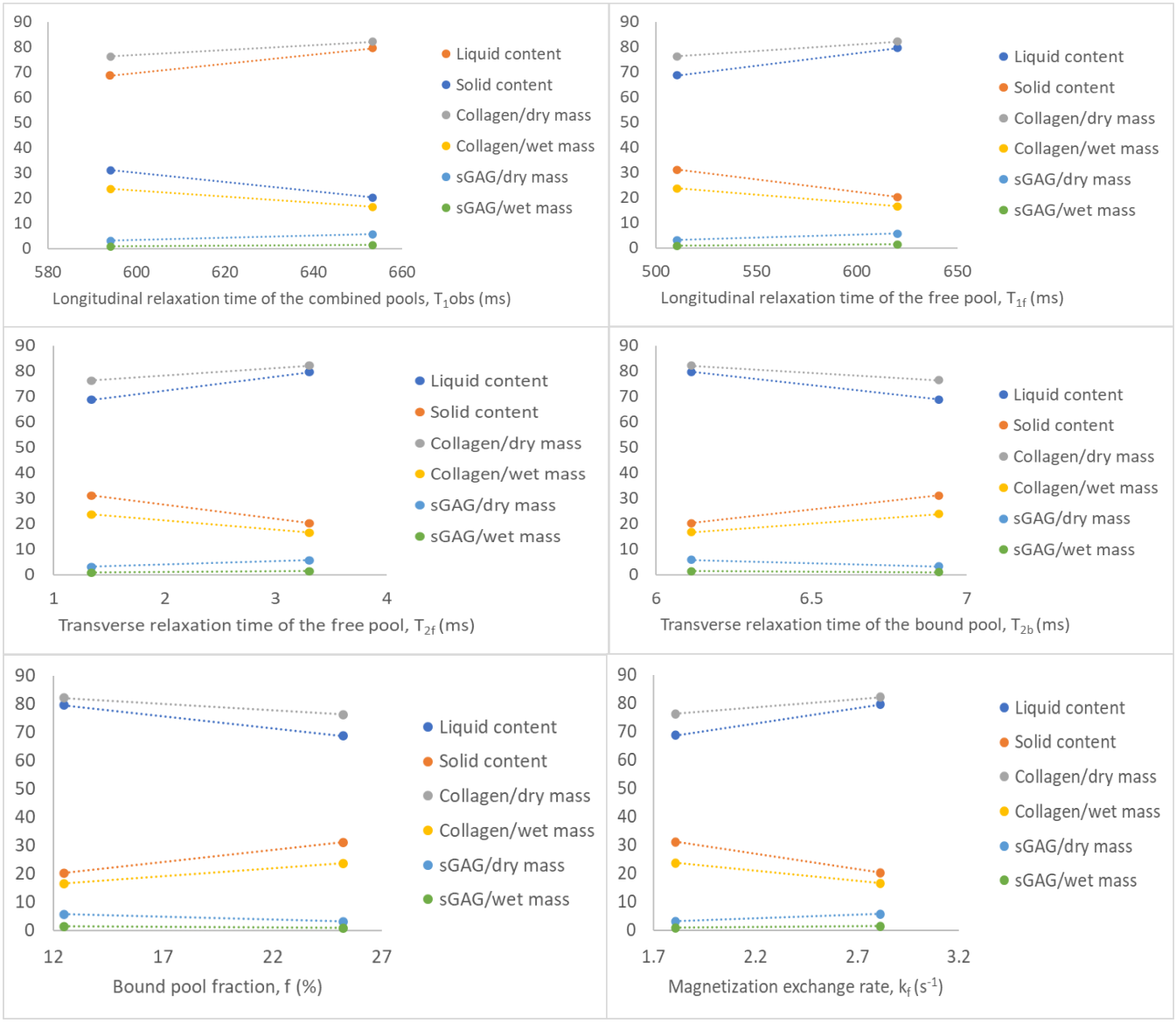

FIGURE O.5: RELATIONSHIPS BETWEEN QMT PARAMETERS AND HISTOLOGY SCORE IN THE *EX SITU* MENISCUS SAMPLES

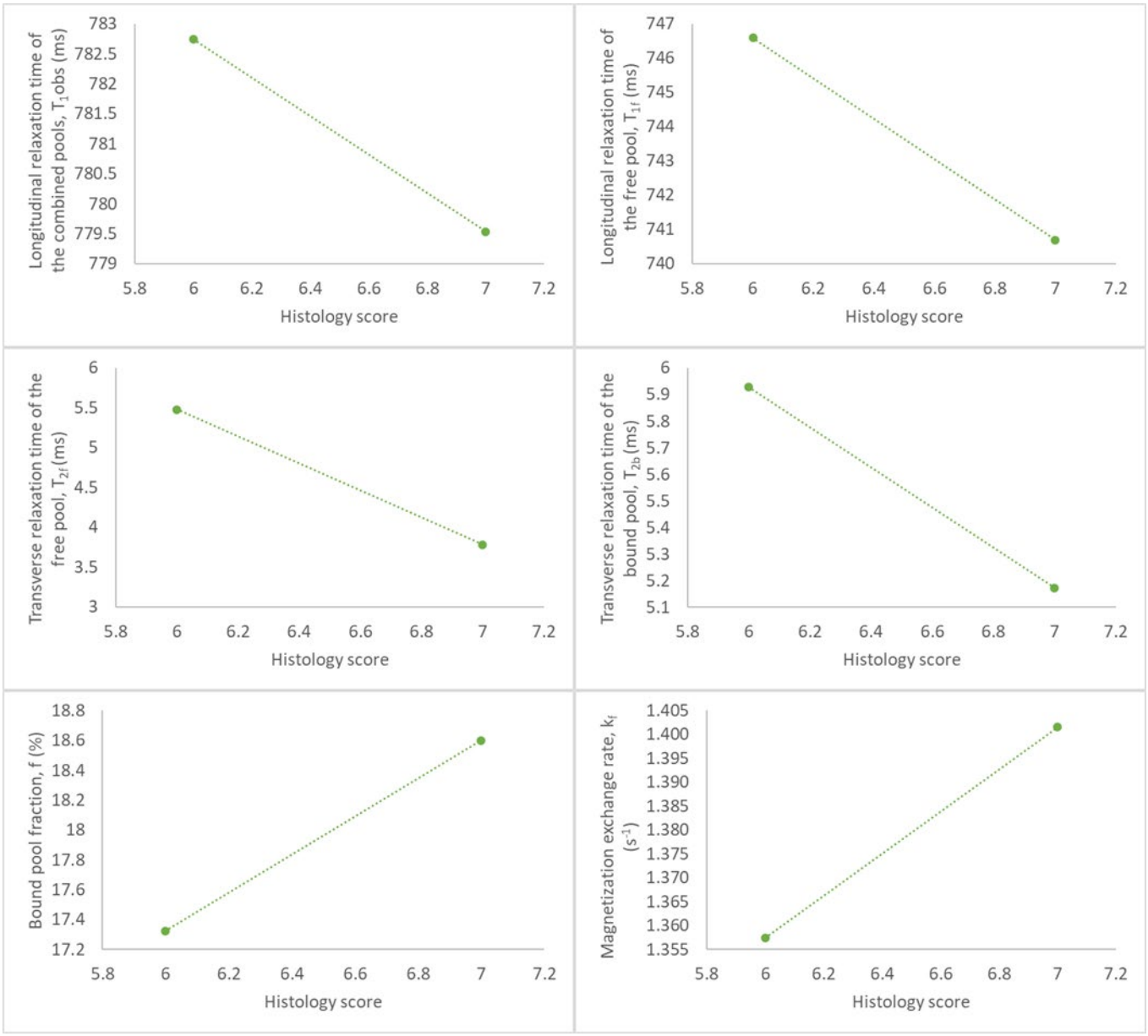

Appendix P: Discussion of connections between the mechanical, biochemistry, and histology results of the TKA study

Aside from information about the qMT parameters of the tissue, my study quantified various tissue properties, which can also be compared to values reported in the literature. In the meniscus, most parameters aligned with what would be expected (Table P.1). In the literature, liquid content increased with damage (72% to 75%)[16,29] and my result (77.7%) aligns with this trend. Interestingly, values reported in the literature for sGAG/dry mass seemed to increase from healthy (1-2%)[29] to damaged (2-4%)[16], even though it would be expected for this to decrease due to the diminishing proteoglycans in diseased tissue. It is important to note however that these results are from different studies and the values are reasonably close, so it is possible experimental errors or slight differences in methods are the cause of the discrepancy. My result (3.47%) falls perfectly into the damaged expectation. My results also line up with the literature for sGAG/wet mass and collagen/wet mass, but the collagen/dry mass result (78.8%) was somewhat unexpected. In the literature, a healthy population had a value of 75%[29] and a damaged population 65%[16]. The reason for my result being higher than both of these values could be due to the potential overestimation of hydroxyproline in the samples (as discussed in section 4.4.3 Connections between biochemistry and histology results).

For the mechanical properties, my results lined up very nicely with all the reported values and trends from the literature. The instantaneous modulus of healthy tissue in the literature was reported as 1.8 MPa[93] and my result for damaged tissue was 0.173 MPa. This is logical on a physical level because the degraded tissue would not be as stiff as healthy tissue, and it also lines up with the literature where a value of 0.212 MPa[16] was reported for a damaged population. From the Mittal *et al* study[156], the thickness was found to not vary greatly between healthy and damaged menisci. It is important to note however that the

resolution for this measurement was not reported and so the accuracy of these measurements is difficult to ascertain. Furthermore, the meniscus is quite a thick tissue (especially in comparison to cartilage), and so changes in its thickness caused by OA may be more difficult to detect unless they are large enough to significantly reduce the overall depth. The average histology score in my study (7) also lined up with the literature (5-9)[71].

Cartilage trends were much like those seen in the meniscus in all properties assessed (Table P.1). My results for liquid content and sGAG followed the expected patterns with my liquid content being higher than healthy populations and sGAG amount lower. Similarly to the meniscus, the collagen amounts that I found were higher than the healthy and damaged values reported in the literature but this could be from the hydroxyproline estimation. Also, the collagen per wet mass values reported in the literature showed higher amounts in a damaged population (5.7%[109]) than healthy (1.78%[108]), which may highlight the variation that exists across the literature. Small differences in procedures could impact the results, and the collagen to hydroxyproline mass ratio chosen especially affects the collagen found. The Li study[109] assumed a collagen to hydroxyproline mass ratio of 10, but other studies do not report what mass ratio they used. This is an important piece of information that may change the quantity of collagen observed.

The cartilage mechanical properties fit reasonably within the values reported in the literature, except for the instantaneous modulus (0.643 MPa), which was much lower than other studies (1.9[142] and 3.72[132]). This may be due to the level of damage of my tissue samples. Upon comparison to the histology results reported in one of the same studies (3.2[142]), my samples were much more damaged (12.5), which could explain the lower moduli values. Clearly, tissue health directly impacts the mechanical and biochemical properties of a tissue.

TABLE P.1: COMPARISON OF MY RESULTS TO THE LITERATURE FOR CARTILAGE AND MENISCUS IN THE TKA STUDY

Parameter	Meniscus			Cartilage		
	Values from literature		My results	Value from literature		My results
	Healthy	Damaged		Healthy	Damaged	
Liquid content (%)	72[29], 65[172], 70-75[51]	75*[16], 85[51]	77.7	65-80[21]	77[142]	80
sGAG/dry mass (%)	1-2[29]	2-4*[16]	3.47			11.7
sGAG/wet mass (%)	0.6-0.8[51]	0.4-0.9*[16]	0.769	10-15[21]	3.9[109]	2.26
Collagen/dry mass (%)	75[29], 69-80[161]	65*[16]	78.8	60[21,22]		64.1
Collagen/wet mass (%)	20-22[29,51]	14*[16]	15.4	1.78[108]	5.7[109]	13.7
Instantaneous modulus (MPa)	1.8[93]	0.212[16]	0.173	2.15[108]	1.9[142], 3.72[132]	0.643
Thickness (mm)	3.7-3.85[156]	3.62-3.94[156]	2.8	2-4[21]	1.39-1.50[156]	1.9
Histology score		5-9[71]	7		3.2[142]	12.5
*Value not stated, estimated from figures						

In order to quantify the relationships between the various tissue properties found in this study, Pearson correlation coefficients were calculated (Appendix Q: Correlations between tissue properties for the TKA study). For this analysis, the properties assessed were the liquid content, sGAG/dry mass, collagen/dry mass, instantaneous modulus, and histology score. These properties were selected as representatives of the tissue property categories and for the sake of brevity, the other biochemistry and mechanical properties were excluded.

In the cartilage (Table Q.1), liquid content was found to increase with histology score ($r=0.492$, $p<0.05$), sGAG per dry mass to increase with decreasing collagen per dry mass ($r=-0.466$, $p<0.05$), and instantaneous modulus to increase with increasing collagen per dry mass ($r=0.464$, $p<0.05$) all at moderate levels. There was one strong relationship found between increasing collagen per dry mass and decreasing histology score ($r=-0.681$, $p<0.01$). The relationship between the collagen and sGAG content is to be expected (Figure P.1A), but the direction of the observed correlation is surprising. It would be expected for the amount of collagen to decrease as the sGAG decreases, but it appears that at higher concentrations of collagen, the sGAG amount is lower. However, the bulk of the data is in a cluster, and all of these samples are from damaged tissue. It is difficult to confidently

determine relationships between these macromolecules without being able to assess a range of tissue health. Histology score is the most direct representation of tissue health, as it depends on the organization and overall condition of the sample. Comparisons between the histology score and the collagen amount (Figure P.1B) and instantaneous modulus (Figure P.1C) roughly show that with increased damage to the tissue, there is expected to be less collagen and a lower instantaneous modulus. Both of these observations align with what was anticipated.

FIGURE P.1: SCATTERPLOTS FOR REPRESENTATIVE TISSUE PROPERTY RELATIONSHIPS IN THE CARTILAGE

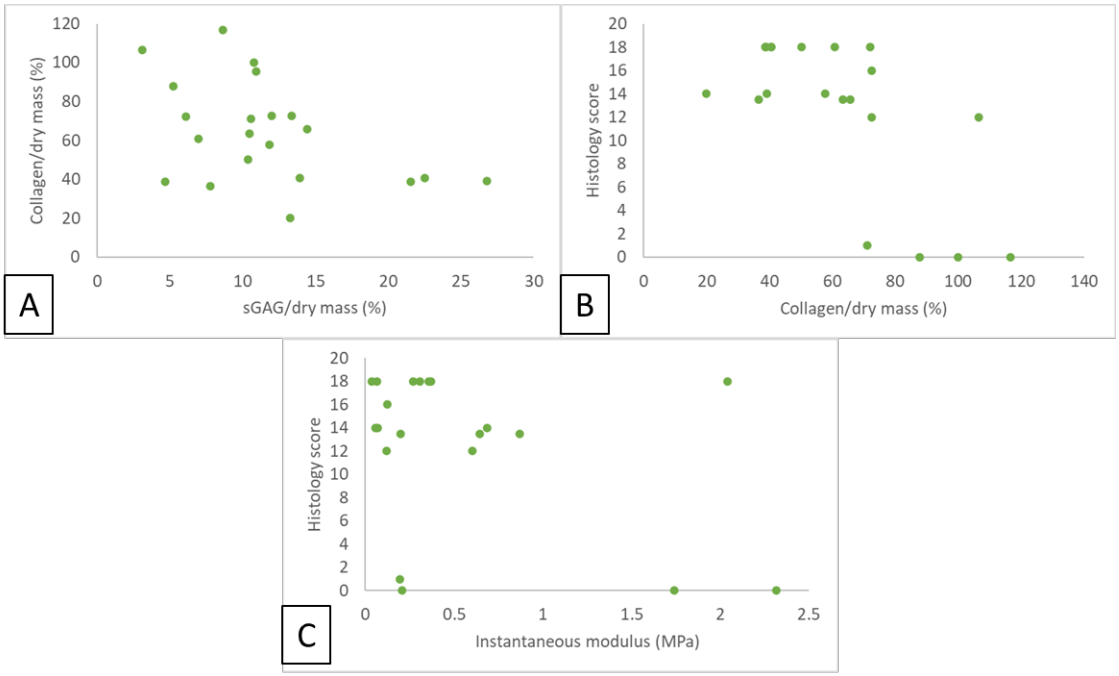

In the meniscus, only one significant correlation was found (Table Q.1) but it was very strong and between the collagen/dry mass and instantaneous modulus ($r=-0.855$, $p<0.01$). This is not alarming however, given that there were only 9 meniscus samples available to determine relationships between. The collagen and sGAG relationship followed the same pattern as for cartilage: increased collagen led to decreased sGAG (Figure P.2A). The connection between the histology score and the collagen content was very pronounced (Figure P.2B), showing a greater amount of collagen with lower histology scores. This was also observed with the

instantaneous modulus (Figure P.2C). Although these connections may seem obvious, they are important to verify to help validate the methods and further understand the correlations achieved in this research.

FIGURE P.2: SCATTERPLOTS FOR REPRESENTATIVE TISSUE PROPERTY RELATIONSHIPS IN THE MENISCUS

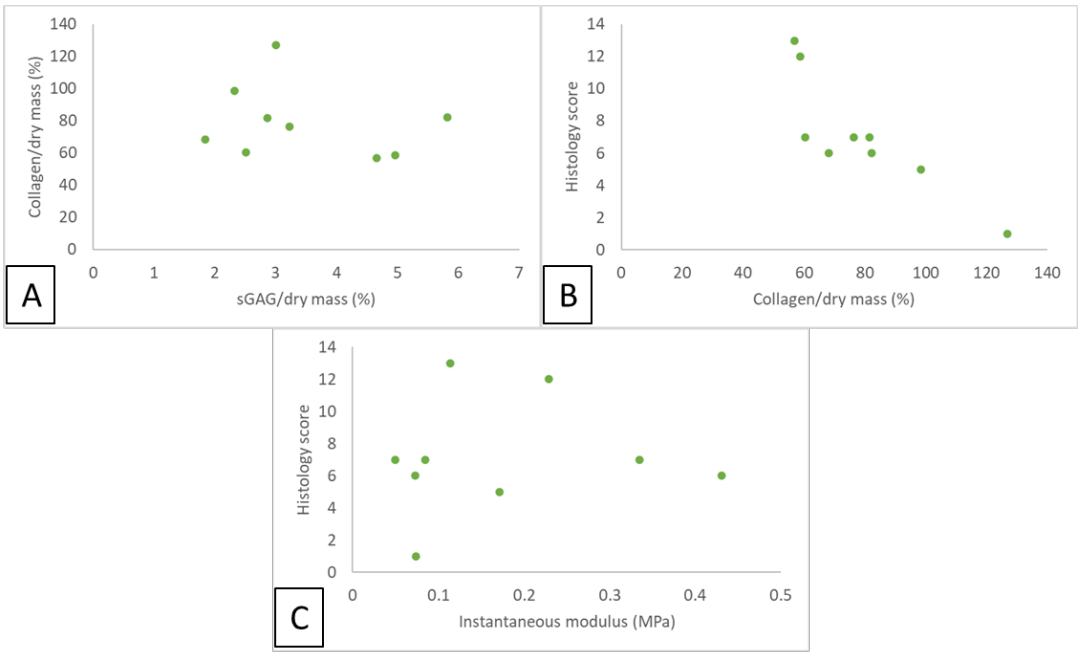

Appendix Q: Correlations between tissue properties for the TKA study

TABLE Q.1: PEARSON CORRELATION COEFFICIENTS CALCULATED BETWEEN VARIOUS REPRESENTATIVE TISSUE PROPERTIES IN THE TKA STUDY

Cartilage		Liquid content (%)	sGAG/dry mass (%)	Collagen/dry mass (%)	Instantaneous modulus (MPa)	Histology score
Liquid content (%)	Pearson Correlation		-0.405	-0.176	-0.138	.492*
	Sig. (2-tailed)		0.069	0.445	0.552	0.028
	N		21	21	21	20
sGAG/dry mass (%)	Pearson Correlation	-0.405		-.466*	-0.214	0.253
	Sig. (2-tailed)	0.069		0.033	0.352	0.282
	N	21		21	21	20
Collagen/dry mass (%)	Pearson Correlation	-0.176	-.466*		.464*	-.681**
	Sig. (2-tailed)	0.445	0.033		0.034	0.001
	N	21	21		21	20
Instantaneous modulus (MPa)	Pearson Correlation	-0.138	-0.214	.464*		-0.388
	Sig. (2-tailed)	0.552	0.352	0.034		0.091
	N	21	21	21		20
Histology score	Pearson Correlation	.492*	0.253	-.681**	-0.388	
	Sig. (2-tailed)	0.028	0.282	0.001	0.091	
	N	20	20	20	20	
Meniscus		Liquid content (%)	sGAG/dry mass (%)	Collagen/dry mass (%)	Instantaneous modulus (MPa)	Histology score
Liquid content (%)	Pearson Correlation		-0.159	0.066	-0.191	-0.276
	Sig. (2-tailed)		0.683	0.866	0.623	0.473
	N		9	9	9	9
sGAG/dry mass (%)	Pearson Correlation	-0.159		-0.243	0.488	-0.318
	Sig. (2-tailed)	0.683		0.529	0.183	0.405
	N	9		9	9	9
Collagen/dry mass (%)	Pearson Correlation	0.066	-0.243		-.855**	-0.252

	Sig. (2-tailed)	0.866	0.529		0.003	0.514
	N	9	9		9	9
Instantaneous modulus (MPa)	Pearson Correlation	-0.191	0.488	-.855**		0.095
	Sig. (2-tailed)	0.623	0.183	0.003		0.808
	N	9	9	9		9
Histology score	Pearson Correlation	-0.276	-0.318	-0.252	0.095	
	Sig. (2-tailed)	0.473	0.405	0.514	0.808	
	N	9	9	9	9	

** Correlation is significant at the 0.01 level	**Correlation legend**	Very weak (0-0.19)	Weak (0.2-0.39)
* Correlation is significant at the 0.05 level	Moderate (0.4-0.59)	Strong (0.6-0.79)	Very strong (0.8-1)